Development of Remaining Life Prediction Models for Instrumentation and Control (I&C) Cables for use in Reliability Assessment of NPP Systems

By

SANTHOSH

(ENGG01200804015)

Bhabha Atomic Research Centre, Mumbai

A thesis submitted to the

Board of Studies in Engineering Sciences

In partial fulfillment of requirements

for the Degree of

DOCTOR OF PHILOSOPHY

of

HOMI BHABHA NATIONAL INSTITUTE

November 2016

Homi Bhabha National Institute

Recommendations of the Viva Voce Committee

As members of the Viva Voce Committee, we certify that we have read thedissertation prepared by SANTHOSH entitled "Development of Remaining Life Prediction Models for Instrumentation and Control (I&C) Cables for use in Reliability Assessment of NPP Systems" and recommend thatit may be accepted as fulfilling the thesis requirement for the award of Degree ofDoctor of Philosophy.

Chairman	Prof. (Smt.) Archana Sharma	**Date:** 04-11-2016
Guide / Convener	Prof. A. K. Ghosh	**Date:** 04.11.2016
Co-guide	Prof. B. G. Fernandes	**Date:** 4/11/2016
Member 1	Prof. V. H. Patankar	**Date:** 04.11.2016
Member 2	Prof. (Smt.) Gopika Vinod	**Date:** 4/11/2016
Member 3	Prof. B. Dikshit	**Date:** 4/11/2016

External Examiner Prof. V. N. A. Naikan 4/11/16

Final approval and acceptance of this thesis is contingent upon the candidate'ssubmission of the final copies of the thesis to HBNI.

I/We hereby certify that I/we have read this thesis prepared under my/ourdirection and recommend that it may be accepted as fulfilling the thesis requirement.

Date: 04.11.2016

Place: Mumbai

Co-guide (if applicable) **Guide**

STATEMENT BY AUTHOR

This dissertation has been submitted in partial fulfillment of requirements for an advanced degree at Homi Bhabha National Institute (HBNI) and is deposited in the Library to be made available to borrowers under rules of the HBNI.

Brief quotations from this dissertation are allowable without special permission, provided that accurate acknowledgement of source is made. Requests for permission for extended quotation from or reproduction of this manuscript in whole or in part may be granted by the Competent Authority of HBNI when in his or her judgment the proposed use of the material is in the interests of scholarship. In all other instances, however, permission must be obtained from the author.

SANTHOSH

DECLARATION

I, hereby declare that the investigation presented in the thesis has been carried out by me. The work is original and has not been submitted earlier as a whole or in part for a degree / diploma at this or any other Institution / University.

SANTHOSH

DEDICATIONS

I dedicate this dissertation to

My father Late Venkatarayappa and mother Gangulamma who taught me to trust in god and believe in hard work

My wife Vani and daughters Divyansha and Shravya for their constant support and unconditional love throughout the preparation of this dissertation

My brothers, sisters and in-laws for their generous support and encouragement throughout my life

ACKNOWLEDGEMENTS

I would like to express my deep and sincere gratitude to my guides, Prof. A. K. Ghosh, Former Director, Health Safety and Environment Group, BARC and Prof. B. G. Fernandes, Head, Electrical Engineering Department, IIT Bombay for their helpful guidance, suggestions and encouragement throughout this research work. I am grateful to both of them for their constant review, comments and suggestions, and directions on every aspect of my thesis work despite of their busy schedule.

My sincere thanks are due to Dr. Kallol Roy, Chairman and Managing Director, Bhavini and Former Chairman, Doctoral Committee VII, Prof. (Smt.) Archana Sharma, Chairperson, Doctoral Committee VII, and Prof. V. H. Patankar, Prof. (Smt.) Gopika Vinod and Prof. B. Dikshit, Members of Doctoral Committee VII for their critical evaluation of my research activities, sincere review, suggestions and kind cooperation throughout this research work.

I express my sincere gratitude to my reviewers Prof. Uday Kumar, Lulea University of Technology, Sweden and Prof. V. N. A. Naikan, IIT Kharagpur for their timely review and valuable suggestions for further improvement of the thesis.

Special thanks are extended to Shri K. K. Vaze, Former Director, Reactor Design and Development Group, BARC, Dr. R. K. Singh, Former Associate Director, Reactor Design and Development Group, BARC and Dr. (Smt.) Gopika Vinod, Head, Probabilistic Safety Section, Reactor Safety Division, BARC for permitting me to carry out several experiments at Radiation Technology Development Division, BARC and National Centre for Photovoltaic Research and Education, IIT Bombay, Powai.

I take this opportunity to thank Shri A. Rama Rao, Associate Director, Reactor Design and Development Group and Head, Reactor Safety Division, BARC for his kind support and encouragement towards research activities.

I extend my sincere gratitude to Prof. B. K. Dutta, Dean, HBNI and Prof. G. K. Dey, Dean, Engineering Sciences, HBNI for their kind support and cooperation during the period of my research work.

Experimental evaluations would not have been possible without the generous support of Shri P. K. Ramteke, Shri A. K. Ahirwar and Shri N. B. Shrestha, Reactor Safety Division, BARC; Dr. Lalit Varshney, Dr. Y. K. Bhardwaj, Dr. K. A. Dubey, Shri C. V. Chaudhari and Shri S. P. Shejwal, Radiation Technology Development Division, BARC; Dr. K. Sudarshan, Radiochemistry Division, BARC; Prof. Sagar Mitra, Prof. Diksha Makwani and Shri N. Thirmaliah, National Centre for Photovoltaic Research and Education, IIT Bombay. I express my sincere thanks to all of them for their kind help and support in carrying out various experiments.

I convey my sincere gratitude to Smt. R. Rajalakshmi, Shri S. S. Jana and Shri R. G. Kamath, Reactor Engineering Division, BARC and Shri M. G. R. Kumar, Heavy Water Division, BARC for their kind support and help towards arranging the cables for experimental studies.

I express my sincere gratitude to Shri A. K. Babar, Shri R. K. Saraf and Dr. V. V. S. Sanyasi Rao, Former Heads of Probabilistic Safety Section, Reactor Safety Division, BARC, and Prof. A. K. Verma, Stord/Haugesund University, Norway and Prof. A. Srividya, University of Stavanger, Norway for their valuable advises and directions towards achieving the important research milestones.

I would express my sincere thanks to my friends and colleagues Dr. K. A. Dubey, Dr. K. Sudarshan, Dr. R. N. Singh, Dr. M. Hari Prasad, Dr. K. Durga Rao, Shri S. Karimulla and Dr. K. Tirumalesh for their active support and technical discussions during the entire period of my thesis work.

I would like to pay my sincere gratitude to all my teachers who have taught me and inspired me right from my school days and provided their blessings for all the success I have achieved.

I acknowledge my wife Mrs. N. S. Vani and my daughters Ms. Divyansha and Ms. Shravya who have supported me throughout my thesis work. I could not have been successful in completing my thesis without their constant support and understanding.

Finally, I express my gratitude to all persons who have not been listed here but helped directly or indirectly to complete this research work.

SANTHOSH

ACRONYMS AND ABBREVIATIONS

AE	Auger electrons
AF	Acceleration factor
ALT	Accelerated life testing
ANN	Artificial neural networks
Anova	Analysis of variance
AX	Antioxidant
BR	Butyl rubber
BSE	Back scattered electrons
CM	Condition monitoring
COMREL	Component reliability analysis software tool
COMSOL	Multiphysics finite element analysis software tool
COV	Coefficient of variation
CSPE	Chlorosulphonated polyethylene
DBA	Design basis accident
DBE	Design basis event
DED	Dose to equivalent damage
DLO	Diffusion limited oxidation
DSC	Differential scanning calorimeter
EAB	Elongation at break
EDS	Energy dispersive X ray spectroscopy
EMC	Electromagnetic correction
EMI	Electromagnetic interference
EPDM	Ethylene propylene diene monomer
EPR	Ethylene propylene rubber

ETFE	Ethylene tetrafluro ethylene
EVA	Ethylene vinyl acetate
FEA	Finite element analysis
FESEM	Field emission scanning electron microscopy
FORM	First order reliability method
FRLS	Flame retardant low smoke
FTIR	Fourier transform infrared spectroscopy
HALT	Highly accelerated life testing
HDPE	High density polyethylene
HMWPE	High molecular weight polyethylene
HR	Heat resistant
I&C	Instrumentation and control
ICEA	International cable engineer's association
IR	Insulation resistance
ISOGRAPH	Fault tree analysis software tool
LDPE	Low density polyethylene
LMWPE	Low molecular weight polyethylene
LOCA	Loss of coolant accident
MCS	Monte Carlo simulation
NPP	Nuclear power plant
OIT	Oxidation induction time
OITp	Oxidation induction temperature
PALS	Positron annihilation lifetime spectroscopy
PE	Polyethylene
PEEK	Ploy ether ether ketone

PET	Polyethylene terephthalate
PI	Polarization index
PPO	Polyphenylene oxide
PSA	Probabilistic safety assessment
PVC	Polyvinyl chloride
RUL	Remaining useful life
SDS	Shutdown system
SE	Secondary electrons
SEM	Scanning electron microscopy
SiR	Silicone rubber
SORM	Second order reliability method
SSI	Stress-strength interference
TDR	Time domain reflectometry
TED	Time to equivalent damage
TTF	Times-to-failure
UHF	Ultra high frequency
UTM	Ultimate tensile machine
VHF	Very high frequency
XLPE	Cross-linked polyethylene
XLPO	Cross-linked polyolefin

CONTENTS

ACKNOWLEDGEMENTS vi

ACRONYMS AND ABBREVIATIONS ix

CONTENTS xii

SYNOPSIS xx

List of Publications arising from the Thesis xxiv

List of Figures xxvii

List of Tables xxxiii

Chapter 1 Introduction 1

1.1 Background 1

1.2 Electrical cables in NPPs 2

1.3 Properties of polymeric insulation materials 5

1.4 Cable failure modes and their effects 6

1.5 Ageing and degradation in electrical cables 7

1.6 Qualification and condition monitoring guidelines 10

1.7 Motivation 11

1.8 Scope 13

1.9 Organization of the thesis 14

1.10 Summary 15

Chapter 2 Literature Review 16

2.1 Introduction 16

2.2 Performance indicators and acceptance criteria for electrical cables 17

2.3 State-of-the-art condition monitoring techniques for performance assessment of electrical cables 18

2.3.1 Measurement of insulation resistance and polarization index 19

2.3.2 Measurement of elongation-at-break 23
2.3.3 Determination of oxidation induction time and temperature 24
2.3.4 Density measurement 27
2.3.5 Fourier transform infrared spectroscopy 28
2.3.6 Positron annihilation lifetime spectroscopy 30
2.3.7 Time domain reflectometry 32
2.3.8 Tan delta measurement 33
2.3.9 Measurement of characteristic impedance of a cable 35
2.3.10 Scanning electron microscopy 37
2.4 Important aspects of accelerated ageing and life estimation of electrical cables 39
2.4.1 Thermal ageing 40
2.4.2 Radiation ageing 41
2.4.3 Limitations of the methods 42
2.4.4 Life estimation 43
2.5 Discussion and research objective 44
2.6 Summary 49
Chapter 3 Degradation Mechanisms in Polymeric Insulation Materials 50
3.1 Background 50
3.2 General features of ageing in polymers 51
3.3 Basic effects of ageing 52
3.3.1 Effect of microvoids in polymers 53
3.3.2 Energy criterion for breaking chemical bonds 53
3.4 Understanding ageing mechanisms 54
3.4.1 Competition between HCl elimination and evaporation of plasticizers in plasticized PVC 55

3.4.2 Ageing through a physical transition in semi-crystalline polymers 55
3.4.3 Compatibility of materials in construction of the cable.....56
3.5 Key concerns on accelerated ageing 57
3.5.1 Accelerated thermal ageing 57
3.5.2 Accelerated radiation ageing 59
3.6 Traditional mechanisms of polymer degradation.....60
3.6.1 General chemical mechanisms.....62
3.6.2 Chain-scission mechanisms in polymers 66
3.7 Physical ageing mechanisms.....69
3.7.1 Evaporation of plasticizers.....69
3.7.2 Migration of plasticizers 70
3.7.3 Reverse temperature effect 70
3.7.4 Oxidation reaction.....71
3.8 Summary 73
Chapter 4 Reliability Prediction of I&C Cables by Stress Strength Interference Theory 74
4.1 Introduction 74
4.2 Methodology 75
4.3 Analysis and results.....80
4.4 Summary 84
Chapter 5 Reliability Prediction of I&C Cables by Artificial Neural Networks ...86
5.1 Introduction 86
5.2 Methodology 87
5.2.1 Prediction of times-to-failure.....87
5.2.2 Reliability prediction 91

5.3 Selection of learning algorithm and network architecture 92
5.3.1 Selection of learning algorithm 93
5.3.1.1 Resilient back propagation algorithm 95
5.3.1.2 Learning rate factors 95
5.3.1.3 Step size 95
5.3.1.4 Working principle 95
5.3.1.5 Sigmoid activation function 96
5.3.1.6 Mean square error function 97
5.3.2 Selection of network architecture 97
5.4 Times-to-failure prediction and development of life-stress model 101
5.5 Determination of life distribution and reliability prediction 105
5.6 Summary 111
Chapter 6 Simulation of Thermal and Radiation Ageing Effects in I&C Cables 113
6.1 Introduction 113
6.2 Insulation degradation due to Joule heating 113
6.2.1 Joule heating 113
6.2.2 Simulation and results 114
6.2.2.1 Joule heating effect in single core I&C cable 115
6.2.2.2 Joule heating effect in multicore I&C cable 120
6.3 Effect of microvoids on electric field in I&C cable 122
6.3.1 Simulation and results 123
6.4 Effect of radiation ageing on mechanical properties 126
6.4.1 Simulation and results 126
6.5 Summary 130
Chapter 7 Experimental Determination of Performance Indicators 131

7.1 Introduction 131
7.2 Research plan for experimental studies 132
7.3 Cable samples for experimental studies 133
7.4 Insulation resistance measurement 133
7.4.1 Experimental 133
7.4.2 Results 134
7.4.3 Insulation resistance model 137
7.4.4 Discussion 139
7.5 Accelerated radiation ageing 140
7.5.1 Infrared spectroscopy 141
7.5.1.1 Results and discussion 141
7.5.1.2 Anova 143
7.5.2 Elongation at break measurement 146
7.5.2.1 Correlation of infrared transmittance with EAB 151
7.5.2.2 Discussion 153
7.5.3 Oxidation induction time and temperature measurement 154
7.5.3.1 Determination of oxidation induction time (OIT) and temperature (OITp) 155
7.5.3.2 Determination of oxidation induction time from the measured oxidation induction temperature 157
7.5.3.3 Correlation between oxidation induction time and EAB 160
7.5.3.4 Discussion 161
7.5.4 Scanning electron microscopy 162
7.5.5 Positron annihilation lifetime spectroscopy 164
7.5.5.1 Estimation of free volume hole size 165

7.6 Accelerated thermal ageing 166
7.6.1 Determination of oxidation induction time and temperature 167
7.6.1.1 Determination of oxidation induction temperature 167
7.6.1.2 Determination of oxidation induction time from the measured oxidation induction temperature 170
7.6.2 Measurement of elongation at break 171
7.6.2.1 Tensile elongation of cable insulation 171
7.6.2.2 Tensile elongation of cable sheath 174
7.6.2.3 Correlation between oxidation induction time and EAB 175
7.6.3 Scanning electron microscopy 178
7.6.3.1 Fracture surface examination 178
7.6.3.2 Surface examination 183
7.7 Summary 184
Chapter 8 Reliability Prediction from Experimentally Determined Performance Indicators 186
8.1 Introduction 186
8.2 Reliability prediction from EAB 186
8.2.1 Results with lognormal distribution of parameter A 187
8.2.2 Results with Gumbel (min) distribution of parameter A 188
8.3 Reliability prediction from OIT 190
8.4 Application to PSA of NPP 192
8.5 Summary 196
Chapter 9 Conclusions and Future Scope 197
9.1 Conclusions 197
9.2 Future scope 201

Bibliography 202

Appendix A. Experimental Studies and Results 220

A.1 Insulation resistance measurement 220

A.2 Elongation at break measurement 226

A.2.1 Stress-strain curves of thermally aged insulation materials 226

A.2.1.1 Stress-strain curves of insulation aged at 110^0C 226

A.2.1.2 Stress-strain curves of sheath aged at 110^0C 228

A.2.1.3 Stress-strain curves of insulation aged at 135^0C 230

A.2.1.4 Stress-strain curves of sheath aged at 135^0C 231

A.2.1.5 Images of thermally aged samples after tensile test 233

A.2.2 Stress-strain curves of radiation aged insulation materials 237

A.2.2.1 Stress-strain curves of radiation aged insulation 237

A.2.2.2 Stress-strain curves of radiation aged sheath 239

A.3 Infrared spectroscopy 242

A.3.1 Infrared spectra of insulation 242

A.3.2 Infrared spectra of sheath 244

A.4 Oxidation induction time and temperature measurement 247

A.4.1 Calibration of DSC 247

A.4.2 Determination of oxidation induction time (OIT) 248

A.4.3 Determination of oxidation induction temperature (OITp) 254

Appendix B. Determination of Life Distribution for Reliability Prediction 261

B.1 EAB data of irradiated insulation 261

B.1.1 Normal distribution fit of the data 261

B.1.2 Lognormal distribution fit of the data 262

B.1.3 Smallest extreme value distribution fit of the data 263

B.1.4 Weibull distribution fit of the data 264
B.1.5 3-Parameter Weibull distribution fit of the data 265
B.1.6 Largest extreme value distribution fit of the data 266
B.1.7 Summary of the distributions 268
B.2 EAB data of irradiated sheath 270
B.2.1 Normal distribution fit of the data 270
B.2.2 Lognormal distribution fit of the data 271
B.2.3 Smallest extreme value distribution fit of the data 272
B.2.4 Weibull distribution fit of the data 273
B.2.5 3-Parameter Weibull distribution fit of the data 274
B.2.6 Largest extreme value distribution fit of the data 275
B.2.7 Summary of the distributions 276

SYNOPSIS

Instrumentation and control (I&C) cables are one of the most important components in nuclear power plants (NPPs) because they provide power to safety-related equipments and also to transmit signals to and from various controllers to perform safety operations. The polymer materials used for insulation and jacket materials in I&C cables are susceptible to ageing and degradation mechanisms caused by exposure to many of the stressors encountered in NPP service conditions. Ageing of components in NPP is an important concern since the degradation caused by ageing can impact the performance of susceptible equipment. Although, there exists several condition monitoring and life estimation techniques, currently there is no any standard methodology or an approach towards estimating the time dependent reliability of I&C cables. The state-of-the art for incorporating cable ageing effects into probabilistic safety assessment (PSA) is still evolving and current assumptions that need to be made on the failure rates and common cause effects are based on sparse data. Therefore, identification and quantification of ageing of electrical cables is very much essential for an accurate prediction of system reliability for use in PSA of NPPs.

The objective of this thesis work is to develop a methodology to assess the susceptibility of polymeric cable insulation to various ageing mechanisms and to predict the state of the insulation at any chosen time in order to evaluate the remaining lifetime of operating cables in NPPs. In this context, several concepts such as stress-strength interference (SSI) theory, artificial neural networks (ANNs) and Weibull theory have been employed to develop reliability prediction frameworks based on the measured performance indicators such as elongation at break (EAB), insulation resistance (IR) and oxidation induction time (OIT). A framework based on SSI theory has been developed to estimate the reliability of I&C cables from the measured IR by subjecting to thermal ageing. The performance of the cable when

the degradation process is linear or exponential has also been modeled. The methodology has been demonstrated for predicting the time dependent reliability of a typical I&C cable consisting of cross-linked polyethylene (XLPE) as insulation however it can be applied to other polymeric insulation materials such as polyvinyl chloride (PVC), polyethylene (PE) etc. Another approach based on ANNs has been developed to predict the reliability of I&C cables from the initial few readings of the IR measured during accelerated life testing. The use condition time-to-failure was predicted from the ANN model and time dependent reliability was estimated from the Weibull reliability model. The methodology has been demonstrated with the accelerated life testing data on a typical XLPE insulated I&C cable. The reliability or probability of failure estimated from these approaches is used in system reliability evaluation for accounting the cable failures in PSA of NPPs.

I&C cables are generally composed of several conductors, polymeric insulation, and a shield/screen for accounting the effect of electromagnetic interference and correction (EMI/EMC). The polymeric insulation is subjected to both internal (resistive losses in the conductor and shield) and external (environmental temperature) heating. In order to study the effect of such thermal ageing in electrical cables, finite element simulation studies have been carried out using COMSOL Multiphysics solver. The effect of aluminium screen present in PVC insulated I&C cable was simulated and the heat transfer was studied. The cable was modeled considering maximum outer surface temperature of the conductor being 90^0C due to resistive losses in the conductor and the time dependent analysis were performed to study the maximum temperature rise in the outer surface of the cable insulation and sheath. Study revealed that presence of aluminum screen in the cable significantly contributes to the thermal degradation of insulation materials. Hence, in the remaining life assessment studies the presence of non-polymeric materials which contribute to thermal degradation of the insulation may also be accounted for realistic lifetime evaluations. COMSOL Multiphysics

simulations have also been carried to study the impact voids, generated due to radiation ageing, on electrical parameters such as electric field, space charge, etc. It was observed from the finite element analysis study that the voids of size beyond 0.01mm radius have significant effect on the electric field and other parameters.

In order to assess the performance of cables received from various manufacturers and subsequent reliability prediction from the proposed approaches for use in PSA of NPP, experimental studies such as insulation resistance measurement, elongation at break measurement, Fourier transform infrared (FTIR) spectroscopy, oxidation induction time and temperature measurement, scanning electron microscopy (SEM) and positron annihilation lifetime spectroscopy (PALS) were carried out. It was evident from the experimental evaluations that, although all the cables meet the required specifications there was a significant variation in the initial IR amongst various manufacturers. However, not much variation in the polarization index (PI) was noticed amongst all the five similar cables. Hence, a cable with high value of IR does not necessarily be of having high performance.

Since all the five cables were of similar types, one of the control cable was subjected to gamma radiation and the degradation due to radiation ageing was assessed by various condition monitoring techniques. An increase in mechanical and chemical properties at lower dose levels was observed in the insulation materials. However, these properties deteriorate with increased dose levels in both insulation and sheath materials. This change in properties is due to the changes in the polymer structure due to chain scission and cross-linking process by gamma radiation. The thermal and radiation stability of insulation materials were carried out using DSC. The samples did not exhibit a clear exothermic peak under isothermal condition due to slow kinetics however; they have shown an excellent oxidation peak under continuous ramp heating. The OITs were determined from the measured oxidation induction temperature (OITp) and found to be in good agreement with the EAB findings. It was

apparent from the data analysis that the EAB follows an exponential function of OIT for both thermal and radiation ageing of insulation materials. The SEM and energy dispersive spectroscopy (EDS) performed on fresh and aged samples also support the correlation from chemical and mechanical measurements. From the SEM micrographs, a significant structural damage was noticed in the samples subjected to high thermal and radiation ageing. The PALS performed on fresh and irradiated samples also indicate a substantial free volume in the polymer matrix due to gamma radiation. It is also evident from the PALS study that a large size voids were generated in the samples aged at lower dose levels due to chain scission. From the performance indicators determined using experimental techniques, the time dependent reliabilities have been estimated by employing the developed reliability approaches. The study demonstrates the significance of accounting cables failures in PSA of NPP by modelling cable failure in shutdown system of advanced heavy water reactor. Considering the significant increase in the unavailability of shutdown system with cable failure accounted, the overall study demonstrates that the cables connected to various NPP systems may be included in the PSA study.

List of Publications arising from the Thesis

Refereed Journals

1. Remaining Life Prediction of I&C Cables for Reliability Assessment of NPP Systems, **T. V. Santhosh**, A. K. Ghosh and B. G. Fernandes, *Nuclear Engineering and Design*, 2012, no. 245, pp. 197– 201.

2. Reliability Prediction of I&C Cable Insulation Materials by DSC and Weibull Theory for Probabilistic Safety Assessment of NPPs, **T. V. Santhosh**, V. Gopika, A. K. Ghosh, B. G. Fernandes and K. A. Dubey, *Nuclear Engineering and Design*, 2015, no. 296, pp. 51-61.

3. Performance Assessment of I&C Cable Insulation Materials by DSC and SEM for NPP Ageing Management, **T. V. Santhosh**, A. K. Ghosh, B. G. Fernandes and K. A. Dubey, *International Journal of Systems Assurance Engineering and Management*, *Springer*, 2016, vol. 7, no. 1, pp. 6-15.

4. Lifetime Prediction of I&C Cables using OIT and OITp Measurements for PSA of NPPs, **T. V. Santhosh**, A. K. Ghosh and B. G. Fernandes, *Current Trends in Reliability, Availability, Maintainability and Safety: An Industry Perspective*, *Springer*, 2016, ISBN 978-3-319-23596-7.

5. Assessment of Insulation Degradation of I&C Cables from Chemical and Mechanical Measurements, **T. V. Santhosh**, A. K. Ghosh and B. G. Fernandes, *SRESA Journal of Life Cycle Reliability and Safety Engineering*, 2015, vol. 4, issue 3, pp. 16-24.

6. Condition Monitoring and Reliability Prediction of I&C Cables for use in Probabilistic Safety Assessment of NPPs, **T. V. Santhosh**, V. Gopika, A. K. Ghosh and B. G. Fernandes, *IEEE Transactions on Reliability*, 2016, Manuscript No. TR-2016-058, **Revision submitted**.

7. An Approach for Reliability Prediction of I&C Cables by Artificial Neural Networks and Weibull Theory for PSA of NPPs, **T. V. Santhosh**, V. Gopika, A. K. Ghosh and B. G. Fernandes, *Reliability Engineering and System Safety*, 2016, Manuscript No. RESS-D-16-00141, **Revision submitted**.

Conferences

1. Ageing of Instrumentation and Control Cables in NPPs, **T. V. Santhosh**, A. K. Ghosh and B. G. Fernandes, *4th National Conference on Nuclear Reactor Technology*, Mumbai, March 4-6, 2011.
2. Lifetime Prediction of I&C Cables using Artificial Neural Networks for PSA Applications, **T. V. Santhosh**, A. K. Ghosh and B. G. Fernandes, *6th International Conference on Quality, Reliability, Infocom Technology and Industrial Technology Management*, New Delhi, November 26-28, 2012.
3. Performance Assessment of I&C Cables for Nuclear Power Plant Safety and Reliability, **T. V. Santhosh**, A. K. Ghosh, B. G. Fernandes, P. K. Ramteke, N. B. Shrestha and R. K. Singh, *1st SRESA National Conference on Reliability and Safety Engineering*, Anna University, Tiruchirappalli, February 13-15, 2014.
4. Infrared Spectra and Tensile Elongation of Irradiated Cable Insulation Materials used in Nuclear Power Plants, **T. V. Santhosh**, A. K. Ghosh, B. G. Fernandes, K. A. Dubey and P. K. Ramteke, *SRESA National Conference on Reliability and Safety Engineering*, Anna University, Tiruchirappalli, February 13-15, 2014.
5. Life Estimation of I&C Cables from Oxidation Induction Time and Temperature Measurements, **T. V. Santhosh**, A. K. Ghosh and B. G. Fernandes, *4th International Conference on Reliability, Infocom Technologies and Optimization*, Amity University Uttar Pradesh (AUUP), Noida, September 2-4, 2015.

6. Life Estimation of I&C Cable Insulation Materials based on Accelerated Life Testing, **T. V. Santhosh**, P. K. Ramteke, N. B. Shrestha, A. K. Ahirwar and V. Gopika, *2nd SRESA National Conference on Reliability and Safety Engineering*, CEG Campus, Anna University, October 8-10, 2015.

List of Figures

Figure 1.1: Structure of a multicore shielded control cable 3

Figure 2.1: IR testing of cable 20

Figure 2.2: Currents in cable insulation 20

Figure 2.3: Universal tensile testing machine 23

Figure 2.4: Principle sequence of OIT measurements 25

Figure 2.5: Principle sequence of OITp measurements 26

Figure 2.6: Typical absorption regions in polymers 29

Figure 2.7: Working principle of TDR 33

Figure 2.8: Tan delta measurement 34

Figure 2.9: Typical coaxial cable 35

Figure 2.10: The block diagram of SEM 38

Figure 2.11: Proposed plan of research work (Part 1) 47

Figure 2.12: Proposed plan of research work (Part 2) 48

Figure 3.1: Traditional chemical reaction schema of polymer oxidation 61

Figure 3.2: General decomposition mechanisms 63

Figure 3.3: Chain scission in polymers 64

Figure 3.4: Cross-linking in polymers 65

Figure 3.5: (a) Intramolecular H transfer, (b) intermolecular H transfer, (c) unzipping 67

Figure 3.6: Evoporation of plasicizers 70

Figure 4.1: Temperature vs. insulation resistance 81

Figure 4.2: Insulation resistance vs. time 82

Figure 4.3: Probability of failure vs. time 84

Figure 5.1: Performance of various networks 99

Figure 5.2: Calculated TTF from various networks 100

Figure 5.3: Predicted TTF from various networks.....100
Figure 5.4: Network architecture 102
Figure 5.5: ANN performance 102
Figure 5.6: TTF from ANN and HALT [124] 102
Figure 5.7: Exponential fit of TTF of experimental data.....103
Figure 5.8: Exponential fit of TTF of ANN data 104
Figure 5.9: Weibull plot of experimental TTFs 105
Figure 5.10: Weibull plot of ANN predicted TTFs 106
Figure 5.11: Weibull plot of experimental TTFs with use condition TTF 106
Figure 5.12: Weibull plot of ANN predicted TTFs with use condition TTF.....106
Figure 5.13: Reliability from the Weibull fit of TTFs 108
Figure 5.14: Exponential plot of experimental TTF 108
Figure 5.15: Exponential plot of ANN predicted TTFs.....109
Figure 5.16: Exponential plot of experimental TTF with the use condition TTF.....109
Figure 5.17: Exponential plot of ANN predicted TTF with the use condition TTF 110
Figure 5.18: Reliability from the exponential fit of TTFs 111
Figure 6.1: Cable model with aluminium screen 115
Figure 6.2: Cable model without aluminium screen 115
Figure 6.3: Temperature distribution in the cable with aluminium screen 116
Figure 6.4: Temperature distribution in the cable without aluminium screen.....116
Figure 6.5: Temperature gradient in the cable with aluminium screen 117
Figure 6.6: Temperature gradient in the cable without aluminium screen 117
Figure 6.7: Time dependent temperature distribution in cable with aluminium screen 118
Figure 6.8: Time dependent temperature distribution in cable without aluminium screen ...118
Figure 6.9: Mean effective thermal conductivity of cable with aluminium screen 119

Figure 6.10: Mean effective thermal conductivity of cable without aluminium screen 119
Figure 6.11: Geometry of a 7 core I&C cable 120
Figure 6.12: Temperature distribution in multicore I&C cable 121
Figure 6.13: Space charge density in multicore I&C cable across the arc length 121
Figure 6.14: Power distribution in multicore I&C cable 122
Figure 6.15: 2D finite element model geometry 123
Figure 6.16: 2D finite element model 124
Figure 6.17: Electric potential across the sheath 124
Figure 6.18: Electric field across sheath with void size 0.001mm 125
Figure 6.19: Electric field across sheath with void size 0.01mm 125
Figure 6.20: Electric field across sheath with void size 0.1mm 126
Figure 6.21: Tensile testing sample for FEM analysis 127
Figure 6.22: Total displacement along the axial direction 128
Figure 6.23: Stress-strain curve 128
Figure 6.24: Strain energy density 129
Figure 6.25: von Mises stress 129
Figure 7.1: Block diagram of experimental research plan 132
Figure 7.2: Test pattern 134
Figure 7.3: IR comparison 136
Figure 7.4: PI comparison 137
Figure 7.5: Exponential fit of individual cables 138
Figure 7.6: The mean exponential fit of all the cables 139
Figure 7.7: Mean IR spectra for insulation material 142
Figure 7.8: Mean IR spectra of sheath material 142
Figure 7.9: Elongation of insulation after 50MRad radiation ageing 146

Figure 7.10: Elongation of sheath after 50MRad radiation ageing.....147
Figure 7.11: Exponential fit of EAB for insulation 149
Figure 7.12: Exponential fit of EAB for sheath.....149
Figure 7.13: Mean elongation and mean transmittance with dose for insulation 151
Figure 7.14: Mean elongation and mean transmittance with dose for sheath.....152
Figure 7.15: Heat flow signal for sample 1.....154
Figure 7.16: Heat flow signal for sample 2.....155
Figure 7.17: DSC thermogram of insulation.....156
Figure 7.18: DSC thermogram of sheath 156
Figure 7.19: OIT vs. dose for insulation 159
Figure 7.20: OIT vs. dose for sheath.....159
Figure 7.21: Exponential fit of EAB for insulation 160
Figure 7.22: Exponential fit of EAB for sheath.....161
Figure 7.23: SEM micrograph of unaged insulation.....162
Figure 7.24: SEM micrograph of unaged sheath 162
Figure 7.25: SEM micrograph of insulation aged at 5MRad.....163
Figure 7.26: SEM micrograph of sheath aged at 5MRad 163
Figure 7.27: SEM micrograph of insulation aged at 10MRad.....163
Figure 7.28: SEM micrograph of sheath aged at 10MRad 163
Figure 7.29: SEM micrograph of insulation aged at 25MRad.....163
Figure 7.30: SEM micrograph of sheath aged at 25MRad 163
Figure 7.31: SEM micrograph of insulation aged at 50MRad.....164
Figure 7.32: SEM micrograph of sheath aged at 50MRad 164
Figure 7.33: Relative free volume vs. dose.....165
Figure 7.34: Probability distribution of free volume holes in sheath 166

Figure 7.35: DSC thermogram of insulation aged at 110^0C 168

Figure 7.36: DSC thermogram of insulation aged at 135^0C 168

Figure 7.37: DSC thermogram of sheath aged at 110^0C 169

Figure 7.38: DSC thermogram of sheath aged at 135^0C 169

Figure 7.39: OIT vs. ageing time for insulation 170

Figure 7.40: OIT vs. ageing time for sheath 170

Figure 7.41: Elongation of thermally aged cable insulation at 110^0C 171

Figure 7.42: Elongation of thermally aged cable insulation at 135^0C 171

Figure 7.43: Sample elongation for 36 days of ageing at 110^0C and 135^0C 172

Figure 7.44: Sample elongation for 91 days of ageing at 110^0C and 135^0C 173

Figure 7.45: EAB vs. ageing time for insulation 173

Figure 7.46: Tensile elongation of sheath material at 110^0C 174

Figure 7.47: Tensile elongation of sheath material at 135^0C 174

Figure 7.48: Mean elongation vs. ageing time of sheath material 175

Figure 7.49: Exponential fit of EAB for insulation 176

Figure 7.50: Exponential fit of EAB for sheath 176

Figure 7.51: SEM micrograph of unaged insulation 178

Figure 7.52: SEM micrograph of insulation after 22 days of ageing at 110^0C 178

Figure 7.53: SEM micrograph of insulation after 22 days of ageing at 135^0C 178

Figure 7.54: SEM micrograph of insulation after 36 days of ageing at 110^0C 179

Figure 7.55: SEM micrograph of insulation after 36 days of ageing at 135^0C 179

Figure 7.56: SEM micrograph of insulation after 61 days of ageing at 110^0C 179

Figure 7.57: SEM micrograph of insulation after 61 days of ageing at 135^0C 179

Figure 7.58: SEM micrograph of insulation after 91 days of ageing at 110^0C 180

Figure 7.59: SEM micrograph of insulation after 91 days of ageing at 135^0C 180

Figure 7.60: SEM micrograph of unaged sheath 180

Figure 7.61: SEM micro graph of sheath after 22 days of ageing at 110^0C 181

Figure 7.62: SEM micrograph of sheath after 22 days of ageing at 135^0C 181

Figure 7.63: SEM micrograph of sheath after 36 days of ageing at 110^0C 181

Figure 7.64: SEM micrograph of sheath after 36 days of ageing at 135^0C 181

Figure 7.65: SEM micrograph of sheath after 61 days of ageing at 110^0C 182

Figure 7.66: SEM micrograph of sheath after 61 days of ageing at 135^0C 182

Figure 7.67: SEM micrograph of sheath after 91 days of ageing at 110^0C 182

Figure 7.68: SEM micrograph of sheath after 91 days of ageing at 135^0C 182

Figure 7.69: Image of unaged insulation 183

Figure 7.70: Image of unaged sheath 183

Figure 7.71: Image of insulation aged at 110^0C after 36 days 183

Figure 7.72: Image of sheath aged at 110^0C after 36 days 183

Figure 8.1: Reliability as a function of time in days at 110^0C of ageing 188

Figure 8.2: Probability of failure as a function of time at 110^0C of ageing 188

Figure 8.3: Reliability as a function of time in days at 110^0C of ageing 189

Figure 8.4: Probability of failure as a function of time at 110^0C of ageing 189

Figure 8.5: Reliability vs. time 191

Figure 8.6: Fault tree of SDS-2 without cable failures (Part 1) 193

Figure 8.7: Fault tree of SDS-2 without cable failures (Part 2) 193

Figure 8.8: Fault tree of SDS-2 without cable failures (Part 3) 194

Figure 8.9: Fault tree of SDS-2 with cable failures (Part 1) 195

Figure 8.10: Fault tree of SDS-2 with cable failures (Part 2) 195

Figure 8.11: Fault tree of SDS-2 with cable failures (Part 3) 196

List of Tables

Table 1.1: Main polymer types used in cables in NPPs....4

Table 1.2: Properties of insulating materials....6

Table 2.1: Minimum IR values....21

Table 2.2: Typical PI values....22

Table 2.3: Comparison of the oxidation induction measuring principles....26

Table 4.1: Insulation resistance data on XLPE cable....80

Table 4.2: Insulation resistance values from proposed methodology....81

Table 4.3: Input data for structural reliability problem....83

Table 5.1: Accelerated life testing data on XLPE cable....89

Table 5.2: Training data for first value prediction....90

Table 5.3: Training data for second value prediction....91

Table 5.4: Results of optimization study....94

Table 5.5: Training dataset....97

Table 5.6: Testing dataset....98

Table 5.7: Prediction dataset....98

Table 5.8: Network architectures....99

Table 5.9: Experimental data model....103

Table 5.10: ANN data model....104

Table 5.11: Parameters of the Weibull distribution and use condition TTF....107

Table 5.12: Parameters of the exponential distribution and use condition TTF....110

Table 6.1: Boundary conditions....116

Table 6.2: Material properties....123

Table 6.3: Material properties for FEM analysis....127

Table 7.1: Cable specimens for experimental studies....133

Table 7.2: Mean IR values 135

Table 7.3: IR values corresponding to 1000 feet length cable 135

Table 7.4: PI values 136

Table 7.5: Model parameters 139

Table 7.6: Specifications of cable for radiation ageing 140

Table 7.7: Descriptive statistics for insulation at $669cm^{-1}$ 144

Table 7.8: Anova results for insulation at 669cm-1 144

Table 7.9: Descriptive statistics for sheath at $669cm^{-1}$ 145

Table 7.10: Anova results for sheath at $669cm^{-1}$ 145

Table 7.11: Mean tensile strength and elongation for insulation 147

Table 7.12: Mean tensile strength and elongation for sheath 148

Table 7.13: Model parameters for insulation 150

Table 7.14: Model parameters for sheath 150

Table 7.15: Cable specimen for thermal ageing 167

Table 7.16: Test matrix for thermal ageing 167

Table 7.17: Model parameters for insulation 177

Table 7.18: Model parameters for sheath 177

Table 8.1: Model parameters for insulation aged at 110^0C 186

Table 8.2: Input data for structural reliability problem 187

Table 8.3: Unavailability of SDS-2 196

Chapter 1 Introduction

1.1 Background

Electric cables are one of the most important components in nuclear power plant (NPP) because they provide power to operate safety-related equipment and also to transmit signals to and from various controllers used to perform safety operations. Depending on their location and application, these cables are exposed to a wide range of stressors such as temperature, radiation, humidity etc. If an accident such as a loss of coolant accident (LOCA) occurs, the aged cable must have sufficient properties remaining after normal ageing so that it will remain viable during design basis accident (DBA) conditions [1-2]. Operating experience in the existing nuclear reactors has shown that the number of cable failures increases with plant age resulting in plant transients, shutdowns, and in some cases, the loss of safety functions. As a result, cable condition monitoring (CM) and remaining useful life (RUL) estimation have become increasingly important in recent years [3].

The integrity and function of electrical cables are monitored indirectly through the performance assessment of in-service testing of safety-related systems and equipments. While these tests can demonstrate the function of the cables under test conditions they do not provide assurance that they will continue to perform successfully when they are called upon to operate for extended periods or under design basis conditions. The results of I&C system calibration and functional surveillance tests, equipment performance tests, or other related technical specification surveillance testing and preventive maintenance program testing, can provide useful information and trends regarding the functional performance of a cable. However, specific information on the physical integrity and dielectric strength of the cable insulation and jacket materials is not revealed by this type of testing [1]. There have been

some cases where cables which had initially been qualified for a 40 year design life failed a design basis event test after removal from the NPP after less than 10 years of operation [4].

As electrical cables are one of the long life items that have not been considered for replacement during the design life of NPPs, assessing their degradation state and predicting their remaining lifetime are very critical issues. The prediction of long-term aging performance has been practiced for years by accelerated aging tests; however, the relationship between artificial and natural aging is still under discussion. Researchers have faced the challenge of simulating the environmental and operational conditions of low-voltage cables located inside and outside the containment and predicting the degradation processes caused by these stressors. The challenge is even more difficult considering that each cable manufacturer uses proprietary formulations, including many additives (antioxidants (AX), flame retardants, dyes, fillers, curing agents, plasticizers and other chemicals for thermal and radiation stability) to the base polymer. Additives strongly affect the ageing characteristics of insulation or jacket compounds. Furthermore, geometry and design of the cables, as well as the fabrication procedures, can affect the overall aging characteristics. Lastly, synergistic effects due to combined radiation and thermal ageing have complicated the understanding of this topic even further [5].

1.2 Electrical cables in NPPs

The construction of a typical electrical cable consists of a polymeric insulating material covering a metallic copper or aluminum conductor. The metallic conductor may be a single strand of solid wire or a bundled group of smaller diameter wires. The insulating material of individual cable conductors is often covered by a layer of polymer jacket material known as sheath to protect the integrity of the insulating material from physical and mechanical damage. Multiple conductor cables will typically include an overall polymer jacket to protect

the individual insulated cables that make up a multicore cable. The structure of typical multicore control cable is shown in Figure 1.1 [6-7].

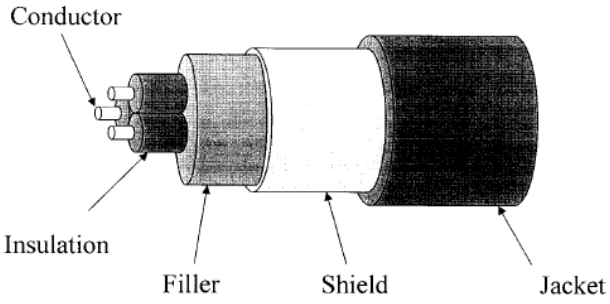

Figure 1.1: Structure of a multicore shielded control cable

The main components of a typical I&C and low voltage power cables are: (i) Conductor(s) (ii) Electrical insulation or dielectric (iii) Shielding and (iv) Outer jacket. In some cable constructions, particularly the control and low voltage power cables, there may be a jacketing layer over the insulation on the individual conductors, providing fire retardant features. This is usually referred to as a conductor jacket or inner jacket. In general, the term jacket would normally refer to the outer layer of the cable construction. Other subcomponents which may be present include: (i) filler or bedding materials, which occupy the gaps between insulated conductors in multi-conductor cables, to improve mechanical stability of the cable structure (ii) tape wraps, which may provide additional electrical, mechanical or fire protection, or identify conductor groupings. Insulation and jacket materials used in electrical cables are based on polymeric materials combined with a number of additives and fillers to provide the required mechanical, electrical and fire retardant properties [8].

The insulation and jacket materials used in I&C cables are of polymer-based and cover a wide range of materials such as polyvinyl chloride (PVC), cross-linked polyethylene (XLPE), ethylene propylene rubber (EPR), etc. These are the base polymers for the cables, but each manufacturer will use their own specific formulation for additives and compounds used in the material. For this reason, there can be significant variations in ageing behaviour between

cables of the same base polymer type from different manufacturers [4]. The main polymer types and their usage in cables in NPPs are shown in Table 1.1.

Table 1.1: Main polymer types used in cables in NPPs

Material	Insulation	Jacket	Extent of use
Cross-lined polyethylene/polyolefin (XLPE/XLPO)	√		Wide
Low and high molecular weight polyethylene (LMWPE, HMWPE)	√		Some
Ethylene propylene based elastomers (EPR, EPDM)	√		Wide
Chlorosulphonated polyethylene (CSPE), also known as Hypalon®		√	Wide
Ethylene vinyl acetate (EVA)	√	√	Some
Polyvinyl chloride (PVC)	√	√	Wide
Silicone rubber (SiR)	√	√	Some
Polyether ether ketone (PEEK)	√		Limited
Ethylene tetrafluro ethylene (ETFE), also known as Tefzel®	√		Limited
Polyphenylene oxide (PPO), also known as Noryl®	√		Limited
Butyl rubber (BR)	√	√	Limited
Polyimide, also known as Kapton®	√	√	Limited
Polychloroprene, also known as Neoprene®		√	Limited
Polyethylene terephthalate (PET), also known as Mylar® (used as a tape wrap)			Limited

Of these materials, the most commonly used insulation materials are PVC, XLPE, EPR, and EPDM. PVC is widely used as insulation, particularly in older plants, but is not generally used in-containment in more modern plants. Most of the other insulation materials are used in relatively small quantities, often in specialist applications, which utilize their specific

properties. For example, PEEK insulation is used in high radiation, high temperature areas. CSPE is primarily used as a jacket material, both as inner and outer jackets. EVA is also mainly used as a jacket material [6-7].

1.3 Properties of polymeric insulation materials

Thermoplastic materials are high molecular weight polymers that are not cross-linked, while the polymer chain of thermoset materials are cross-linked in covalent bonded networks. While thermoplastic materials can be reshaped by heating and cooling within the proper temperature ranges for the materials, thermoset materials cannot be reshaped once they have been cross-linked. Thermoplastic polyethylene was the first material to be used for an extruded type of insulation, followed by high density polyethylene (HDPE), XLPE and finally EPR. XLPE and EPR have higher operating voltages compared to LDPE and HDPE cables. However, EPR is not used for higher voltage cables as it has higher voltage dielectric loss as compared to XLPE cables. Table 1.2 shows the dielectric constant, dissipation factor, thermal resistivity and operating temperature for these insulating materials [9].

Conductor insulating materials are typically polymers, with XLPE and EPR being the most commonly used. For special applications such as very high temperatures or radiation exposure, other materials may be used. Examples are silicon rubber for very high temperature and polyimides for high radiation exposure [10].

Table 1.2: Properties of insulating materials

Insulation type	Dielectric constant	Dissipation factor	Thermal resistivity (K.m/W)	Operating temperature (0C)
PVC	3.6	0.0096	6.5	70
LDPE	2.3	0.01	3.5	70
HDPE	2.3	0.01	3.5	80
XLPE	2.5	0.01	3.5	90
EPR	3.0	0.5	5.0	90

1.4 Cable failure modes and their effects

The basic failure modes of low-voltage and medium-voltage power and I&C cables are the following [1]:

1. Conductor short circuit to ground
2. Conductor-to-conductor short circuit
3. Degraded insulation resistance (excessive leakage current)
4. Open circuit

For low-voltage and medium-voltage AC power cables, the first two failure modes are electrical faults that would normally cause circuit protection devices to trip and result in loss of electric power transmitted through the affected circuit. For low-voltage DC power cables, depending on the operating configuration of the DC system (grounded vs. ungrounded), the electrical fault will result in a trip of the circuit by protective devices or a degraded system alarm. The third failure mode is an incipient failure of low-voltage power cables, except in the presence of a conductive medium (e.g., water, dirt, high humidity, chemical deposits) that could quickly degrade the condition into one of the other two failure modes. In medium-voltage power cables, the third failure mode can lead to partial discharge, or corona,

phenomenon that could cause excessive heating and degradation of the cable insulating materials, and ionization of the air in the vicinity of the current leakage. The fourth power cable failure mode can result from: a physical event breaking the conductor; vaporization of the conductor by an electrical fault (failure modes 1 & 2) that is not cleared by the circuit protective device; extreme corrosion breaking conductor continuity; electromechanical force from a short circuit transient breaking the conductor; vibration fatigue breaking the conductor; or disconnection of the electrical conducting joint at a splice, termination, or other connection accessory.

In the case of I&C cables, the first two failure modes will interrupt transmission of analog or digital control signals over the affected circuit. Similarly, analog or digital instrumentation signals will be interrupted by either of the first two failure modes resulting in loss of signal throughout the affected instrumentation circuit. I&C circuits may experience degraded function or an increased level or rate of error, or may not be affected at all, by the third failure mode, degraded insulation resistance, depending upon the type of signal that is transmitted and the design of the receiving-end circuits and devices [1].

1.5 Ageing and degradation in electrical cables

Ageing is the continuous time-dependent degradation of materials due to service conditions, which include normal operation as well as transient conditions. The polymer materials used for the insulation and jacket materials in electric cables, cable splices, and terminations are susceptible to ageing and degradation mechanisms caused by exposure to many of the stressors encountered in NPP service conditions. The dominant stressors are temperature, radiation dose rate and the presence of oxygen for the majority of reactor systems. It should be emphasized that real service conditions usually involve synergistic effects between two or more of the stressors. In particular, dose rate effects can be a major

factor in the degradation of cables in plants. In many polymers the dose required to reach a specific level of degradation is significantly lower when the dose is applied at low dose rates.

High humidity and the design of cable trunking and conduits will often expose cables to excessive moisture within NPPs. Its presence within the cable insulation can have a significant effect on the electrical properties of the cables, but little is known of its effects on changes in the mechanical properties. For many of the polymers of interest in cables, oxidation is the dominant ageing mechanism and is initiated both thermally and by irradiation [11]. In PVC, the loss of plasticizer from thermal ageing is also an important degradation mechanism. Both of these mechanisms can result in embrittlement of the cable materials, increasing the probability of cracking of the insulation under mechanical stresses. Such stresses can arise in the plant from handling, vibration, thermal cycling or from the way in which the cable is routed. In practice it is this loss of mechanical integrity which is the prime cause of failure of low voltage cable, resulting in the loss of electrical integrity.

Polymer degradation is the result of two main causes. The first is chemical degradation due to changes in the chemical structure of the polymer sample. The second cause of degradation is associated with physical changes in the polymer, e.g. changes in composition due to the diffusion of low-molecular-weight components, such as plasticizer or water, out of the amorphous regions [12-15]. The main chemical aging mechanisms are:

- Scission of macromolecular chains, when two shorter chains are created by the breaking up of one. It is usually a scission of alkoxy or peroxide radicals. The effect is usually a mechanical weakening of the polymer.
- Cross-linking reactions, this corresponds to the formation of a covalent link of two adjacent macromolecules. The increment of crosslink density forms a three

dimensional network. With the increase of the density of those bonds, material stiffness usually increases too. Prolonged cross-linking causes embrittlement.

- Oxidation, which is the main cause of degradation in the ambient atmosphere, and is accelerated by increased temperatures and by ionizing radiation.

Recently, research work on the degradation of cables in NPPs has been reported [16], where several insulation materials, such as polyethylene (PE), ethylene–propylene rubber (EPR), polyvinyl chloride (PVC) and silicone rubber (SiR) were evaluated by thermal and radiation–thermal combined ageing tests for a long period over the temperature range of 80–120^{0}C. The reported activation energy of these polymers was 100–150kJ/mol at degradation temperatures above 120^{0}C. The estimated lifetime at the application temperature is greatly influenced by different values of activation energy, so the determination of activation energy is the key point for the condition assessment of the cable insulation materials. Since the activation energy is dependent on the type of chemical degradation mechanism caused by thermal or radiation ageing, and the correct degradation mechanism plays a significant role in the life extension, it is therefore highly useful to identify the potential ageing mechanism for decision making.

Another important aspect of ageing and degradation is the generation of voids during thermal and radiation ageing. Quantification of voids during manufacturing is not possible in online processing; however sample sets can be tested in specialized laboratories. At the start, the insulation resistance (IR) values and characteristic impedance values are usually met. These micro voids are not a matter of concern and hence often not tested. However, with ageing these micro voids tend to play significant role in the performance of safety function. Since the stability of fluorinated polymers under radiation ageing is expected to be high, the degradation mechanisms related to fluorinated polymers are not a matter of concern.

1.6 Qualification and condition monitoring guidelines

A nuclear power plant may contain more than 50,000 electric cable circuits, of which about 60% are control circuits, 20% are instrumentation, 13% are AC power, 1% are DC power, and the remainder are miscellaneous communications circuits [1]. Most of these electric cable circuits are located in dry, mild operating environments that are well within their qualified operating limits, and therefore perform reliably throughout their qualified service life [1]. Many cable circuits, however, may normally be exposed to one or more of the stressors and must be qualified to operate under more harsh operating environments. Electric equipment important to safety, including electric cables, that are required to continue to successfully perform their safety function in the harsh environment throughout the duration of and following design basis events occurring at the end of their qualified life, must be environmentally qualified in accordance with the requirements of IEEE standards [17-18].

Cables are qualified by their manufacturers to provide a specified service life (typically 40 years for NPPs) for a specified voltage class (based on the qualified dielectric strength of the polymer insulation) operating continuously at or below a specified maximum ambient temperature (e.g. 90^0C). If the insulation and outer jacket material are undamaged, most cables can tolerate occasional wetting, but are not qualified for extended operation in a submerged state. Since the existence of IEEE standards, a better understanding has evolved over the years for studying the degradation behaviour of organic materials. In particular, it is now realized that the high acceleration factors (elevated temperature, high radiation dose rates) typically used in qualification programs may not adequately simulate the degradation seen in-service. An example of this has been seen in some types of ethylene tetrafluro ethylene (ETFE) insulated cables which failed DBE tests after low dose rate exposure to a dose one tenth of that survived in qualification tests [19]. Also, a qualified life of 40 years

based on the qualification procedures in IEEE standards is not now accepted by some countries. A shift towards more on-going tests is occurring, either via formal on-going qualification or by additional testing or condition monitoring [20]. A recent literature review on environmental qualification of electrical cables has highlighted some of the concerns that have not yet been resolved in this area [21].

It should be noted that the failure criteria normally defined in IEEE standards may not be appropriate for DBE tests. Considerably lower values can be accepted for the duration of the test provided that they do not affect the safe operation of the circuit. For example, insulation resistance is normally limited to a minimum value of 1MΩ but during a DBE test, a more appropriate limit could be a maximum leakage current for the whole circuit of 1% of total current, provided that this does not affect the functionality of the circuit. Qualification procedures are aimed primarily at radiation and thermal degradation of cable materials but do not take into account other degradation mechanisms. For example, in one type of Chlorosulphonated polyethylene (CSPE) insulated cable, significant cable failures were observed in the first few years of operation [22], specifically linked to the effects of moisture on this particular type of CSPE cable insulation, which contained MgO. The hygroscopic nature of the MgO made this particular cable type susceptible to the effects of long term exposure to high humidity. Degradation of the cable materials may also cause variation in electrical resistivity arising from plasticizer migration between the shield and insulation in PVC insulated cables [23].

1.7 Motivation

The electrical cables in NPPs are exposed to a variety of environmental and operational stressors. Over time, these stressors and combinations of these stressors can cause ageing and

degradation mechanisms that will result in a gradual degradation of the cable insulation and jacket materials. Much of the degradation due to ageing is controlled through periodic maintenance and/or component replacement. However, I&C cables do not receive periodic maintenance or monitoring once they are installed. Moreover, replacing a cable in an NPP can be a complex and expensive task. Most of the work on degradation of cable insulation and life assessment discusses about the traditional methods of monitoring the cable degradation through parameters such as elongation at break (EAB), insulation resistance (IR), oxidation induction time (OIT), etc. In general, many plants perform IR testing or measure polarization index (PI), and some plants additionally perform time domain reflectometry (TDR), Fourier transform infrared (FTIR) spectroscopy, etc. [24-26]. However, attempts at gleaning any useful information on the remaining life from such measurements also raise few questions. The best conclusion that can be drawn from such testing is the electric insulation is acceptable at present with no guarantee for future continued integrity of operational acceptability [27].

The state-of-the-art for incorporating cable ageing effects into probabilistic safety assessment (PSA) is still evolving and current assumptions that need to be made on the failure rate and common cause effects are based on sparse data. In the assessment of reliability of NPP systems, the ageing effect of electrical cable insulation is not considered and also, there is no standard methodology or framework that exists for incorporating such ageing effects into the system reliability. Therefore, identification and quantification of ageing of electrical cables is very much essential for an accurate prediction of system reliability for PSA applications. The main objective of this thesis work is to develop a methodology to estimate the reliability of I&C cables subjecting to various ageing mechanisms for incorporating the cable ageing into PSA of nuclear power plants.

1.8 Scope

The main focus of this thesis work is on performance assessment of polymeric insulation of I&C cables which are extensively being used in safety-related systems of NPPs. The polymers such as polyvinylchloride (PVC) and cross-linked polyethylene (XLPE) are studied as these materials are widely being used in I&C cables. The main activities involved are identification of failure modes, characterization of the ageing process, development of life models, and estimation of reliability. The model, which will be function of one or more stresses, will eventually describe the state of the insulation with the help of time-dependent degradation of insulating materials. Development of remaining life models for cable insulation consists of looking for adequate relationships between insulation life and the applied stresses from both the life testing data and the physics of failure considering the time dependent degradation. In order to validate the developed life prediction models based on the physical-chemical properties, experimental studies are conducted under accelerated ageing conditions. The experimental data available in the literature is also used (if required) to validate the proposed models.

The polymeric insulation is subjected to accelerated thermal and radiation ageing and the performance properties such as insulation resistance, elongation-at-break, oxidation induction time, etc. are measured to develop the models for reliability prediction. The experimental results obtained from condition monitoring techniques such as insulation resistance measurement, tensile testing, Fourier transform infrared spectroscopy, etc. are used to support the developed methodologies for use in PSA applications. Data analyses are also performed to build the statistical confidence in the experimental results for extrapolation to use condition. Finite element simulation studies are also carried out on typical I&C cable to determine various ageing effects on insulation materials. The results obtained from the

simulation studies are correlated with the experimental findings. From the experimentally determined performance indicators, time dependent reliabilities are predicted from the developed reliability models. The importance of considering the cable failure in PSA of NPP is demonstrated with the reliability analysis of a typical safety system.

1.9 Organization of the thesis

The thesis consists of nine Chapters and two Appendices. Chapter 1 discusses the background on electrical cables used in NPP and their ageing and degradation phenomenon. Chapter 2 deals with the review of state-of-the-art literature on various aspects of cable ageing, degradation mechanisms, life assessment techniques, performance indicators, condition monitoring techniques and their limitations, and accelerated ageing aspects. The important damage mechanisms in polymeric insulation materials due to thermal and radiation ageing have been discussed in Chapter 3. Chapter 4 presents a an approach for reliability prediction of I&C cables based on stress-strength interference theory and Chapter 5 presents another reliability prediction methodology based on artificial neural networks. The finite element analysis simulation studies on electrical cables used in NPP are discussed in Chapter 6. Chapter 7 is devoted to experimental determination of performance indicators for reliability prediction by accelerated radiation and thermal ageing of insulation materials. Chapter 8 deals with the reliability prediction from the performance indicators determined from experimental studies in Chapter 7. The conclusions and future scope of the thesis are presented in Chapter 9. The detailed experimental results of various condition assessment techniques are presented in Appendix A. The results of data analysis for determining the failure distribution of the ageing data has been presented in Appendix B.

1.10 Summary

The general background on various types of I&C cables used in NPPs are discussed in this chapter with respect to insulation type and their properties, cable failure modes, ageing and degradation mechanisms, equipment qualification and condition monitoring guidelines. The main objective of the thesis work and scope of the research area have also been discussed in this chapter. The organization of the thesis is also described in this chapter.

Chapter 2 Literature Review

2.1 Introduction

The integrity and function of power and I&C cables are monitored indirectly through the performance of in-service testing of the safety-related systems and components. Unfortunately, while these tests can demonstrate the function of the cables under test conditions, they do not verify their continued successful performance when they are called upon to operate fully loaded for extended periods as they would under anticipated normal service operating conditions or under design basis conditions. Nor does in-service testing of a cable provide specific information on the status of ageing degradation processes, or the physical integrity and dielectric strength of its insulation and jacket materials [28]. Consequently, a cable circuit with undetected damaged or degraded insulation could pass an in-service functional test, but still fail unexpectedly when called upon to operate under anticipated environmental conditions, or the more severe stresses encountered in emergency operation during a design basis event.

In view of this, an extensive literature survey has been carried out to study and identify the state-of-the-art research work carried on various insulation life prediction methodologies, tools and techniques for insulation condition assessment, equipment qualification guidelines, and ageing management programs relating to instrumentation and control cables in nuclear power plants. A few widely used condition assessment techniques, accelerated ageing methods and life estimation approaches for I&C cables have been discussed in this chapter.

2.2 Performance indicators and acceptance criteria for electrical cables

The acceptance criteria are usually the limiting values of properties beyond which the degree of deterioration is considered to reduce the ability of the cable to withstand stresses encountered in normal service, and during and following accidents [29]. During qualification, a number of functional properties are tested. The extent of the measured properties and their acceptance criteria may vary and are generally based on the specific cable application. The most frequently tested parameters are insulation resistance, voltage withstand tests and mechanical properties. Mechanical properties have no direct influence on the functionality of the cable but demonstrate the retention of a degree of flexibility and ability to withstand mechanical stress and vibration during normal operation as well as during postulated accidents. Since embrittlement is a major result of ageing degradation, the elongation at break (EAB) of a cable insulation material is an indicator of the state of degradation.

Conventionally, the reduction in elongation to 50% absolute is taken as the failure criterion for a cable insulation material. It is generally accepted that 50% EAB after a DBE test represents a material that is still in a functional state electrically with a satisfactory degree of margin before failure. In many of the polymers used in cables, there is little change in elongation values in the early stages of ageing degradation. In some cable materials, significant reductions in elongation are only seen in the last quarter of total service life. For this reason, although elongation is used as the prime indicator of degradation, other parameters which show changes in the earlier stages of degradation are particularly useful in assessing the state of cables. Examples of these types of degradation parameter are oxidation induction time or temperature, dielectric loss, indenter value [30]. The service limits of the various polymer materials are stipulated in the standard IEC-544-2 [31].

For a cable in an oxygen-containing environment, the surface of the insulation will first react with the oxygen. If the radiation dose rate is sufficiently high, the reaction rate in the interior of the cable insulation will be limited by the rate of oxygen diffusion. Thus a greater time, and therefore a greater dose, will be required to reach a given level of degradation in the interior of the cable than on the surface. This phenomenon is known as diffusion-limited oxidation (DLO). Since EAB depends on the level of degradation throughout the entire cross-section of the cable insulation, the EAB for a given dose rate and total dose will be higher if DLO is present than it would be otherwise.

During service conditions the dose rates are lower, and one does not expect DLO phenomenon. The main goal is to determine the probability that a cable inside the NPP containment will reach a critical level of embrittlement. This probability will depend primarily on the temperature and dose rate that the cable is exposed to during normal plant operation, and the time of exposure to these conditions [32]. If a LOCA occurs after the cable insulation reaches a critical level of embrittlement, as measured by the EAB of the cable, the cable may fail to perform its function, although cables with severely embrittled insulation have performed successfully in environmental qualification tests.

2.3 State-of-the-art condition monitoring techniques for performance assessment of electrical cables

Currently many promising condition monitoring (CM) techniques [33-34] including indenter modulus, oxidation induction time (OIT), and density measurements, have been recognized to be very useful for monitoring insulation degradation. Unfortunately, one major limitation of these CM methods is that they are only suitable for monitoring termination or accessible portion. For inaccessible locations such as conduits, and cable trenches, these CM

methods cannot be used when inaccessible cable is exposed to localized adverse environment caused by moisture/water submergence, high temperature, or radiation. Therefore, it is important to understand the ageing effects of cable caused by moisture, high temperature, radiation, and their combinations, and to further develop effective CM methods for cable ageing management program and license renewal in nuclear power plant [35]. Electrical condition monitoring techniques have great advantage in evaluating the insulation system performance and ageing condition for inaccessible cable. Insulation resistance measurement is most commonly used for checking the insulation performance of electrical equipment.

There is a general consensus that there are yet no definitive CM techniques available that can assess insulation degradation or predict remaining life, but there are a number of potentially useful CM methods. No one technique can measure the degradation. A combination of tests would be required to provide an indication of degradation. The information obtained from condition monitoring techniques is used to determine the ability of a cable, in its current condition, to perform its intended function within certain acceptance criteria. To obtain useful information, it is important that an appropriate technique be selected for the cable being monitored. A brief overview of the commonly used condition monitoring techniques is presented in subsequent sections.

2.3.1 Measurement of insulation resistance and polarization index

Insulation resistance measurement is a standard industry technique that is commonly performed to determine the current condition of cable insulation. It involves the application of a voltage between the cable conductor and a ground to determine the resistance of the insulation separating them [36-37]. Typical IR testing of an electrical cable is shown in Figure 2.1. It is based on the principle that when a DC voltage is applied to an insulated conductor, a small but measurable current will flow through the insulation to ground. The

total current flowing in the insulation from the conductor to ground is equal to the sum of the capacitive charging current, the leakage current and the dielectric absorption current.

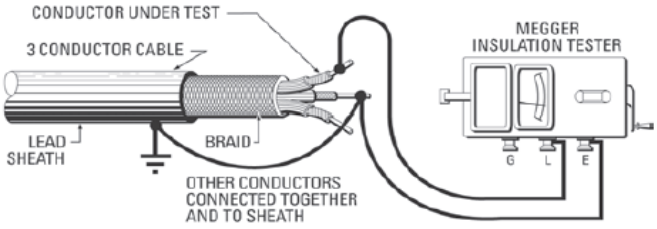

Figure 2.1: IR testing of cable

These three component currents change with time. Various currents in cable insulation system are shown in Figure 2.2. The capacitive charging current and the dielectric absorption current will initially be relatively high when the test voltage is first applied to the test specimen. Since the insulation behaves like a capacitor, after it is energized and charges have aligned across the insulation these currents will taper off and eventually approach zero. However, leakage current will typically start at zero and then gradually increase.

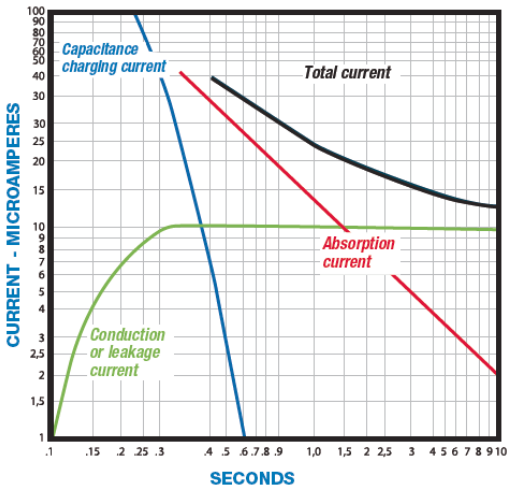

Figure 2.2: Currents in cable insulation

In high integrity insulation, leakage current will reach and maintain a steady value after a certain amount of time. If the insulation is badly deteriorated, wet, or contaminated, the leakage current will be greater than that found in good insulation and it could continue to increase over time. As a result, the total current flowing in a test specimen will start out high

when a test voltage is first applied, and vary in different ways over the next several minutes depending on the condition of the insulation. To account for this behavior, insulation resistance is normally measured at one minute and again at ten minutes; then the ratio of the two measurements is calculated. This ratio is known as the polarization index (PI). IEEE Standard 400 [38-39], IEEE Standard 141 [40], and ASTM Standard D257 [41] provide guidance on performing insulation resistance testing. IEEE Std. 400 mentions that the international cable engineers association (ICEA) recommends a minimum insulation resistance of R megohms for 1000 ft. (305 m) as per the following equation:

$$IR = Klog_{10}(\frac{D}{d}) \tag{2.1}$$

where, IR is insulation resistance in megohms for 1000 ft. of cable, K is a constant for the specific type of cable insulation, D is the outside diameter of the insulation and d is the diameter over the conductor shield. The minimum values for IR tests vary depending on the type of equipment and the nominal voltage. They also vary according to international standards. The minimum recommended IR values as per IEC 60364-6 [42] are shown in Table 2.1.

Table 2.1: Minimum IR values

Nominal circuit voltage (Vac)	Test voltage (Vdc)	Insulation resistance (MΩ)
Extra low voltage	250	≥0.5
Upto 500V	500	≥1.0
Above 500V	1000	≥1.0

Polarization index, the ratio of the IR at 10 minutes to the IR at one minute, can be a more consistent and repeatable indicator of cable insulation integrity since it accounts for the time-dependent behavior of capacitive charging current, leakage current and dielectric absorption current. Another advantage of PI is that the temperature correction factor required for

normalizing the IR readings drops out of the calculation. The recommended values of PI as per IEEE 43-2000 [43] are shown in Table 2.2.

Table 2.2: Typical PI values

PI	Insulation condition
<2	Problematic
2 to 4	Good
>4	Excellent

It is recommended that insulation resistance/polarization measurements and data trending be considered along with the results from one or more other cable condition monitoring techniques to assess the condition and rate of degradation for cable insulation.

Advantages of this test are that it is relatively easy to perform and requires inexpensive equipment. IR is often regarded as a simple pass/fail test for the dielectric integrity of electrical equipment and cables since the results are very sensitive to environmental conditions, making them too irregular for trending purposes. The results can be corrected for environmental effects, such as temperature. Measurements are normally corrected to a single temperature, such as 15.6ºC for electric cables. This allows the comparison of measurements taken at different times when the cable might be at different temperatures.

A disadvantage of the IR and PI techniques is that the cable under test must be disconnected in order to attach the test instrument. This is undesirable since it requires handling of the cable, which could result in unintentional damage, particularly for aged cables that may be embrittled. Another disadvantage is that this test is not as sensitive to insulation degradation as other techniques. In some cases, such as in dry air, severe damage to the insulation may result in little change in insulation resistance.

2.3.2 Measurement of elongation-at-break

Elongation-at-break is a measure of a material's resistance to fracture under an applied tensile stress and is often termed the "ductility" of a material. When exposed to stressors such as elevated temperature and radiation levels, polymers tend to lose their ductility. The rate of ductility loss is determined by the material composition, as well as the severity of the stressors; however, in general, ductility will decrease with age. Since many cable insulation and jacket materials are polymers, EAB has proven to be an excellent condition monitoring technique for electric cables [44-45]. EAB tests are typically performed using a calibrated tensile tester in accordance with ASTM Standard D638 [46] and D412 [47]. Typical universal tensile testing machine is shown in Figure 2.3.

Figure 2.3: Universal tensile testing machine

EAB measurements provide a useful quantitative assessment of the condition of cable insulation materials and are widely used as a benchmark for characterizing such materials. It is a reliable technique for determining the condition of polymers and provides trendable data that can be directly correlated with material condition [48]. Currently, there is no standardized acceptance criterion for the minimum EAB for a cable material that will define

the end of its useful service life for normal, mild or harsh environments. However, a conservative value of at least 50% absolute elongation has been used as an acceptance criterion; however, research testing has shown that there is usually some useful service life remaining at levels well below this.

ASTM D638 recommends testing at least five specimens in the case of isotropic materials and at least ten specimens, five normal to, and five parallel with, the principal axis of anisotropy, for each sample point in the case of anisotropic materials. It is also recommended that specimens that break as a result of a fortuitous flaw, improperly prepared test specimen or at a location outside of the predetermined gage marks be discarded and retested with another specimen. The primary disadvantage of the EAB test is that it is a destructive test, and relatively large amounts of cable are required. The necessary samples can only be obtained if a cable is removed from service, or if surveillance-type cables are installed specifically for periodic EAB testing.

2.3.3 Determination of oxidation induction time and temperature

Oxidation induction time is a measure of the time at which oxidation of a test material occurs when exposed to a predetermined constant test temperature in a flowing oxygen environment. It is measured with a differential scanning calorimeter (DSC), which is essentially an oven with the capabilities for very precise control and measurement of the heat energy supplied to a test sample. The sequence of a standardized OIT measurement using the DSC method according to ISO 11357-6 [49] is shown in Figure 2.4.

After positioning an uncovered sample pan in calibrated DSC oven nitrogen is subjected to the measuring cell. The DSC cell is heated rapidly to the temperature at which the OIT value should be determined. After reaching the required temperature for the first time, an

isothermal step of 3 minutes follows. The end of this phase is indicated as t_1 in Figure 2.4. At t_1 the atmosphere is switched to oxygen and the DSC oven is held at the same temperature until an exothermal signal (oxidation) can be recognized. The onset of this oxidation signal corresponds to a time t_2.

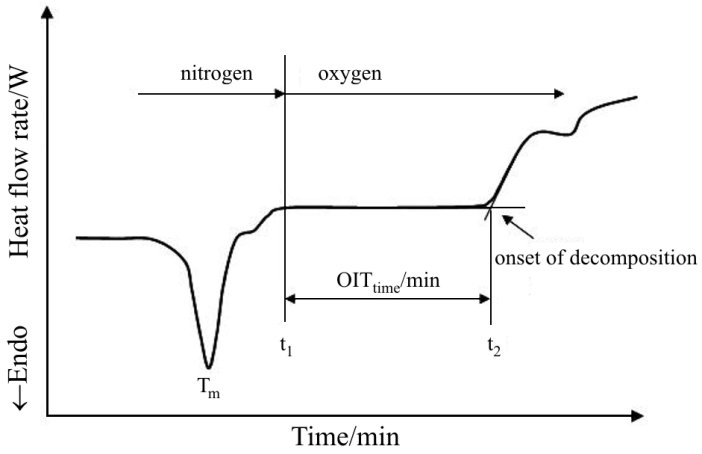

Figure 2.4: Principle sequence of OIT measurements

The OIT value can now be determined as the time between t_1 and t_2, as described in Figure 2.4. Frequently however, the oxidation signal is less pronounced than indicated in Figure 2.4, making the determination of a clearly defined onset temperature difficult. Finding a suitable measuring temperature for the isothermal phase often causes further difficulties with OIT measurements. If the temperature is too low there is a substantial increase of the duration of the measurement. And if the temperatures are too high, oxidation takes place immediately after the introduction of oxygen. The onset temperature of the decomposition signal (t_2) can no longer be determined [50].

The oxidation induction temperature (OITp) is evaluated in accordance with Figure 2.5. The sample is heated up continuously under a pure oxygen gas flow. A change of gases at a defined time, as stated under OIT measurement, is not necessary. OITp is determined as the onset of the decomposition signal results. OITp is usually more clearly pronounced as the onset time t_2 in OIT measurements (t_2 is necessary for the determination of the OIT values).

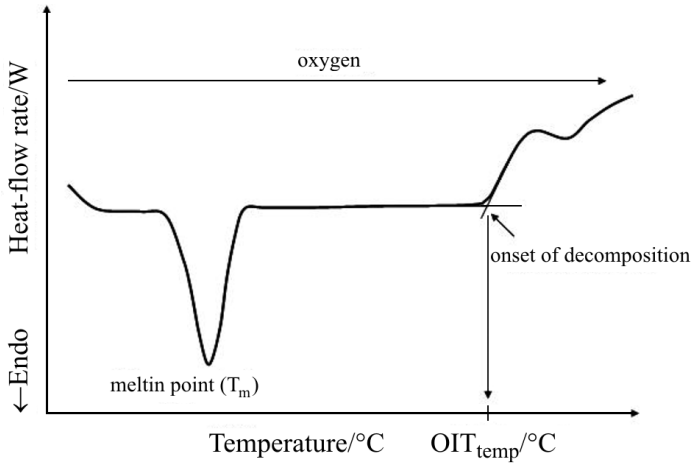

Figure 2.5: Principle sequence of OITp measurements

To give an overview, the essential characteristics of both methods (determination of OIT vs. OITp) are summarized in Table 2.3 [50]. By comparing the statements in Table 2.3 it is obvious, that OITp needs less effort in setting up the measurements and in the majority of cases it delivers clear defined onset points.

Table 2.3: Comparison of the oxidation induction measuring principles

Features	OIT	OITp
Standardized	Yes	No
Measuring principles	Static	Dynamic
Preliminary tests	Yes	No
Gas change	Yes	No
Onset of oxidation signal	Partially difficult to recognize and to analyze	Mostly expresses very well and clear analyzable

OIT/OITp is a destructive test from the standpoint of the test sample used; however, many consider this test to be non-destructive from the standpoint of the cable being tested since only a very small sample is required (i.e., 10 mg). It is possible that a sample of this small can be obtained without damaging the cable, although the cable would have to be handled at some level. For inaccessible cables, the sample would have to be obtained from a remote location, which may not be representative of the location of interest.

2.3.4 Density measurement

If a polymer is aged in air, oxidation normally is the dominating cause of degradation, leading to both cross-linking and chain scission, and also resulting in the formation of oxidation products together with the release of gases. The density of the polymer is increased by most of these processes. The oxidation products increase the density through the substitution of hydrogen atoms with oxygen atoms, which are significantly heavier. As many polymers have fillers of high densities, the release of degradation products from the comparatively low-density polymer chain leads to a higher density through a decrease in the polymer to filler ratio. Shrinkage from a tightening of the polymer chain is often a result from cross-linking, and this is also a cause of an increase in density [51].

This method is considered essentially non-destructive because of the small size of the samples required (< 1 mg). The density can be measured in a couple of ways. The older way consists of placing the sample in a column with a density gradient. The sample then falls to a position where the density of the sample corresponds to the density of the surrounding liquid. This method is time consuming, as the time required to reach density equilibrium is comprised between a few minutes for large samples to hours for small ones [52].

A more recent way for measuring the density is using the Archimedes' principle, and weighing the samples, both in air and in a liquid with a density lower than that of the polymer, on a precision balance. The density of the polymer is then determined as:

$$\rho_{polymer} = \left[\frac{w_{air}}{w_{air} - w_{liquid}}\right] \rho_{liquid} \tag{2.2}$$

where w_{air} and w_{liquid} are the measured weights in air and liquid respectively, and ρ_{liquid} is the density of the liquid. This method is fast and produces results of good accuracy [51, 53]. This method can give satisfactory information about the ageing for a number of

different materials. However, in many cases, the density increase is slow at the beginning of the ageing, with an increase at later stages, showing the so-called induction time-effect. Materials that have a near-linear increase in density with ageing, and show no such induction time include PVC and LDPE [51]. As for OIT, the results from this kind of measurements need to be correlated to a property such as elongation at break.

2.3.5 Fourier transform infrared spectroscopy

Fourier transform infrared spectroscopy is a well-known laboratory technique for studying the molecular structure of materials. It is performed using a spectroscope, in which a small material sample is exposed to infrared radiation. The absorbance or transmittance of this radiation by the material at various wavelengths is then measured [54]. In studying the oxidation of cable materials an important wavenumber in the FTIR spectrum occurs at 1730 cm^{-1}, which indicates the presence of the carbonyl (C=O) peak. This peak is a direct indication that the polymer is undergoing oxidation and carbonyl bonds are being generated. A second important wavenumber occurs at 2915 cm^{-1} representing the $–CH_2$ bond that is part of the polymer's backbone structure. These bonds may also be present in the other constituents that are additives in the polymer material formulation [54].

The magnitudes of the peaks in the spectra reflect the changes in the polymer molecular structure as it oxidized over time increasing the presence of carbonyl bonds and decreasing the number of $–CH_2$ bonds. The transmittance percent at the selected wavenumber peaks also changes as the polymer materials aged due to thermal and radiation. Because of the variations in the polymer formulations for each manufacturer, the effects of additives and colorizers, and the distribution of antioxidants throughout the material, an absolute acceptance criterion is not practical. The best approach is to establish baseline transmittance spectra and transmittance percent values at the selected significant peak wavenumbers for each material.

As the materials ages, subsequent periodic measurements can then be compared to those baseline spectra and transmittance percent values for the selected peak wavenumbers to assess the progress and rate of ageing degradation in the insulating material for the cables being monitored. The chemical bonds and their typical absorption regions of polymers are shown in Figure 2.6.

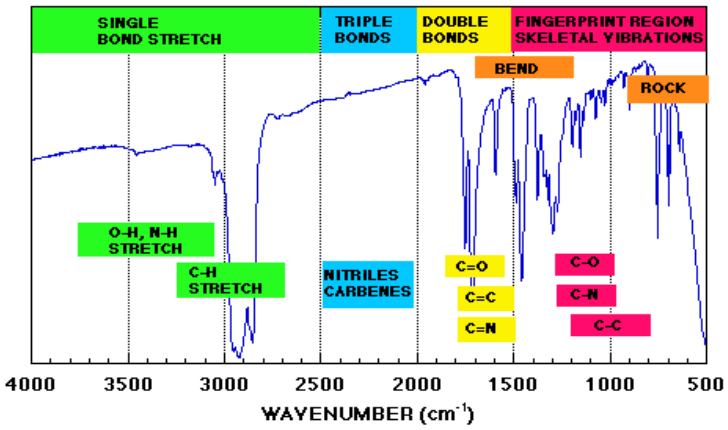

Figure 2.6: Typical absorption regions in polymers

An advantage of this technique is that samples can be obtained from very small areas of cable; therefore, it can be considered a non-destructive technique. In addition, quantitative results are provided that can be trended over time for use in tracking the condition of the cable. A disadvantage of the FTIR spectroscopy technique is that it is a surface examination procedure in which the infrared radiation passes into the surface of the specimen and is refracted back into the spectroscope crystal. The material's transmittance is determined through analysis of the intensity of the incident and reflected rays. Under harsh environment condition (i.e., elevated temperatures and high radiation) an oxidation gradient could develop at the specimen surface, resulting in the spectroscope detecting a higher amount of oxidation than the average bulk value. Correlation of FTIR results for such cables with results from other techniques that accurately reflect average bulk properties, such as EAB, could be problematic.

2.3.6 Positron annihilation lifetime spectroscopy

Positron is an antiparticle of electron. When energetic positrons are implanted in matter, they thermalize and annihilate with the electrons of the matter giving annihilation gamma-rays. In condensed matter, besides direct annihilation, positrons form positronium, a bound state of positron and electron. The positronium is analogous to hydrogen atom, with positive nucleus replaced by positron [55]. Like hydrogen atom, the positronium can also be ortho-positronium (denoted as o-Ps; triplet spin state of electron and positron) or para-positronium (p-Ps; singlet spin). The free positron and positronium has propensity to get trapped or localized in the defects (in metals, semiconductors) and free volumes (in polymers) due to the repulsion with nuclear cores. That is they are trapped in the low electron density areas of the material.

The intrinsic lifetimes (if in perfect vacuum) of ortho and para-positronium are 142 ns and 125 ns respectively. The p-Ps lifetime is too short to be effect much by the condensed matter. However, the o-Ps lifetime is shortened to few nanoseconds in polymer by the process called pick-off annihilation. That is positron from o-Ps can pick up an electron of opposite spin from the surrounding medium and annihilate (by conservation laws, the annihilation with electron of opposite spin giving two gamma-rays of 511 keV is more probably). Since the positronium is trapped in the free volume holes in the polymer, the pick-off annihilation rate (and hence the positronium lifetime) depends on the size of the free volume hole. Larger the size of the free volume hole less is the overlap of the positronium wave function with electrons of the medium and hence positronium can survive longer. The semi-empirical relation between the radius of the free volume hole (R) from which the o-Ps is annihilating and positronium lifetime (τ_3) is given as:

$$\frac{1}{\tau_3} = \lambda_3(ns^{-1}) = 2 \times \left(1 - \frac{R}{R+\Delta R} + \frac{1}{2\pi} sin\left(\frac{2\pi R}{R+\Delta R}\right)\right) \quad (2.3)$$

where ΔR is the fitted empirical electron layer having thickness of 0.166nm. The fraction of positrons forming o-Positronium (I_3- o-Ps intensity) is directly related to the number of free volume holes. The fractional free volume is calculated using the following relation:

$$f_V = C.V_f.I_3 \quad (2.4)$$

where V_f is the volume of the holes calculated using radius R (spherical hole) obtained from Eq. (2.3), I_3 is the intensity (%) of the o-Ps pick-off lifetime component in the spectra and C is an empirical constant (0.018 nm^{-3}).

Though it is common practice to assume all the free volume holes are uniform and spherical in size, it is definitely an approximation. In many instances, the free volume size distribution becomes much more important than the average size. There is no denying that the positronium trapped in free volume holes of different sizes should have different lifetime. But unless the sizes are very different, extraction of indefinite number of positron lifetimes from positron lifetime spectra is mathematically not possible. To overcome this difficulty, assuming that the positron lifetimes follow a distribution in τ, the lifetime spectrum may be described by a continuous form as given as:

$$F(t) = \int_0^\infty \frac{I(\tau)}{\tau} e^{-\left(\frac{t}{\tau}\right)} dt \quad (2.5)$$

where $\int I(\tau)dt = 1$. The CONTIN-PALS computer program calculates the annihilation rate distribution function, λα(λ), via Laplace inversion technique where λ=1/τ. The intensities are related to the annihilation rate distribution function as:

$$I(\tau) = \lambda^2 \alpha(\lambda) \quad (2.6)$$

Using the relation between the o-Ps annihilation rate and the free volume hole radius (Eq. (2.3)) and considering the difference in the o-Ps capture probability in different hole sizes the free volume hole radius probability density f(R) is calculated as:

$$f(R) = -2\Delta R\left[cos\left(\frac{2\pi R}{R+\Delta R}\right) - 1\right].\frac{\alpha(\lambda)}{(R+\Delta R)^2(1+8R)} \quad (2.7)$$

The positron annihilation lifetime spectrum of silicon single crystal is used as reference in analyzing the lifetime spectra.

2.3.7 Time domain reflectometry

Time domain reflectometry (TDR) is a commonly used technique for assessing the condition of instrumentation, control, and power cables in inaccessible locations. The working principle of TDR is shown in Figure 2.7. The TDR works on the same principle as radar. A non-destructive pulse of energy is transmitted down a cable from one end, and is reflected back when it encounters (i) the far end of the cable, (ii) a fault along the cable, or (iii) some other problem that causes a change in the electrical impedance of the cable. The time for the signal to travel to where the impedance change is located and return back is measured by the TDR and converted into a distance. This distance is used to locate the impedance change [56].

The simplest form of TDR will display the distance to an impedance change, which could be a fault. Impedance variations can be caused by degradation due to ageing. TDR testing can be used to monitor cable condition by first obtaining an initial in situ baseline cable signature for a specific cable, and then comparing future TDR signatures to the baseline to identify and trend in-service degradation over time. Once the characteristic velocity of propagation for specific insulating materials and cable configurations has been determined, an experienced

operator can use the TDR to detect and physically locate any cable damage that may have occurred since the last cable inspection.

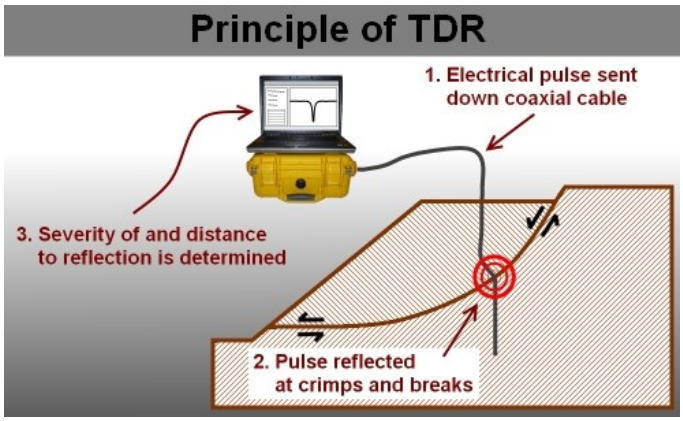

Figure 2.7: Working principle of TDR

An advantage of TDR testing is that it is a non-destructive test that can be performed in situ to monitor the condition of low-voltage or medium-voltage cables. It provides information that can be used to determine the severity and location of a discontinuity, which could represent a fault. In addition, the test equipment needed is only moderately expensive, and the data can be trended against historic baseline reflectograms. Disadvantages of the TDR are that the cable under test must be disconnected in order to perform the test. Also, training and experience are required of the testing personnel in order to obtain useful results, and transient conditions, such as immersion, are only detected if they are present during the TDR test.

2.3.8 Tan delta measurement

The tan delta technique or Tan δ can be derived from one of Maxwell's four equations, which relates the magnetic field intensity to the electric field intensity. Expressed in phasor form, the equation contains the relationship between the conduction current density (σE) and the displacement current density ($j\omega\varepsilon'$) for dielectric materials [57].

$$\nabla \times H = \sigma E + j\omega\epsilon' E \ (Am^{-2}) \tag{2.8}$$

where, H = magnetic field intensity (A/m)

E = electric field intensity (V/m)

σ = conductivity (℧/m)

ω = angular frequency (rad/sec)

ε" = real portion of the complex permittivity where ε=ε'-jε" (F/m)

The relative permittivity ε_r describes how a specific material will interact with an applied electric field known as the dielectric constant of the material. It is derived from the permittivity of free space as:

$$\varepsilon = \varepsilon_r \varepsilon_0 \tag{2.9}$$

where, $\varepsilon_0 = 8.854^{-12}$ F/m,

This complex permittivity can therefore be written as $\varepsilon_r = \varepsilon_r' - j\varepsilon_r''$ and shown on a simple vector diagram (Figure 2.8).

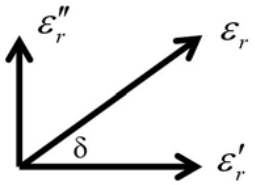

Figure 2.8: Tan delta measurement

The tangent of the angle δ between them is the ratio of these two vector quantities and is a measure of the ratio of energy from the applied electric field that is stored in a specific material to the amount dissipated or lost. This quantity is known as the loss tangent and defined as:

$$\text{Tan}\delta = \frac{\varepsilon_r''}{\varepsilon_r'} \tag{2.10}$$

2.3.9 Measurement of characteristic impedance of a cable

Any type of coaxial cable as shown in Figure 2.9 is typically chosen based on the characteristic impedance. The main consideration is that impedance levels should match both at the transmitting and receiving end. Although there are many standard impedances levels, the most common ones by far are the 50Ω and 75Ω impedances [58]. These two standards are used for most coaxial cable applications, but other standards are also available in lesser quantities.

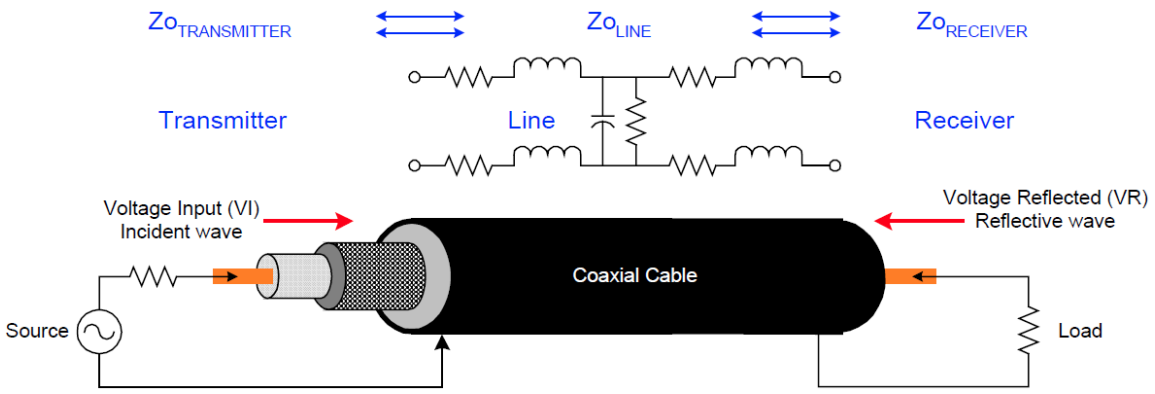

Figure 2.9: Typical coaxial cable

For ordinary signal and data transmission applications, the cable that almost always chosen is the 50Ω type, while the 75Ω type is almost exclusively used for video signal and high-frequency RF applications, such as very high frequency (VHF) and ultra high frequency (UHF) [59]. The characteristic impedance corresponds to the input impedance of a uniform transmission line of infinite length, i.e.,

$$Z_{in} = \frac{V_i}{I_i} \tag{2.11}$$

It also corresponds to the input impedance of a transmission line of finite length that is terminated in its own characteristic impedance. In general, the characteristic impedance is a complex number with a resistive and reactive component. Characteristic impedance is of

prime importance for good transmission. Maximum power transfer occurs when the source has the same impedance as the load. Thus for sending signals over a line, the transmitting equipment must have the same characteristic impedance as the line to get the maximum signal into the line. At the other end of the line, the receiving equipment must also have the same impedance as the line to be able to get the maximum signal out of the line. Where impedances do not match, some of the signal is reflected back towards the source. In many cases this reflected signal causes problems and is therefore undesirable.

As the length of cable increases, it becomes more like a transmission line, and it becomes more important to make sure the impedance of cable is matched with the receiving end termination impedance. For shorter cables that have lengths that are less than about $1/10^{th}$ of the wavelength of the carried signal, the transmission line characteristics do not apply. In these cases, there is usually no need to match impedance levels, and the basic principles of circuit analysis can be employed instead. When using the transmission line concept, a coaxial cable can be represented as a series of capacitances and inductances as shown in Figure 2.9. In this way, it behaves somewhat like a low-pass filter, where the cable passes most of the signal at lower frequencies and attenuates the signal at higher frequencies.

For frequencies above about 1MHz, the characteristic impedance of a coaxial cable line depends only on the dielectric constant of the inner insulator and the ratio of the diameter of the inner conductor to the inner diameter of the outer conductor (shield). Unlike the impedances for individual capacitors and inductors, the coaxial cable impedance is independent of cable length and frequency for frequencies above 1MHz. The impedance is about the same both for short and long cables, and for 2MHz and 20MHz signals as expressed by:

$$Z_0 = \sqrt{\frac{R+j\omega L}{G+j\omega C}} \tag{2.12}$$

where Z_o is the characteristic impedance. Characteristic impedance changes considerably with frequency, particularly from DC to about 100 kHz. Simplified formula may be derived from the above equation. At high frequencies (>100 kHz), the characteristic impedance reduces to Eq. (2.13).

$$Z_0 = \sqrt{\frac{L}{C}} \tag{2.13}$$

There are a few reasons why 50Ω and 75Ω were chosen as the standard characteristic impedances. For a coaxial cable with air as the dielectric, the minimum attenuation occurs at around 75-77Ω. As other dielectric materials are used, the lowest attenuation drops to a value between 52–64Ω. The second consideration is power-handling capability, which is maximized at about 30Ω regardless of the dielectric used [59].

The characteristic impedance of coaxial cable can be determined from the measured open circuit impedance and short circuit impedance from the formula [60]:

$$Z_0 = \sqrt{Z_{oc} Z_{sc}} \tag{2.14}$$

where, $Z_{oc}$is the open circuit impedance and Z_{sc} is the short circuit impedance.

2.3.10 Scanning electron microscopy

Scanning electron microscopy (SEM) can image and analyze bulk specimens. In general, SEM is a vacuum system containing the electron source, focus optics and a detector. Electrons from a thermionic (Schottky) or field-emission cathode are accelerated by a voltage difference between cathode and anode that may be within the range 0.1 – 50 keV. The electron probe of diameter 100 nm – 1 nm, carrying the electron-probe current of 10 nA – 1 pA, is formed at the specimen surface [61]. The deflection coil system scans the electron probe in a raster across the specimen synchronously with the observation screen, where its

intensity is modulated by detected signal from the specimen. The diameter of the electron probe determines the geometrical resolution of SEM. The block diagram of SEM is shown in Figure 2.10.

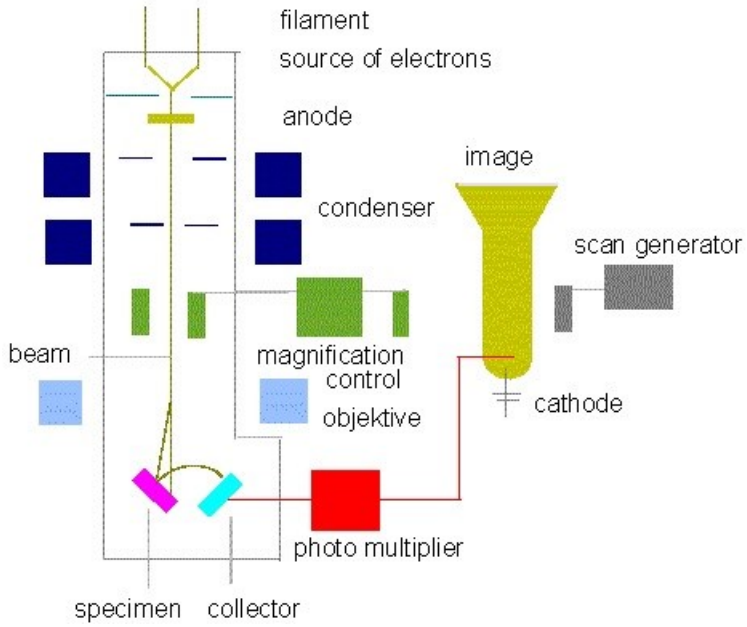

Figure 2.10: The block diagram of SEM

The focused electron beam impacts the specimen and interacts with its atoms. Elastic and inelastic scattering are the elementary atomic interaction processes, but the final signal is not the result of the single scattering process but of complete electron diffusion connected with gradual loss of the electron energy and lateral spreading caused by multiple elastic large-angle scattering. The electrons have a finite range R of the order of 10 nm – 10 μm, in dependence on electron energy and target density. The information and interaction volumes are not strictly limited and in most cases contribution to the signal decreases exponentially with increasing depth. The electrons that escape from the sample are called signal electrons and we can divide them into three basic parts: secondary electrons (SE), backscattered electrons (BSE) and Auger electrons (AE). The energy spectrum of the signal electrons is

within the range from zero up to the primary beam energy. Furthermore, X-ray emission and cathodoluminescence can also be excited from the specimen [62].

Final image contrast depends not only on electron interaction with the specimen, but also on the part of the emitted electrons detected. The knowledge of the angular and energy sensitivity of the detector allows for a better interpretation of the final image contrast. Detected signals in the SEM are mostly weak; therefore it is necessary to obtain the most effective conversion of electrons to the electrical signal that modulates brightness to achieve the highest possible signal to noise ratio.

2.4 Important aspects of accelerated ageing and life estimation of electrical cables

Accelerated life tests are becoming increasingly popular in today's industry due to the need for obtaining life data quickly and reliably. Life testing of products under higher stress levels without introducing additional failure modes can provide significant savings of both time and money. Correct analysis of data gathered via such accelerated life testing will yield parameters and other information for the product's life under use stress conditions. To be of practical use in assessing the operational behaviour of cables in NPPs, laboratory ageing aims to mimic the type of degradation observed under operational conditions. Conditions of testing therefore need to be carefully chosen to ensure that the degradation mechanisms occurring in the accelerated tests are similar to those which occur in service. Accelerated life testing involves acceleration of failures with the single purpose of the quantification of the life characteristics of the product at normal use conditions [63].

Lifetime (or service life, or long term performance) of a polymer material at ambient temperature or at elevated temperature is a crucial property, which determines the scope of

application of polymer materials. Reasonable lifetime predictions can be obtained from accelerated ageing tests when results of such tests are extrapolated to service conditions, using an appropriate time-temperature model. Various degradation tests, usually based on determination of time-dependent mechanical properties, e.g. tensile strength or ultimate elongation, as well as based on weight loss can be applied.

2.4.1 Thermal ageing

Polymeric cable materials used in NPP have a finite life in an environment featuring elevated temperatures and radiation. Recognizing this fact, industry standards and the Nuclear Regulatory Commission (NRC) have obligated nuclear utilities to provide evidence showing that degradation caused by ageing will not critically affect the performance of these materials and will not pose any safety hazards during their qualified service life of 40 years [64]. Because it is impractical to test these materials under normal plant conditions (natural aging), accelerated aging is usually employed for qualification. To allow for uncertainties, conditions for accelerated aging tests are often made purposefully conservative [65]. Experience has suggested that they may be unrealistically conservative, leading to frequent and expensive replacements, and the use of materials which may not be otherwise optimal.

According to standards, the simulation of long-term service thermal ageing is performed isothermally at elevated temperature using Arrhenius methodology [66-67]. For reliable simulation of long-term thermal ageing, the temperature of accelerated ageing should not be too far from the service temperature. The standards [68-69] recommend using not more the 25^0C difference. But to simulate 40 years of service ageing, such a small difference would lead to very long testing time. Hence, the test temperature is usually higher. The maximum allowed ageing temperature is limited by the range of chemical stability (the temperature range in which for specific time no chemical changes are detected) or by any thermo-

dynamical transition in the material, like glass transition (Tg), softening or melting point [70]. Eyring relationship is also commonly used for analyzing data for which temperature is the accelerated stress [71]. The inverse power law relationship is commonly used for analyzing data for which the accelerated stress is non-thermal in nature [72]. The temperature-humidity relationship is a two-stress relationship. It is commonly used for predicting the life at use conditions when the temperature and humidity are the accelerated stresses in a test [73].

2.4.2 Radiation ageing

In ageing by radiation, four basic methods of predicting the radiation ageing behaviour of cable materials have been developed in recent years based on laboratory ageing test. They are:

- The power law extrapolation method
- The superposition of time dependent data
- The superposition of dose to equivalent damage (DED) data
- The kinetic model

All of the methods utilize data on changes in elongation at break as a function of ageing time under accelerated test conditions, by applying higher dose rates and/or higher temperatures than are normally seen under service conditions. In each of the methods, it is emphasized that care must be taken to ensure homogeneous oxidation conditions when assessing the results. The methods differ mainly in the amount of data required for predicting the behaviour of cable materials and in the way the test data are extrapolated to the service conditions.

For example, the power law extrapolation method utilizes data obtained at a single temperature over several dose rates [74]. The dose to equivalent damage (DED) values are

assessed at each of the test conditions and plotted as a function of log DED against log dose rate. Typical DED values for evaluation could be e/e0 = 0.5 or e = 50% absolute. This plot is linear in a number of polymers, particularly polyolefins, enabling an extrapolation to be made of the predicted DED at lower dose rates. Note that the IEC 544 standard for radiation testing recommends the use of e/e0 = 0.5 as the failure criterion [31].

2.4.3 Limitations of the methods

All of the accelerated ageing and life estimation methods are dependent on data being obtained at dose rates low enough for homogeneous oxidation to occur in the test samples and assume that the temperatures used do not span any physical transitions of the polymer, such as crystalline melting or glass transition. This means that the time-scales for carrying out testing are typically in the range of 6 to 18 months. Extrapolation to service time-scales of the order of decades is therefore likely to introduce significant errors in the prediction of lifetimes [74]. However, such errors will be reduced if longer term testing programs, which can verify the data trends, extend over a period of several years.

The power law extrapolation method can only be safely used for those service conditions where thermal degradation is insignificant compared with radiation-induced degradation. In practice, this limits the method to temperatures up to approximately 40°C, dependent on the polymer. The method has so far only been demonstrated to work satisfactorily on some polyolefins, but it may well have a wider application [74].

The superposition of time dependent data is only possible where the general shape of the elongation vs. log time curve does not vary with changes in temperature and dose rate. This implies that all of the degradation mechanisms are equally accelerated by an increase in temperature or dose rate. This is generally the case when the degradation is dominated by a

single mechanism (e.g. oxidation), as is the case with many of the commonly used cable materials. If more than one degradation process is significant in the temperature and dose rate range tested, then the curve shapes will not be the same and the data cannot be superposed. The method has been successfully applied to a range of polymers, including ethylene vinyl acetate (EVA), XLPE and EPR [74].

The superposition of DED data can be used even for those polymers which do not have one dominant degradation mechanism. The method does however require a large data set to obtain sufficient DED values for superposition to be carried out. It is not very successful in those materials which show little or no dose rate effect, but can generally be used on a wide range of materials. The kinetic model can be applied to a range of materials, including EPR and EVA. The main limitation in its wider application is the extensive matrix of test data required [75].

2.4.4 Life estimation

Several researchers have estimated the remaining life of insulating materials by correlating the measured parameters against benchmark parameters suggested by international standards. For example, Y. T. Hsu [76] has used the minimum insulation resistance requirement as an acceptance criterion after correlating with the voltage stresses as stated in IEEE 323. In [77] authors have estimated the life by correlating the break down voltage with the EAB. In yet another [78] article, the remaining life of an electrical cable has been estimated through a simple linear relationship for a given insulation property. It was concluded in [78] that many factors affect the rate of degradation of a cable system and that the degradation mechanisms vary between different types of cables and accessories. The authors in [79] have reported the life estimation by correlating the surface modulus with the EAB. It is apparent from the existing literature that the life estimation of cables involves

establishing the correlation with the benchmark parameters suggested by international standards and guidelines. In order for the reliability estimation, the performance indicators determined from experimental studies are first correlated with the standard benchmark parameters and their failure distribution is determined.

2.5 Discussion and research objective

It has been discussed in several research papers [80-89] that the integrity and function of electrical cables are monitored indirectly through the performance of in-service testing of the safety-related systems and components. However, while these tests can demonstrate the function of the cables under test conditions, they do not verify their continued successful performance for extended periods as they would under anticipated normal service operating conditions or under design basis conditions. Nor does in-service testing of a cable provide specific information on the status of ageing degradation processes, or the physical integrity and dielectric strength of its insulation and jacket materials. Currently many promising material condition monitoring (CM) techniques [90-91] including indenter, oxygen induction time (OIT), and density measurements, have been recognized to be very useful for monitoring material degradation condition. Unfortunately, one major limitation of these CM methods is that they are only suitable for monitoring termination or accessible portion. For inaccessible locations such as conduits, and cable trenches, these CM methods cannot be used when inaccessible cable is exposed to localized adverse environment caused by moisture/ water submergence, high temperature, or radiation. Therefore, it is important to understand the ageing effects of cable caused by moisture, high temperature, radiation, and their combinations, and to further develop effective CM methods for cable ageing management program and license renewal in nuclear power plant [92-93].

In many countries, qualification of safety-related I&C cables is based on compliance with IEEE-323 (1983) and IEEE-383 (1974) standards, which detail testing procedures aimed at demonstrating the ability to survive a design basis event (DBE) after a 40 year service life. However, since these standards were written, a better understanding of the degradation behavior of cable materials has been reached. This has led to a need for improved methods for assessing and mitigating ageing of cables in NPPs since it is now recognized that the standard qualification tests may have been inadequate in assessing long term degradation in service, particularly for cables inside the NPP containment. There have been some cases where cables which had initially been qualified for a 40 year design life failed a design basis event test after removal from the NPP after less than 10 years. The procedures used for qualification of cables include in-laboratory accelerated ageing using higher temperature and dose rates which may not adequately simulate the cable ageing in long-term operational conditions. Most of the work on qualification and remaining life estimation of I&C cables has been carried out experimentally which is very expensive and time consuming.

Also, despite the development of several accelerated ageing tests, there is still no simple ageing test that can reliably assess and/or predict the performance of cables for use in reliability assessment. This problem can be attributed to three main reasons: (1) Basic insulation ageing mechanism is still not fully understood, (2) Simulation of what occurs in service is difficult to reproduce in the laboratory, and (3) Various service stresses are not accurately defined. In life estimation studies, the impact of non-polymeric material on insulation ageing has never been addressed and there are no guidelines to account such effect.

From the literature survey, it is apparent that most of the work discusses about the traditional methods of assessing degradation through one or more experimental means and correlating with the benchmark acceptance criterion suggested by standards and guidelines. The present acceptance criterion used for installed cables is 50% absolute elongation-at-break

and is based on years of experience in testing and analysis of accelerated and field aged cables. It is assumed, generally, that this elongation value will provide sufficient margin to ensure that the insulation maintains its electrical properties during a design basis event. However, it has been noted in the literature that, in certain cases, an elongation of only 5% of the original value may be sufficient for the cable to function electrically during a design basis event. The state-of-the-art for incorporating cable ageing effects into probabilistic safety assessment (PSA) is still evolving and current assumptions that need to be made on the failure rate and common cause effects are based on sparse data. One of the key assumptions of the risk assessment is that operating environments are less severe than or the same as those assumed during qualification testing. Further, in the assessment of reliability of NPP systems the cable insulation is generally not considered. Also, there is no any standard methodology available for incorporating the ageing of cable insulation into system reliability.

The objective of this research is to develop a methodology to assess the susceptibility of polymeric cable insulation to various ageing mechanisms; and to predict the state of the insulation at any chosen time in order to evaluate the remaining life-time of operating cables. Confirmation of the acceptability of cable insulation remaining life is essential to ensure continued long-term reliable nuclear power plant operation. Therefore, an accurate approach is needed to confirm the continued acceptable margin in cable insulation life or to establish end of life for insulation subjected to ageing and post design basis event harsh environments. This thesis work study aims to develop the background and technical basis for incorporating the ageing effects of I&C cables in the reliability assessment of safety related systems in nuclear power plants for probabilistic safety assessment applications.

The proposed plan of thesis work is shown in Figure 2.11 and 2.12. The chemical changes in the polymers occur due to thermal, radiation and moisture intrusion. Because of these

chemical changes in the polymer structure, there could be change in the physical, mechanical and electrical properties which are indicative of the ageing and degradation.

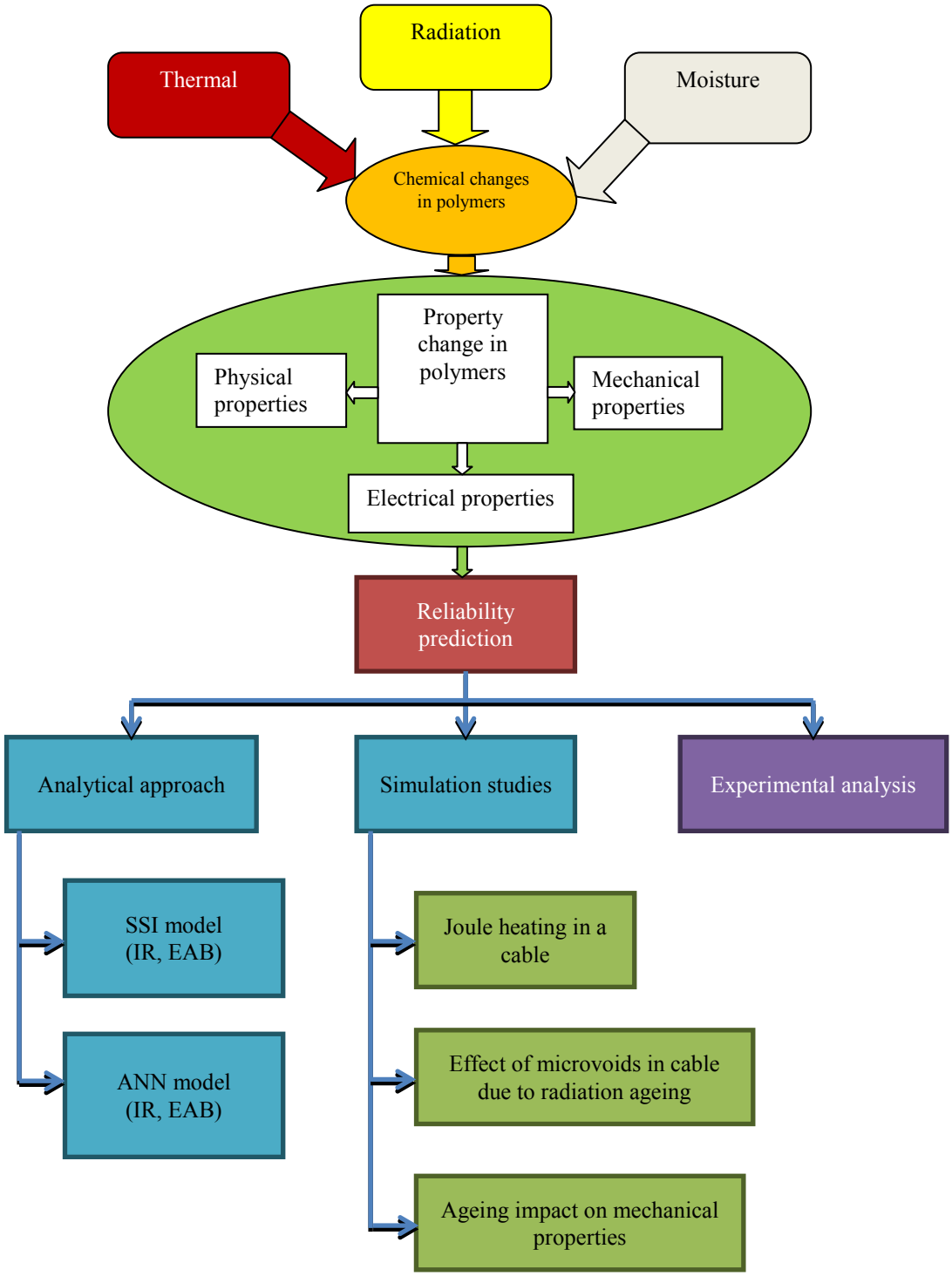

Figure 2.11: Proposed plan of research work (Part 1)

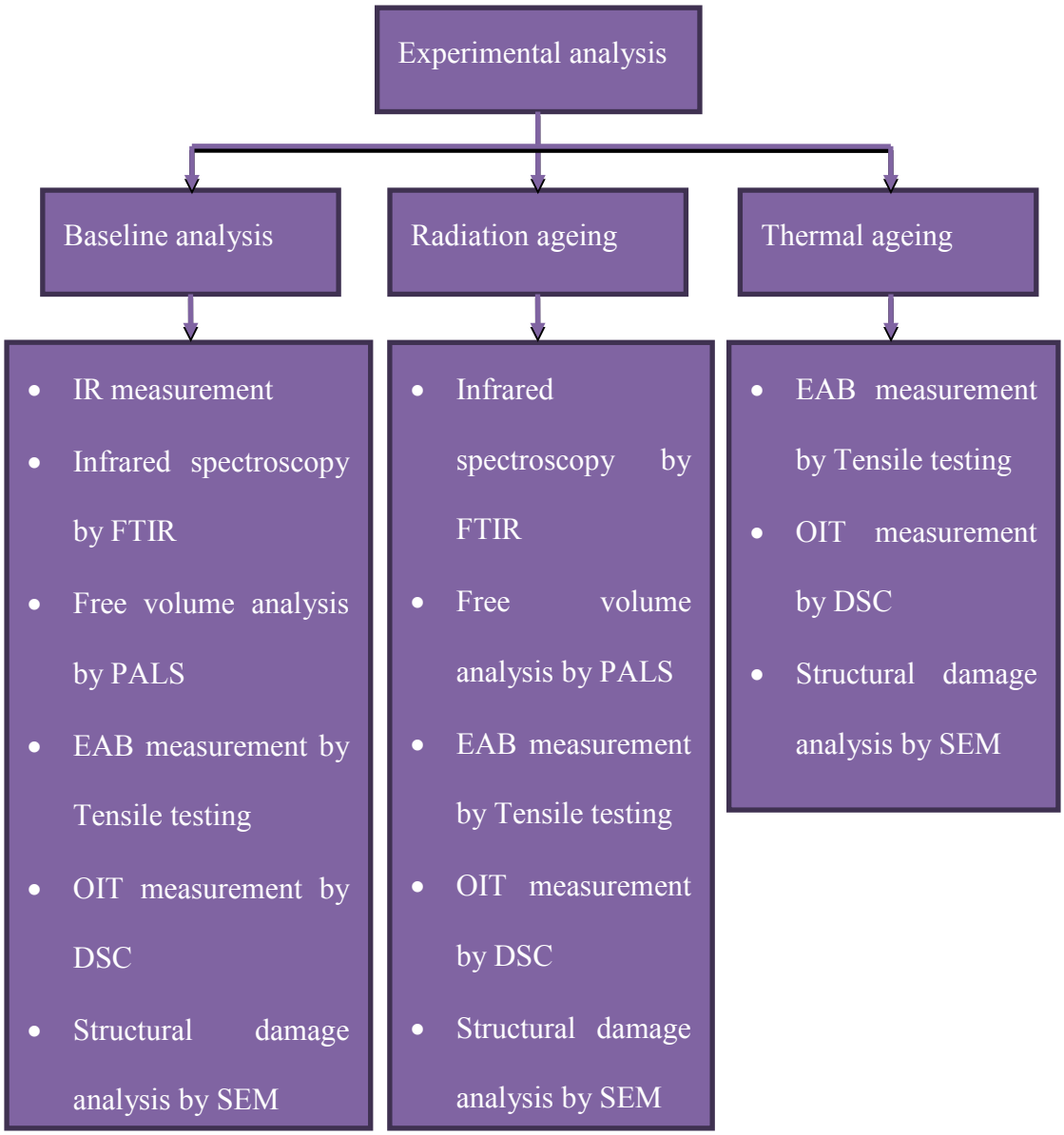

Figure 2.12: Proposed plan of research work (Part 2)

The parameters thus measured are used for degradation assessment and reliability prediction. The key performance indicators such as IR, EAB, and OIT are determined from analytical, simulation and experimental approaches by subjecting the cable samples to thermal and radiation ageing. The time dependent reliability is estimated from the reliability prediction models developed based on stress-strength interference theory and Weibull

reliability concepts. The significance of considering the cable failures in PSA of NPP is also demonstrated by carrying out reliability analysis of a typical safety system of NPP.

2.6 Summary

The performance parameters and their acceptance criteria for degradation assessment and life estimation have been discussed with regard to the international standards and guidelines followed in the cable industry. The most widely used condition monitoring techniques such as IR measurement, EAB measurement, oxidation time and temperature measurement, etc. have also been discussed. The accelerated thermal and radiation ageing methods commonly employed in cable life assessment studies and their limitations have also been discussed in this chapter. The research objective of the thesis work and the proposed research plan has also been discussed with respect to the identified stressors, ageing mechanisms, model development, accelerated laboratory ageing and experimental determination of performance parameters for reliability prediction.

Chapter 3 Degradation Mechanisms in Polymeric Insulation Materials

3.1 Background

Polymeric insulation materials used in (I&C) cables of nuclear power plants are exposed to radiation and thermal oxidation. The lifetime for long-term ageing has been evaluated by the accelerated testing methods, namely the radiation accelerated testing is done by irradiation with high dose rates as well as by ageing at elevated temperatures. The differences between degradation by accelerated ageing and actual ageing have been investigated by many researchers and a lot of data have been reported [94-96]. For acceleration of radiation degradation, dose rate effects on the polymer degradation were analyzed to be the distribution of oxidation area due to oxygen diffusion control at the higher dose rate range, and to be the chemical chain reaction of oxidation at lower dose rate range. However, quantitative analysis of the chemical chain reaction was not yet been resolved.

For thermal degradation, the degradation rates at several different higher temperatures are generally plotted using the Arrhenius equations and extrapolated to lower temperature. The main problem with the application of the Arrhenius equation was that the activation energy of degradation might change over the wide temperature ranges. The synergistic effect on the degradation between radiation and thermal oxidation has been an important factor for the accelerated ageing, but it is still not clear. This chapter presents various degradation mechanisms that occur due to thermal and radiation ageing in I&C cables used in NPPs.

3.2 General features of ageing in polymers

The ageing of polymeric materials is dependent on three basic factors [6-7]:

- the polymer system itself,
- the pre-service and service environmental conditions, and
- the time scale (generally long periods).

The external jacket and the insulating materials are formulated organic compounds. They are made up of a basic polymer (a macromolecular chain obtained by multiple replications of a unitary monomer) or co-polymer and of additives which provide the material with specific properties. These additives are mainly protective agents (anti-oxidants, thermal stabilizers, fire retardants, mineral fillers, plasticizers, oil (used to aid manufacture of the material), pigments etc. Some complex compounds may contain up to ten or fifteen different constituents. Variations in formulation can affect both the activation energy and the rate of thermal ageing and the maximum dose for radiation ageing.

The electrical cables inside the containment building of an NPP are exposed to various environmental conditions. The most important factors are temperature and ionizing radiation, to which should be associated the nature of the environment, typically the presence of oxygen in most reactor types and the presence of water vapour (the relative humidity being possibly above 80%). Mechanical influences should also be considered, e.g. vibration, for cables connected to running machines; connection/disconnection operations during maintenance, installation anomalies where bending stresses are excessive, which may locally affect some cables. For I&C cables, electrical stresses are not significant in ageing, since this type of cable is exposed to voltages less than 1 kV.

3.3 Basic effects of ageing

The environmental service conditions will induce chemical and/or physical processes at the molecular level of the material; these processes are the ageing mechanisms. The consequence at the macroscopic level is a slow and irreversible change in the properties (electrical, mechanical) of the material, which can lead to the functional failure of the cable. Typical macroscopic changes in the properties of common cable materials include [6-7]:

- decrease in the tensile elongation of the material, often associated with a decrease in the tensile strength
- increase in the hardness or compressive modulus (particularly for materials commonly used as jackets)
- increase in the density, and
- change in the electrical properties, e.g. small increase in dielectric loss is observed in some materials.

In most cable types, the changes in electrical properties are not at large. Loss of cable functionality is usually determined by the changes in the mechanical properties, cracking of the insulation preceding electrical failure (i.e. loss of insulation resistance). PVC cables, however, may fail electrically during a DBE test before becoming severely embrittled.

The ageing mechanism may include various elementary mechanisms which may have cumulative, competitive, synergistic and/or antagonistic effects. Two large categories of ageing mechanisms (chemical/physical) are usually distinguished, depending on whether they imply a change in the chemical structure or not of the macromolecular chains or the additives. The following sections describe the practical aspects of ageing and why ageing mechanisms

need to be understood, how to identify ageing mechanisms and recommendations on how to carry out meaningful accelerated ageing tests and subsequent life estimation.

3.3.1 Effect of microvoids in polymers

Many microvoids exist in polymer due to its condensed structure feature. The electrons moving in these microvoids do not get scattered. Therefore the ability of electrons to accumulate energy is only limited by the size of the microvoids [97]. If the size of microvoids is large enough for electrons to gain enough kinetic energy due to its acceleration in electric field direction to break the polymer chain, then electrical breakdown would occur. Experimental results show that the number of microvoids in a typical polymer is more than $10^{14}/cm^3$ [98]. In terms of the free volume theory of breakdown, the correlation between breakdown strength (EB) and radius of maximum microvoid (Rmax) may be written as follows [98]:

$$E_B = \frac{\Delta W}{2eR_{max}} \tag{3.1}$$

where ΔW is the accumulated energy of electron, i.e. the energy required for breaking chemical bonds of molecular chain; e is the charge of electron.

3.3.2 Energy criterion for breaking chemical bonds

The breakdown of polymers is always accompanied with the scission of chemical bonds. The previous studies on electrical breakdown of polymers are mostly concentrated on the physical process such as electron transport and energy accumulation [99], but a little on the chemical process, being a certain lack of understanding the breakdown process from the viewpoint of molecular structure. Usually the conventional electrical breakdown theories suggest that breakdown will occur if electrons (or photons) with an energy equal to the

bonding energy of chemical bonds impact on the molecules of polymer [100]. As is well known, the bonding energy of general chemical bonds such as C-C, C-H, CH_3-CH_3, CH_3-H, Si-H and Si-O is in the range of 3.05-4.40 eV. However previous investigations confirmed that polymers involve many microvoids, and the electronic processes causing electrical breakdown occur in the microvoids instead of polymer chains [97]. The size of maximum microvoid measured in typical polypropylene (PP) sample in the investigation exceeds 50 nm. According to electron mean free path of 50 nm, within which electrons gain energy of 3.05-4.40 eV, the calculated breakdown strength is on the order of 10^7 V/m, which is much smaller than the measured electrical breakdown strength [101]. Obviously, it would be inadequate to take the bonding energy of chemical bonds as the energy criterion for electrical breakdown of polymers.

3.4 Understanding ageing mechanisms

Ageing mechanisms are active when a sensitive/susceptible material is exposed to suitable environmental conditions. As a result, changes occur in material properties (ageing effects) which may cause changes/degradation in the functional characteristics of cable. Although the best scientific solution for appreciating the long term behaviour of cable materials would consist in removing cables after a 40 to 50-year operating period in an NPP, such a solution is generally unrealistic, except where samples are available from redundant circuits or from specific deposits of cable materials. Another possible solution would be to simulate ageing in an accelerated manner by carrying out in a few months (short term) what happens over long periods of time. In order to be satisfactory, accelerated ageing should include a fundamental concept that the simulation of ageing must be representative. It is therefore necessary to select the conditions for the accelerated tests to simulate the ageing mechanisms involved in NPPs. Numerous studies, over the past 20 years, have generated a

great number of examples which enable this key notion to be appreciated [102]. Some examples of practical aspects of ageing mechanisms that needs to be considered in accelerated ageing tests are given in the following sections.

3.4.1 Competition between HCl elimination and evaporation of plasticizers in plasticized PVC

For thermal ageing at temperatures below 70–80°C in the absence of radiation, the main ageing mechanism for plasticized PVC is evaporation of plasticizers from the surface of the external sheath of the cable. At higher temperatures (>80°C) and under irradiation, this mechanism is in competition with intramolecular elimination of hydrochloric acid (HCl) from the macromolecular chains of PVC. Thus, increasing of temperature of the accelerated ageing reduces the validity of the ageing simulation.

3.4.2 Ageing through a physical transition in semi-crystalline polymers

Some of the polymeric materials used in cables are semi-crystalline, with a crystalline melting region close to the temperature range used in service. Studies have shown the influence of the crystalline phase on physical properties, particularly for polyethylene based materials. For this type of material, care must be taken in extrapolation of data from accelerated thermal ageing tests. If the extrapolation is through the crystalline melting region, then the Arrhenius equation will not be valid and the accelerated tests will not be a representative simulation of natural ageing [103]. In accelerated radiation ageing, semi-crystalline polymers, such as XLPE, will often show a reverse temperature effect, with ageing

occurring more rapidly at lower temperature than at higher temperature. This is because of the complex repairing mechanism of the macromolecules when recrystallization takes place.

3.4.3 Compatibility of materials in construction of the cable

For some cable configurations, the external jacket is in direct contact with the insulation material. In the specific case of plasticized PVC cables, this can lead to diffusion of plasticizers from one material to another. This is a physical ageing mechanism (mass transfer). This mechanism is not observed when a solid metallic screen is placed between the two materials, but can occur if the metallic screen is braided. The degradation observed will not be the same when ageing is performed separately on dumbbells cut from the jacket or insulation of PVC materials, compared with ageing of complete cable samples.

The diffusion of plasticizers has also been observed with polyethylene external jacket/PVC insulation and PVC jacket/PE insulation materials. Materials compatibility may also affect connectors or terminations. Interaction between the degradation products of the jacket and insulation materials can also occur, affecting the observed behaviour, particularly in accelerated tests. This is the case for PVC jacketed cables with PE insulation, which are radiation aged or thermally aged at temperatures >80°C, when HCl elimination is a dominant mechanism. The selected sample geometry (pre-cut dumbbells, complete cable) for an ageing study may strongly affect the ageing mechanisms because of interaction between the cable components. A study highlights that the activation energy of a chlorosulfonated polyethylene (CSPE) material depends upon the sample geometry during thermal ageing [104].

3.5 Key concerns on accelerated ageing

3.5.1 Accelerated thermal ageing

Thermal degradation refers to the chemical and physical processes in polymers that occur at elevated temperatures. Increased temperature accelerates most of the degradation processes that occur in polymers such as oxidation, chemical attack and mechanical creep. Oxidation is generally considered to be the most serious problem when using polymers at elevated temperatures [105]. The influence of temperature on the oxidation processes will depend on the chemical structure of the polymer. Thermo-oxidation is initiated by the reaction of free radicals P· with oxygen to form peroxide radicals:

$$P\cdot + O_2 \rightarrow POO\cdot \tag{3.2}$$

All polymers contain these free radicals due to their polymerization and processing history. However, the concentration of free radicals can be significantly increased by interaction with light, ionizing radiation or the presence of transition metals. Once formed the peroxide radicals undergo slower propagation reactions that breakdown the polymer chains. The overall degradation process will normally involve a relatively long induction period during which little degradation is observed [105]. At the end of this period there is a rapid increase in degradation leading to a significant reduction in the mechanical properties of the polymer. This induction period is temperature sensitive and is reduced significantly at elevated temperatures. The induction period of the degradation process can normally be regarded as the serviceable lifetime of the polymer.

Thermal ageing is always present, to some degree, for cables installed inside containment. Accelerated thermal ageing is achieved by exposing the cables to temperatures significantly higher than the expected service temperature. The assumption of an Arrhenius relationship

between temperature and rate of degradation is typically used for determination of the acceleration factor. A qualification margin is applied in the establishment of the qualified life. This margin is dependent on a number of factors, including: knowledge of the cable temperature during operation. Less margin is needed if the temperature is controlled (and measured) throughout the cable's qualified life, knowledge of the characteristics of the materials from which the cable insulation is constructed, especially access to measured activation energies within the actual temperature range of service, test tolerances, e.g. the tolerances on temperature in the working space of the dry heat test chamber, and the number of samples tested.

Several studies have shown that the activation energy and degradation rate may vary with the composition of the insulation material (fillers, additives, etc.) and with the temperature. It is recommended that the activation energy of the cable insulation materials be measured as part of the preparation for the testing. Values taken from studies based on similar, but not identical materials or at temperatures other than the specific application temperature may be of limited use. In cases where such values are used instead of measurements on the actual cable materials, a high degree of conservatism is required.

Test temperature tolerances are stated in standards used for climatic testing, e.g. IEC 60068-2-2 [106] for high temperature testing. Studies of the relationship between required qualification margin and the number of samples tested show that a high margin may be needed to account for the deviation between individual cable samples, if very few samples are used in the qualification test. However, the margin needed can be significantly reduced by increasing the number of samples tested. The accuracy of the qualified life established through laboratory testing is limited by the factors discussed above, but also by the inaccuracy inherent in the application of the Arrhenius formula to a complex component. The inaccuracy grows with increasing acceleration factor; that is with increasing difference

between test temperature and operating temperature. In establishing a qualified condition, care must be taken that the accelerated thermal ageing is carried out at a temperature where the ageing degradation mechanism is the same as that seen in service.

3.5.2 Accelerated radiation ageing

Ionizing radiation covers a wide range of different forms of radiation including x-rays, gamma rays, neutrons, alpha particles and beta particles. When a polymer is irradiated the ionizing radiation induces degradation by the formation of free radicals or ions in the polymer. These reactive intermediates are capable of initiating chemical reactions which occur by free radical or ionic mechanisms and which result in scission as well as in cross-linking reactions. Free radicals with a long lifetime, which are present in the bulk of the material after irradiation, are responsible for changes in properties even a long time after exposure [107-108].

The radiation ageing component of an accelerated ageing test normally includes subjecting the test specimen to the total expected lifetime dose (before DBE) in a short time, which means a much higher dose rate than under normal operating conditions. The acceleration factor is defined by the ratio between the dose rate used in the artificial ageing and the dose rate in operating conditions. The qualification margin applied in radiation ageing for establishing of the qualified life depends on [6]:

- knowledge of the dose rate during normal operation. Less margin is needed if the dose rate is controlled (and measured) throughout the cables qualified life,
- knowledge of the dose rate effect on the cable insulation materials,
- test tolerances, and
- the number of samples tested.

For many insulation materials, the degradation due to a specific total radiation dose depends on the dose rate. The observed degradation during accelerated ageing will be dependent on whether oxygen is able to diffuse into the cable material during the test period. Unless it has been proven by tests that the dose rate effect is negligible, it is recommended that the dose rate be limited in the artificial ageing test. Very low dose rates (20–30 Gy/hr) have been found necessary for testing certain materials particularly sensitive to the dose rate. In establishing a qualified condition, care must be taken to avoid the development of heterogeneous oxidation which occurs when diffusion limited oxidation takes place. This is a particular concern in the whole cable samples used for DBE testing.

3.6 Traditional mechanisms of polymer degradation

Over the years, the chemical reactions of polymer degradation (oxidation) mechanisms have been accepted as following equations (3.3 to 3.7), especially for polyolefin polymers, for both thermal and radiation ageing [109].

$$Polymer\ (RH) \rightarrow R\cdot\ (polymer\ radical) + H\cdot\ (proton) \tag{3.3}$$

$$R\cdot\ +\ O_2\ \rightarrow R-O-O\cdot\ (peroxy\ radical) \tag{3.4}$$

$$R-O-O\cdot\ +RH\ \rightarrow R-O-OH\ (hydro-peroxide) + R\cdot \tag{3.5}$$

$$R-O-OH\ \rightarrow RO\cdot\ +\ \cdot OH\ (thermal\ decomposition) \tag{3.6}$$

$$RO\cdot\ \rightarrow Chain\ scission\ (carbonyl, alcohol)$$

$$R-O-O\cdot\ (RO\cdot) + AX\ \rightarrow R-O-OX\ (R-OX) + AY\ (AX: antioxidant) \tag{3.7}$$

Eq. (3.2) as initiation step is radical formation on polymer chain by thermal or radiation energy, (3.3) radical reacts with oxygen to form peroxy radical, (3.4) peroxy radical abstracts hydrogen from the neighbor polymer to form same radical in (3.2) on polymer, and the

peroxy radical forms hydro-peroxide, (3.5) hydro-peroxide decomposes to poly-oxy radical and hydro-oxy radical, (3.6) poly-oxy radical decomposes to chain scission and oxidation products (carbonyl groups, alcohols), (3.7) antioxidant reacts with radicals to terminate the oxidation reactions. The combination of (3.3) and (3.4) produces the cycle reaction, i.e. the chain reaction of oxidation until the radicals are recombined. Antioxidant stops the chain reaction by the quench of free radicals. The chemical reaction schema is illustrated in Figure 3.1.

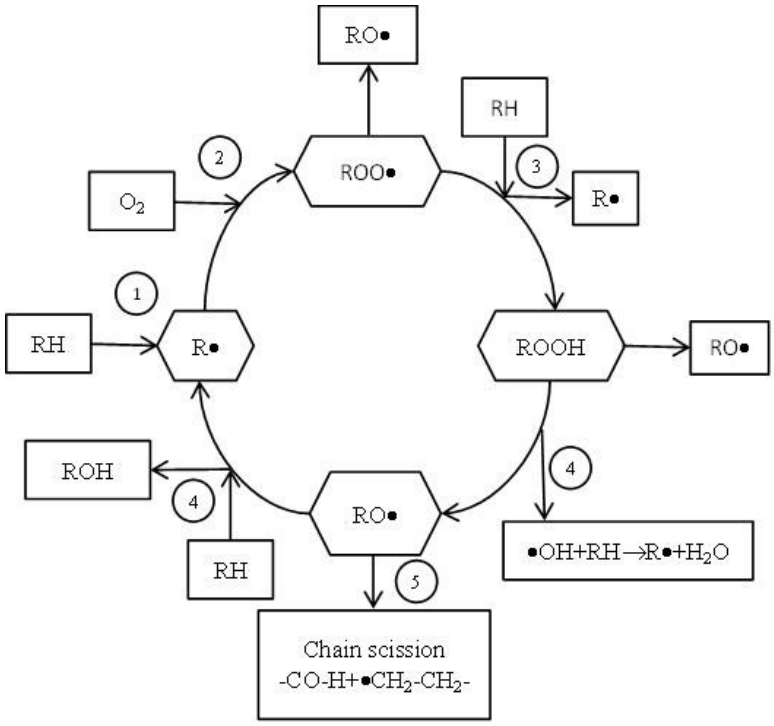

Figure 3.1: Traditional chemical reaction schema of polymer oxidation

According to above traditional mechanisms, the following facts might be observed: (i) antioxidant is consumed with the progress of the oxidation, (ii) the oxidation is reduced much with the high concentration of antioxidant, and (iii) the effect of antioxidant should much depend on the type and molecular weight of antioxidant. Reactions which result in oxidative degradation are not identical for all polymers, but vary with the chemical structure of the polymer and with the conditions at which oxidation occurs. Nevertheless some generalities

are evident and have resulted in a reaction mechanism which is now generally accepted for the oxidation of hydrocarbon polymers. This same mechanism is believed to contribute to the oxidation of many other polymers which are not completely hydrocarbon in structure, but do contain hydrocarbon groups or segments. Oxidation of polymers, though basically a series of chemical reactions, may also be modified by the physical (morphological) structure.

The kinetics of polymer degradation has been constructed on the basis of above mechanisms. The activation energy of thermal degradation is estimated to be the intrinsic value for each polymer materials. The dose rate dependency on the degradation for radiation ageing is derived in principle from chain reactions (3.4) and (3.5). The other dose rate effects are caused from the oxygen diffusion control into polymer materials during irradiation in the ageing at relatively high dose rate irradiation. In a low dose rate irradiation free from the oxygen diffusion control, the dose rate dependency of the degradation is analyzed to be proportional to square root of reverse dose rate when the antioxidant is absent. Even if the antioxidant is present, the dose rate effect cannot be neglected by considering the contribution of the chain reactions. Although the most of reports on radiation ageing of polymer degradation had pointed out the dose rate effect, the effect had not been explained reasonably or quantitatively.

3.6.1 General chemical mechanisms

The thermal decomposition of polymers may occur due to oxidative processes or simply due to the presence of heat. In many polymers, the thermal decomposition processes are accelerated by oxidants (such as air or oxygen). In that case, the minimum decomposition temperatures are lower in the presence of an oxidant. This significantly complicates the problem of predicting thermal decomposition rates, as the prediction of the concentration of oxygen at the polymer surface during thermal decomposition or combustion is quite difficult

[110]. Despite its importance to fire, there have been fewer studies of thermal decomposition processes in oxygen or air than in inert atmospheres.

Four general mechanisms common in polymer decomposition are illustrated in Figure 3.2. These reactions can be divided into those involving atoms in the main polymer chain and those involving principally side chains or groups. While the decomposition of some polymers can be explained by one of these general mechanisms, others involve combinations of these four general mechanisms. Nonetheless, these categorizations are useful in the identification and understanding of particular decomposition mechanisms.

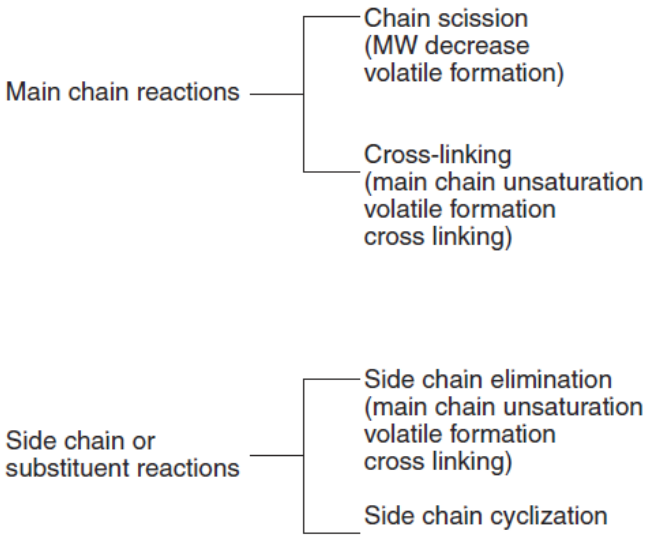

Figure 3.2: General decomposition mechanisms

Among simple thermoplastics, the most common reaction mechanism involves the breaking of bonds in the main polymer chain. These chain scissions may occur at the chain end or at random locations in the chain. End chain scissions result in the production of monomer, and the process is often known as unzipping. Random-chain scissions generally result in the generation of both monomers and oligomers (polymer units with 10 or fewer monomer units) as well as a variety of other chemical species. The type and distribution of volatile products depend on the relative volatility of the resulting molecules.

Cross-linking is another reaction involving the main chain. It generally occurs after some stripping of substituents and involves the creation of bonds between two adjacent polymer chains. This process is very important in the formation of chars, since it generates a structure with a higher molecular weight that is less easily volatilized. The main reaction types involving side chains or groups are elimination reactions and cyclization reactions. In elimination reactions, the bonds connecting side groups of the polymer chain to the chain itself are broken, with the side groups often reacting with other eliminated side groups. The products of these reactions are generally small enough to be volatile. In cyclization reactions, two adjacent side groups react to form a bond between them, resulting in the production of a cyclic structure. This process is also important in char formation because, as the reaction scheme shows, the residue is much richer in carbon than the original polymer as seen, for example, for polyvinyl chloride [111]:

$$-CH_2 - CHCl- \Longrightarrow CH = CH - + HCl \tag{3.8}$$

which leads to a hydrogenated char or for polyvinylidene chloride:

$$-CH_2 - CCl_2- \Longrightarrow -C \equiv C - + 2HCl \tag{3.9}$$

which yields a purely carbonaceous char with an almost graphitic structure. These chars will tend to continue breaking down by chain scission, but only at very high temperatures.

Scission of macromolecular chains: two new chains are created after the breaking up of one. It is usually a scission of alkoxyl or peroxide radicals. This is shown schematically below.

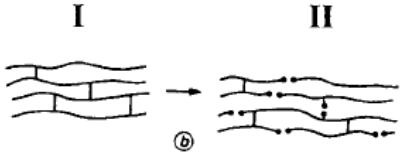

Figure 3.3: Chain scission in polymers

Cross-linking reactions: cross-linking corresponds to the formation of a covalent link of two adjacent macromolecules. As the number of cross-links increases, the cross-link density also increases as shown schematically below forming a three dimensional network.

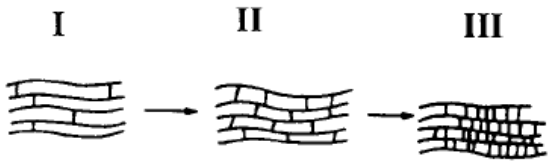

Figure 3.4: Cross-linking in polymers

Oxidation reaction: this is a free radical chain mechanism whose classical series of reaction steps can be found in numerous reference works. The reaction scheme is summarized below.

- initiation step = formation of free radicals
- propagation step = formation of peroxy radicals and hydroperoxide
- chain branching step = decomposition of hydroperoxide
- termination step = deactivation of radicals in inert products (alcohol, acid).

The initiation step leads to the formation of reactive species, i.e. radicals, because of the initial break of a covalent link under the effect of temperature and/or radiation. Oxidation leads both to chain scission and cross-linking, dependent on the detailed kinetics of the individual steps in the oxidation chain reaction. These kinetics are strongly dependent on the additives present in the polymeric compound and will therefore vary with the detailed formulation of the material [112].

Process controlled by oxygen diffusion: the kinetics of ageing is governed by the diffusion of oxygen when the free radical initiation rate is faster than the rate of dissolved oxygen diffusion in the polymeric material. This behaviour leads to a concentration profile in oxidation products in the material thickness (heterogeneous degradation). An oxidized

surface layer with a cross-linked core is observed. Oxygen diffusion controlled processes depend on the oxygen permeability of the polymer, the radiation dose rate, and the sample thickness. Diffusion-limited oxidation is the first type of radiation dose rate effect identified in polymer ageing. This diffusion-limited process can also occur in thermal ageing of polymers.

Synergistic effect: this is observed in a number of polymeric materials when the combined effects of environmental conditions are higher than the individual effects of the conditions applied separately. It is particularly evident in combined thermal and radiation ageing for some polymers, but can also be observed for other conditions, e.g. moisture and radiation in polyurethane and polyimide materials. Elimination of hydrochloric acid: this corresponds to the elimination of a molecule of hydrochloric acid (dehydrochlorination) from the macromolecular chain of PVC. A similar mechanism occurs in fluorinated polymers, with the elimination of hydrofluoric acid (HF). It goes together with the formation of conjugated polyenes. When the degradation is advanced enough, the material becomes coloured.

3.6.2 Chain-scission mechanisms in polymers

Decomposition by chain scission is a very typical mechanism for polymer decomposition. The process is a multistep radical chain reaction with all the general features of such reaction mechanisms: initiation, propagation, branching, and termination steps. Initiation reactions are of two basic types: (1) random chain scission and (2) end-chain scission. Both, of course, result in the production of free radicals. The random scission, as the name suggests, involves the breaking of a main chain bond at a seemingly random location, all such main chain bonds being equal in strength. End-chain initiation involves the breaking off of a small unit or group at the end of the chain. This may be a monomer unit or some smaller substituent. These two types of initiation reactions may be represented by the following generalized reactions [113]:

$$P_n \Longrightarrow R_r + R_{n-r} \qquad \text{(random-chain scission)} \qquad (3.10)$$

$$P_n \Longrightarrow R_r + R_E \qquad \text{(end-chain initiation)} \qquad (3.11)$$

where Pn is a polymer containing n monomer units, and Rr is a radical containing r monomer units. RE refers to an end group radical.

Propagation reactions in polymer decomposition are often called depropagation reactions, no doubt due to the polymer chemist's normal orientation toward polymer formation (polymerization) rather than decomposition. Regardless, there are several types of reactions in this class as shown in Figure 3.5(a) -3.5(b).

$$R_n \Longrightarrow R_{n-m} + P_m \qquad \text{(intramolecular H transfer, random-chain scission)} \qquad (3.12)$$

$$P_m + R_n \Longrightarrow P_{m-j} + P_n + R_j \qquad \text{(intermolecular H transfer)} \qquad (3.13)$$

$$R_n \Longrightarrow R_{n-1} + P_1 \qquad \text{(unzipping, depropagation, depolymerization)} \qquad (3.14)$$

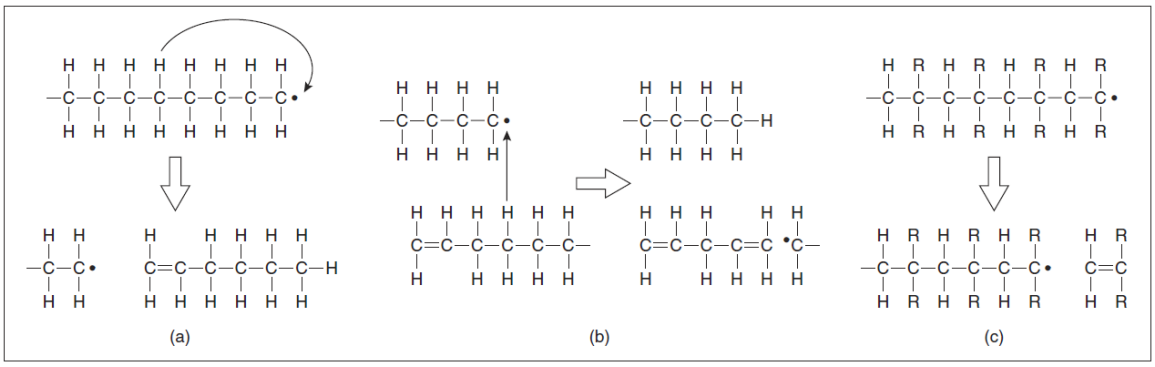

Figure 3.5: (a) Intramolecular H transfer, (b) intermolecular H transfer, (c) unzipping

The first of these reactions involves the transfer of a hydrogen atom within a single polymer chain, i.e., intramolecular hydrogen atom transfer. The value of m is usually between one and four as polymer molecules are often oriented such that the location of the nearest available H within the chain is one to four monomer units away from the radical site. The

value of m need not be a constant for a specific polymer as the closest available hydrogen atom in the chain may vary due to conformational variations.

Decomposition mechanisms based on this reaction are sometimes known as random-chain scission mechanisms. The second reaction involves the transfer of a hydrogen atom between polymer chains, i.e., intermolecular hydrogen atom transfer. The original radical, Rn, abstracts a hydrogen atom from the polymer, Pm. As this makes Pm radical with the radical site more often than not within the chain itself (i.e., not a terminal radical site), the newly formed radical breaks up into an unsaturated polymer, Pm–j, and a radical, Rj. In the final reaction, no hydrogen transfer occurs. It is essentially the reverse of the polymerization step and, hence, is called unzipping, depropagation, or depolymerization. Whether the decomposition involves principally hydrogen transfer reactions or unzipping can be determined by examining the structure of the polymer, at least for polymers with only carbon in the main chain. If hydrogen transfer is impeded, then it is likely that the unzipping reaction will occur.

Vinyl polymers, strictly speaking, are those derived from a vinyl repeating unit, namely:

$$—[CH_2—CH_2]_n—$$

where n is the number of repeating monomers. Here, the hydrogen atoms can be substituted, leading to a repeating unit of the following form:

$$\begin{array}{c} W \quad Y \\ | \quad | \\ —[C—C]_n— \\ | \quad | \\ X \quad Z \end{array}$$

where W, X, Y, and Z are substituent groups, perhaps hydrogen, methyl groups, or larger groups. Consider that the C–C bond connecting monomer units is broken and that a radical site results from the scission shown as:

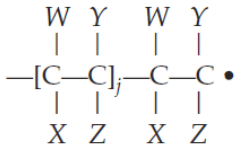

where the symbol • indicates an unpaired electron and, hence, a radical site. In order for a hydrogen atom to be transferred from the chain to the radical site, it must pass around either Y or Z. If Y and Z are hydrogens, this is not at all difficult due to their small size. However, if the alpha carbon has larger substituents bound to it (i.e., Y and Z are larger groups), the transfer of hydrogen to the radical site is more difficult. This type of interference with hydrogen transfer is known as steric hindrance [114].

While chain-branching reactions seem to be of little importance in polymer decomposition, termination reactions are required in all chain mechanisms. Several types of termination reactions are common.

$$R_m \Longrightarrow P_m \text{ (unimolecular termination)} \tag{3.15}$$

$$R_m + R_n \Longrightarrow P_{m+n} \text{ (recombination)} \tag{3.16}$$

$$R_n + R_m \Longrightarrow P_m + P_n \text{ (disproportionation)} \tag{3.17}$$

3.7 Physical ageing mechanisms

3.7.1 Evaporation of plasticizers

Plasticizers will evaporate at the surface of the material. The surface is then replenished by plasticizer diffusion from the core as shown in Figure 3.6. There can be competition between these two kinetic regimes (evaporation and diffusion), depending on temperature. This ageing mechanism is of particular concern in PVC based materials, which usually have high plasticizer content.

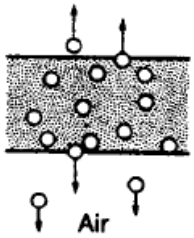

Figure 3.6: Evoporation of plasicizers

3.7.2 Migration of plasticizers

This phenomenon appears in multilayer cables using plasticized materials. The migration of plasticizers occurs until equilibrium is reached corresponding to a uniform distribution of each plasticizer, in each material.

3.7.3 Reverse temperature effect

The reverse temperature effect is a phenomenon which has only been recognized in the last few years. It has been seen in polyolefin materials which have been radiation aged in air at temperatures below their crystalline melting point. Under these conditions, degradation is more rapid at the lower temperatures than at higher temperatures, which is opposite to what would be expected from normal kinetics of chemical reactions [115-116]. However it is now realized that the reverse temperature effect is a function of the semi crystalline nature of the polyolefins.

Polyethylene based materials, such as XLPE, are semi-crystalline and their mechanical properties are determined by their microstructure at the super molecular level. The material contains randomly oriented crystalline regions linked by amorphous tie molecules. During radiation ageing, reactive species such as radicals are generated uniformly throughout both crystalline and amorphous regions. In the crystalline regions at temperatures well below the

melting point, these species are trapped and are unable to react to form oxidative products because of the low chain mobility and the low oxygen diffusion rate in the crystalline region.

Degradation then proceeds primarily through oxidative scission reactions in the amorphous regions, where both chain mobility and oxygen diffusion rates are higher. Since the amorphous regions form the tie molecules between the crystalline blocks, chain scission in these regions has a marked effect on the mechanical properties. If the radiation ageing occurs at slightly higher temperatures, nearer the melting region for the crystalline portion, then chain mobility is high enough for the trapped species to react to form chemical crosslinks. In addition, the enhanced mobility enables some recrystallization to occur which can reform tie molecules which were broken by oxidative scission in the amorphous regions. The combination of these effects is to effectively 'heal' some of the damage which is created by the radiation ageing. The overall macroscopic effect is a reduced rate of degradation at the higher temperature during radiation ageing.

3.7.4 Oxidation reaction

The basic reactions in the classical oxidation reaction scheme are shown in below equations.

$$Initiation \qquad RH \longrightarrow R\cdot \tag{3.18}$$

$$Propagation\ and\ bracnching \qquad R\cdot + O_2 \rightarrow RO_2\cdot \tag{3.19}$$

$$RO_2\cdot + RH \rightarrow RO_2H + R\cdot \tag{3.20}$$

$$RO_2H \rightarrow RO\cdot + OH\cdot \tag{3.21}$$

$$RO\cdot \rightarrow R\cdot + -CO- \tag{3.22}$$

$$Termination \qquad 2R \cdot \rightarrow RR \tag{3.23}$$

$$2RO_2 \cdot \rightarrow RO_2R + O_2 \tag{3.24}$$

$$or \quad ROH + -CO - + O_2 \tag{3.25}$$

Initiation of the radical chain mechanism can be either via thermal or radiation activation. Propagation and branching of the reactions can then occur with the production of unstable hydroperoxide groups as well as intermediary radicals. Termination of the chain reaction occurs with the recombination of radicals to form stable groups. The detailed kinetics of the individual steps within the oxidation scheme will be determined by the formulation of the polymeric compound, particularly the nature and amount of additives included in the material.

One important physical effect of radiation dose rate is diffusion-limited oxidation, which takes place when degradation reactions occur faster than oxygen diffusion processes from the ambient air, such that the oxygen dissolved in the polymer cannot be readily replenished. In these circumstances, the concentration of oxygen in the polymer interior is reduced from its equilibrium value to lower or even nonexistent levels. Apart from reducing the dose rate, two other approaches can be taken to help solve the problem of diffusion-limited oxidation due to high dose rate in accelerated aging experiments: thinner samples and/or higher oxygen pressures may be used.

Clough & Gillen [117] observed in their study on polyvinylchloride and polyethylene that the thermal decomposition of hydrogen peroxides, a radiation oxidation product, can lead to an important chemical dose-rate effect. Hydroperoxide breakdown gives free radicals (R•) via chain branching, as shown in above equations. The free radicals (R•) produced then reinitiate the sequence of scission and/or cross-linking. Under long-term irradiation at low dose-rate conditions, this step is thought to contribute substantially or even dominate the direct action

of the radiation as a source of free radicals [117-118]. Under conditions of short-term, high-dose rate exposure, however this hydroperoxide-mediated chain branching step may not emerge, even at the same total dose as in a long-term low dose-rate experiment. Physical effects of polymer aging that depend on radiation dose rate can be eliminated by the approaches mentioned above, but the chemical dose rate effect is hard to eliminate. For this reason, the best practice is to use as low dose rate as possible to achieve the desired total dose, in an accelerated aging experiment.

3.8 Summary

The important features of ageing and its effect on performance of the cable insulation have been discussed. The energy criterion for breaking of various chemical bonds due to thermal and radiation ageing has also been discussed in this chapter. The traditional ageing mechanisms of polymer degradation such as chain scission, cross-linking and oxidation are explained with the help of chemical reactions. In addition, the physical ageing mechanisms such as evaporation of plasticizers, migration of plasticizers, etc. have been discussed in this chapter.

Chapter 4 Reliability Prediction of I&C Cables by Stress Strength Interference Theory

4.1 Introduction

Development of remaining life models for cable insulation consists of looking for adequate relationships between insulation life and the applied stresses from both the life testing data and the physics of failure considering the time dependent degradation. The main activities are identification of failure modes, characterization of the ageing process, derivation of life expressions and validating the models. The approach is mainly based on the study of physical-chemical properties of insulating materials subjected to various stressors that are present in nuclear power plants. The model, which will be function of one or more stresses, will eventually describe the state of the insulation with the help of time-dependent degradation of insulating materials. In order to validate the developed models based on the physical-chemical properties, experiments will be conducted under accelerated ageing conditions. The experimental data available in the literature may also be used to validate (if required) the proposed remaining life prediction models.

Although, the stress-strength interference (SSI) theory has well been recognized and successfully applied to various fields of risk and reliability assessment, it has not yet been applied to remaining life estimation of electrical cables in NPPs. In this section a framework for estimating the life time of I&C cable is discussed. The main aim of developing this framework is to perform reliability evaluation of safety-related and safety critical system taking into account the reliability or probability of failure of associated I&C cables for PSA of NPP. The XLPE cables are extensively being used in safety systems of Indian NPPs and

their failure will not only interrupt the plant performance but also causes the malfunctioning of associated systems essential during emergency shutdown. Therefore, the prior knowledge of their remaining life time is very much essential to maintain the adequate plant safety.

4.2 Methodology

The performance of an electrical cable depends on its insulation resistance (conductor to ground or shield, conductor to conductor) and dielectric strength. High temperature, humidity, radiation and voltage can degrade the insulation resistance beyond a point which may not be acceptable for I&C circuits to maintain the accuracy [119]. A cable failure occurs when the stress is higher than the strength or capacity. For a random loading or strength, the probability that the strength is always greater than the load in mission duration provides product reliability for that time period. From the stress-strength interference (SSI) theory, a cable failure will occur when the current insulation resistance is less than a specified threshold value. The SSI model for stress (S_1) and strength (S_2) relationship is as follows [120]:

$$R = P(S_2 > S_1) \tag{4.1}$$

In regard to the cable life assessment, the insulation resistance of the cable represents the strength of the material and the temperature, humidity, voltage etc. represent various stresses that act on the cable insulation to degrade and result in its eventual failure. Furthermore, if both stress and strength are treated as continuous random variables and their probability density functions denoted by $f_1(S_1)$ and $f_2(S_2)$ respectively, then Eq. (4.1) can be rewritten as the following [121]:

$$R = \int_{-\infty}^{\infty} f_2(S_2) \left[\int_{-\infty}^{S_2} f_1(S_1) dS_1 \right] dS_2 \tag{4.2}$$

The strength, in this case the insulation resistance of cable material, is a function of one or more stresses. The insulation system of a cable consists of a primary insulation, a secondary insulation and a jacket material. All these materials are usually organic compounds typically made from a family of polymers such as polyethylene, polyvinyl chloride; ethylene propylene rubber etc. and they are subjected to various stresses. Therefore, the insulation resistance of a cable can be a time dependent function of stresses such as temperature, humidity, voltage etc. and can be formulated as the following:

$$IR = f(T, H, V, t) \tag{4.3}$$

where, IR is the insulation resistance of the cable material, T is the temperature H is the humidity, V is the applied voltage, t is the time.

Since, temperature is one of the dominant stressors present in an NPP; the proposed methodology has considered temperature as the ageing stress. However, the other stressors such as humidity, radiation, etc. can also be modeled accordingly. The insulation resistance of the insulating system depends upon the number of free electrons available to conduct electricity between the conductor to ground/shield or between conductor to conductor. The number of free electrons in an organic compound depends upon temperature. Keeping the applied voltage V constant at some fixed value V_0, the leakage resistance of the cable insulation system is given by the following equation [119]:

$$IR = R_0 e^{\alpha T} \tag{4.4}$$

where, R_0 = constant depending upon material property (Ω), IR = resistance at temperature T (Ω), α = voltage dependent constant (1/K), T = Ambient temperature (K).

At some ambient temperature T_1, Eq. (4.4) becomes:

$$IR_1 = R_0 e^{\alpha T_1} \tag{4.5}$$

Similarly at an ambient temperature of T_2, Eq. (4.4) becomes:

$$IR_2 = R_0 e^{\alpha T_2} \tag{4.6}$$

Dividing Eq. (4.5) by Eq. (4.6) yields,

$$\frac{IR_1}{IR_2} = e^{\alpha[T_1 - T_2]} \tag{4.7}$$

Taking natural logarithm on both sides of Eq. (4.7) and rearranging for α,

$$\alpha = \frac{ln\frac{IR_1}{IR_2}}{[T_1 - T_2]} \tag{4.8}$$

Similarly at an ambient temperature of T_3, Eq. (4.7) becomes:

$$\frac{IR_1}{IR_3} = e^{\alpha[T_1 - T_3]} \tag{4.9}$$

Substituting for α and rearranging,

$$IR_3 = IR_1 e^{\left(ln\frac{IR_1}{IR_2}\right)\left(\frac{T_1 - T_3}{T_2 - T_1}\right)} \tag{4.10}$$

Due to the upgradation of I&C systems in NPPs, a periodic PSA is carried out to ensure that the adequate safety levels are maintained. Therefore, a time dependent reliability of cables and other equipment taking into account the degradation needs to be evaluated. In order to account for a time dependent degradation of the insulation resistance, let IR_3 be the initial insulation resistance at a given temperature, T and λ be the linear degradation rate due to normal ageing over a time period t, then IR at a given temperature for a period of time t can be formulated as:

$$IR(T,t) = IR_3(1 - \lambda t) \tag{4.11}$$

If the degradation process is assumed to be exponential, then Eq. (4.11) becomes,

$$IR(T,t) = IR_3 e^{-\lambda t} \tag{4.12}$$

Using Eq. (4.11) or Eq. (4.12), the remaining insulation resistance of a cable at time t can be estimated. Now, IR_3 becomes the remaining strength of the cable insulation material. From Eq. (4.2), the reliability of an electrical cable can be estimated at any temperature T as stress. This is further formulated as a structural reliability problem as follows:

A cable is said to be failed when the remaining insulation resistance is less than or equal to a specified threshold value IR_{th} when subjected to one or more stresses. Therefore, the probability of a cable failure is then formulated by the following equation:

$$P_f = P\ (IR \leq IR_{th}) \tag{4.13}$$

Now, this is in the form of a load-resistance relationship and can be solved by using the structural reliability concepts through first or second order reliability methods or Monte Carlo simulation method. However, in this study this problem has been solved by using structural reliability methods through limit state concepts [122].

The limit state function for structural reliability problem can be formulated as:

$$g(IR, IR_{th}) = IR_3 - IR_{th} \tag{4.14}$$

Substituting for IR_3, Eq. (4.14) becomes,

$$g(IR, IR_{th}) = IR_1 e^{\left(ln\frac{IR_1}{IR_2}\right)\left(\frac{T_1 - T_3}{T_2 - T_1}\right)} - IR_{th} \tag{4.15}$$

From the structural reliability methods, the probability of failure is computed from the following relation:

$$P_f = P\ (g(IR, IR_{th}) = IR_3 - IR_{th} \leq 0) \tag{4.16}$$

Substituting for IR_3, Eq. (4.16) becomes,

$$P_f = P\ (g(IR, IR_{th}) = IR_1 e^{\left(ln\frac{IR_1}{IR_2}\right)\left(\frac{T_1 - T_3}{T_2 - T_1}\right)} - IR_{th} \leq 0) \tag{4.17}$$

From structural reliability,

$$P_f = \Phi(-\beta) \tag{4.18}$$

where, P_f is the probability of failure, $\Phi(.)$ is the standard normal cumulative distribution function (CDF) and β is the reliability index, which is defined as the minimum distance from the origin to the limit state surface in the standard normal space [123]. Accordingly, the reliability is given by:

$$R = 1 - P_f \tag{4.19}$$

Thus, reliability of an electrical cable can be estimated from Eq. (4.19) for use in PSA applications as a part of ageing management programs.

In general, when cables are exposed to extreme ambient temperatures their insulation resistance typically drops several orders of magnitude following an exponential behaviour. The acceptable IR level depends on the application; therefore, it is different for a cable used in control circuit, than for a cable used in a power supply circuit. Based on the insulation resistance approach, the USNRC has established a minimum acceptance criterion of $10^6\ \Omega$ over a 1000 foot length of a conductor or cable for applications using less than 1000 volts [1].

This is based on the assumption that for most modern cable insulations such as XLPE, PVC, EPR, etc. the IR drops exponentially as temperature increases and most of the cable insulation materials commonly used in nuclear power plants behave in similar manner; so the IR drops by order of magnitude at the temperature surrounding the cable increases. Since, most of the I&C cables in Indian nuclear power plants operate within the range of 1000 volts the minimum criterion suggested by NUREG/CR-7000 can be adopted as failure criterion in evaluating the life time of cables in this study.

4.3 Analysis and results

In order to validate the proposed methodology and to show the usefulness in assessing the cable life and subsequent application in PSA studies of NPPs, an accelerated life testing data on a typical XLPE I&C cable has been taken from the literature and the probability of failure has been estimated using structural reliability method. The data obtained from the literature is shown in Table 4.1 [124].

Table 4.1: Insulation resistance data on XLPE cable

Sl. No.	Temperature (K)	IR (Ω)
1	375	1.0E+06
2	475	1.0E+05
3	575	1.0E+04
4	675	1.0E+03

From Table 4.1,

IR_1 = 1.0E+06Ω, corresponding to T_1 = 375K,

IR_2 = 1.0E+05Ω, corresponding to T_2 = 475K.

From Eq. (4.10), the new IR can be estimated corresponding to a given temperature T. Table 4.2 shows the predicted values of insulation resistance corresponding to various temperatures from Eq. (4.10).

Table 4.2: Insulation resistance values from proposed methodology

Sl. No.	Temperature (K)	IR Model (Ω)	IR Expt. (Ω)
1	273	1.05E+07	----
2	313	4.17E+06	----
3	333	2.63E+06	----
4	353	1.66E+06	----
5	375	1.0E+06	1.0E+06
6	475	1.0E+05	1.0E+05
7	575	1.0E+04	1.0E+04
8	675	1.0E+03	1.0E+03

Figure 4.1 shows the plot of temperature verses predicted insulation resistance from the IR model.

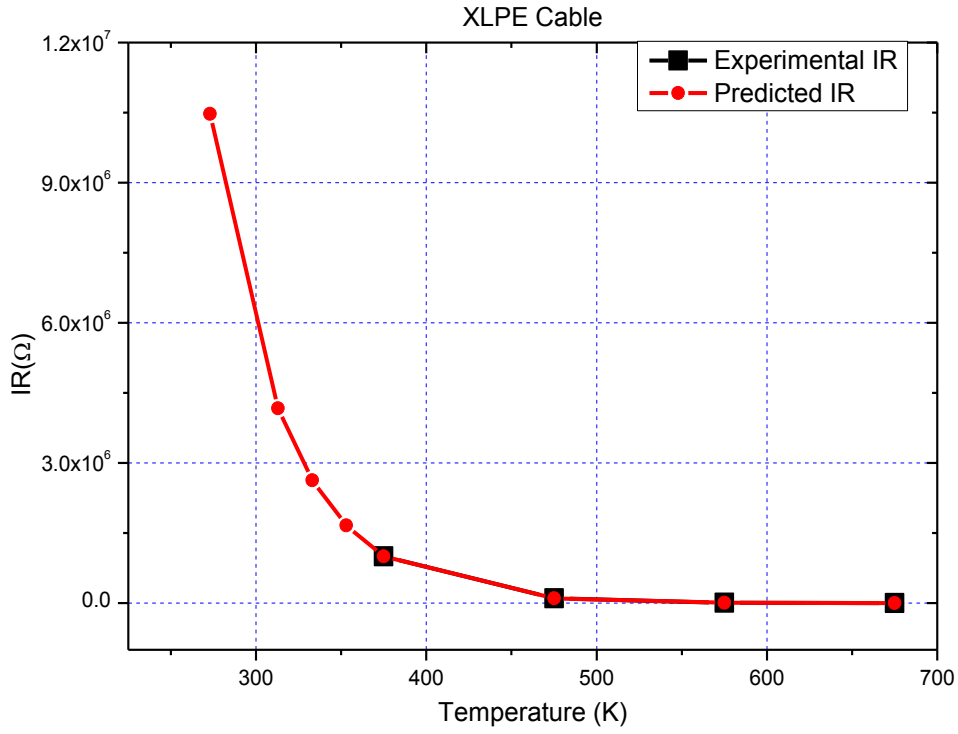

Figure 4.1: Temperature vs. insulation resistance

Considering the degradation rate of 0.02Ω/yr the behaviour of insulation resistance of a typical XLPE cable when exposed to temperature with the degradation rate being either linear or exponential is shown in Figure 4.2.

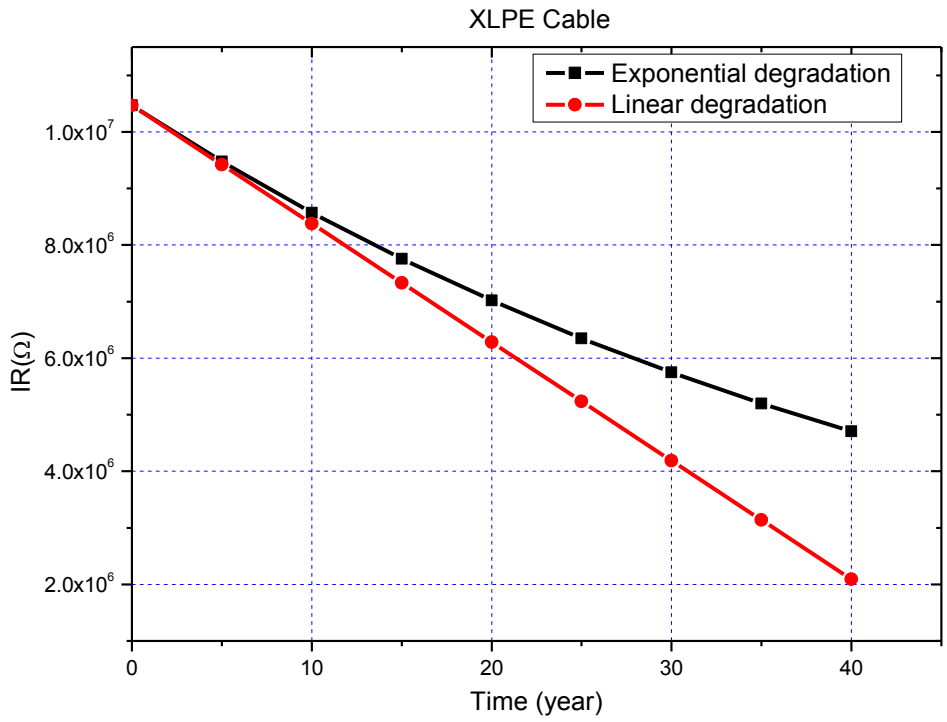

Figure 4.2: Insulation resistance vs. time

The degradation rate considered in this study is only for illustration. However, the actual degradation rate should be considered when performing reliability analysis of specific cable systems of NPP. A periodic insulation resistance measurement yields results on the state of insulation. However, it is practically not possible to carry out an IR measurement on an installed cable in the field. Other alternate methods may include storing the similar cables within the installed environment and carrying out periodic experiments for determining the actual degradation rate.

Now, using the data from Table 4.1, the probability of failure of a typical cable corresponding to a temperature of 40^0C (313K) can be calculated from the structural reliability method. This temperature is chosen under the assumption that most of these I&C

cables in a typical Indian nuclear power plant are operating at this temperature. The input data considered for calculating the reliability of an XLPE cable from the structural reliability method is shown in Table 4.3. The coefficient of variation (COV) values for basic random variables have been taken from the literature.

Table 4.3: Input data for structural reliability problem

Parameter	Distribution	Mean	COV
IR_1	Normal	1.0E+06Ω	0.1
IR_2	Normal	1.0E+05Ω	0.1
IR_{th}	Constant	1.0E+06Ω	----
T_1	Constant	375K	----
T_2	Constant	475K	----
T_3	Constant	313K	----

This problem has been solved by using the first order reliability method from the COMREL [125] tool, which is a standard software tool for solving structural reliability problems. COMREL stands for COMponent RELiability, a module of STRUREL [126] which stands for STRUctural RELiability developed by Reliability Consulting Programs, Germany. Both time-variant and time-invariant reliability evaluations can be performed using COMREL software. COMREL comprises the several structural reliability methods such as first order reliability method (FORM), second order reliability method (SORM), and Monte Carlo simulation (MCS) techniques. The reliability index β corresponding to a temperature of 313K is found to be 5.789 and consequently the probability of failure is 3.56e-9. This is without the consideration of time dependent degradation.

Now, considering the degradation rate of 0.02Ω/yr, the time dependent probability of failure of an XLPE cable corresponding to a temperature of 40^0C (313K) is shown in Figure

4.3. It is evident from Figure 4.3 that P_f increases suddenly after about 30 years of service when the degradation process is linear. This shows that the safety margin is significantly less after about 30 years of service. However, when the degradation is due to temperature the insulation resistance behaviour will usually be exponential. From Figure 4.3, a time dependent probability of failure value obtained can be directly used in the reliability analysis of cable systems for PSA applications as a part of ageing management of NPPs.

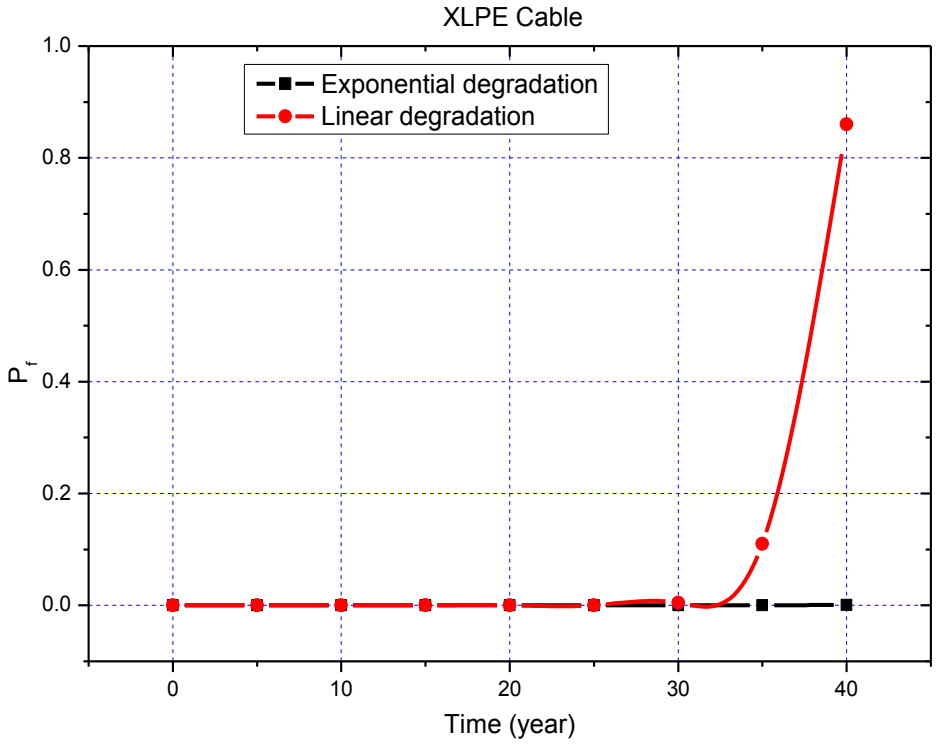

Figure 4.3: Probability of failure vs. time

4.4 Summary

A framework for time dependent reliability prediction of I&C cables for use in PSA of NPP has been developed by considering the thermal aging of XLPE cable as a part of ageing management. The proposed methodology has been illustrated with the data obtained from the literature on a typical XLPE I&C cable. It is clear from the results that with a few sets of accelerated life testing data on a typical XLPE cable the remaining life can be estimated from

the developed methodology. The behaviour of insulation resistance when the degradation process is linear or exponential has been modeled. Also, the time dependent probability of failure model has been developed in order to account for time dependent degradation. The degradation rate considered in this study is only for illustration. However, the actual degradation rate should be considered when performing reliability analysis of specific cable systems. The reliability index or probability of failure obtained from this framework is used in system reliability analysis to account for cable ageing. The proposed methodology can be extended to other degradation mechanisms such as humidity, voltage etc.

Chapter 5 Reliability Prediction of I&C Cables by Artificial Neural Networks

5.1 Introduction

Generally, the lifetime of electrical cables is determined based on accelerated life testing experiments which are not only expensive but also time consuming. Unfortunately, accelerated test procedures normally require a number of specimens to be aged at several temperatures above the normal operating limits. Moreover, the conventional life prediction models may not predict the lifetime accurately as the cable insulation materials have significantly improved over the years in order to account for highly reliable performance features [127-129]. In addition, the test could take a long time and require the compilation of a significant amount of data. In previous works, as one of the intelligent methods, artificial neural networks were used efficiently to assess insulation condition of paper insulated power cables and predict the thermal ageing in transformer oil.

Recently, the use of ANNs has perhaps been the most promising technique in diagnosis and condition monitoring of electrical and other equipment [130-135]. However, their use in degradation assessment and reliability prediction for I&C cables is very limited due to lack of well-established approaches based on ANN. A few researchers [136-137] have applied ANN for lifetime prediction of electrical cables; however there is still no well-defined approach that can be directly applied on the limited accelerated ageing data to obtain the cable reliability. Therefore, one of the important objectives of this study is to develop an integrated approach based on ANN and accelerated laboratory ageing data to predict the reliability of an electrical cable for use in PSA of nuclear power plants. This chapter deals with the reliability

prediction methodology based on ANN from the data collected during accelerated life testing. The methodology has been illustrated for a typical XLPE cable reliability evaluation.

5.2 Methodology

5.2.1 Prediction of times-to-failure

When electrical cables are exposed to extreme ambient temperatures, radiation, voltages, and moisture related environmental conditions encountered in NPP, their properties such as dielectric constant, insulation resistance, Tanδ, elongation at break (EAB) etc. change which are a direct indicative of insulation degradation. Insulation resistance (IR), which is one of the important performance parameter typically, drops several orders of magnitude under such extreme ageing conditions. When IR drops below $10^6\Omega$, as suggested in NUREG/CR-7000 [1] or EAB going below 50% absolute [4], the cable will no longer fulfill the desired performance and therefore considered to be failed. The property, such as IR or EAB measured at regular intervals of time during accelerated ageing will serve as an input to ANN. And the trend of the times-to-failure against stressor such as temperature or voltage is used for modelling ANN for lifetime prediction.

In this study, the approach is illustrated considering IR as performance parameter and temperature as stressor; however the procedure can be extended to any other performance indicator and stressor of interest. The acceptance criterion adopted in this study while developing the methodology is that the cable is said to be failed when IR drops below $10^6\Omega$ at any given temperature as suggested in NUREG/CR-7000 [1]. The accelerated ageing experiments are carried out and the performance parameters such as IR, elongation at break (EAB), oxidation induction time (OIT), etc. are measured at regular intervals of time to capture the trend of the failure distribution. This trend is used to train the ANN for predicting

the future value of performance parameter. The formulation of ANN based life prediction methodology is explained in the following sections:

Let T be the accelerated ageing temperature in K, IR be the insulation resistance in Ω, and t be the time to failure (TTF) of an electrical cable under accelerated ageing test condition. Let (T_i, IR_i, t_i) for $i = 1, \dots, n$ be the accelerated life test result-set for training the ANN. Here, n is the size of result-set. To predict the future value of t_{n+1} from a set of measured data t_i the algorithm will be trained with a set of samples having the form (T_i, IR_i, t_i) for $i = 1, \dots, n-1$. After this iteration, the weights of the network are updated so that when the network receives the value t_i, its response will be t_{i+1}. The training is repeated with $n+1$ values of t_i, $i = 1, \dots, n+1$. The training is repeated from the beginning in order to predict the value t_{n+2}, the new set of data will now contain $n+2$ values of t_i, $i = 1, \dots, n+1$. This training process is repeated until the prediction of all values that constitute the remainder of the property of the studied curve is obtained.

In order to improve the efficiency of the network, after each future value prediction, the first value can be omitted from the set of data. For example, t_1 can be omitted after predicting t_{n+1}, and t_2 after predicting t_{n+2}, etc. Thus, the size of the training data is same for any future value prediction. However, care must be taken to ensure that the trend of parameter predicted from ANN is relatively in good agreement with that of experimental trend. Otherwise the entire previous data should be used for training the ANN for future property prediction.

In order to account for a synergistic effect, multiple stressors such as temperature, humidity, radiation (generally present in any NPP) can be easily modeled with neural networks. In such case, the sample training set becomes $(T_i, RH_i, D_i, IR_i, t_i)$ for $i = 1, \dots, n$. Here, T_i is the accelerated temperature, RH_i is the relative humidity and D_i is the radiation

dose. Thus, the combined effect of various stressors can be accounted in the assessment of cable reliability.

To validate the proposed methodology and to show the strength of ANN in predicting the cable reliability for use in PSA application of NPPs accelerated life testing data (as shown in Table 5.1) on a typical cross-linked polyethylene (XLPE) I&C cable has been referred from the literature [124]. The times to failure shown in Table 5.1 correspond to IR below the suggested value [1] which is considered as the failure criterion for the cable. For training ANN, reasonably large amount of data is required. However, it is not possible to generate sufficiently large amount of data by subjecting many samples under long accelerated life testing experiments. Generally, only the trend of the data is sufficient for ANN to learn the patterns [138].

Table 5.1: Accelerated life testing data on XLPE cable

Sl. No.	Temperature (^{0}C)	TTF (min)
1	330	28
2	350	13
3	370	9
4	390	7
5	410	5
6	430	4
7	450	3
8	470	2
9	490	1

The training and testing sets have been prepared from the data shown in Table 5.1. Since the data shown in Table 5.1 correspond to IR below $10^6\Omega$, which is same in every data set, it is therefore appropriate to omit IR data from the training set and the resulting training set will

have the form (T_i, t_i), i.e. only ageing temperature and TTF are sufficient to train the ANN. However, when the ageing experiments are terminated before the end-of-life criterion is met (i.e. if IR is greater than $10^6\Omega$); in such cases the IR values should also be part of training data for future value prediction. The data in Table 5.1 have been obtained after a complete failure of the sample by subjecting to a highly accelerated life test (HALT) [124]; however tests can be terminated well in advance once the successful trend of the failure distribution is obtained when ANN is employed. To predict the TTF corresponding to temperature 410^0C (Sl. No. 5 in Table 5.1), the previous four data sets are used for training.

Similarly, to predict the TTF corresponding to temperature 430^0C (Sl. No. 6 in Table 5.1), the preceding four data sets are used for training (i.e., data at Sl. No. 1 in Table 5.1 is omitted if the predicted trend is relatively in good agreement with experimental trend) and so on. Thus, the accelerated life testing experiment is terminated once the prediction from ANN is found satisfactory. The training data for two sample cases is shown in Table 5.2 and Table 5.3 respectively. The data in Table 5.1 is obtained under failure-terminated accelerated life testing experiment, however in general it is not practical to subject all the samples to fail under test. The main aim of using ANN is to save samples from complete failure and collect the trend of the failure at the early degradation state and terminate the experiment so that the future property can be predicted without further experiment.

Table 5.2: Training data for first value prediction

Sl. No.	Temperature (^{0}C)	TTF (min)
1	330	28
2	350	13
3	370	9
4	390	7

Table 5.3: Training data for second value prediction

Sl. No.	Temperature (^{0}C)	TTF (min)
1	350	13
2	370	9
3	390	7
4	410	5.23

After successful prediction is obtained from the ANN model, the TTF corresponding to a normal operating temperature can be predicted. The environmental temperature in NPPs under normal conditions is usually about 40^0C. As can be seen in Table 5.1 there is no data reported in [124] between 40^0C and 330^0C, hence predicting TTF corresponding to normal operating condition may require the regression analysis of the predicted data to derive an empirical model. Therefore, when conducting accelerated ageing experiments care must be taken to ensure that data collected could be easily transformed to the operating condition for life assessment studies.

5.2.2 Reliability prediction

Once the TTF corresponding to normal operating condition is predicted from the ANN model or from the regression model (if applicable), the reliability or probability of failure can be estimated using the generalized Weibull reliability model [139]. The Weibull distribution is commonly used in reliability studies. It is well suited to fitting the 'weakest-link' properties of typical lifetime data [140]. Different mechanisms of failure can sometimes be differentiated by the Weibull parameters. The hazard rate function of a two-parameter Weibull distribution is given by:

$$\lambda(t) = \frac{\beta}{\eta}\left(\frac{t}{\eta}\right)^{\beta-1};\ \eta > 0, \beta > 0, t \gg 0 \tag{5.1}$$

where, η is the scale parameter or characteristic life, β is the shape parameter or slope of the distribution and t is the time. The probability density function is given by:

$$f(t) = \frac{\beta}{\eta}\left(\frac{t}{\eta}\right)^{\beta-1} e^{-\left(\frac{t}{\eta}\right)^{\beta}} \tag{5.2}$$

The reliability function for Weibull distribution is given by:

$$R(t) = e^{[-\int_0^t \lambda(t)dt]} \tag{5.3}$$

Substituting Eq. (5.1) in Eq. (5.3) and integrating, we get the following expression for Weibull reliability.

$$R(t) = e^{-\left(\frac{t}{\eta}\right)^{\beta}} \tag{5.4}$$

Consequently, the unreliability or probability of failure is given by:

$$F(t) = 1 - R(t) \tag{5.5}$$

$$F(t) = 1 - e^{-\left(\frac{t}{\eta}\right)^{\beta}} \tag{5.6}$$

In this study, the probability of failure corresponding to normal operating condition cannot be estimated as the use condition TTF may not be accurately predicted from ANN due to the absence of TTF data between 40^0C to 330^0C. However, regression analysis of the predicted data results in an empirical life-stress model which can be used to determine the TTF under use condition. With this TTF, the probability of failure of cable corresponding to normal operating condition is estimated for use in reliability analysis of NPP systems.

5.3 Selection of learning algorithm and network architecture

Artificial neural network is an information processing paradigm that is inspired by the way the biological nervous systems, such as the brain, process information etc. ANN is a

system modeled based on human brain. The field goes by many names, such as connectionism, parallel distributed processing, neuro-computing, natural intelligent systems, machine learning algorithms, and artificial neural networks. ANNs, like humans, learn by examples [141-143]. It is an attempt to simulate, within specialized hardware or sophisticated software, the multiple layers of neurons. Each neuron is linked to a few of its neighbours with varying coefficients of connectivity that represent the strengths of these connections. Learning is accomplished by adjusting these strengths to cause the overall network to produce appropriate results [144-145].

5.3.1 Selection of learning algorithm

In order to find an efficient learning algorithm for the life prediction problem, an optimization study has been carried out considering several learning algorithms [146]. The algorithms considered in this study are the Standard Back Propagation, Resilient Back Propagation, Quick Propagation, Manhattan, Delta Bar Delta, etc. Before selecting any algorithm for training, network architecture has to be defined for the selected problem. In order to define the architecture, a set of input and output parameters needs to be identified. Since, the number of input and output neurons in a neural network is fixed for a given problem; the optimum network architecture depends on the selection of number of hidden layers and neurons in each hidden layer.

In a neural network, the number of hidden layer neurons is usually determined from trial and error approach. But, if the number of neurons in the hidden layer is too large, the network will get an over fit. The training set of data will be memorized and thus, making the network ineffective on test data. Again, in order to maintain the computational efficiency, only one or two hidden layers are generally considered for most of the problems. It is found from the experience that, 2/3rd of input plus the number of output neurons would be a good choice for

the hidden layer [147-148]. With these parameters, a network consisting of 39 inputs, 27 hidden and one output neuron was defined for optimization study. The sigmoid activation and the mean square error functions were used for training. The target error considered in all these algorithms was 1.0E-10. The results of the optimization study are shown in Table 5.4.

Table 5.4: Results of optimization study

Learning algorithm	Epochs	Minimum error	Percentage error (%)	CPU time (sec)
Resilient back propagation (Batch)	95463	3.82E-11	3.25	5472.204
Standard back propagation (Pattern)	325611	9.95E-11	8.98	21866.031
Back propagation with momentum (Pattern)	262335	9.96E-11	7.59	12242.47
Back propagation with momentum (Batch)	550100	5.50E-09	8.62	23561.66
Quick propagation (Batch)	484793	3.60E-10	10.92	25537.04
Manhattan (Batch)	459126	4.90E-09	11.74	23729.23
Delta bar delta (Batch)	504532	8.20E-10	9.67	27836.45

It is seen from the study that the resilient back propagation learning algorithm has converged to an optimum solution more efficiently than the other algorithms. Moreover, some of the algorithms were forced to terminate as they were taking too many iterations without considerable reduction in the error. Hence, resilient back propagation algorithm is employed for life prediction. The batch mode and the pattern mode of training are the two training schemes of the learning algorithms. Although, it is not possible to describe all these algorithms, it is however appropriate to discuss the concepts of the resilient back propagation algorithm in this study.

5.3.1.1 Resilient back propagation algorithm

Resilient back propagation algorithm is a local adaptive learning scheme performing supervised batch learning in multi-layer perceptrons. The basic principle of this algorithm is to eliminate the harmful influence of the size of the partial derivative on the weight step. Consequently, only the derivative is considered to indicate the direction of the weight update.

5.3.1.2 Learning rate factors

There are two factors associated with the learning rate: The learning-rate increment factor η^+, and the learning-rate decrement factor η^-. The most suitable values for η^+ and η^-, found experimentally, are 1.2 and 0.5 respectively [146].

5.3.1.3 Step size

While learning starts, all the update-values are set to an initial value Δ_0. In order to prevent the weights becoming too small, the lower bound is set to the minimum weight-step by Δ_{min}, and to prevent the weights becoming too large, the upper bound is set to the maximum weight-step by Δ_{max}.

5.3.1.4 Working principle

Here, the update value Δ_{ij}, for each weight, determines the size of the weight update. This adaptive update-value evolves during the learning process based on its local sight of the error function E, according to the following learning rule:

$$\Delta_{ij}(t) = \begin{cases} \eta^{+} * \Delta_{ij}(t-1), if\ \frac{\partial E}{\partial w}(t-1) * \frac{\partial E}{\partial w}(t) > 0 \\ \eta^{-} * \Delta_{ij}(t-1), if\ \frac{\partial E}{\partial w}(t-1) * \frac{\partial E}{\partial w}(t) < 0 \\ \Delta_{ij}(t-1), else \\ For\ 0 < \eta^{-} < 1\eta^{+} \end{cases} \quad (5.7)$$

Once the update-value for each weight is adapted, the weight update is done as under

$$\Delta w_{ij}(t) = \begin{cases} -\Delta_{ij}(t), if\ \frac{\partial E}{\partial w}(t) > 0 \\ +\Delta_{ij}(t), if\ \frac{\partial E}{\partial w}(t) < 0 \\ 0, else \end{cases} \quad (5.8)$$

However, there is one exception: if the partial derivative changes its sign, it indicates that the previous weight step was too large and the minimum was missed. Hence, the previous weight update is reverted as:

$$\Delta w_{ij}(t) = -\Delta w_{ij}(t), if\ \frac{\partial E}{\partial w}(t-1) * \frac{\partial E}{\partial w}(t) < 0 \quad (5.9)$$

In addition, $\frac{\partial E}{\partial w}(t) = 0$ is set to avoid the update being done twice.

5.3.1.5 Sigmoid activation function

This function is continuous and differentiable, rotationally symmetric about some point, and asymptotically approaches their saturation values. The sigmoid acts as a squasher compressing the input function when it takes large positive or large negative values. Large positive values asymptotically approach one, while large negative values are squashed to zero. The sigmoid activation function is given by the following expression:

$$T(f) = \frac{1}{1+e^{-(\lambda f)}} \quad (5.10)$$

The parameter λ is known as the abruptness factor which determines the steepness of the function. The variable *f* is defined as a scalar product of the weights and input vector.

5.3.1.6 Mean square error function

The mean square error is given by the following expression:

$$E = \sum_p \sum_i \frac{1}{2p} e_i^2 \tag{5.11}$$

where E is the error function, e is the difference between the desired and the calculated output, p is the number of patterns in a training set, and i is the number of outputs.

5.3.2 Selection of network architecture

In this study, as there is only one neuron in the input layer (accelerated ageing temperature) and one neuron in the output layer (time-to-failure) it very important to select a suitable number of hidden layers and neurons in each hidden layer such that future property can be predicted efficiently and accurately. Hence, several architectures were tried to arrive at optimum network architecture with the resilient back propagation learning algorithm. The training and testing datasets for selecting best suitable network architecture is shown in Table 5.5 and 5.6 respectively.

Table 5.5: Training dataset

Sl. No.	Temperature (^{0}C)	TTF (min)
1	330	28
2	370	9
3	410	5
4	450	3

The dataset for the prediction of unseen data from the tested network is shown in Table 5.7. The input data is selected such that the training and testing phase will have the data set

uniformly distributed. However, the data at Sl. No. 8 and 9 of Table 5.1 was not used for either training or testing as this is predicted from the tested network.

Table 5.6: Testing dataset

Sl. No.	Temperature (^{0}C)	TTF (min)
1	350	13
2	390	7
3	430	4

Table 5.7: Prediction dataset

Sl. No.	Temperature (^{0}C)	TTF (min)
1	470	2
2	490	1

The various network architectures chosen for selecting a best suitable architecture are shown in Table 5.8. The architecture at Sl. No. 1 refers to 1 input, 1 output and 1 hidden layer with 2 neurons and the architecture at Sl. No. 2 refers to 1 input, 1 output and 2 hidden layers with 2 neurons in each layer, etc.

The performance of various networks is shown in Figure 5.1 and the calculated TTF from various networks are shown in Figure 5.2. The TTFs predicted from various tested networks are also shown in Figure 5.3.

Table 5.8: Network architectures

Sl. No.	Architecture
1	1-2-1
2	1-2-2-1
3	1-2-3-1
4	1-3-2-1
5	1-3-1
6	1-3-3-1
7	1-3-4-1
8	1-4-3-1
9	1-4-1
10	1-4-4-1

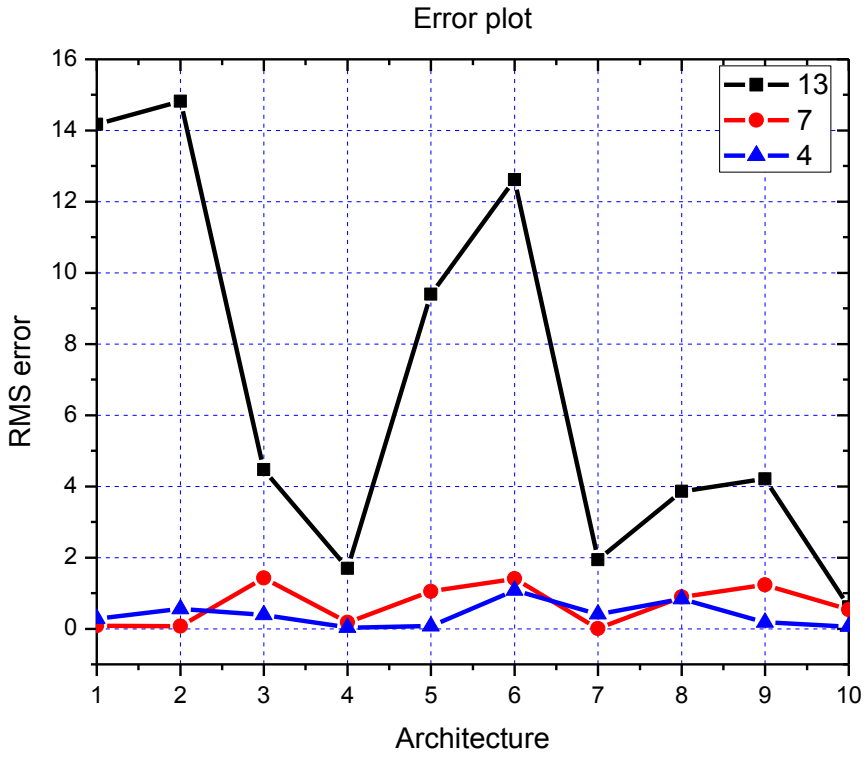

Figure 5.1: Performance of various networks

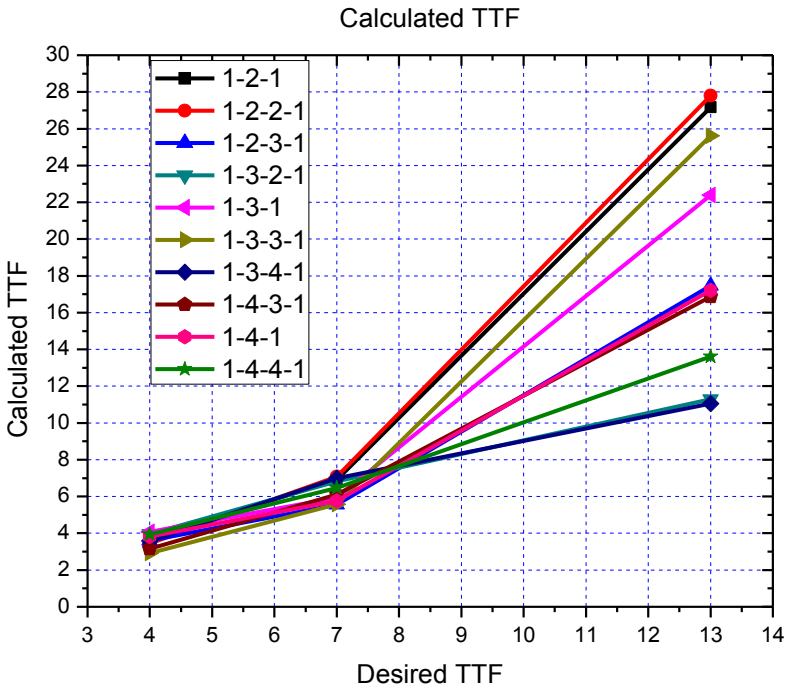

Figure 5.2: Calculated TTF from various networks

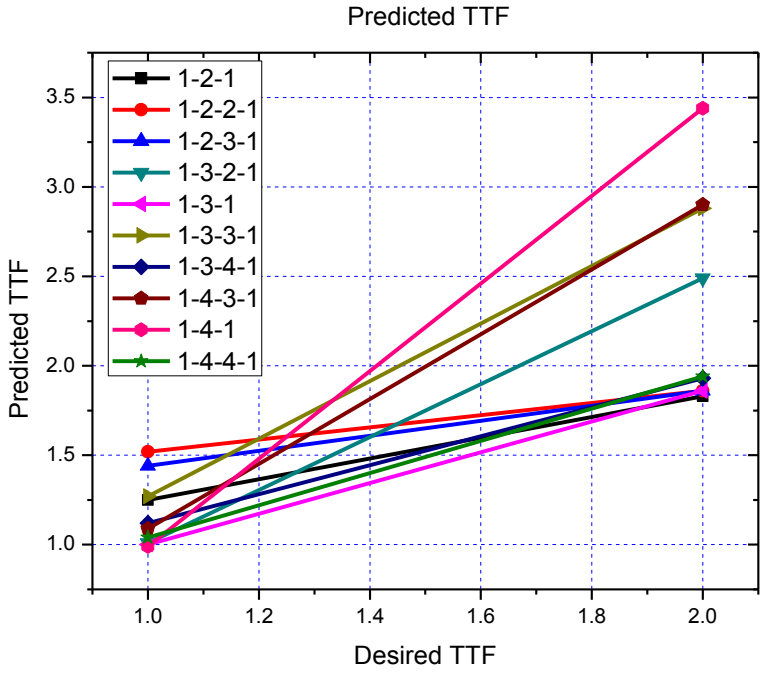

Figure 5.3: Predicted TTF from various networks

It can be observed from the ANN results that in both testing and prediction phase the architecture at Sl. No. 10 of Table 5.8 has performed well for all the TTFs compared to other architectures considered in this study. As there is large gap in the input data between TTFs 9 and 28 all architectures fail to predict the case of TTF 13 however, architecture at Sl. No. 10

of Table 5.8 has managed to predict more closely to the desired TTF. Hence, it is very important to carry out an optimization study on selecting learning algorithm as well as network architecture for more accurate and efficient prediction of the future property.

5.4 Times-to-failure prediction and development of life-stress model

Based on the optimization study discussed in previous section the resilient back propagation learning algorithm and architecture at Sl. No. 10 of Table 5.8 have been employed for predicting the future TTF for reliability prediction of I&C cables. With the selected learning algorithm and network, the best performed network with two hidden layers and four neurons in each layer is shown in Figure 5.4. The performance of ANN with resilient back propagation algorithm is shown in Figure 5.5. The batch learning technique has proved a better performance for the prediction network comparing to the pattern learning technique. There were many parameters to adjust including the number of hidden layers, learning rate parameter and momentum coefficient, etc. to find an efficient network model for this study. The learning rate parameter and the size of the hidden layer were key elements in deciding the best performing network.

Based on the approach discussed, the TTFs of I&C cable have been predicted from the final adopted ANN model and the plot of experimental TTFs and ANN prediction is shown in Figure 5.6.

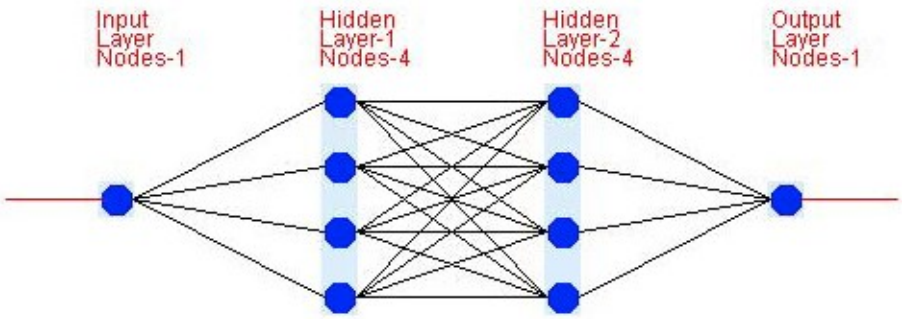

Figure 5.4: Network architecture

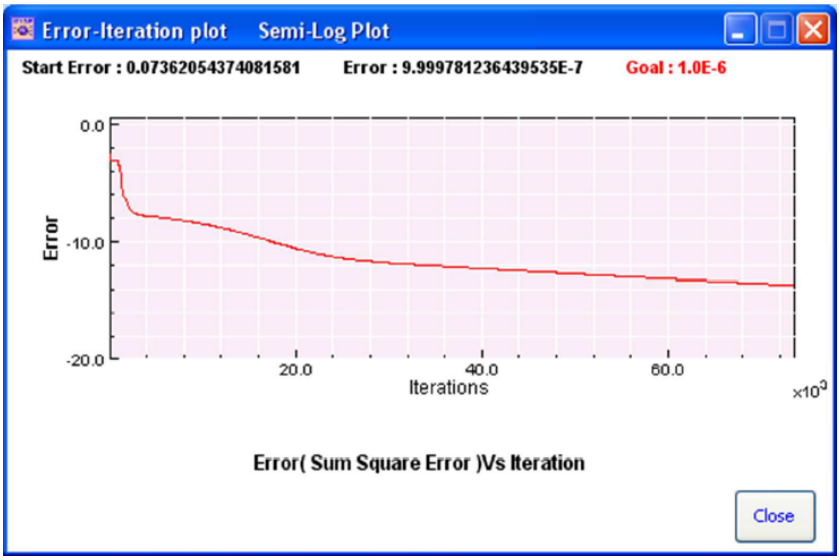

Figure 5.5: ANN performance

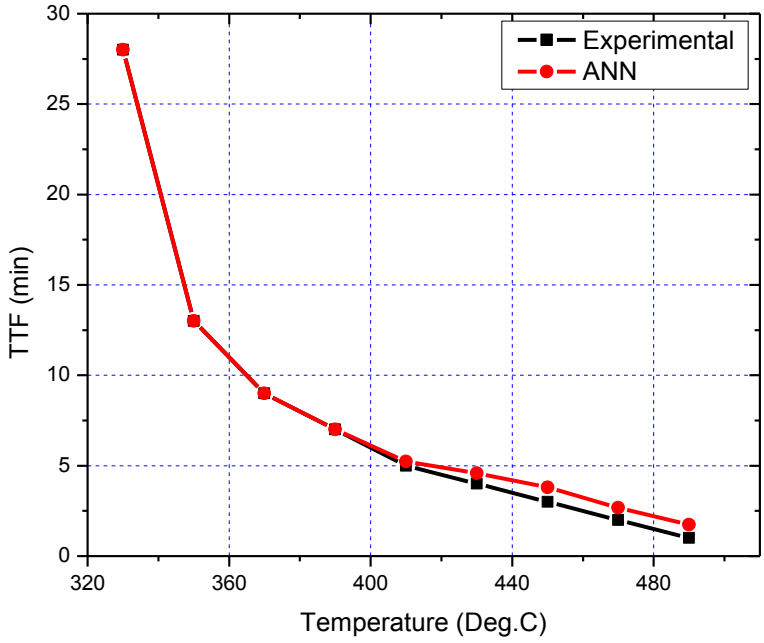

Figure 5.6: TTF from ANN and HALT [124]

In order to determine the reliability of the cable, TTF corresponding to use condition (40^0C) needs to be predicted. In view of this, a life-stress model of the cable has been determined from the regression analysis. The exponential fit of the experimental data with coefficient of determination of 0.97 is shown in Figure 5.7. The life-stress model is shown in Eq. (5.12) and the corresponding model parameters are shown in Table 5.9.

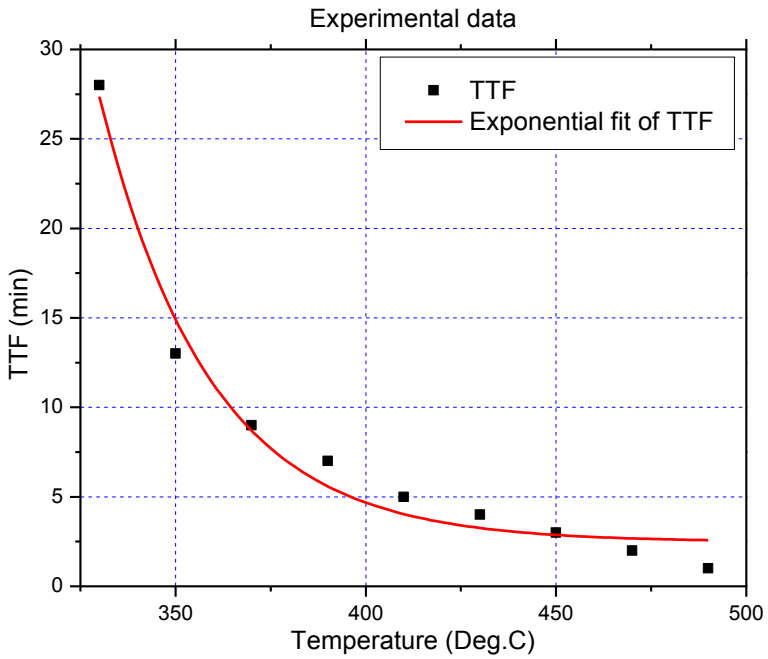

Figure 5.7: Exponential fit of TTF of experimental data

Table 5.9: Experimental data model

Parameter	Value	Standard error
A	2.48297	0.74608
B	2.3164e6	3.6585e6
C	0.03467	0.00478

$$TTF = A + Be^{-cT} \tag{5.12}$$

Similar analysis was carried out to determine the life-stress model from the ANN predicted data and the exponential with coefficient of determination of 0.98 is shown in

Figure 5.8. The life-stress model is shown in Eq. (5.13) and the corresponding model parameters are shown in Table 5.10.

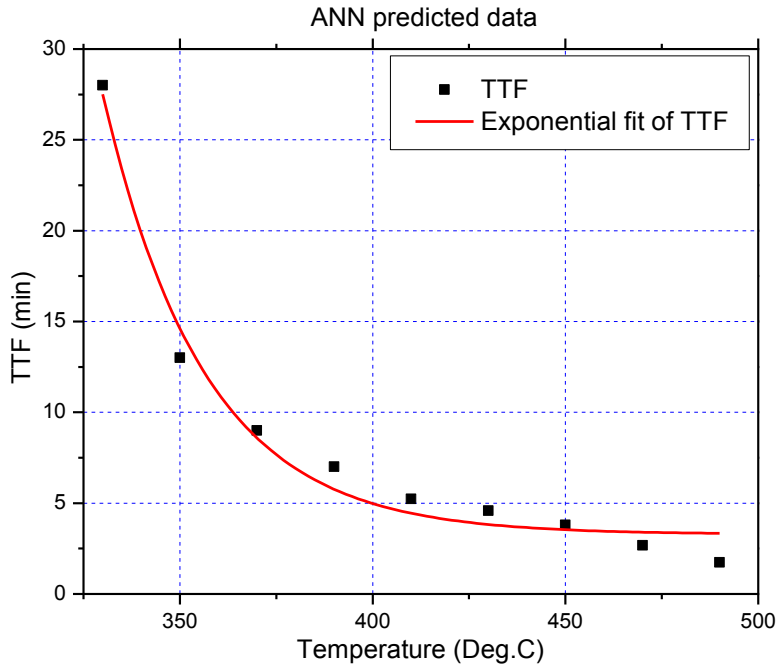

Figure 5.8: Exponential fit of TTF of ANN data

Table 5.10: ANN data model

Parameter	Value	Standard error
A	3.28343	0.64446
B	6.6963e6	1.08564e7
C	0.03797	0.0049

$$TTF = A + Be^{-cT} \tag{5.13}$$

From the above analysis, the TTF corresponding to use condition (40^0C) has been predicted from both experimental and ANN regression models for reliability estimation.

5.5 Determination of life distribution and reliability prediction

The life distribution which explains the failure characteristics of the components under test or use is important information to be required in the reliability analysis. Hence, probability plotting has been carried out to determine the life distribution from the data collected during HALT and predicted from the ANN. The Weibull probability plots for experimental data and ANN data without the use condition TTF are shown in Figure 5.9 and 5.10 respectively. The Weibull probability plots for experimental data and ANN data with the use condition TTF are shown in Figure 5.11 and 5.12 respectively. The parameters of the Weibull distribution and use condition TTFs are shown in Table 5.11.

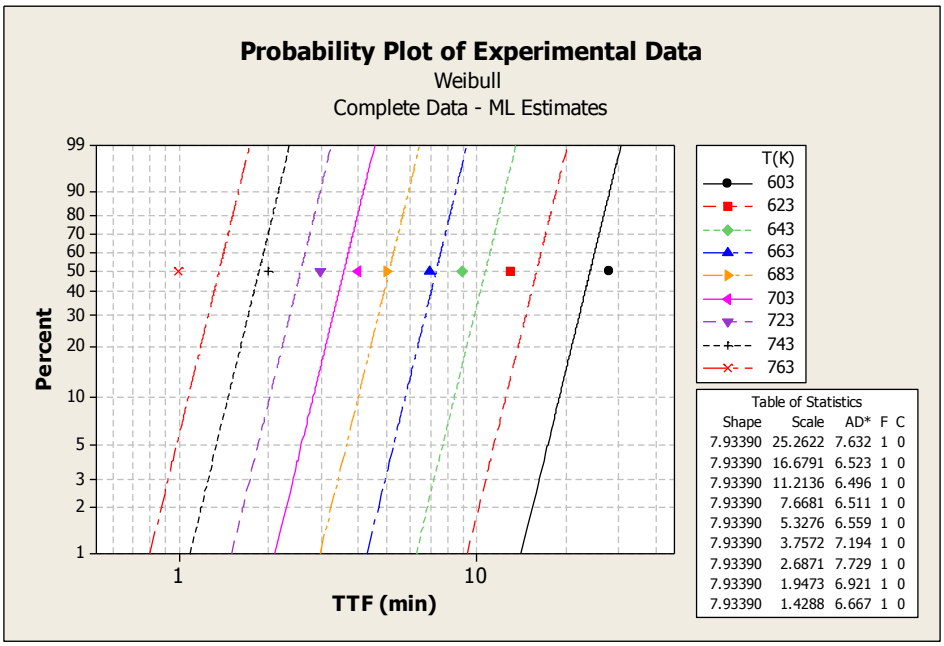

Figure 5.9: Weibull plot of experimental TTFs

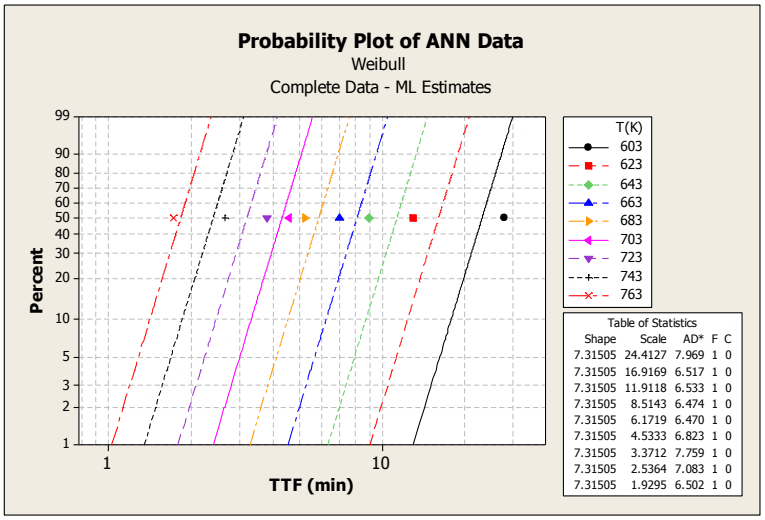

Figure 5.10: Weibull plot of ANN predicted TTFs

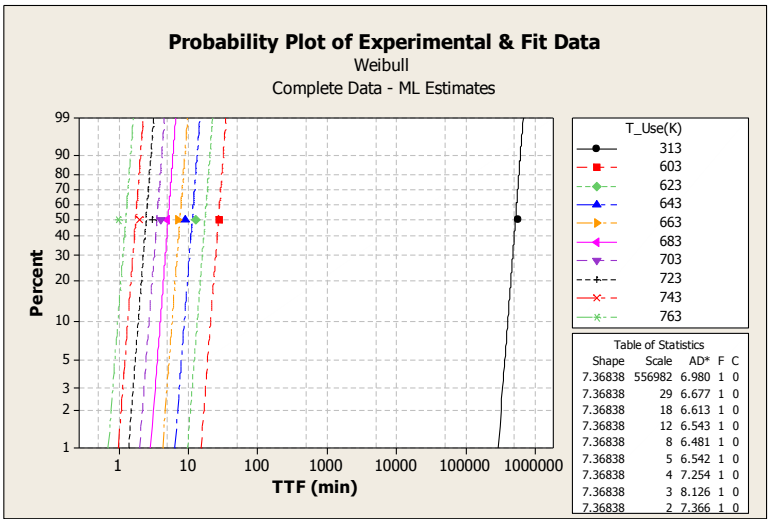

Figure 5.11: Weibull plot of experimental TTFs with use condition TTF

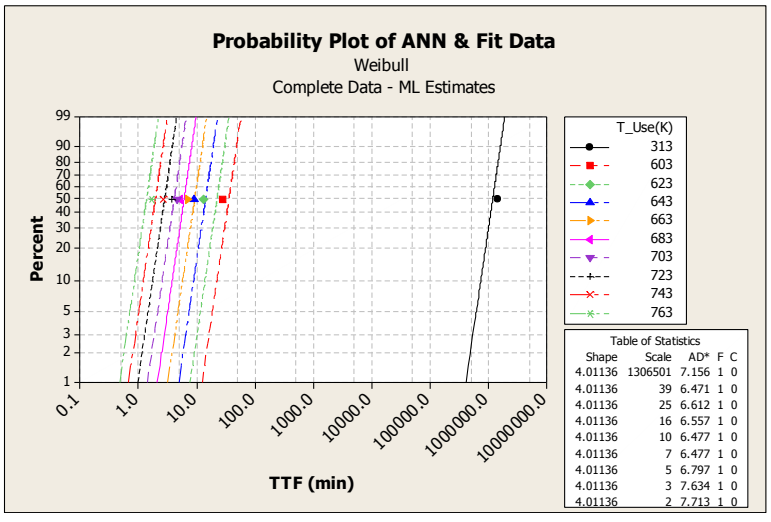

Figure 5.12: Weibull plot of ANN predicted TTFs with use condition TTF

Table 5.11: Parameters of the Weibull distribution and use condition TTF

Weibull plot	β	η (years) at 40^0C	Use condition TTF (min)	Use condition TTF (min)
Experimental	7.9339		-	-
ANN	7.31505		-	-
Experimental with use condition TTF	7.36838	1.0597	578809	1.1
ANN with use condition TTF	4.01136	2.485	1466322	2.8

As can be seen from Table 5.11 the shape parameters obtained from the ANN predicted TTFs are slightly deviated from that of experimental TTFs. This is due to the fact that the regression model arose from ANN study has TTFs with certain degree of deviation from the experimental TTFs during training phase due to insufficient training data. However, this can be taken care by adequate training data with proper network and learning algorithm. From the parameters of the distribution analysed, the time dependent reliability from the experimental TTFs and ANN predicted TTFs is estimated from the two parameter Weibull reliability function as given in Eq. (5.4) and the reliability shown in Figure 5.13.

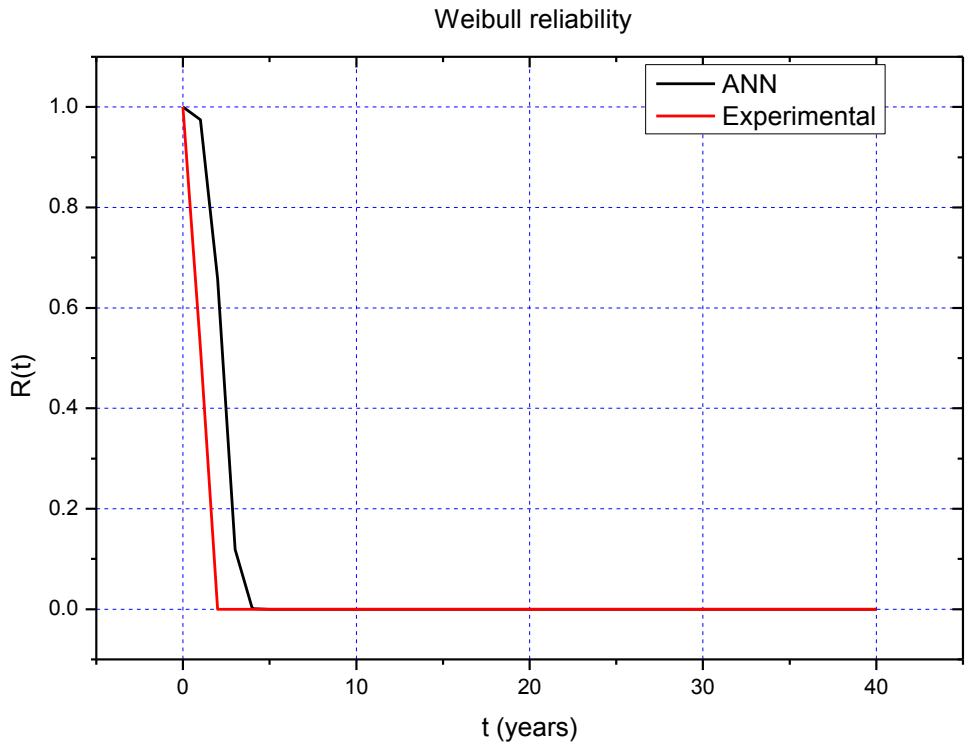

Figure 5.13: Reliability from the Weibull fit of TTFs

The analysis was extended by considering the exponential distribution of the TTF. The probability plots of exponential distribution are shown in Figure 5.14 to 5.17. From the data analysis, the mean time to failure (MTTF) from experimental and ANN predicted TTFs is found to be 1.046 and 2.31 years respectively as shown in Table 5.12.

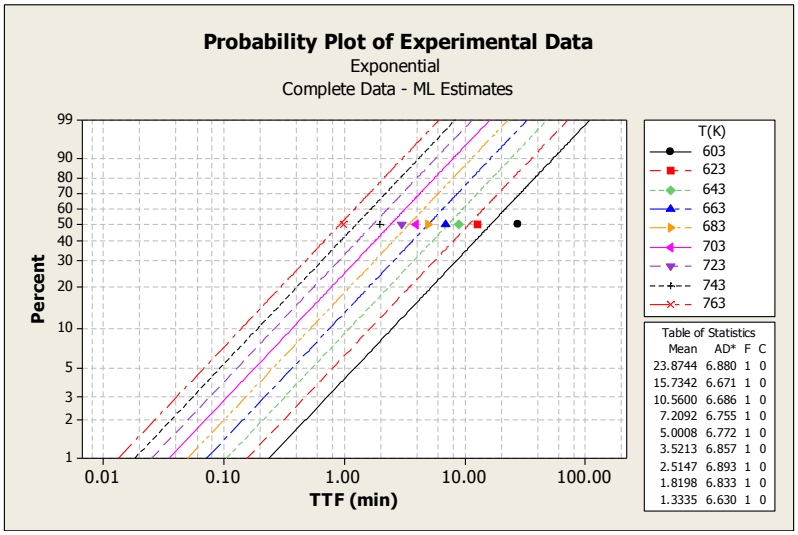

Figure 5.14: Exponential plot of experimental TTF

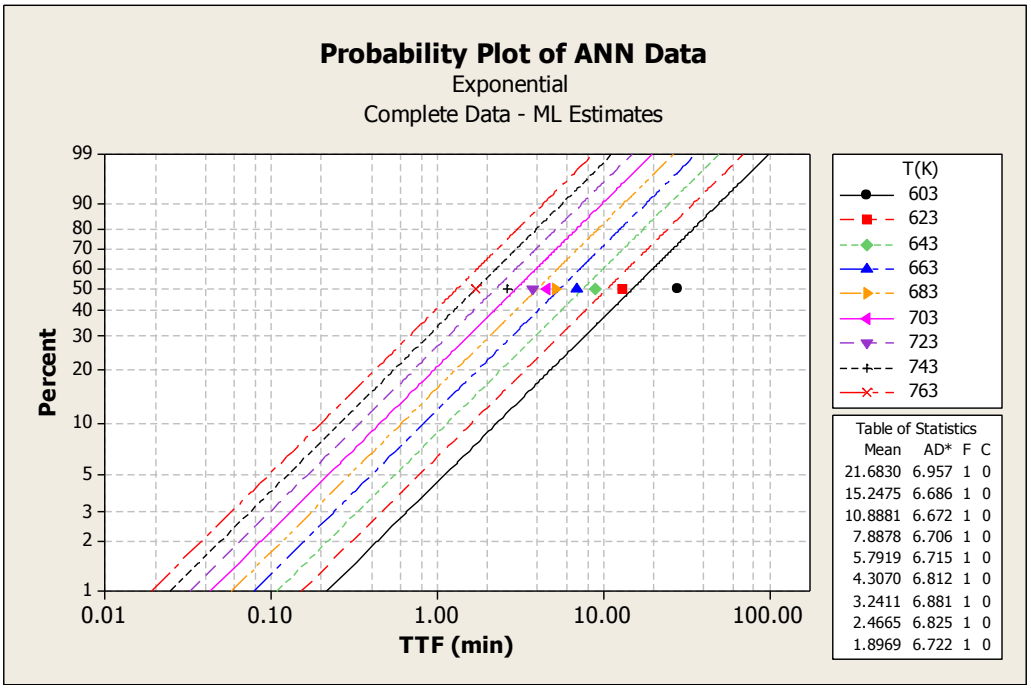

Figure 5.15: Exponential plot of ANN predicted TTFs

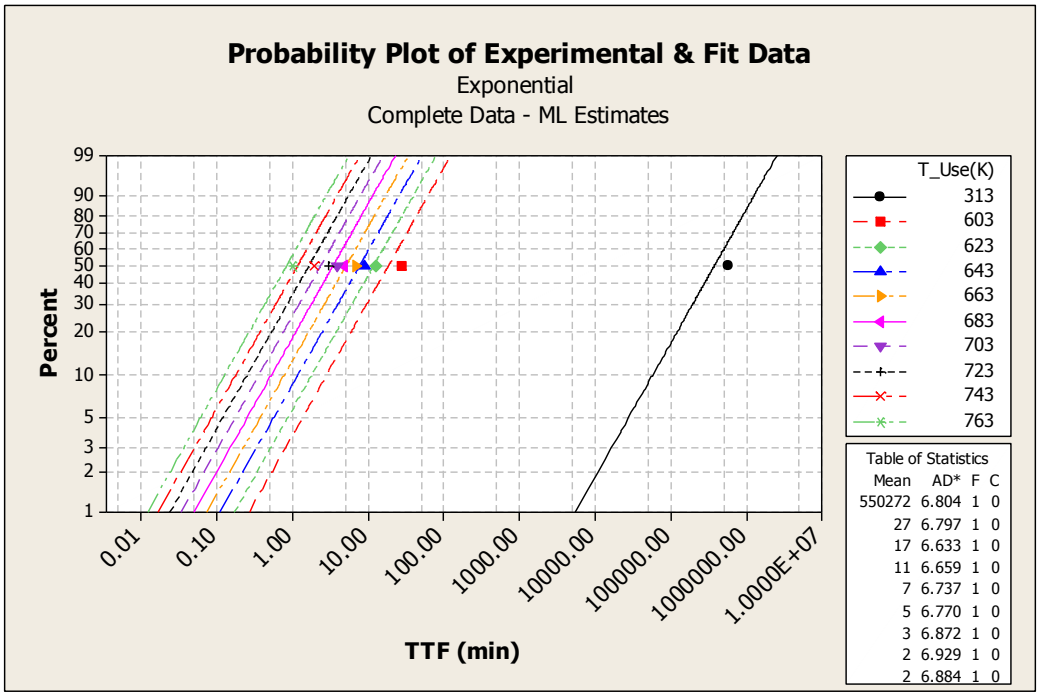

Figure 5.16: Exponential plot of experimental TTF with the use condition TTF

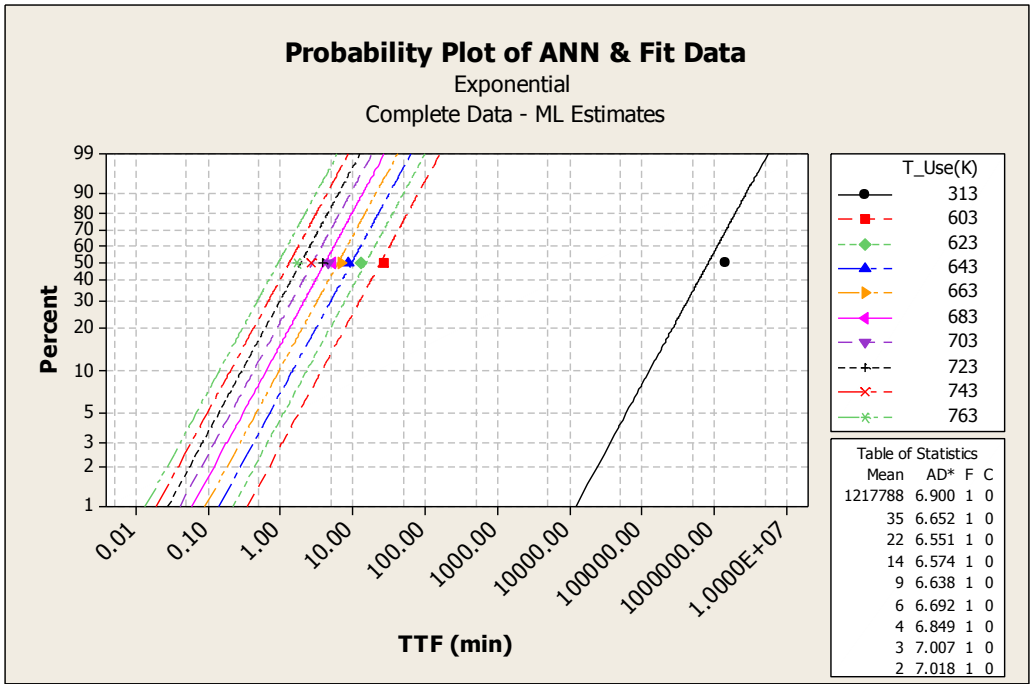

Figure 5.17: Exponential plot of ANN predicted TTF with the use condition TTF

It should be noted here that such low MTTFs are expected as the data reported in [124] is for samples subjected to a highly accelerated condition. The time dependent reliability from the experimental and ANN predicted TTFs is shown in Figure 5.18.

Table 5.12: Parameters of the exponential distribution and use condition TTF

Exponential plot	MTTF (year) at 40^0C	Use condition TTF (min)	Use condition TTF (year)
Experimental	-	-	-
ANN	-	-	-
Experimental with use condition TTF	1.046	578809	1.1
ANN with use condition TTF	2.31	1466322	2.8

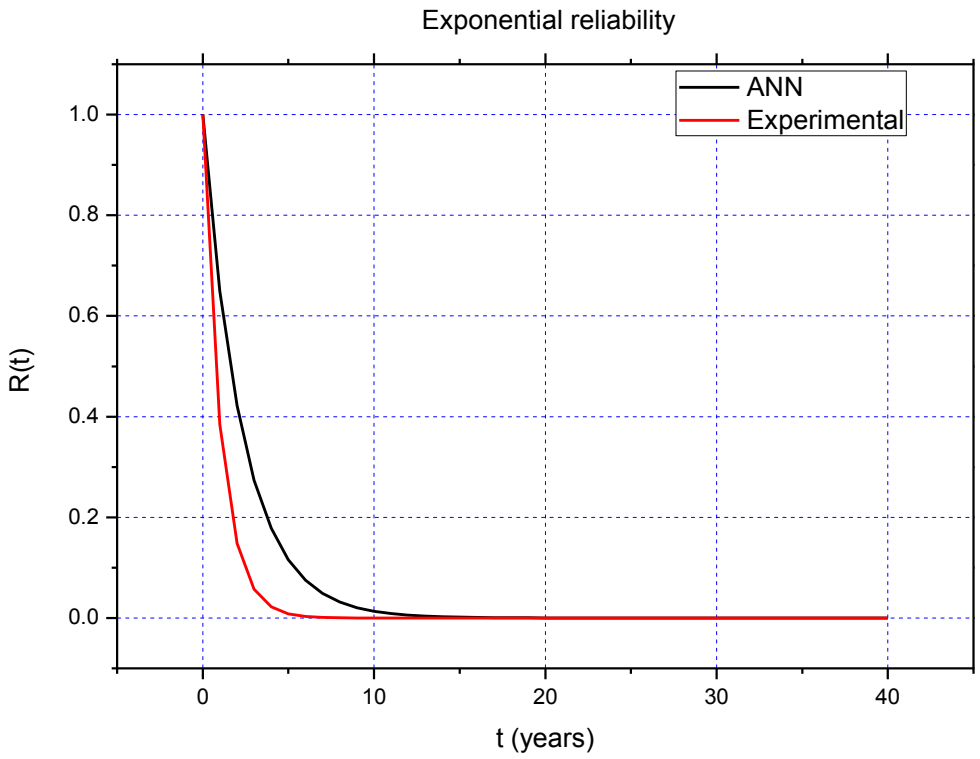

Figure 5.18: Reliability from the exponential fit of TTFs

From Figure 5.13 and 5.18, it can be seen that a high values of β (shape parameter) in Weibull distribution makes reliability decreasing steeply during the early stage of useful life as the components are subjected to HALT. Therefore, it is important to follow the guidelines suggested in [17-18] to design appropriate test conditions such that the use condition can be simulated more accurately. Based on the results obtained from the developed ANN framework, it can be demonstrated that by selecting appropriate training algorithm with suitable network architecture, it is possible to predict the reliability by ANN from the limited accelerated ageing data.

5.6 Summary

An approach based on ANNs has been developed for reliability prediction of I&C cables for use in PSA applications. The methodology has been illustrated with the data referred from

the literature on a typical XLPE I&C cable. It is concluded from the analysis results that with a few sets of accelerated life testing data the reliability can be predicted from artificial neural networks. The reliability or probability of failure obtained from the developed methodology can be used when analyzing the systems through reliability techniques for PSA applications to account for cable failures as a part of ageing management programs. The use of ANNs in life assessment of cables not only reduces the laboratory ageing time but also minimizes the cost by accurately predicting the future property of an electrical cable. Also, when conducting experiments it is important to note that appropriate test conditions play a significant role in predicting the future property. Therefore, test conditions must be designed such that the use condition can be simulated more accurately and that data can be used for reliability prediction.

Chapter 6 Simulation of Thermal and Radiation Ageing Effects in I&C Cables

6.1 Introduction

The most important indicator of the health of electrical plant items is the condition of their insulation. In the case of cables an important issue is the operating temperature and indeed the thermal history of the cable. There are several factors which will determine the thermal behaviour of a given cable installation. These include the assumed ampacity, the cable construction and circumstances of installation, and the ambient temperature [149-150]. The work presented in this study involves the use of COMSOL Multiphysics finite element analysis tool to study the temperature distribution in the cable. The principal heat source in the problem is the Joule heat dissipated in the conductor(s). The transfer of this heat to the surroundings is governed by the geometry and material properties of the conductor, insulation, screen, sheath and ambient conditions.

6.2 Insulation degradation due to Joule heating

6.2.1 Joule heating

When an electric current passes through the cable the material heats up due to its electrical resistance. This is called resistive heating or joule heating. The dielectric core is the part of the cable with lowest maximum allowable value of temperature. The current flow in the cable causes heating in the structure due the Joule's effect, and so the generated resistive

heating, Q (W/m^3), is proportional to the square of the magnitude of the current density J according to Eq. (6.1)

$$Q = \frac{1}{2\sigma}|J|^2 \tag{6.1}$$

where σ is electric conductivity in (S/m).

The electric conductivity is a function of temperature, given by:

$$\sigma = \frac{\sigma_0}{1+\alpha(T+T_0)} \tag{6.2}$$

where σ_0 is the electric conductivity at the reference temperature, T_0 and α is the temperature coefficient of resistivity [151].

The objective here is to study the temperature rise in the insulation and sheath material in the presence of aluminum screen when the outer surface of the copper conductor temperature is set at 90^0C (Joule heating effect). In other words, objective is to study whether the presence of aluminum screen in cable contributes significantly to thermal degradation of the polymer insulation materials.

6.2.2 Simulation and results

Simulation has become an essential part of science and engineering. A computer simulation environment is simply a translation of real world physical laws into their virtual form. How much simplification takes place in the translation process helps to determine the accuracy of the resulting model. It would be ideal, then, to have a simulation environment that includes the possibility to add any physical effect to the model. COMSOL Multiphysics is essentially a software tool to simulate the various phenomena individually or together. The tool has comprehensive built-in models for various physics and significantly a large database of components and material properties. Tool allows carrying out a multidimensional model

simulation and has the capability of solving many coupled physics simultaneously. With this kind of all-inclusive environment, COMSOL gives the confidence to build models with real-world precision.

6.2.2.1 Joule heating effect in single core I&C cable

The cable model for simulation of a high density polyethylene (HDPE) insulated and PVC sheathed cable with and without the presence of aluminum screen are shown in Figure 6.1 and 6.2 respectively.

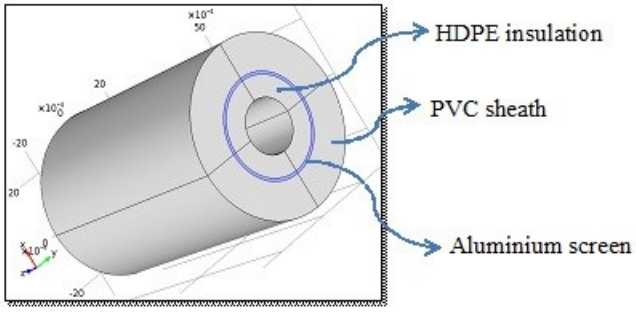

Figure 6.1: Cable model with aluminium screen

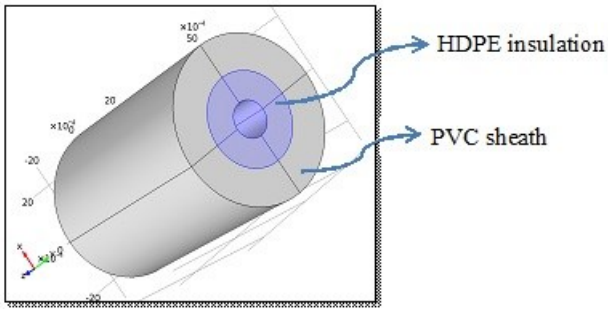

Figure 6.2: Cable model without aluminium screen

The governing heat conduction equation solved in COMSOL Multiphysics software is given by:

$$\rho C_p \frac{\partial T}{\partial t} + \nabla.(k\nabla T) = Q \tag{6.3}$$

$\boldsymbol{\rho}$ = density, C_p = specific heat capacity, k = thermal conductivity, Q = heat source term. The boundary conditions of the problem are shown in Table 6.1.

Table 6.1: Boundary conditions

Boundary condition	Value
Conductor surface temperature	363.15K
External temperature	313.15K

The material properties for PVC and HDPE for simulation have been taken from the standard literature [152]. Time dependent analyses were carried up to 10 minutes to determine the surface temperature and other thermal properties. This time duration is selected to ensure that after about 10 minutes, there can be only resistive leakage current but zero capacitive charging current [42-43]. The temperature distributions in the cable with and without the presence of aluminum screen are shown in Figures 6.3 and 6.4 respectively.

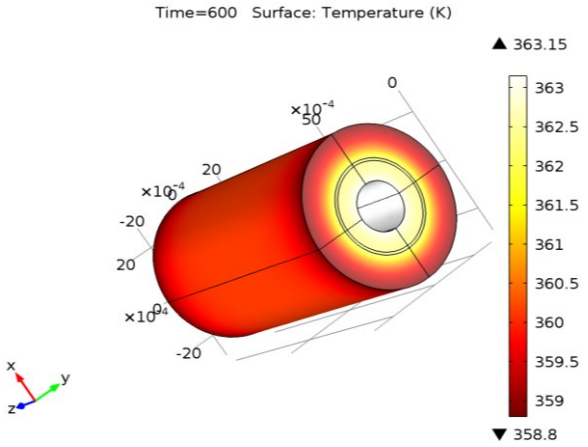

Figure 6.3: Temperature distribution in the cable with aluminium screen

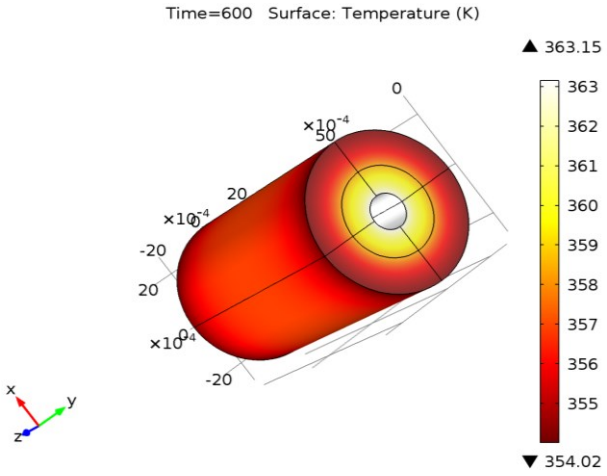

Figure 6.4: Temperature distribution in the cable without aluminium screen

The temperature gradients in the cable for models with and without the presence of aluminium screen are shown in Figures 6.5 and 6.6 respectively.

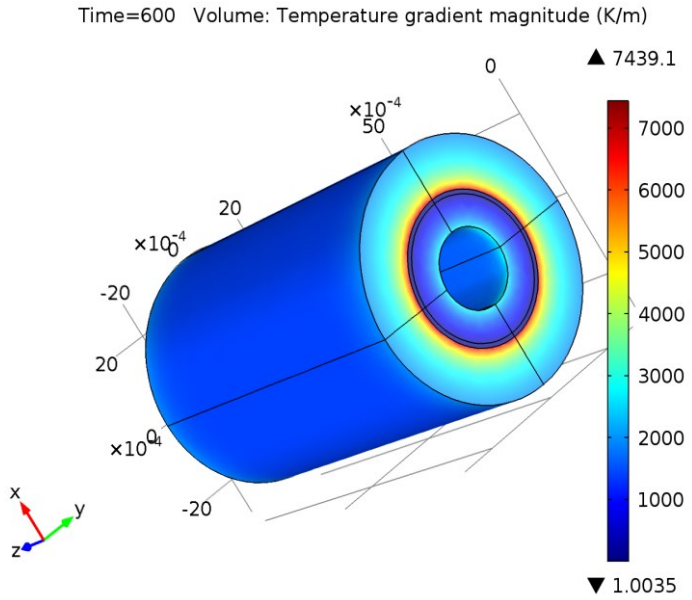

Figure 6.5: Temperature gradient in the cable with aluminium screen

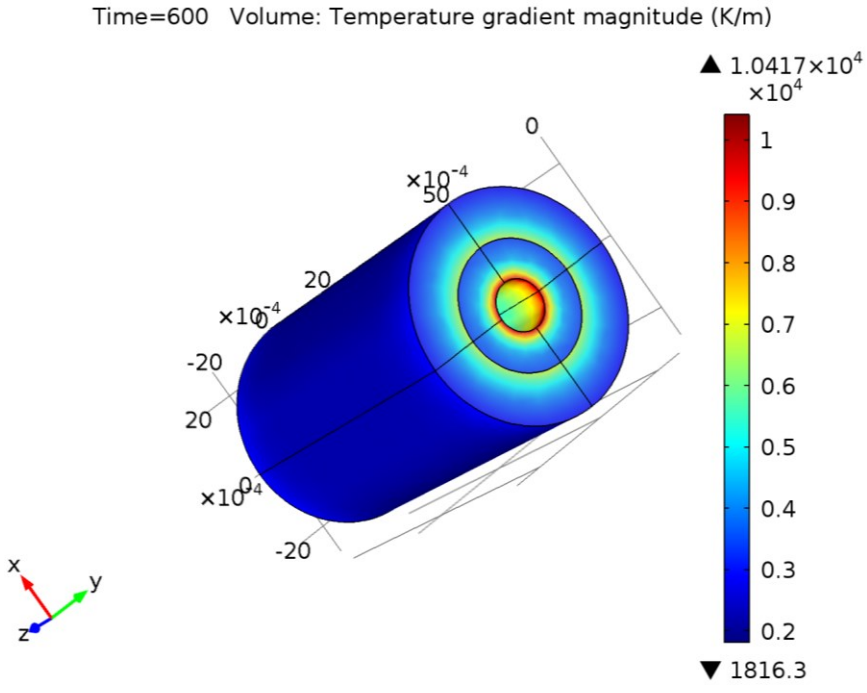

Figure 6.6: Temperature gradient in the cable without aluminium screen

The time dependent temperature distributions in the cable with and without the presence of aluminum screen are shown in Figures 6.7 and 6.8 respectively.

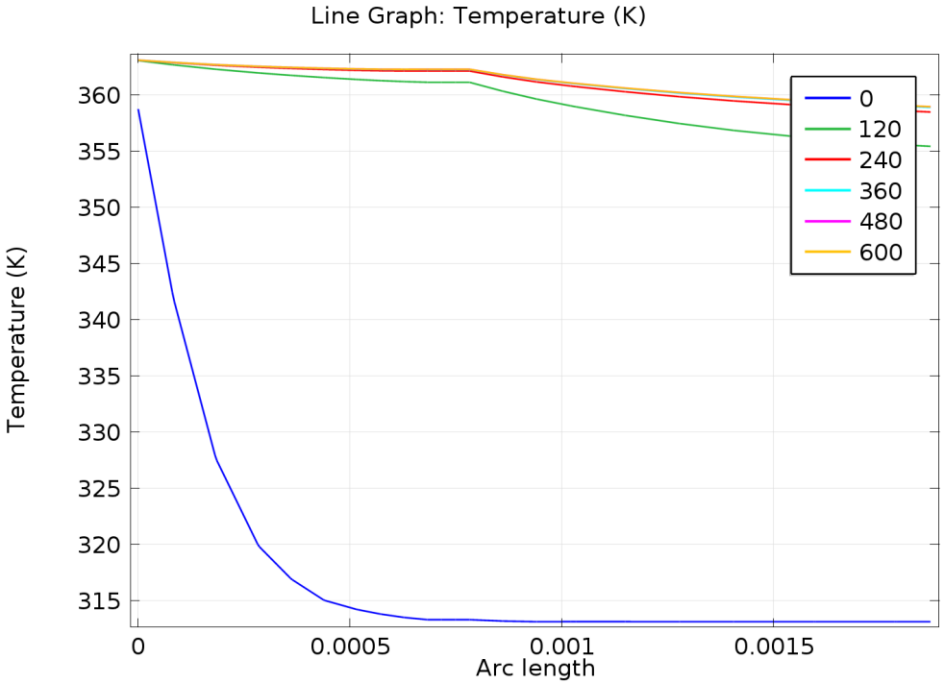

Figure 6.7: Time dependent temperature distribution in cable with aluminium screen

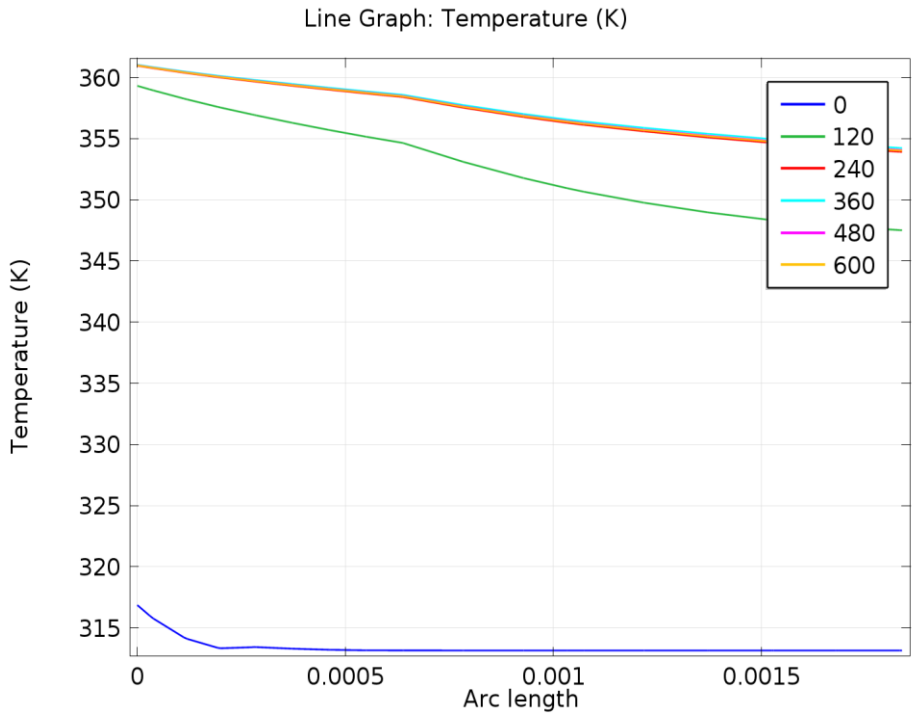

Figure 6.8: Time dependent temperature distribution in cable without aluminium screen

It is observed from Figure 6.8 that there is a significant temperature rise in the insulation material with the presence of aluminium screen. The changes in the thermal conductivities of

cable with and without the aluminium screen are also shown in Figures 6.9 and 6.10 respectively.

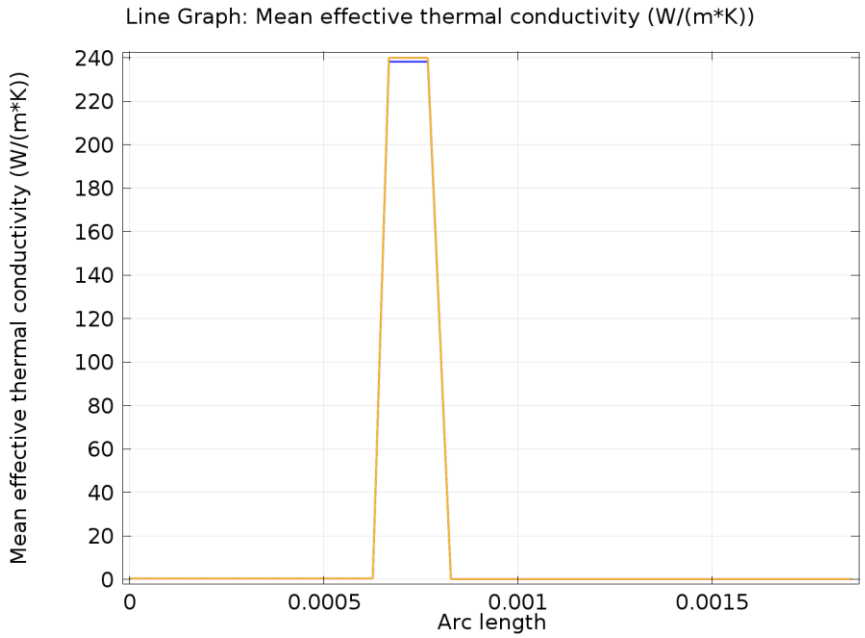

Figure 6.9: Mean effective thermal conductivity of cable with aluminium screen

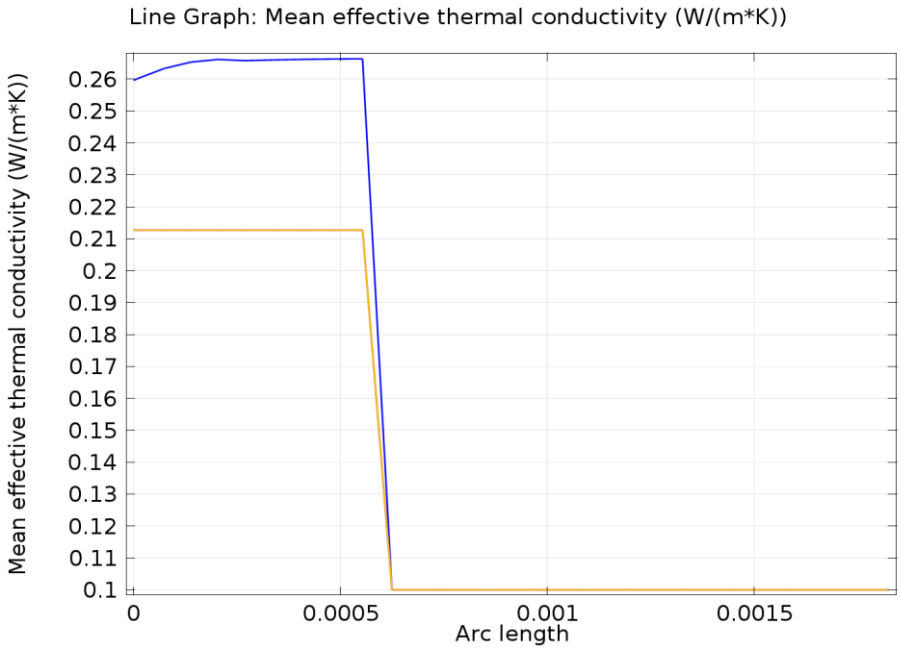

Figure 6.10: Mean effective thermal conductivity of cable without aluminium screen

It is evident from the study that a change in temperature of about 5^0C will contribute to the thermal degradation of insulation materials in the presence of aluminum screen.

Therefore, in the remaining life assessment studies of cables the presence of such components in addition to insulation materials should also be considered for realistic evaluations.

6.2.2.2 Joule heating effect in multicore I&C cable

Since most of the I&C cables used in NPP are of multicore cables for connecting the multiple signals of safety and control systems, the heat generation is substantially high and may contribute to insulation degradation. An attempt has been made to study the heat transfer in such cables. For this study, a 7-core cable has been selected for simulation. The geometry of a 7-core cable is shown in Figure 6.11.

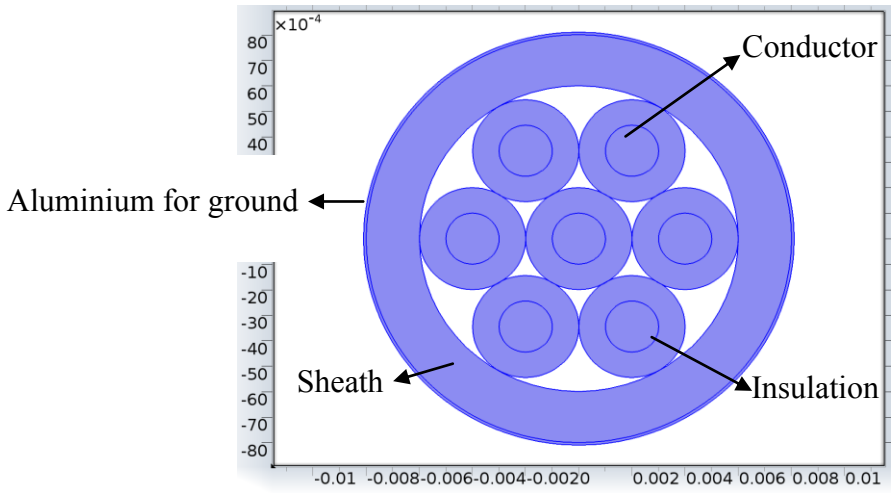

Figure 6.11: Geometry of a 7 core I&C cable

The governing Equations for the Joule heating model in Comsol Multiphysics software tool are:

$$\rho C_P \mu \nabla_{T2} = \nabla \cdot (k \nabla_{T2} + Q \tag{6.4}$$

$$\nabla \cdot J = Q_j \tag{6.5}$$

$$J = \sigma E + J_e \tag{6.6}$$

$$E = -\nabla V \tag{6.7}$$

The material properties for PVC, HDPE and aluminium are taken from the literature. A potential of 20mV is applied to every conductor and the outer sheath of the cable is grounded with an aluminium wrapper around the cable. The temperature distribution in the cable is shown in Figure 6.12.

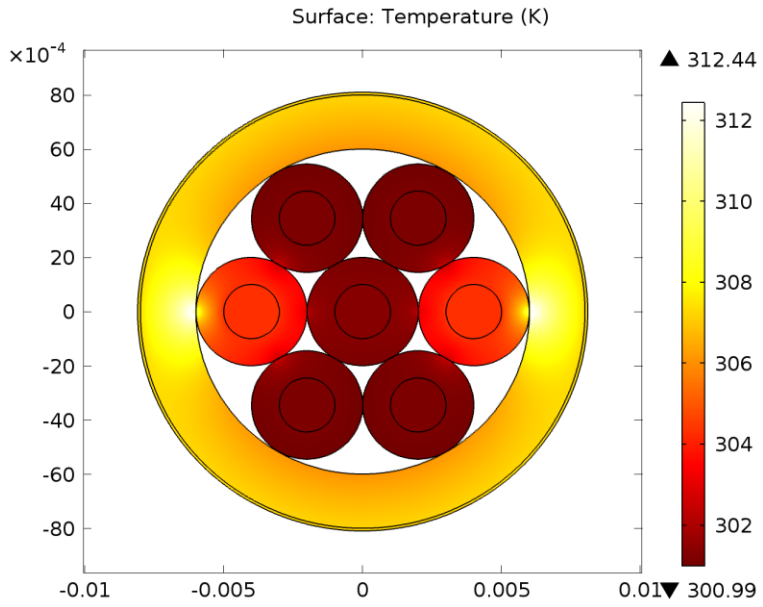

Figure 6.12: Temperature distribution in multicore I&C cable

The space charge density across the arc length is shown in Figure 6.13.

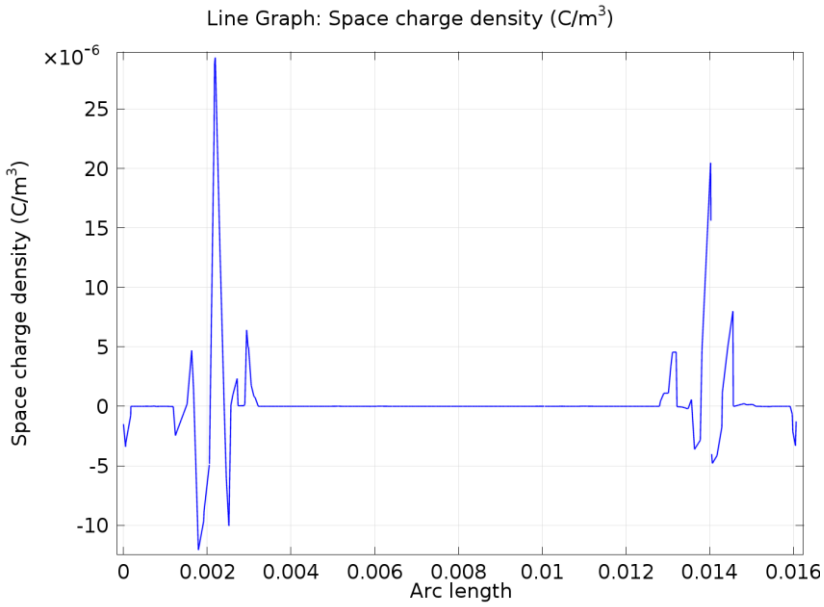

Figure 6.13: Space charge density in multicore I&C cable across the arc length

The power distribution is shown in Figure 6.14. It is evident from the study that the insulation damage is more towards the surface of the outer sheath due to combined effect of internal heating. The space charge dissipation is predominantly more at the peripheral cores.

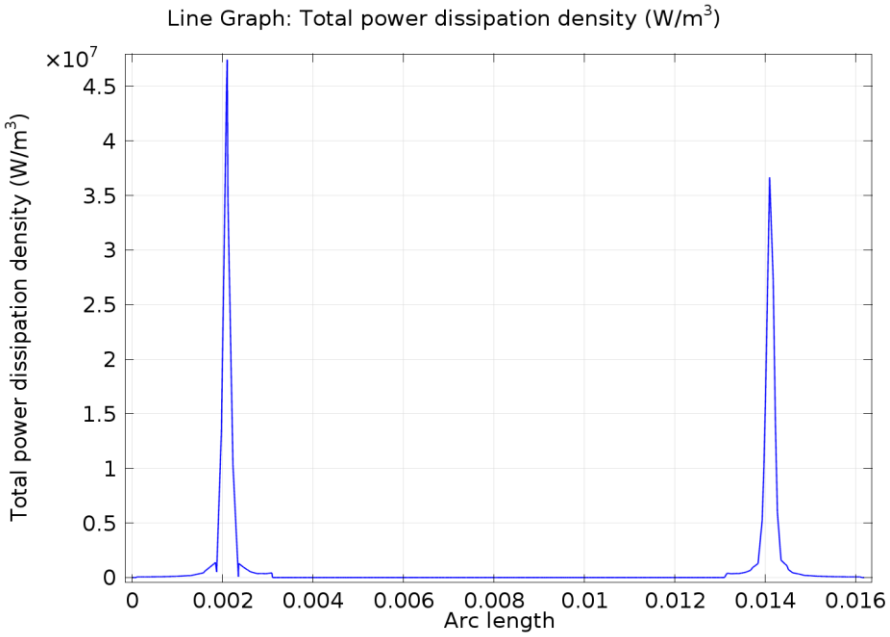

Figure 6.14: Power distribution in multicore I&C cable

6.3 Effect of microvoids on electric field in I&C cable

During the process of gamma radiation the polymeric materials undergo three important chemical reactions such as chain scission, cross-linking and oxidation. During this chemical process a large amount of microvoids are generated in the material leading to free volume formation. When such voids present in the insulation material there could be chance that the electric field in the cable get disturbed causing signal damage. In order to study this effect, Comsol Multiphysics simulation has been carried out by considering a void in the insulation material.

6.3.1 Simulation and results

In order to study the effect of gamma radiation on electric field, a void is considered in the sheath. The finite element analysis of the PVC sheath with free volume hole is carried out using Comsol Multiphysics FEM software. The 2D model geometry considered for the simulation of void is shown in Figure 6.15 and the material properties are shown in Table 6.2.

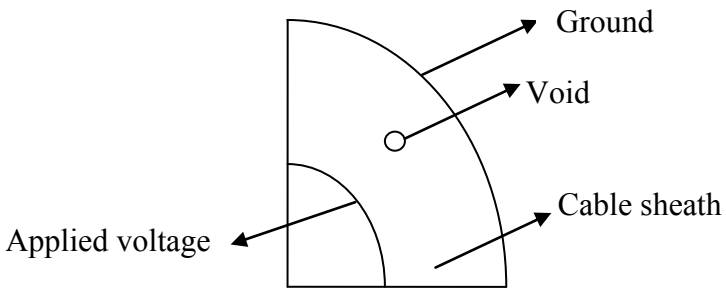

Figure 6.15: 2D finite element model geometry

Table 6.2: Material properties

Parameter	Values
Relative permittivity of cable sheath	2.3
Relative permittivity of void	1
Inner radius of sheath	2mm
Outer radius of sheath	5mm
Applied voltage	1100V

The governing equations solved for electrostatic model are:

$$\nabla \cdot (\epsilon_0 \epsilon_r E) = \rho_V \tag{6.8}$$

$$E = -\nabla V \tag{6.9}$$

Analysis was carried out assuming an applied voltage of 1100V across the sheath to simulate the field condition of I&C applications. The 2D geometry with a void in the sheath

is shown in Figure 6.16. The results of the finite element study are shown in Figures 6.17 to 6.20.

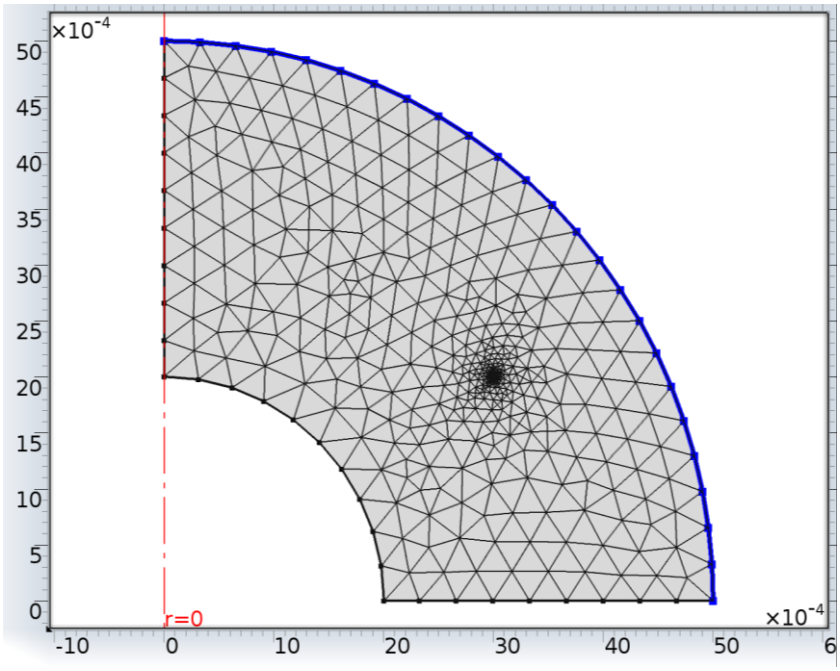

Figure 6.16: 2D finite element model

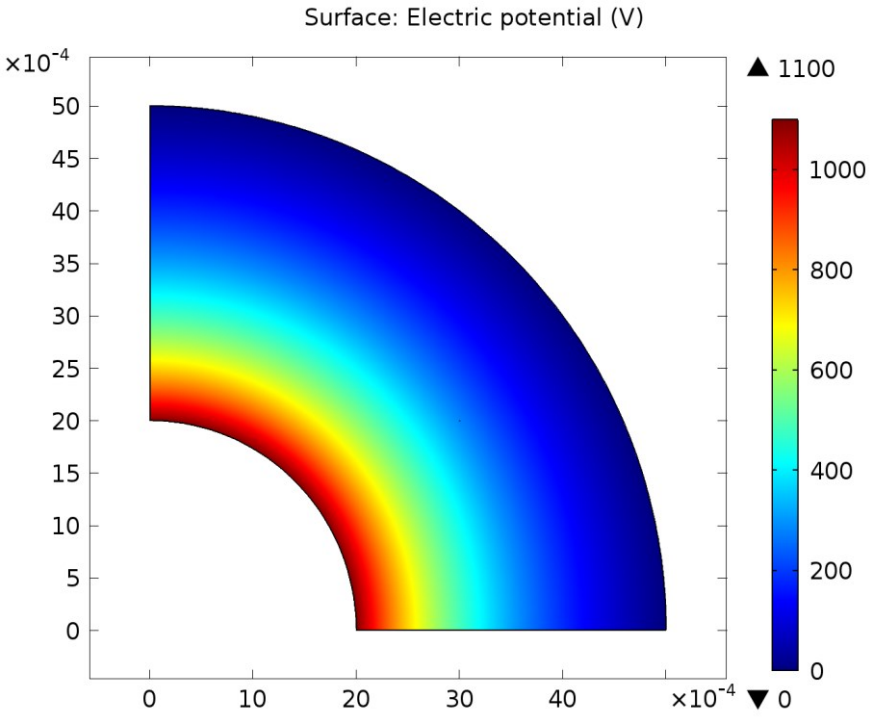

Figure 6.17: Electric potential across the sheath

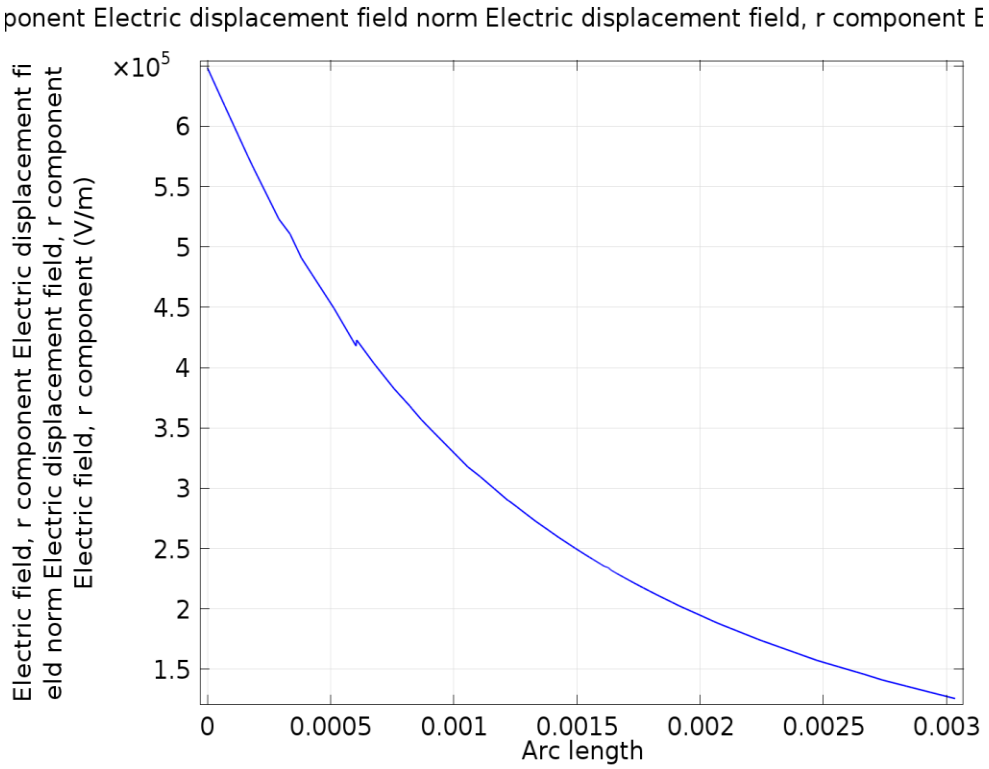

Figure 6.18: Electric field across sheath with void size 0.001mm

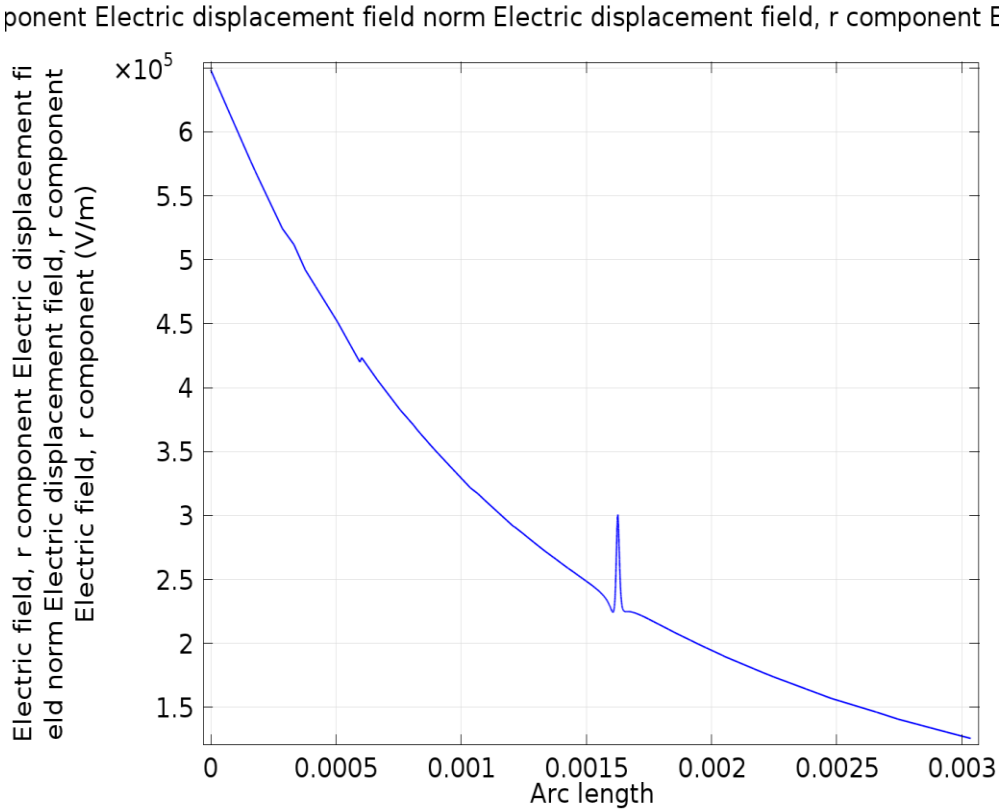

Figure 6.19: Electric field across sheath with void size 0.01mm

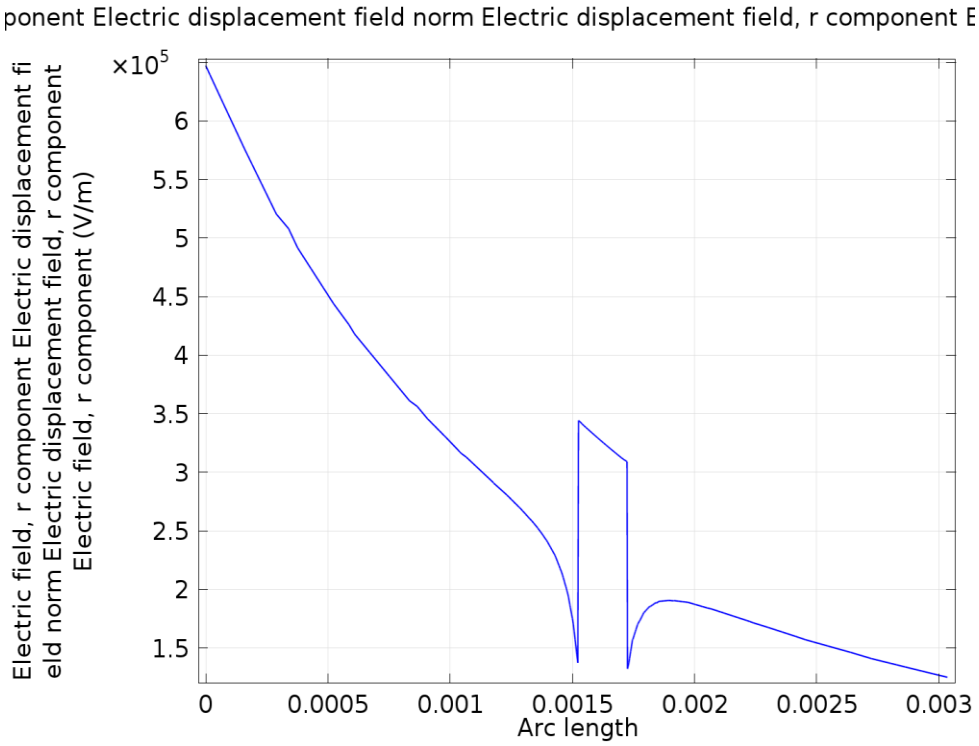

Figure 6.20: Electric field across sheath with void size 0.1mm

The finite element analysis of the sheath with free holes (voids) due to gamma radiation demonstrates that there is no significant change in the electric field distribution in the presence of nano scale voids in the material. However, as the void size increases; a significant increase in the electric filed is possible thereby causing early damage of sheath.

6.4 Effect of radiation ageing on mechanical properties

6.4.1 Simulation and results

As gamma radiation introduces the changes in the chemical structure of the polymer, there can be change in the physical and mechanical properties. The structural damage studied from the SEM is modeled in FEM to study the behaviour of polymer under mechanical loading. The typical ASTM sample specimen used in tensile testing is shown in Figure 6.21. The material properties used in the study are show in Table 6.3.

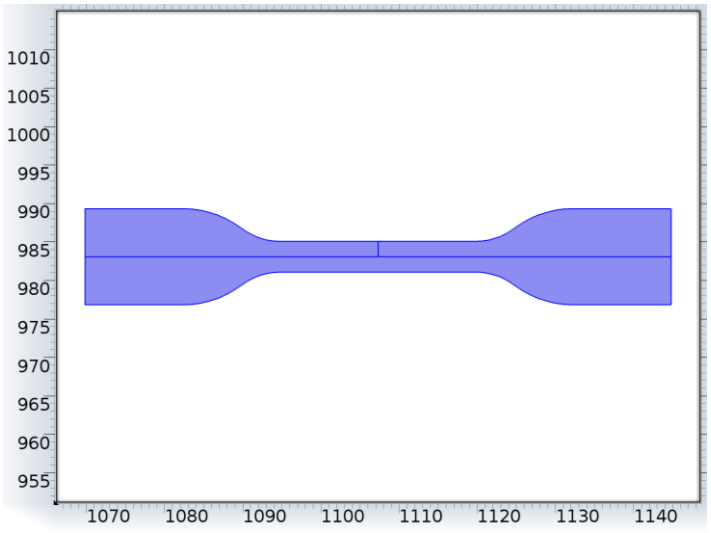

Figure 6.21: Tensile testing sample for FEM analysis

Table 6.3: Material properties for FEM analysis

Parameter	Value	Unit
Young's modulus	3e9	Pa
Poisson's ratio	0.38	1
Density	1450	kg/m^3
Force	2000	N

The governing equations solved in the study are:

$$-\nabla \cdot \sigma = F_V, \quad \sigma = s \tag{6.10}$$

$$s - s_0 = C \cdot (\epsilon - \epsilon_0 - \epsilon_{inel}) \tag{6.11}$$

$$\epsilon = \frac{1}{2}[(\nabla_u)^T + \nabla_u] \tag{6.12}$$

$$\sigma \cdot n = F_A \tag{6.13}$$

$$F_A = \frac{F_{tot}}{A} \tag{6.14}$$

An applied force of 2kN was applied at the one end and the other end was fixed. The results of the study are shown in Figure 6.22 to 6.25.

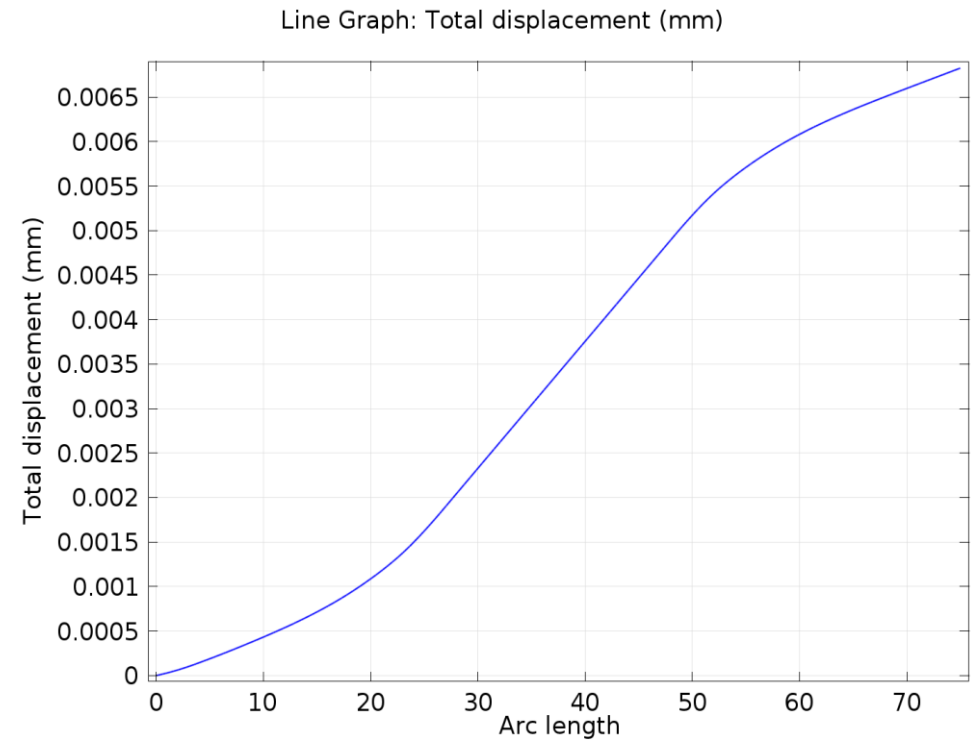

Figure 6.22: Total displacement along the axial direction

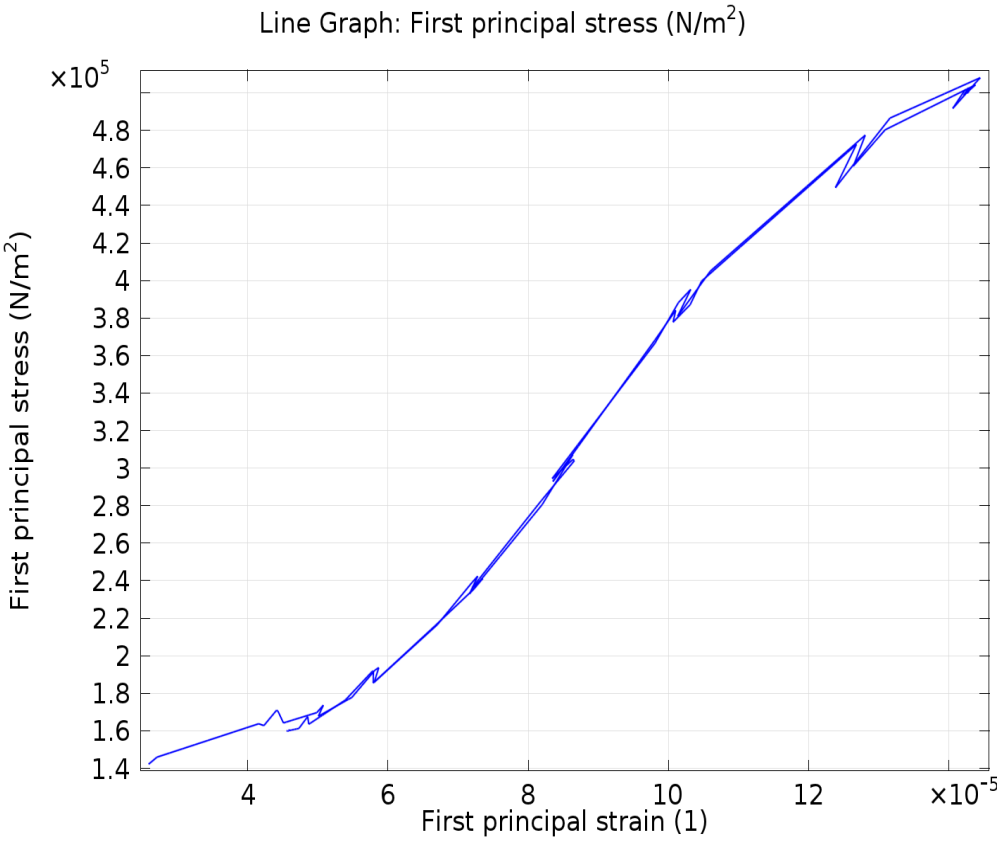

Figure 6.23: Stress-strain curve

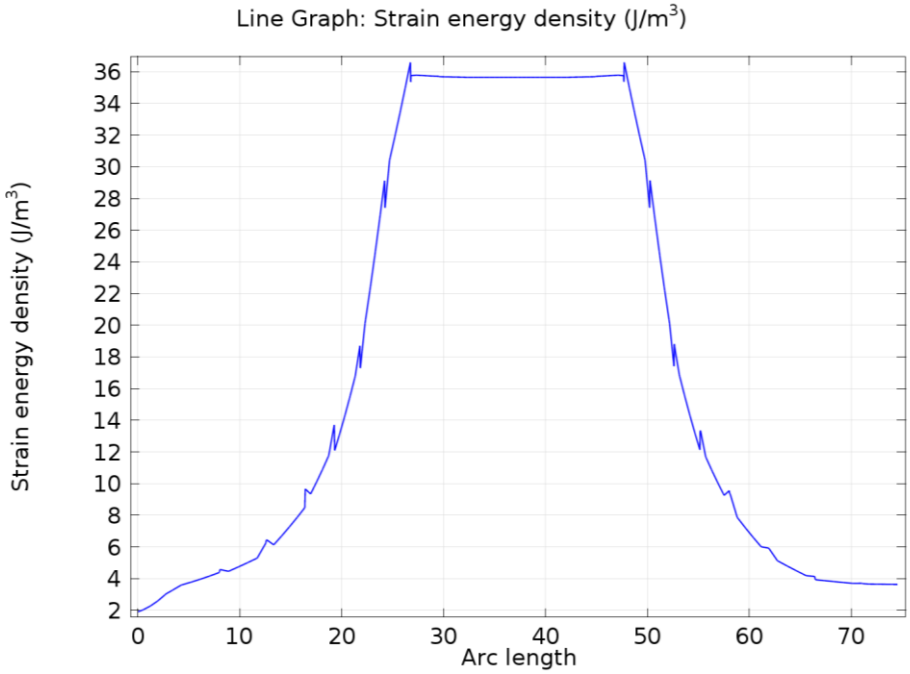

Figure 6.24: Strain energy density

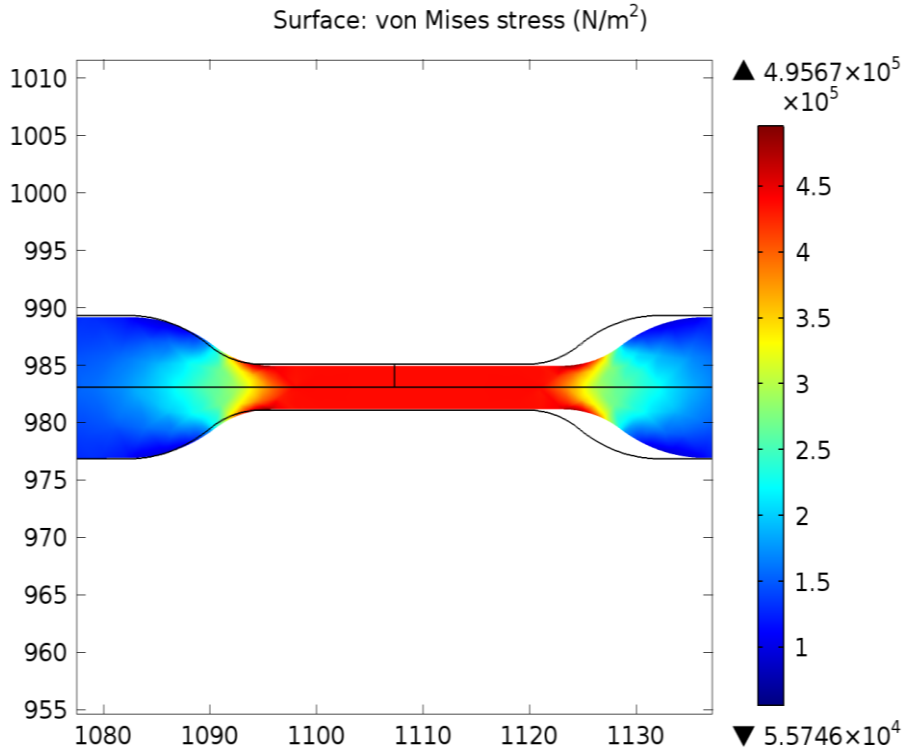

Figure 6.25: von Mises stress

The von Mises stress as shown in Figure 6.25 indicates the point of yield when subjected to tensile loading.

6.5 Summary

The COMSOL Multiphysics simulation have been carried out on a typical low voltage I&C cable in order to determine the ageing effect of aluminium screen in the cable. The cable was modeled assuming an outer surface temperature of the conductor being 90^0C due to Joule heating of the conductor (also known as ohmic heating). The time dependent studies were performed to study the maximum temperature rise in the outer surface of the cable insulation and sheath. It was found from the study that the presence of aluminum screen in the cable contributes to the thermal degradation of insulation materials due to rise in thermal conductivity of aluminium screen. The purpose of aluminium screen in cable is to provide shielding against electromagnetic inferences for the highly sensitive signals. However, such shielding materials significantly contribute to the insulation ageing. Therefore, in the remaining life assessment studies of cables the presence of such components in addition to insulating materials may also be considered for realistic evaluations. COMSOL Multiphysics simulations have also been carried to study the joule heating in a multicore cable and also to study the impact of radiation damage on electrical signal. It was seen from the study that unless the voids are above 0.01mm radius, the electric field is not affected much by the gamma radiation. Simulation has also been carried out to study the mechanical properties such as strain, displacement etc.

Chapter 7 Experimental Determination of Performance Indicators

7.1 Introduction

Experimental techniques provide means for evaluating the level of ageing and degradation of electrical cables. Condition monitoring for electric cable systems involves inspection and measurement of one or more indicators, which can be correlated to the condition or functional performance of the electrical cable on which it is applied [4-9]. Furthermore, it is desirable to link the measured indicators such as elongation-at-break, insulation resistance, etc. with an independent parameter, such as time or cycles, in order to identify trends in the condition of the cable. Ideally, condition monitoring data and trends in performance indicators guide the cable engineer's decisions to effectively manage the ageing and degradation in electrical cables, cable splices, or other accessories in a cable system before they reach the end of life or degraded performance that may adversely affect the safe and reliable operation of the associated components and systems.

Nuclear power plant receives large number of low voltage cables of various manufacturers for I&C applications. Although, all the manufacturers meet the required specifications there can be a significant variation in the performance of cables from manufacturer to manufacturer. This is due to many factors such as design, material processing, purity of the raw materials, workmanship, etc. Also, a few manufacturers add plasticizers and other additives for enhanced performance and ease of manufacturing. The experimental techniques such as insulation resistance testing, tensile elongation, differential scanning calorimetry, Fourier transform infrared spectroscopy, etc. will provide strong basis

on the adequate performance of these cables. These experimental techniques will also help in establishing correlation against standard benchmark characterization techniques for lifetime prediction of insulating materials. Prior to accelerated ageing the insulation resistance measurement was carried out and the key electrical parameters were assessed for the cable samples under study.

7.2 Research plan for experimental studies

The proposed research plan for carrying out experiments on fresh and aged cable samples is shown in Figure 7.1.

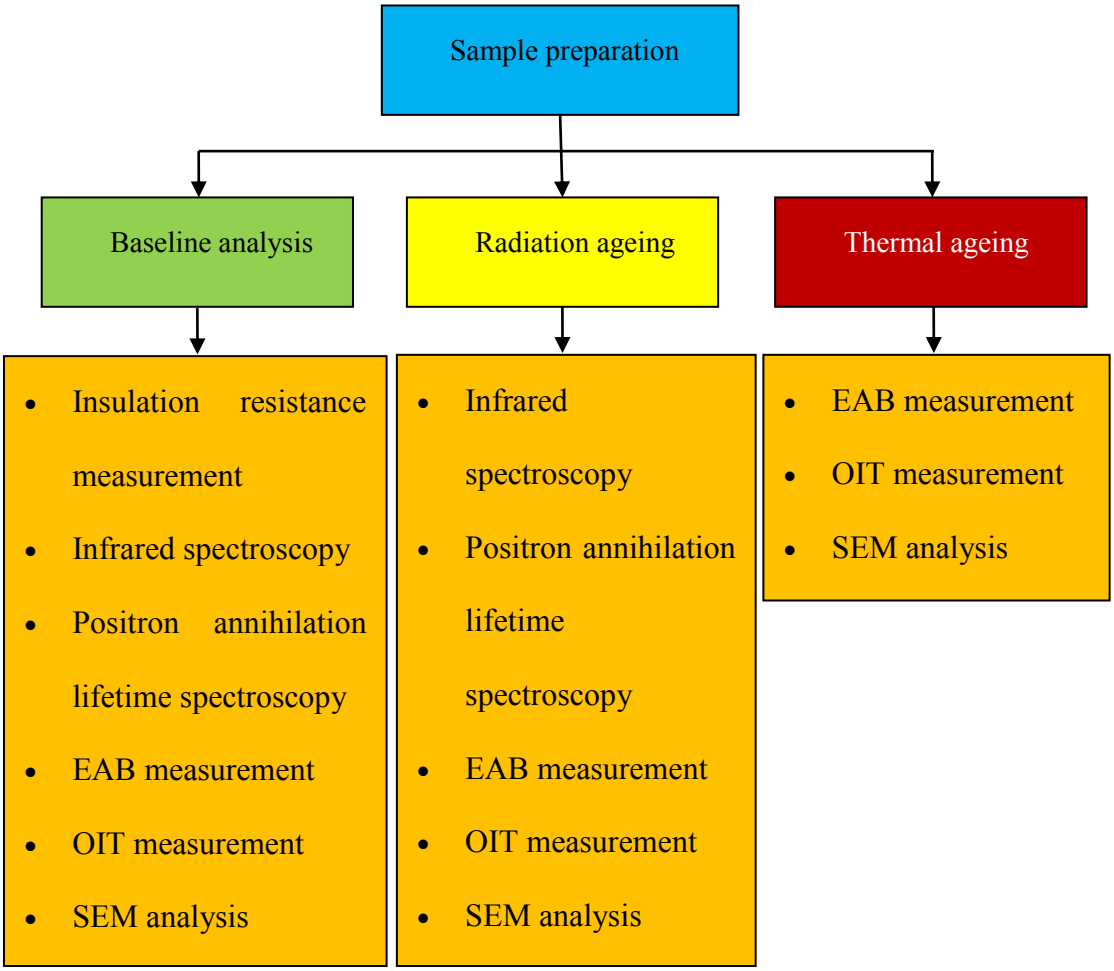

Figure 7.1: Block diagram of experimental research plan

7.3 Cable samples for experimental studies

The cables chosen for experiments are of low voltage type (≤ 1100V) as they are extensively used in nuclear power plant I&C applications. The cables shown in Table 7.1 have been selected for experimental determination of performance parameters.

Table 7.1: Cable specimens for experimental studies

Cable type	Specifications	Polymer type	
		Insulation	Sheath
Manufacturer 1- control cable	10 core, 1.5sq.mm, 650/1100V	PVC	PVC
Manufacturer 2- signal cable 1	37 core, 1.5sq.mm, 1100V	FRLS	HRPVC
Manufacturer 2- signal cable 2	19 core, 1.5sq.mm, 1100V	FRLS	HRPVC
Manufacturer 2- instrumentation cable	30 core, 1.0sq.mm, 1100V	FRLS	HRPVC
Manufacturer 3-control cable	37 core, 1.5sq.mm, 1100V	FRLS	HRPVC

7.4 Insulation resistance measurement

7.4.1 Experimental

IS: 10810 (Part 43) 1984 [153] recommends a minimum 3 meter length cable as a test specimen for insulation resistance testing and test needs to be conducted at an ambient temperature (27±2℃). In case of multicore control cables (i.e. six cores and above) at least five cores have to be taken from the finished cable. The adopted test pattern is shown in Figure 7.2.

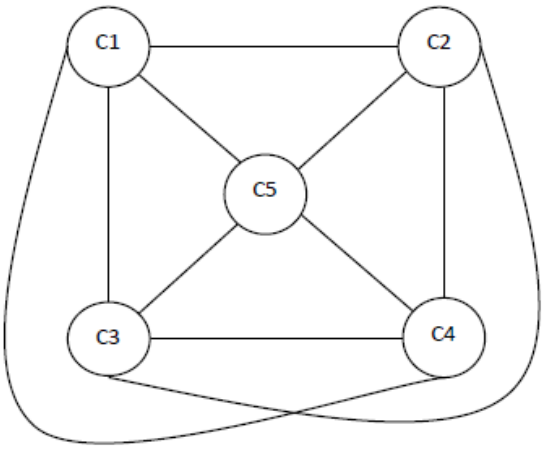

Figure 7.2: Test pattern

For example, in a 37 core control cable five cores have been chosen randomly and the cross insulation between two conductors was measured by earthing the remaining cores along with outer sheath. Test was repeated until all the combinations were reached. However, the proximity effect was not considered in the measurement. The IR testing was performed using Megger S1-1052/2 a 10 kV high current insulation resistance tester. Since all the selected cables are above 1100V rated, the test voltage chosen was 1100V DC for all the cables. The insulation materials were polyvinylchloride with flame retardant additives in both insulation and sheath. The IR test was performed on five cables from three different manufacturers. The cross IR and polarization index readings were measured between 5 cores from each multicore cable. The IR was measured between all the combinations of five conductors by earthling the remaining conductors and screen together.

7.4.2 Results

The mean insulation resistance values obtained from the insulation resistance measurement for all the specimen cables before ageing are shown in Table 7.2.

Table 7.2: Mean IR values

Cable type	Specimen length (Feet)	Mean IR ($10^9\Omega$)
Manufacturer1-control cable	25.6	113.41
Manufacturer2-signal cable 1	27	577.1
Manufacturer2-signal cable 2	26	100.9
Manufacturer2-instrumentation cable	23	2721
Manufacturer3-control cable	26	630.8

The IR values corresponding to a 1000 feet length cable are computed from:

$$IR_{1000} = \frac{IR_{measured} \times Specimen\ length}{1000} \tag{7.1}$$

The IR values obtained from the above equation should be greater than 1MΩ for 1000V rated cables. IR values corresponding to 1000 ft. length cable are shown in Table 7.3.

Table 7.3: IR values corresponding to 1000 feet length cable

Cable type	Mean IR for a 1000 feet length cable ($10^9\Omega$)
Manufacturer 1-control cable	2.9
Manufacturer 2-signal cable 1	15.58
Manufacturer 2-signal cable 2	2.6
Manufacturer 2-instrumentation cable	62.58
Manufacturer 3-control cable	16.4

Because of the sensitivity of insulation resistance measurements to temperature, moisture and other factors, trending of insulation resistance over time compared to a baseline value can be somewhat unreliable. A better choice for data trending would be the polarization index, which is just as easy to perform, and will give more reliable and repeatable results. Also, polarization index is independent of length of the specimen. Hence, a comparison of PI is

more logical than IR values. The polarization index values for all the five cables are shown in Table 7.4.

Table 7.4: PI values

Cable type	Mean PI
Manufacturer 1-control cable	1.331
Manufacturer 2-signal cable 1	1.311
Manufacturer 2-signal cable 2	1.289
Manufacturer 2-instrumentation cable	1.319
Manufacturer 3-control cable	1.548

In order to study the variation in the manufacturing process, the IR and PI values have been compared among the manufactures. The comparison of IR and PI values are shown in Figure 7.3 and Figure 7.4 respectively.

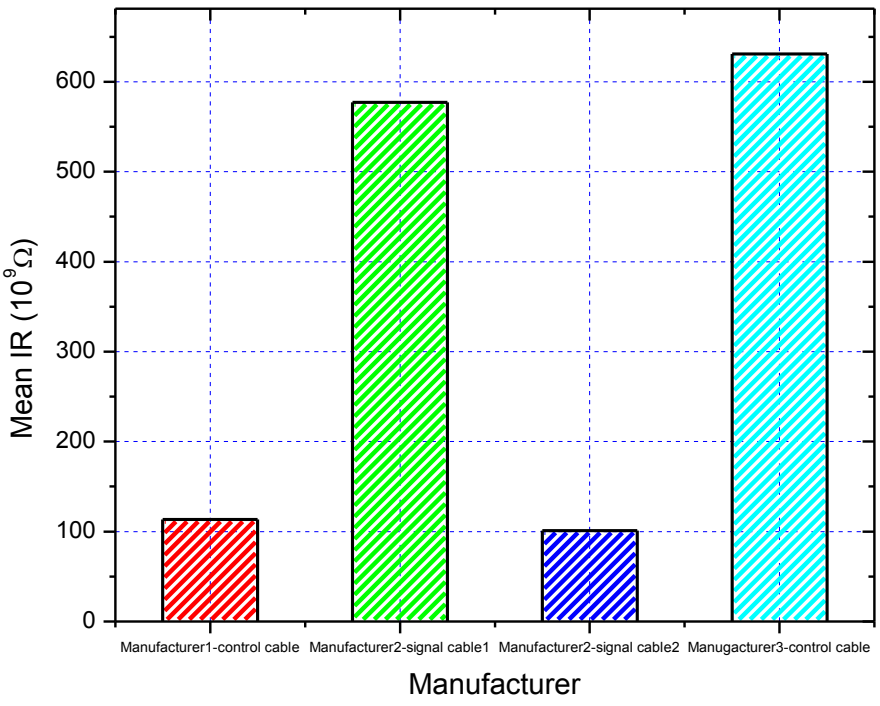

Figure 7.3: IR comparison

It can be noted that the cable 3 from manufacturer 2 has been withdrawn from the comparison as the exact IR values could not be measured as the readings were beyond the capability of the measurement equipment. The detailed results of IR measurement on individual cables are given in Appendix A.

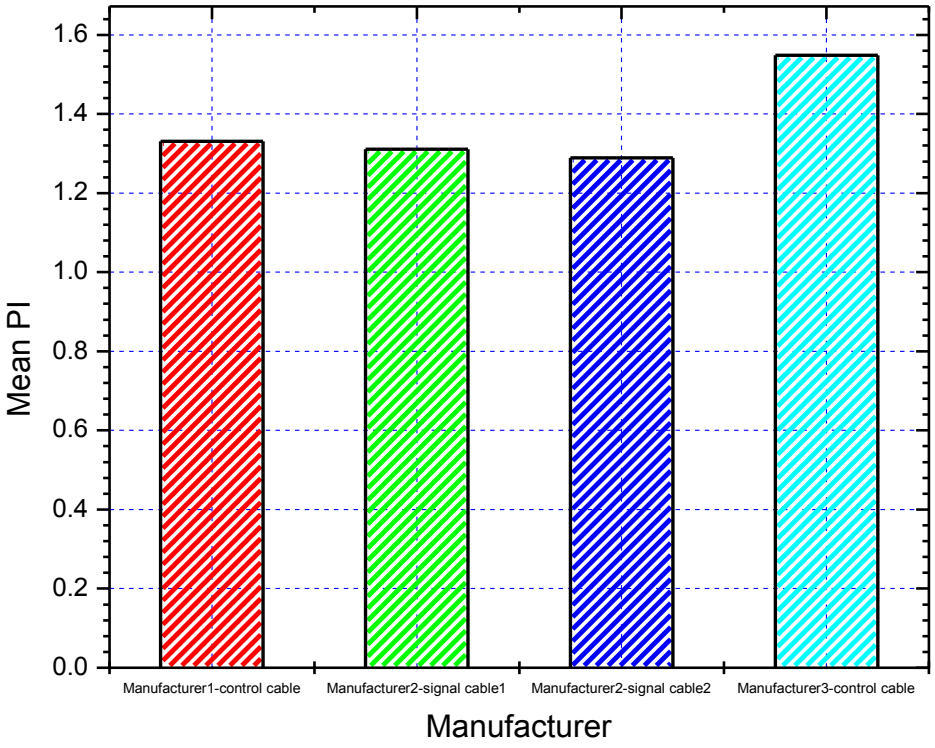

Figure 7.4: PI comparison

It is observed from Figures 7.3 and 7.4 that the control cable from the manufacturer exhibits relatively good IR and PI values. However, it can be noted that the signal cable 1 from manufacturer 2 has significantly high insulation resistance but low PI indicating steady state losses.

7.4.3 Insulation resistance model

In order to study the relationship between leakage current and IR, statistical data analysis was performed on 10 minute IR data. It was found from the study that though there is a large variation in the IR values, there is not much change in the relationship between IR and

leakage current. All cables fit an exponential model with a coefficient of determination being greater than 99%. The individual data models are shown in Figure 7.5 and that of mean model is shown in Figure 7.6. From Figure 7.6, it can be concluded that irrespective of the additives and other filler materials used in cable manufacturing process to improve physical and mechanical parameters, the PI is not affected much though there is a significant variation in IR. The exponential model obtained from the mean IR and leakage current with a coefficient of determination being 0.93 is:

$$IR = A + Be^{-\frac{I_l}{C}} \tag{7.2}$$

Where, A, B and C are model parameters shown in Table 7.5. Here, I_l is leakage current.

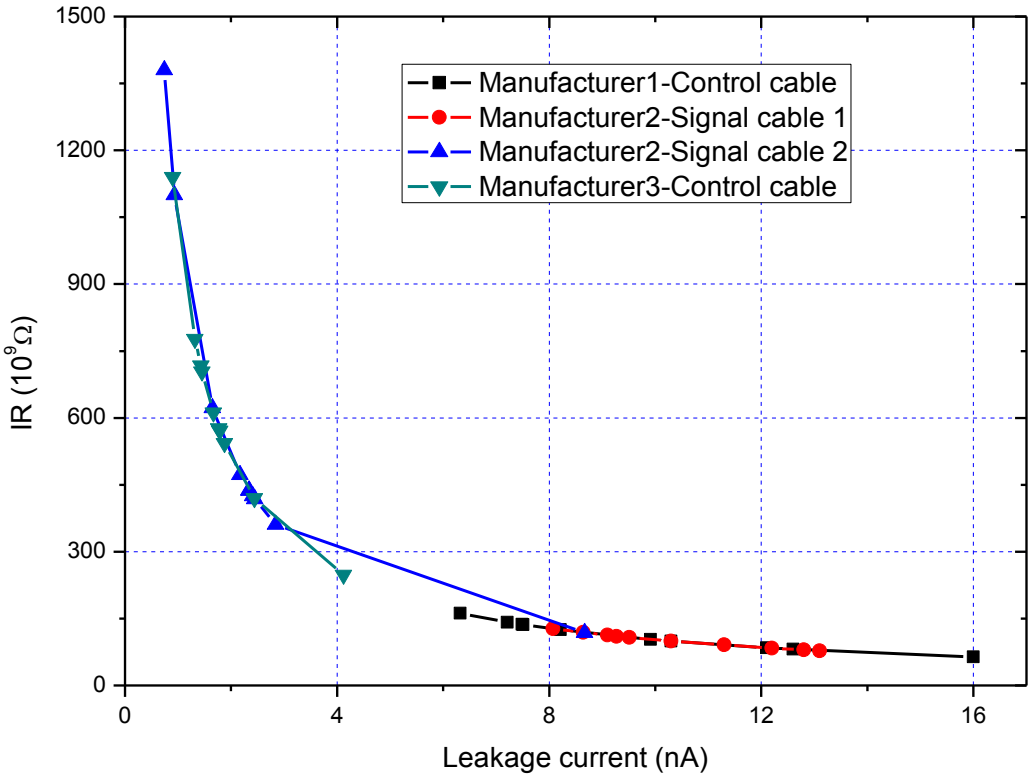

Figure 7.5: Exponential fit of individual cables

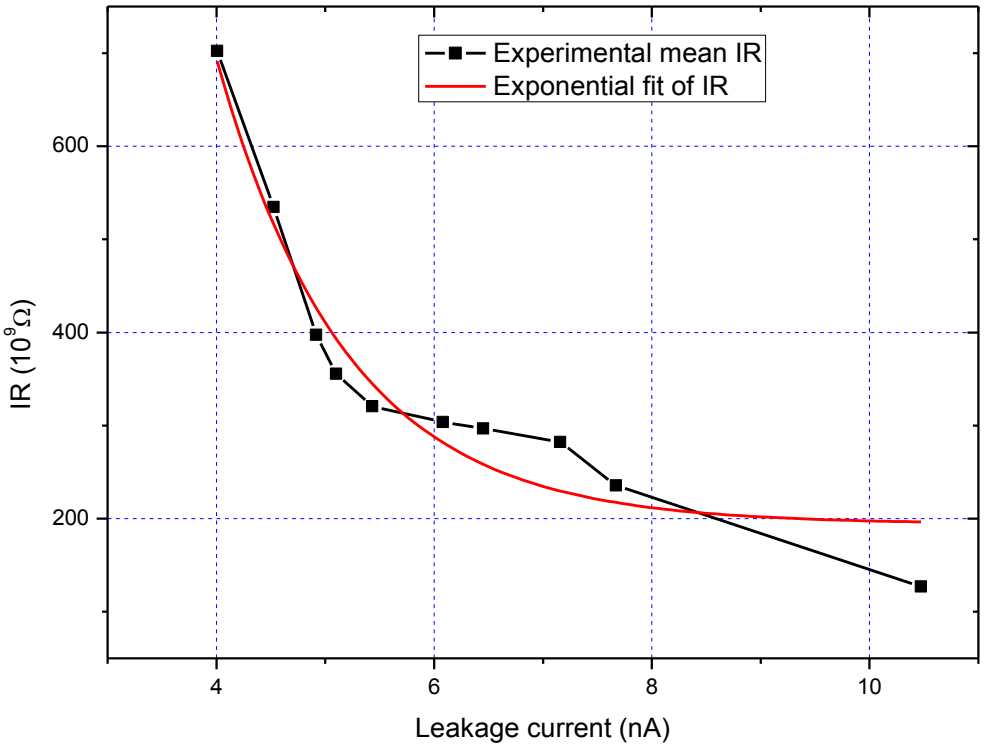

Figure 7.6: The mean exponential fit of all the cables

Table 7.5: Model parameters

Parameter	Value	Standard error
A	194.32	32.65
B	14311.03	10306.21
C	1.1926	0.256

7.4.4 Discussion

Insulation resistance test was performed on five cables from three different manufacturers. IR and polarization index readings were measured and compared against the recommended values from the industry standards. It was observed from the study that, there is a significant variation in the IR values among different manufacturers. This variation is due to the sensitivity of IR measurements to temperature, moisture and other factors, and some manufacturers design cables with significantly high IR. However, a cable with high IR does not always guarantee the reliable performance. As PI being independent of temperature and

length of the specimen; and will give more reliable and repeatable results, it would be logical to compare the PI values against recommended standards for performance assessment. Also, it was found that though there is a significant variation in IR values, there is not much change in the relationship between IR and leakage current. All five cables fit an exponential model with a coefficient of determination being greater than 99%. This indicates that the basic phenomenon is unaffected among the various manufacturers though there is huge variation in the IR values. Hence, polarization index should also be considered along with IR while assessing the cable performance.

7.5 Accelerated radiation ageing

Under normal operating environments in a nuclear reactor, electric cables are subjected to radiation and thermal stress. Qualification standards IEEE 323 and IEEE 384 recommend that cables must withstand doses of 50MRad to simulate normal operation, plus approximately 150MRad in the event of a LOCA, and ageing at a temperature and time deemed equivalent to simulated installed life. The specifications of the chosen cable for radiation ageing experiments are shown in Table 7.6.

Table 7.6: Specifications of cable for radiation ageing

Cable type	Specifications	Polymer type		Year of manufacturing
		Insulation	Sheath	
Control cable	10 core, 1.5sq.mm, 650/1100V	FRLS PVC	HR PVC	2009

The conductors were removed and 75mm length tubular samples were prepared from insulation and a standard dumbbell shape samples were made from sheath material for FTIR, DSC and tensile testing experiments. A minimum of 7 samples were kept under test covering 2.5MRad, 5MRad, 10MRad, 25MRad and 50MRad dose conditions related to normal to

accidental doses conditions encountered in NPP. Radiation ageing was carried out under aerated condition in a gamma chamber having ^{60}Co gamma source at a dose rate of 0.17MRad/Hr.

7.5.1 Infrared spectroscopy

FTIR spectroscopy was performed using Jasco FT/IR 660 Plus Series Spectrometer. A minimum of 7 irradiated samples were kept under each test condition and the tests were repeated whenever samples failed due to improper testing. All the experiments were carried out at a resolution of $4cm^{-1}$ wavenumber with a measurement range being $4000 – 400cm^{-1}$. The detailed results of infrared spectroscopy on individual cables are given in Appendix A.

7.5.1.1 Results and discussion

The mean transmittance of infrared radiation and its absorbance by specific chemical bonds in PVC insulated cable for various dose conditions for insulation and sheath are shown in Figure 7.7 and 7.8 respectively. The mean transmittance for every dose condition was obtained with a minimum of seven samples to build a statistical confidence in the results. Un-irradiated (0MRad) corresponds to the baseline spectra.

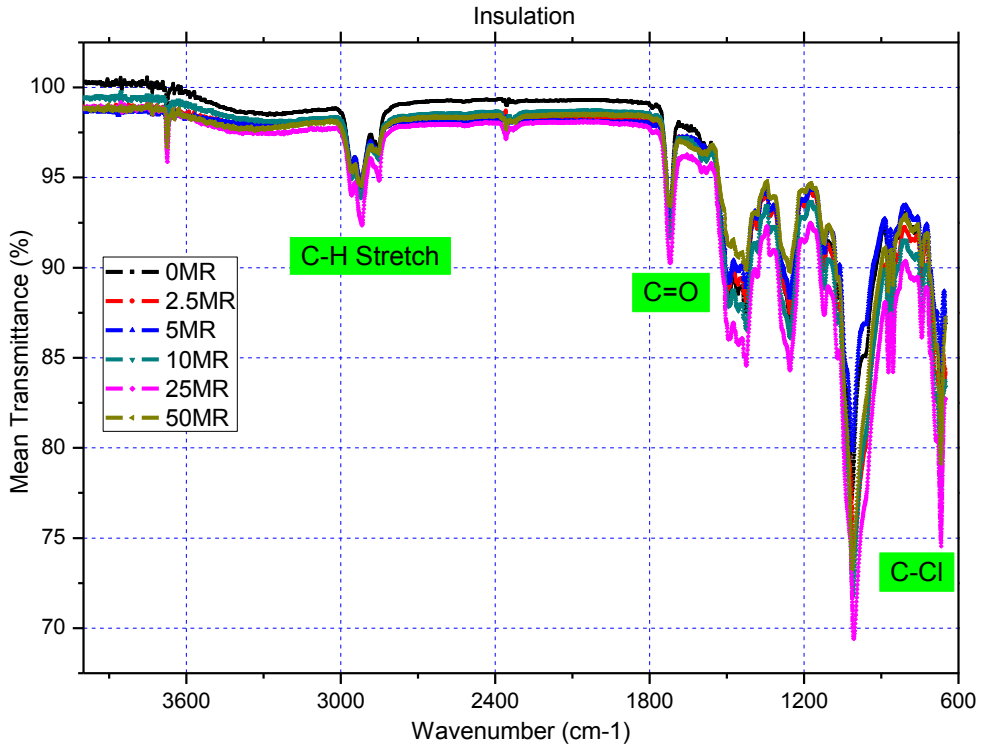

Figure 7.7: Mean IR spectra for insulation material

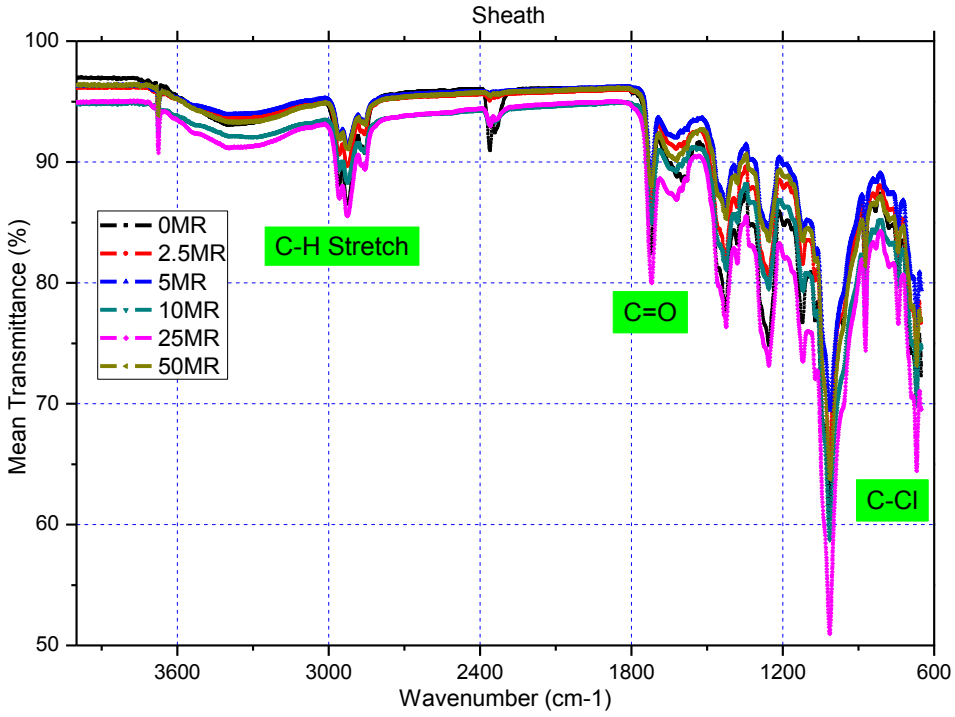

Figure 7.8: Mean IR spectra of sheath material

It is observed from Figure 7.7 and 7.8, the presence of CH peak at around 2950cm^{-1} and C-Cl peak at 669cm^{-1} in both insulation and sheath confirms the polymer belonging to PVC

class [154-155. It is also evident from infrared spectra that there is not much difference in the peaks of insulation and sheath materials. However, a significant change in the infrared transmittance in two materials is of great concern. For example, about 75-85% of the infrared radiation is being transmitted in the C-Cl peak in case of insulation at all dose conditions, whereas about 65-75% is being transmitted at this peak in case of sheath material. Therefore, there is a significant energy absorption by the sheath material compared to insulation. This change in energy absorption by various chemical groups not only depends on the base polymers but also depends upon the additives present in the material. Hence, there can be a significant effect on mechanical properties of sheath can be present although the chemical structure is unaffected. The peak at around 1000cm^{-1} in both insulation and sheath is due to the presence of plasticizers which are added by manufacturers to improve certain thermal and other properties.

The visual examination of infrared spectra provides conclusive results on whether there is any significant radiation effect on the polymer material. Therefore, a suitable data analysis technique is needed to verify the degradation observed from FTIR technique.

7.5.1.2 Anova

Analysis of variance (Anova) is a statistical method for making simultaneous comparisons between two or more means; a statistical method that yields values that can be tested to determine whether a significant relation exists between variables. When there are only two samples, one can use the t-test to compare the means of the samples but it might become unreliable in case of more than two samples. The decision of whether or not to reject the null hypothesis that the sample means are similar to each other requires that the value for F-statistic be compared with a critical value. And, in turn, just as for the t-test, the critical value differs with the number of degrees of freedom. Unlike the t-test, the critical value of F

needed to reject the null hypothesis at any given level of significance (alpha) (e.g. .05, .01, or .001) varies with two rather than only one indicator of degrees of freedom. The alpha level of F-statistic for rejecting the null hypothesis depends on both the "between-subset means squares and the within-subset means squares" of degrees of freedom [127].

One-way Anova was performed on control cable as there is only one factor (radiation ageing) considered in the study so far. Anova was performed at specific peaks (C-Cl) of chemical groups to study the extent of degradation due to gamma radiation at various dose conditions. Since Anova assumes that the data is normally distributed, an Anderson-Darling normality test was also performed at each dose condition. The descriptive statistics for various levels of factor for insulation are shown in Table 7.7. The results of One-way-Anova at 669cm-1 corresponding to C-Cl peak for insulation is shown in Table 7.8.

Table 7.7: Descriptive statistics for insulation at $669cm^{-1}$

Dose (MRad)	Sample size	Mean transmittance (%)	Standard deviation	Standard error of mean
0	9	83.14	2.63	0.87
5	7	84.31	3.40	1.28
10	7	77.67	5.64	2.13
25	6	74.75	3.57	1.46
50	7	79.16	6.80	2.57

Table 7.8: Anova results for insulation at 669cm-1

Parameters	Degrees of freedom	Sum of squares	Mean square	F value	Prob>F
Model	4	426.75	106.68	5.03154	0.00304
Error	31	657.32	21.20		
Total	35	1084.08			

The descriptive statistics for various levels of factor for sheath are shown in Table 7.9. The results of One-way-Anova at 669cm^{-1} corresponding to C-Cl peak for insulation is shown in Table 7.10.

Table 7.9: Descriptive statistics for sheath at 669cm^{-1}

Dose (MRad)	Sample size	Mean transmittance (%)	Standard deviation	Standard error of mean
0	8	70.20	5.17	1.83
5	7	76.49	6.72	2.54
10	7	69.86	7.53	2.85
25	7	64.46	9.39	3.55
50	7	73.17	8.09	3.06

Table 7.10: Anova results for sheath at 669cm^{-1}

Parameters	Degrees of freedom	Sum of squares	Mean square	F value	Prob>F
Model	4	556.21	139.05	2.50748	0.06213
Error	31	1719.13	55.45		
Total	35	2275.35			

It is observed from Anova study that there is a significant change in degradation due to radiation in insulation at different dose conditions at 5% significance level compared to that of sheath material. It is concluded that the infrared spectra do not clearly indicate the extent of ageing effect as there is no substantial shift in the peaks except for some change in infrared transmittance. However, Anova study reveals that both insulation and sheath materials are not exactly the same polymers although FTIR spectroscopy indicates that the base polymers are same except for some changes in energy absorption.

7.5.2 Elongation at break measurement

Tensile tests were performed using Tinius Olsen Universal Testing Machine with a load cell of 10kN in accordance with ASTM Standard D638 [46] and D412 [47]. A minimum of 5 samples were placed under each test condition and tests were repeated wherever the samples failed due to improper testing. Tests were performed with an initial jaw separation of 25mm at a strain rate of 25mm/min. with the extensometer the mechanical properties such as tensile strength, elongation at break, Young's modulus were recorded. Typical elongation curves at dose of 50MRad for insulation and sheath material for a typical control cable are shown in Figure 7.9 and 7.10 respectively. The legend numbers represent sample IDs for test condition. The detailed results of tensile testing on individual cables are given in Appendix A.

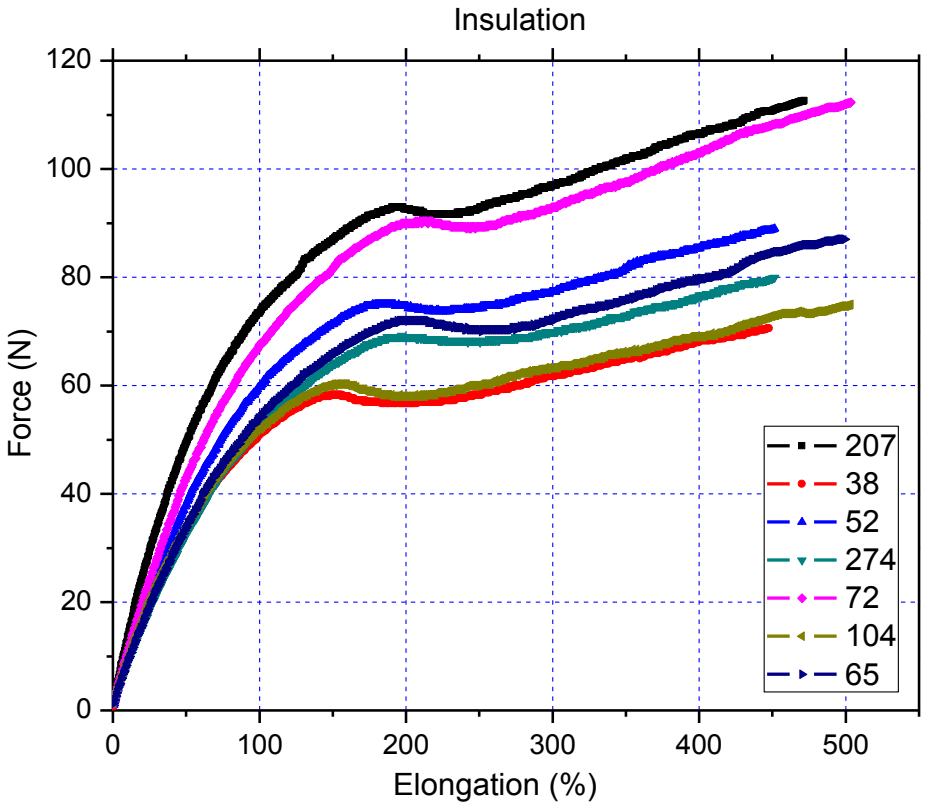

Figure 7.9: Elongation of insulation after 50MRad radiation ageing

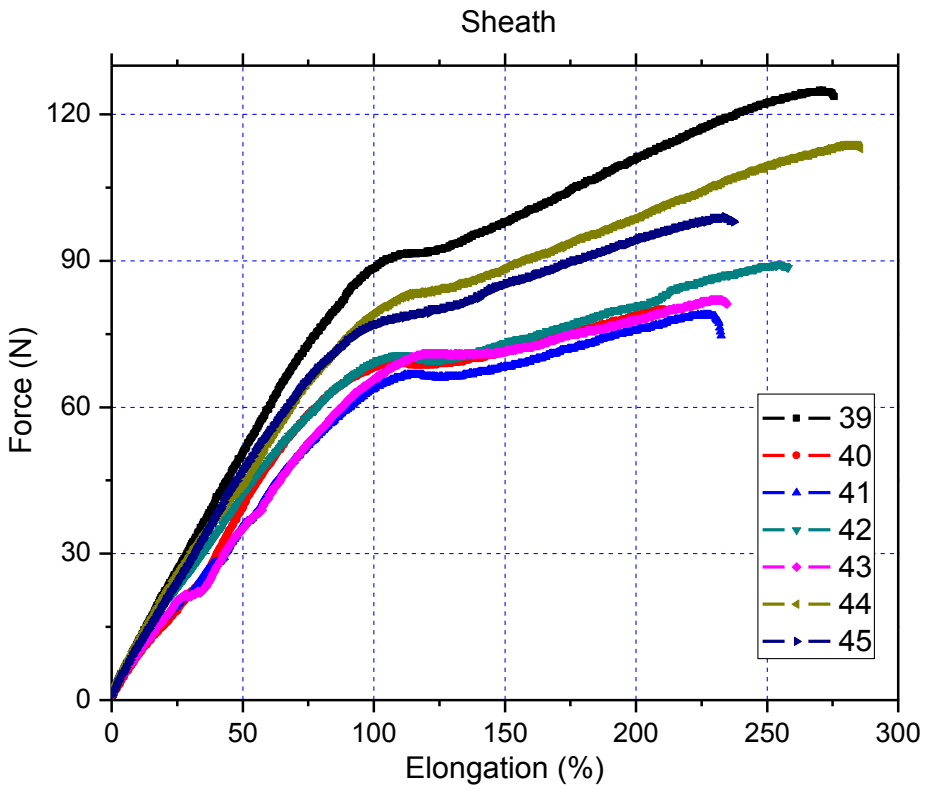

Figure 7.10: Elongation of sheath after 50MRad radiation ageing

It can be seen from Figures 7.9 and 7.10 that the change in percentage transmittance (i.e., energy absorption by specific chemical groups) has reflected in the tensile properties of insulation and sheath materials. The mean tensile strength and elongation for various dose levels of control cable insulation and sheath are shown in Table 7.11 and 7.12 respectively.

Table 7.11: Mean tensile strength and elongation for insulation

Dose (MRad)	Tensile strength (MPa)		EAB (%)	
	Mean	Standard deviation	Mean	Standard deviation
0	23.93	2.12	481	70.22
5	32.35	2.61	589	50.94
10	26.18	1.92	503	59.96
25	21.64	1.87	461	20.66
50	19.02	2.29	456	10.83

Table 7.12: Mean tensile strength and elongation for sheath

Dose (MRad)	Tensile strength (MPa)		EAB (%)	
	Mean	Standard deviation	Mean	Standard deviation
0	14.97	1.11	409	46.03
5	14.96	0.57	375	29.14
10	13.06	0.43	337	16.86
25	9.10	0.69	242	65.07
50	9.22	0.61	248	26.15

It is evident from Table 7.11 and 7.12 that it is the percentage transmittance which is indicating the extent of ageing although the infrared spectra appears similar in both insulation and sheath materials (i.e., no significant shift in the chemical groups were seen in two spectra). It can be seen from Table 7.12 that the tensile strength of sheath material has reduced significantly with the increased doses. This reduction in EAB is due to the presence of other additives in the sheath material for physical strength, mechanical and environmental protection. Generally, a fresh cable should have a minimum tensile strength of about 12.5N/mm^2 and an elongation greater than 200%.

The probability plotting of the EAB data for insulation and sheath has been performed to determine the life characteristic distribution. The detailed results of probability plotting of the EAB data for insulation and sheath are given in Appendix B. The data obtained under tensile testing was analyzed to determine the ageing process in the insulation and sheath material for degradation assessment. The plots obtained from the data analysis for insulation and sheath materials are shown in Figure 7.11 and 7.12 with coefficient of determination being 0.58 and 0.976 respectively.

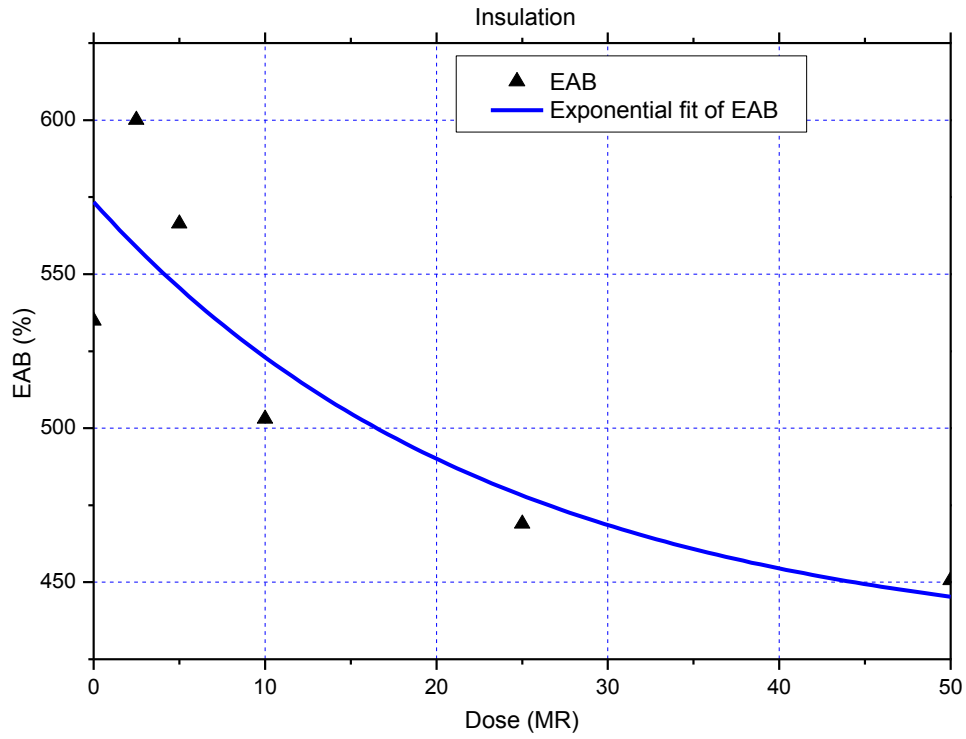

Figure 7.11: Exponential fit of EAB for insulation

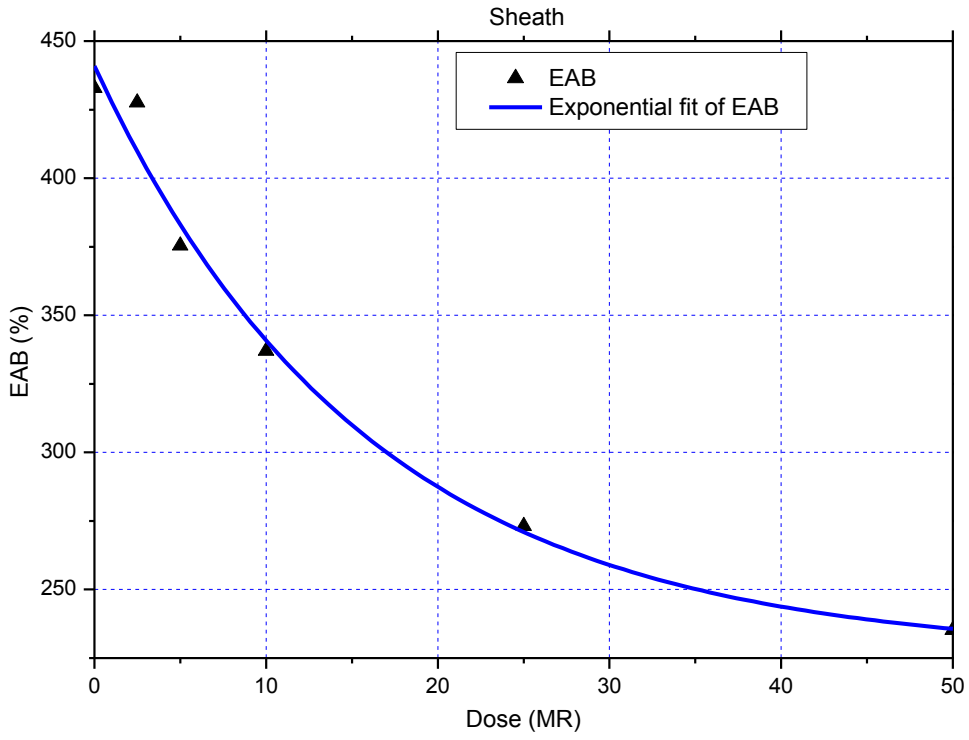

Figure 7.12: Exponential fit of EAB for sheath

It is evident from Figure 7.11 and 7.12 that though the ageing process is exponential in both the cases, the rates of degradation in insulation and sheath are significantly different. This difference in degradation rates is mainly due to the presence of various additives in each of the material. From the data analysis, the empirical relation for insulation and sheath is given by:

$$e = A + Be^{-Cd} \tag{7.3}$$

where, A, B and C are model parameters and d is the applied radiation dose. The model parameter values and the standard error obtained from the regression analysis for insulation and sheath are shown in Tables 7.13 and 7.14 respectively.

Table 7.13: Model parameters for insulation

Parameter	Value	Standard error
A	427.94	87.22
B	145.45	79.74
C	0.043	0.059

Table 7.14: Model parameters for sheath

Parameter	Value	Standard error
A	226.41	17.13
B	214.50	16.92
C	0.062	0.014

From the data analysis, it can be concluded that EAB alone cannot be a performance indicator for life prediction under radiation ageing as the dose required to reach the acceptable value of EAB is significantly large and practically not feasible. Therefore, a further evaluation of accurate performance indicators is needed for accurate life estimation of polymeric insulating materials. The IEC standard 544 [75] recommends that 50% of the initial value of the EAB be chosen as the end point criterion.

7.5.2.1 Correlation of infrared transmittance with EAB

Ultimate tensile elongation represents the parameter most often used to follow the degradation of plastic materials and is therefore the "gold-standard" to compare to data from other condition monitoring approaches. A correlation study between FTIR findings and tensile testing results was conducted and the results are shown in Figures 7.13 and 7.14.

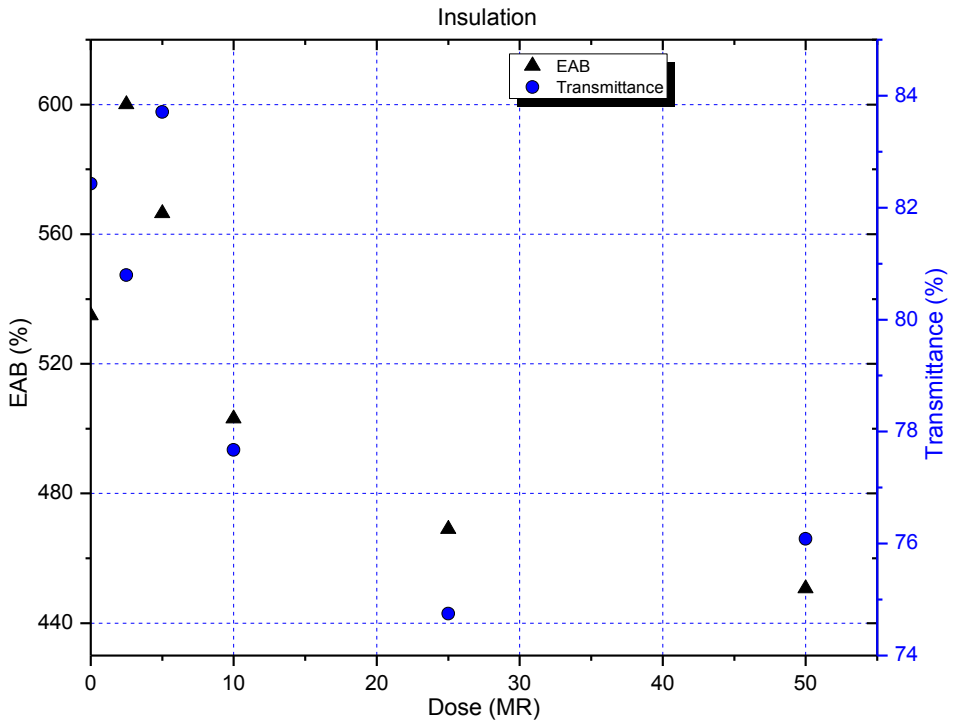

Figure 7.13: Mean elongation and mean transmittance with dose for insulation

It is observed from Figure 7.13 that a near correlation exists between the infrared transmittance and elongation in case of insulation material. However, as seen in Figure 7.14, a significant difference in correlation can be seen in case of sheath material at 5MRad and beyond 25MRad. This deviation is expected as the sheath material has other additives which may not affect the basic chemical structure of the polymer but induces the changes in mechanical properties. This is because, the high energy radiation can either induce cross-

linking or degradation in a polymer matrix depending on the properties of base matrix and the radiation parameters.

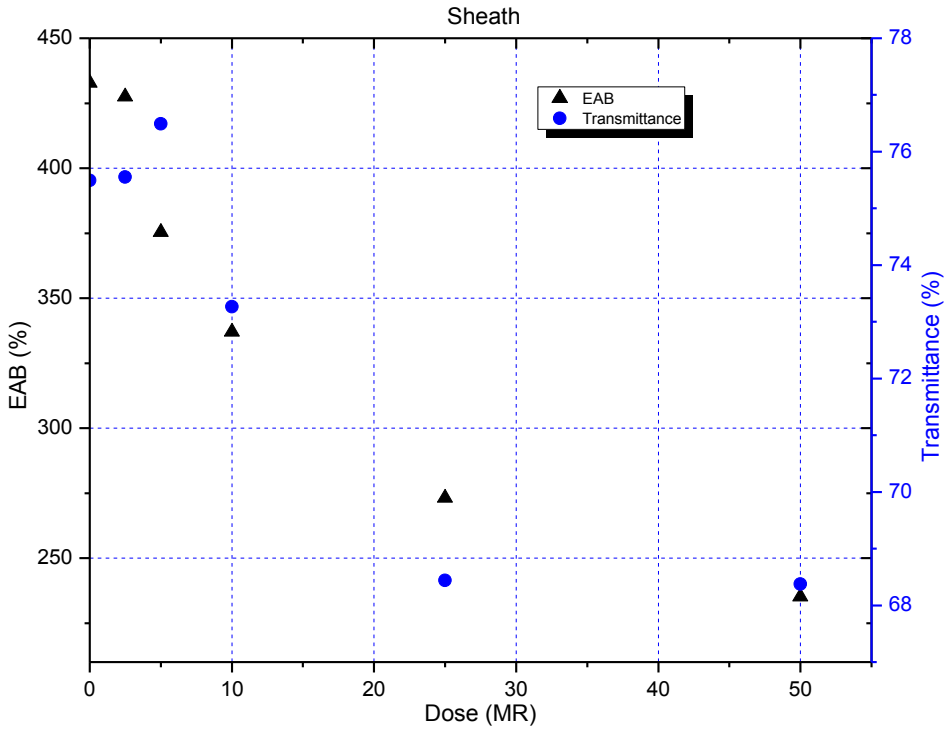

Figure 7.14: Mean elongation and mean transmittance with dose for sheath

PVC generally undergoes dehydrochlorination reaction after gamma irradiation. Due to the dehydrochlorination and inefficient inter-chain recombination of radicals, chain scission is expected to be a predominant process in irradiated PVC matrix. Chain scission of the PVC is expected to lead a reduction in the mechanical properties; the observed correlation between FTIR (C-Cl peak) and EAB supports this hypothesis. More experiments are however needed to clearly understand and quantify such changes. It can be noted that in certain cases where there are some additives present in the base polymer, a more appropriate condition assessment techniques need to be employed to substantiate the findings of infrared spectroscopy.

7.5.2.2 Discussion

A low voltage control cable with PVC insulation and PVC sheath was subjected to gamma radiation and the degradation due to radiation ageing was assessed using FTIR spectroscopy and tensile testing. It was observed that there is an improvement in the tensile properties at lower dose conditions. However, these properties degrade with increased dose levels in both insulation and sheath materials. This change in material properties may be due to the fact that the high energy radiation can either induce cross-linking or degradation in a polymer matrix depending on the properties of base materials and radiation parameters. A near perfect correlation exists between infrared transmittance and elongation in case of insulation material. However, a significant difference in correlation is seen in case of sheath material beyond 25MRad. This deviation is expected as the sheath material has other additives which may not affect the basic chemical structure of the polymer but may induce changes in mechanical properties. Therefore, in certain cases where there are some additives present in the polymers, a more appropriate condition assessment techniques need to be employed in addition to chemical characterization techniques when mechanical properties are major concern.

It was concluded from Anova study that there is a significant change in degradation due to radiation in insulation at various dose conditions at 5% significance level compared to that of sheath material. It can be seen from this study that the infrared transmittance can be directly related to EAB for polymeric insulation materials where there are no additives. However, precaution must be taken when correlating infrared transmittance with EAB in case of non-standard polymeric materials. It was concluded from the study that the elongation decreases rapidly under early stages of radiation ageing. However, under prolonged ageing condition the rate of degradation reduces significantly. Whereas, the degradation rate in

sheath material follows a homogeneous-exponential process throughout the ageing period. From the data analysis, it is concluded that EAB alone cannot be a performance indicator for life prediction under radiation ageing as the dose required to reach the acceptable value of EAB is significantly large and practically not feasible. Therefore, further evaluation of performance indicators is needed for life estimation of polymeric insulating materials.

7.5.3 Oxidation induction time and temperature measurement

The calibration of DSC on standard materials needs to be performed prior to any measurements on actual samples. The first sample to be tested is the Indium or Tin reference material as recommended by ASTM D3895-07 standard [156]. In this study, Indium has been used as a reference material for calibration of DSC131. The recommended heating cycle for Indium is as follows: Nitrogen atmosphere with a gas flow rate of 50ml/min, heating rate of 10^0C/min from 120^0C to 180^0C, sample mass of approximately 5-10mg in sealed aluminium pan. The standard melting point of Indium is about 156.63^0C. The calibration of DSC 131 was carried out with the recommended procedure and the heat flow profiles obtained for two samples of different masses of Indium are shown in Figures 7.15 and 7.16.

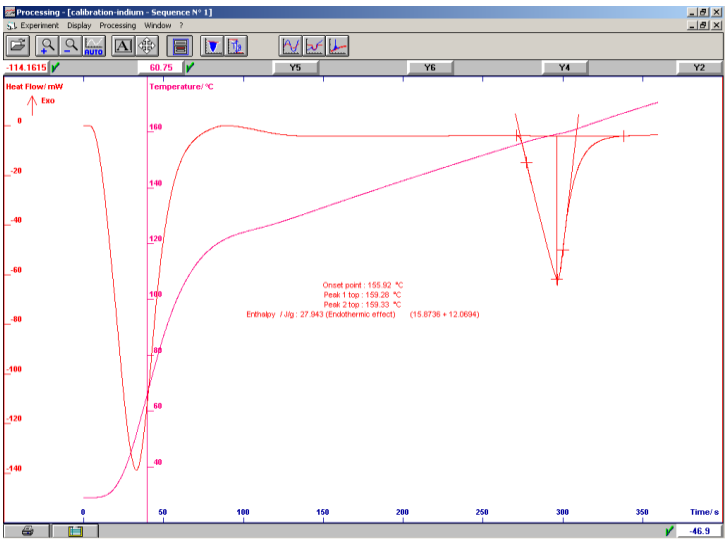

Figure 7.15: Heat flow signal for sample 1

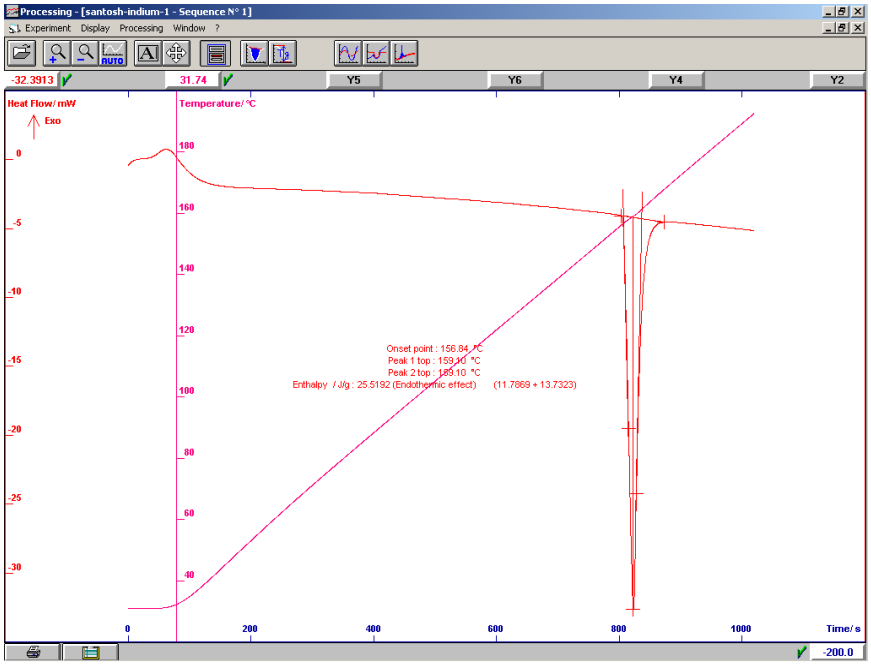

Figure 7.16: Heat flow signal for sample 2

It is observed from the calibration curves that the melting temperature of Indium obtained from DSC131 is very close to the standard melting point of Indium. Hence, the equipment is said to be calibrated for further experimental analysis on samples of I&C cables of NPPs.

7.5.3.1 Determination of oxidation induction time (OIT) and temperature (OITp)

The OIT measurements were carried out using SETARAM DSC131 differential scanning calorimeter in accordance with ASTM D3895-07 standard [156] in the range from 180^0C to 220^0C, and up to 8 hours on fresh and irradiated cable insulation materials. However, none of the heat flow signals showed a clear onset oxidation under isothermal condition. Hence, an alternative method known as oxidation induction temperature was employed to determine isothermal OIT. The OITp measurements were carried out on fresh and irradiated samples of upto 50MRad dose conditions. The DSC thermograms for insulation and sheath are shown in Figure 7.17 and 7.18 respectively. A clear exothermic peak can be seen between 220^0C and

270^0C for both insulation and sheath material at different dose levels. The detailed results of OIT and OITp measurements on individual cables are given in Appendix A.

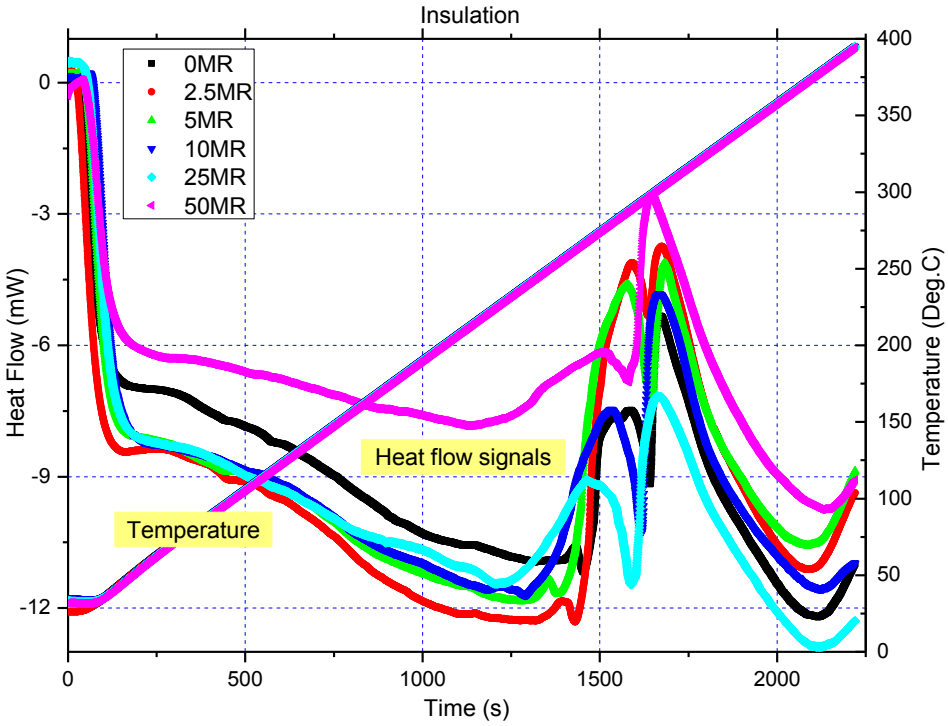

Figure 7.17: DSC thermogram of insulation

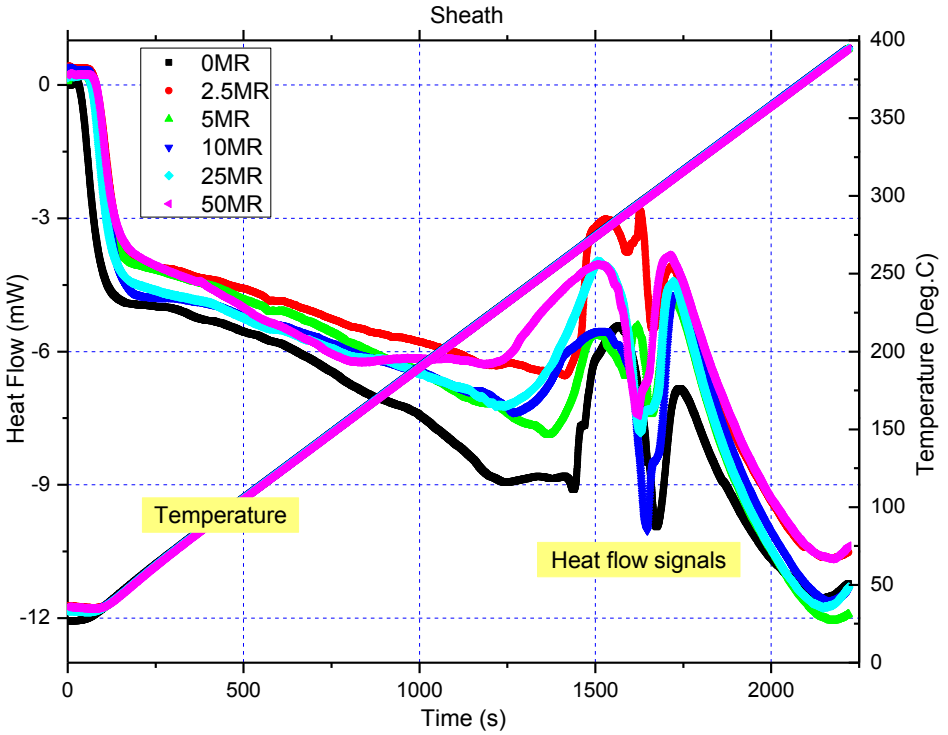

Figure 7.18: DSC thermogram of sheath

7.5.3.2 Determination of oxidation induction time from the measured oxidation induction temperature

The approach employed in this study is the one developed by Gimzewski [157]. The primary thermally induced oxidation reaction that occurs in the DSC is given by:

$$RH + O_2 \rightarrow R\cdot + HO_2\cdot \tag{7.4}$$

where, RH is an undamaged polymer chain, $R\cdot$ is a polymer free-radical, and $HO_2\cdot$ is a hydroperoxide free-radical. Assuming that the reaction in Eq. (7.4) follows an Arrhenius relationship, as was assumed by Gimzewski [157]. The corresponding rate equation for reaction (7.4) is:

$$\frac{d}{dt}[RH] = -[RH][O_2]Ae^{-\frac{E_a}{kT}} \tag{7.5}$$

where, A is a constant related to the initial polymer concentration, Ea is the activation energy, k is Boltzmann's constant, and T is the test temperature. Direct measurement of the OIT is done in the isothermal mode of the DSC which is known as time-scanning method. In this mode, letting $T = T_{iso}$, Eq. (7.5) can be integrated until the antioxidant is exhausted to give the following:

$$\int \frac{d[RH]}{[RH][O_2]A} = -\int_0^{OIT} e^{-\frac{E_a}{kT}}\,dt = -(OIT)e^{-\frac{E_a}{kT_{iso}}} \tag{7.6}$$

Although OIT cannot be solved from this equation, this result will be used in the second method for determining OIT as described below. Alternatively, the DSC can be operated in the temperature scanning mode. This provides a measure of the oxidation induction temperature (OITp), which is the temperature at which the antioxidant is entirely consumed. In this mode the temperature of the polymer sample is raised at a constant rate until the

antioxidant is exhausted, i.e., until the oxidation induction temperature is reached. The temperature ramp rate, dT/dt, can be introduced into Eq. (7.6) as follows:

$$\frac{d}{dT}[RH]\left(\frac{dT}{dt}\right) = -[RH][O_2]Ae^{-\frac{E_a}{kT}} \tag{7.7}$$

Integration of Eq. (7.7) from the initial temperature, T_0 to OITp and denoting the ramp rate by α gives:

$$\int \frac{d[RH]}{[RH][O_2]A} = -\frac{1}{\alpha}\int_{T_0}^{OIT_p} e^{-\frac{E_a}{kT}}\,dt \tag{7.8}$$

The integrals on the LHS of Eq. (7.6) and (7.8) are equal because both are integrated until the antioxidant is exhausted. Therefore the RHS of Eq. (7.6) and (7.8) can be set equal. This gives for OIT:

$$OIT = \frac{1}{\alpha} e^{\frac{E_a}{kT_{iso}}} \int_{T_0}^{OIT_p} e^{-\frac{E_a}{kT}}\,dt \tag{7.9}$$

Thus, by measuring OITp and E_a, the integral in Eq. (7.9) can be evaluated numerically. Eq. (7.9) provides the basis for a comparison between the OIT measured directly and the OIT calculated from the measured thermal parameters OITp and Ea.

The activation energy for most of the PVC based insulation materials is found to be between 0.92 to 1.25eV [5,127,154]. Comparing the initial EAB from Figure 7.11 and 7.12, a factor of about 1.27 times higher EAB is found for insulation. Hence, activation energy of 0.92eV for sheath and 1.18eV for insulation was assumed for OIT calculations. The plots of calculated isothermal OITs corresponding to the observed OITp as a function of radiation dose for insulation and sheath are shown in Figure 7.19 and 7.20 respectively.

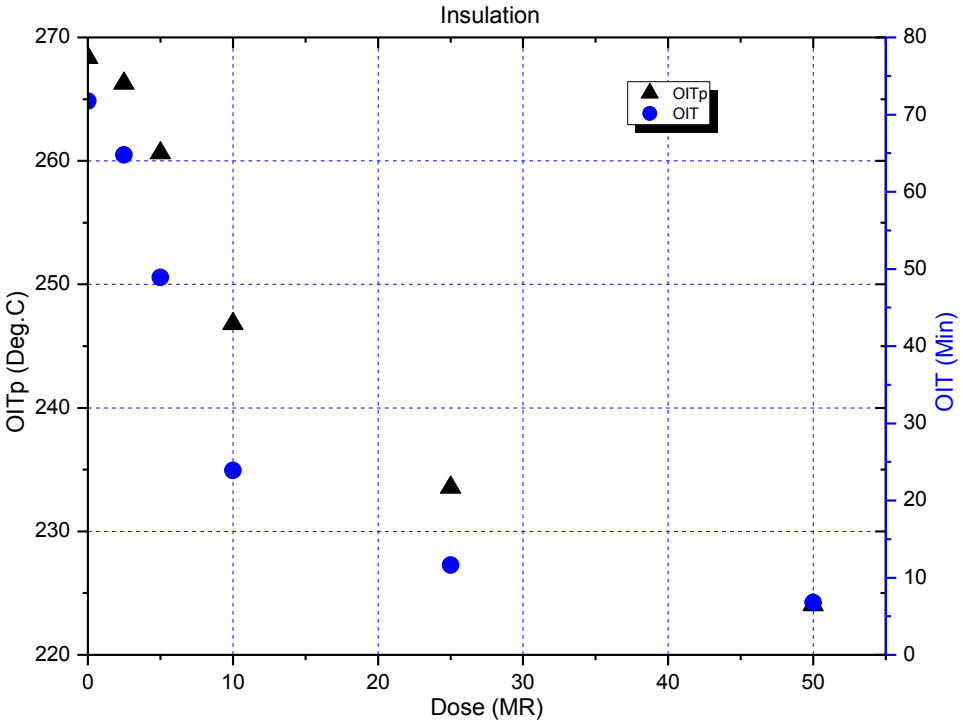

Figure 7.19: OIT vs. dose for insulation

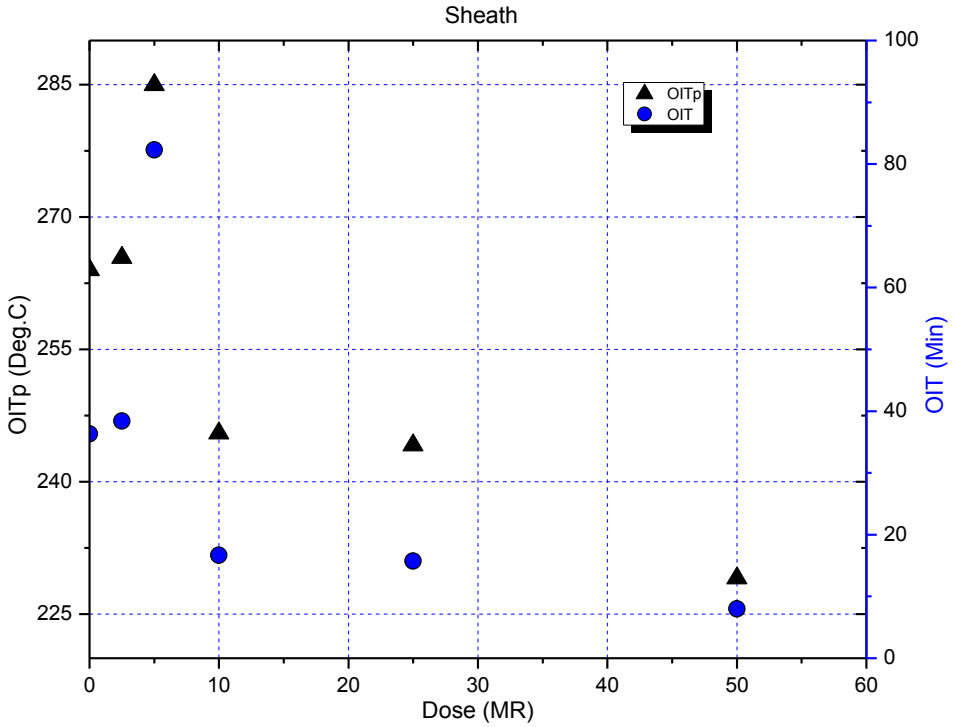

Figure 7.20: OIT vs. dose for sheath

7.5.3.3 Correlation between oxidation induction time and EAB

Since elongation is an accepted benchmark characterization technique for polymeric materials, the calculated OITs need to be correlated with EAB for degradation assessment and life prediction purposes. The correlation between EAB and OIT with coefficient of determination being 0.99 for insulation and 0.93 for sheath is shown in Figure 7.21 and 7.22 respectively.

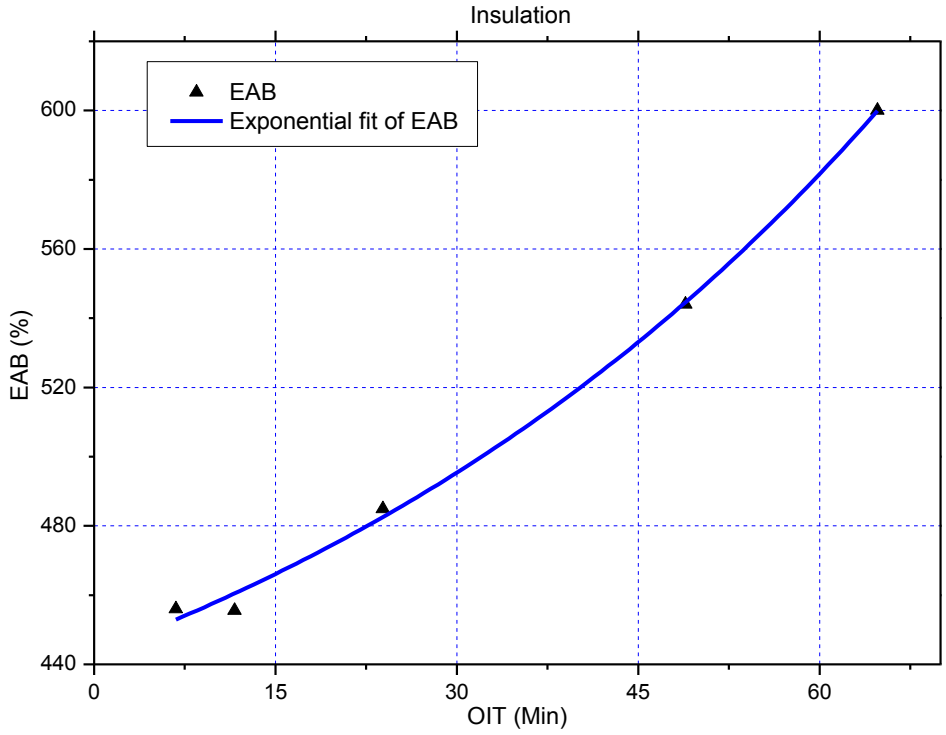

Figure 7.21: Exponential fit of EAB for insulation

It is observed from Figure 7.21 and 7.22 that the relationship between EAB and OIT for both insulation and sheath is found to be exponential under radiation ageing, however their rates of degradation are relatively different. This is mainly due to the generation of free-radicals, chain scission, cross-linking process during gamma radiation and with the presence of different antioxidants in the insulation and sheath.

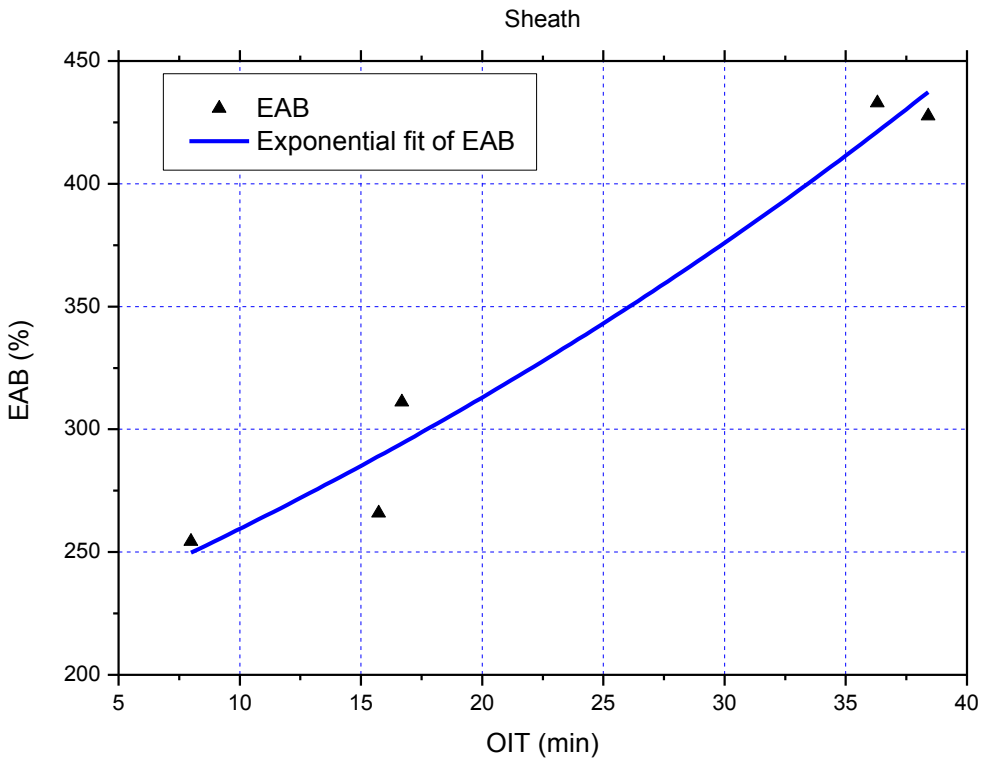

Figure 7.22: Exponential fit of EAB for sheath

7.5.3.4 Discussion

The DSC findings for radiation aged cable insulation are relatively in good agreement with the EAB. From the experimental evaluations, it was found that the EAB fits an exponential function of OIT for both insulation and sheath material under radiation ageing. From the empirical models obtained from the correlation study, the OITs corresponding to 50% elongation were predicted for both insulation and sheath. It should be noted here that, the OITs estimated in this study are at non-isothermal conditions. This predicted OIT values will be further related to the OITs under isothermal condition and the remaining life estimation evaluations will be carried out for reliability assessment studies.

7.5.4 Scanning electron microscopy

Scanning electron microscopy is an important technique in materials research. Field emission scanning electron microscopy (FESEM) is used to visualize very small topographic details on the surface or entire or fractioned objects. This examination can yield information about the topography, morphology, composition and crystallographic information [61-62].

In order to monitor the state of the fresh and aged cable insulation, the samples of the insulating materials mentioned in Table 7.6 were observed under SEM. The samples were initially made conductive for current by coating them with an extremely thin layer (1.5 - 3.0 nm) of gold. The SEM images for fresh and irradiated insulation and sheath are shown in Figure 7.23-7.32. The SEM images show a significant change in the material geometry and structure for radiation aged samples. Both cross-sectional and surface topography of the SEM indicates material becoming brittle at high radiation.

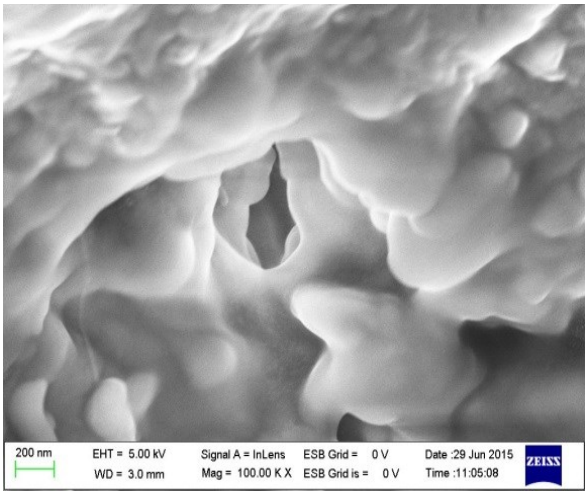

Figure 7.23: SEM micrograph of unaged insulation

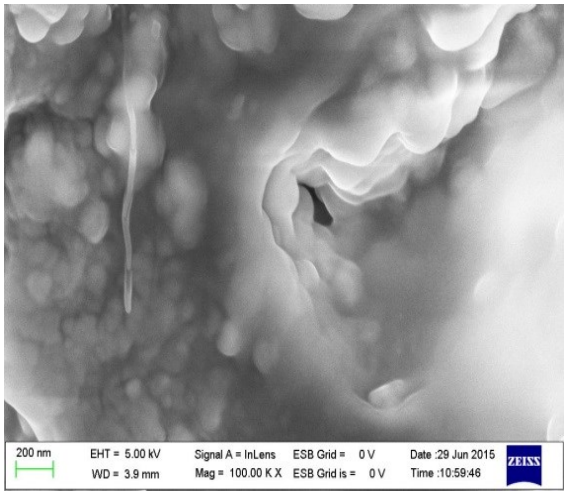

Figure 7.24: SEM micrograph of unaged sheath

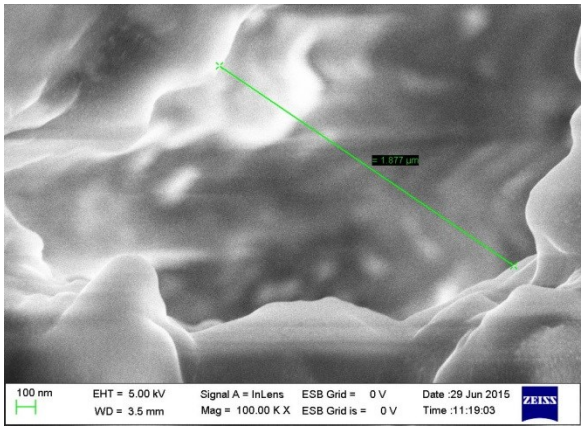

Figure 7.25: SEM micrograph of insulation aged at 5MRad

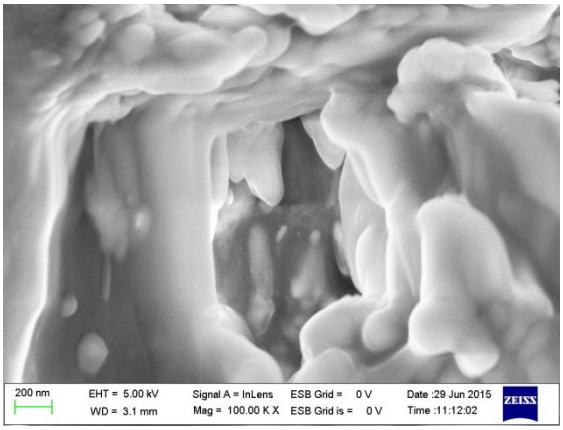

Figure 7.26: SEM micrograph of sheath aged at 5MRad

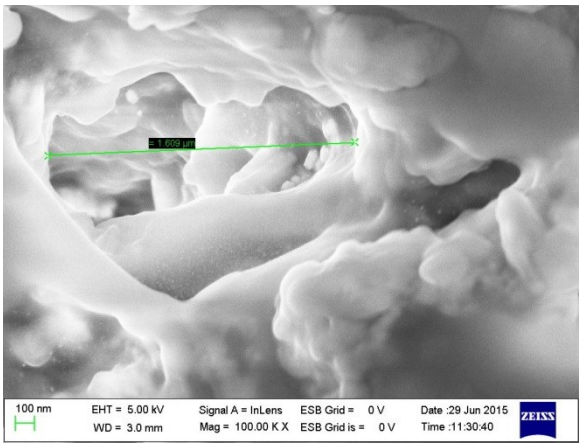

Figure 7.27: SEM micrograph of insulation aged at 10MRad

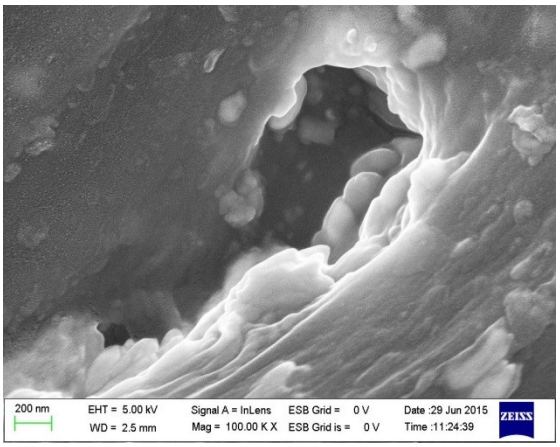

Figure 7.28: SEM micrograph of sheath aged at 10MRad

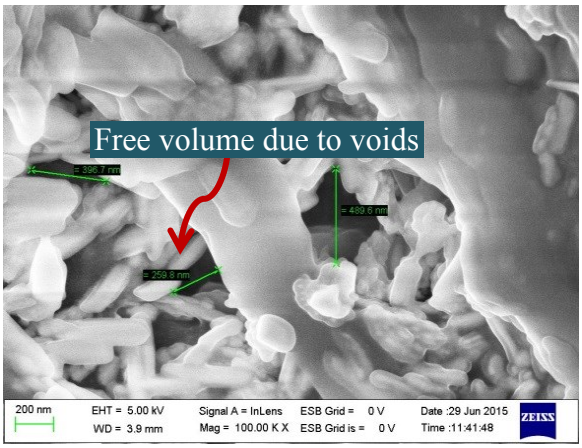

Figure 7.29: SEM micrograph of insulation aged at 25MRad

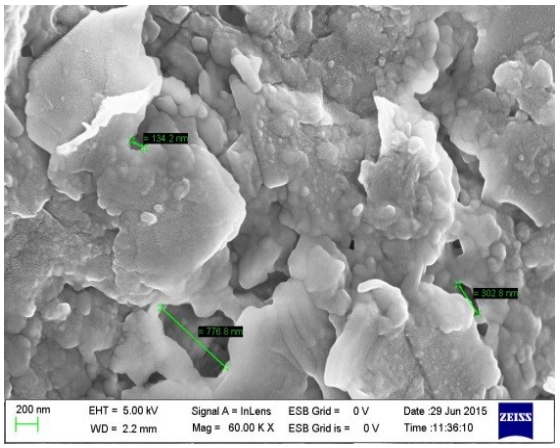

Figure 7.30: SEM micrograph of sheath aged at 25MRad

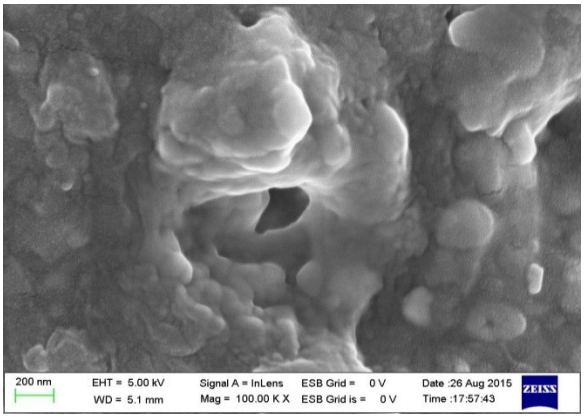

Figure 7.31: SEM micrograph of insulation aged at 50MRad

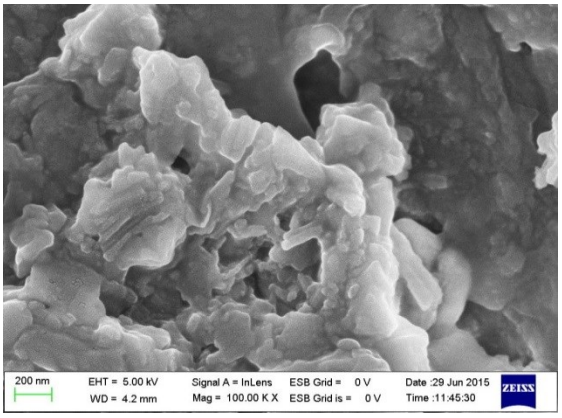

Figure 7.32: SEM micrograph of sheath aged at 50MRad

It is observed from the SEM micrographs that the surface is uniformly smooth and homogeneous in the case of unaged materials whereas irregular structure with discrete objects is seen in the micrographs of aged samples. This is mainly due to the fact that the gamma irradiation of polymeric materials may result in (a) cross-linking, (b) chain scission and (c) oxidation reaction. The cross-linking and chain scission reactions modify the macro-molecular chains of the material. The chain scission leads to the scissoning of macro-molecular chains. Oxidation leads to both chain scission and cross-linking which may result in the embrittlement of the insulation [158]. It is concluded that the SEM findings support the degradation behaviour assessed from several other CM techniques.

7.5.5 Positron annihilation lifetime spectroscopy

The PALS was carried out on irradiated cable sheath materials (aged from 2.5MRad to 50MRad) and the free volume fraction was estimated. The initial estimate of free volume fraction in sheath (heat resistant PVC) is estimated by assuming that all the free volume holes are of same size and are spherical in shape (usual assumption in PALS). The relative free volume is shown in Figure 7.33.

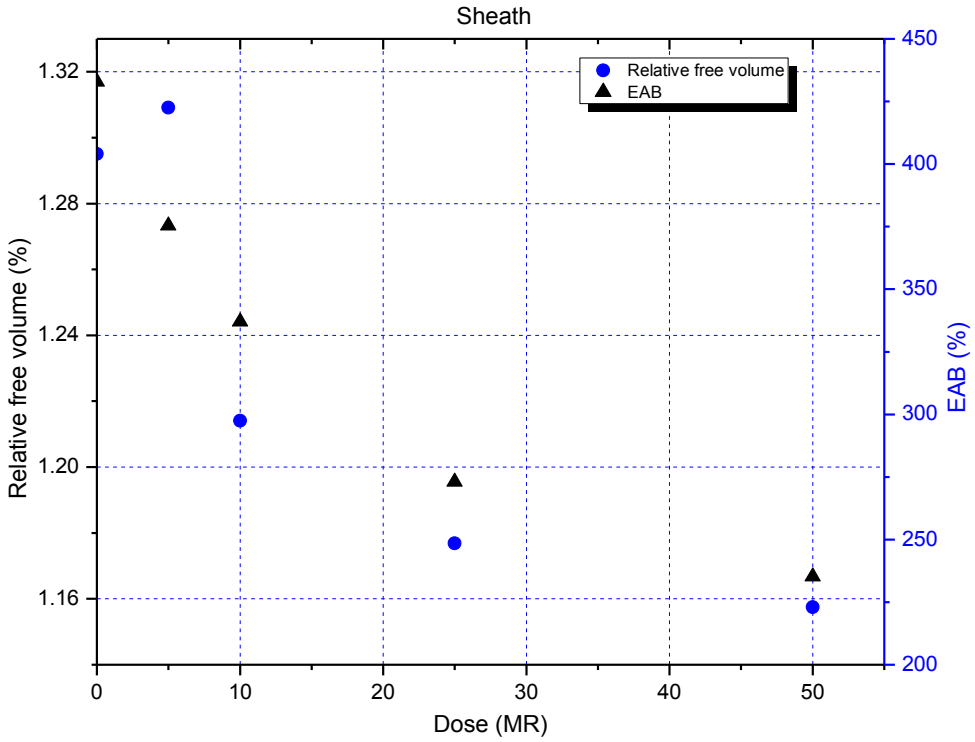

Figure 7.33: Relative free volume vs. dose

Generally, gamma radiation causes the chain scission in the polymer structure thereby evolving free volume in the bulk material. This process is found to be predominant at lower doses (upto 5MRad in this case). As the more free volume is available in the polymer structure, crosslinking takes place thereby forming a dense structure which makes the polymer chain more rigid resulting reduction in elongation [159]. The effect of chain scission was observed in DSC and FTIR analysis as well. However, this effect of chain scission due to gamma radiation was not observed in tensile testing.

7.5.5.1 Estimation of free volume hole size

The study was further extended to assess the free volume hole size and their probability with respect to gamma radiation for use in structural damage analysis [160-161]. Analysis is done considering the free volume holes to have distribution of sizes around certain mean

value and shape are assumed to be spherical. The probability distributions of free volume holes at various dose levels are shown in Figure 7.34.

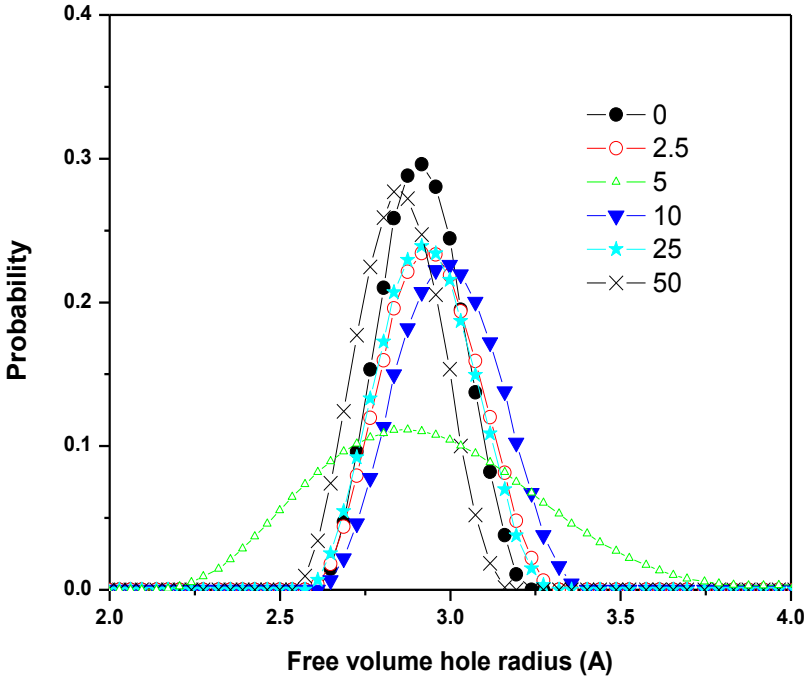

Figure 7.34: Probability distribution of free volume holes in sheath

It is observed from Figure 7.34 that, a large variation in size of the free volume holes exists at 5MRad dose level. This is attributed to the formation of free volume due to chain scission. As the radiation dose increases, the free volume is occupied by the newly formed crosslinks thereby reducing the free volume hole radius. By looking at the probability curves, mean free hole radius in all dose levels is near 3Angstrom. During gamma radiation and in the process of chain scission and crosslinking, oxidation also occurs, which causes the polymer to become more brittle.

7.6 Accelerated thermal ageing

The cable chosen for experiments is of low voltage cables (≤ 1100V) as they are extensively used in nuclear power plant for I&C applications. The specifications of cable are shown in Table 7.15.

Table 7.15: Cable specimen for thermal ageing

Cable type	Specifications	Polymer type		Year of manufacturing
		Insulation	Sheath	
Signal cable	37 core, 1.5sq.mm, 1100V	FRLS PVC	HRPVC	2011

The samples were prepared from insulation and sheath materials and thermal ageing experiments were conducted in forced air circulating ovens at temperatures from 110^0C to 150^0C, for time periods as shown in Table 7.16. The test temperatures were selected based on the guidelines suggested in IEC 60216 [162]. A minimum of 3 samples (as shown in Table 7.16) were kept under each test condition. The samples were taken out periodically as per the schedule shown in Table 7.16 to perform tensile elongation and oxidation induction time/temperature measurements.

Table 7.16: Test matrix for thermal ageing

Time (days)	Temperature (^{0}C)		
	110	135	150
21	3	3	3
36	3	3	3
61	3	3	3
91	3	3	3
119	3	3	3

7.6.1 Determination of oxidation induction time and temperature

7.6.1.1 Determination of oxidation induction temperature

The OIT measurements were carried out in the range from 180^0C to 220^0C, and up to 8 hours on fresh and thermally aged polymeric insulation materials. Additionally, OITp

measurements were carried out on these samples. The DSC thermograms of insulation and sheath at 110^0C and 135^0C are shown in Figure 7.35 to 7.38. The legend, for example, 110T22D in Figures refers to samples aged at 110^0C and up to 22 days.

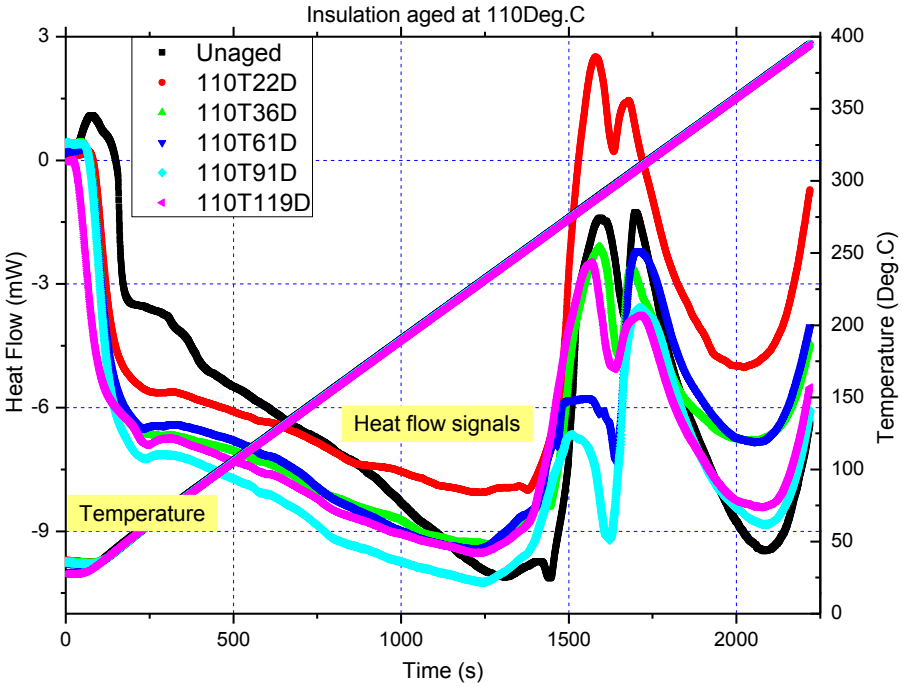

Figure 7.35: DSC thermogram of insulation aged at 110^0C

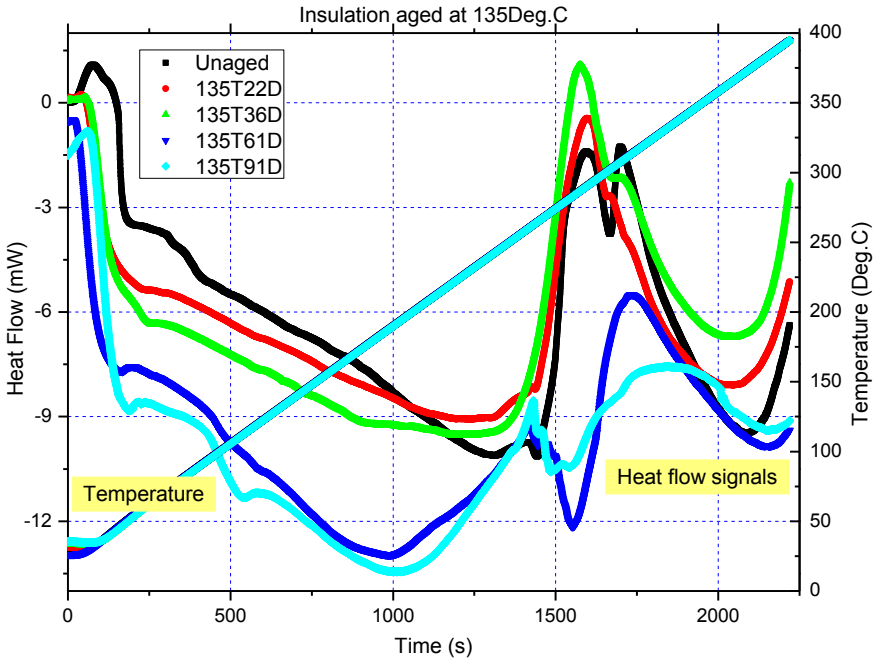

Figure 7.36: DSC thermogram of insulation aged at 135^0C

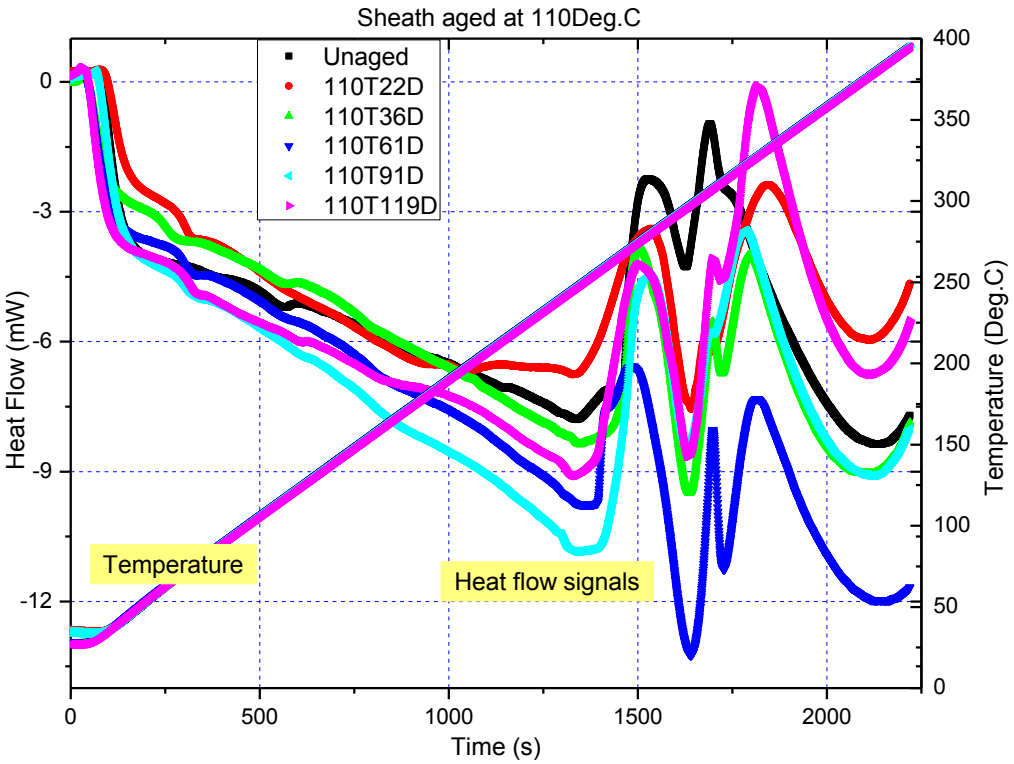

Figure 7.37: DSC thermogram of sheath aged at 110^0C

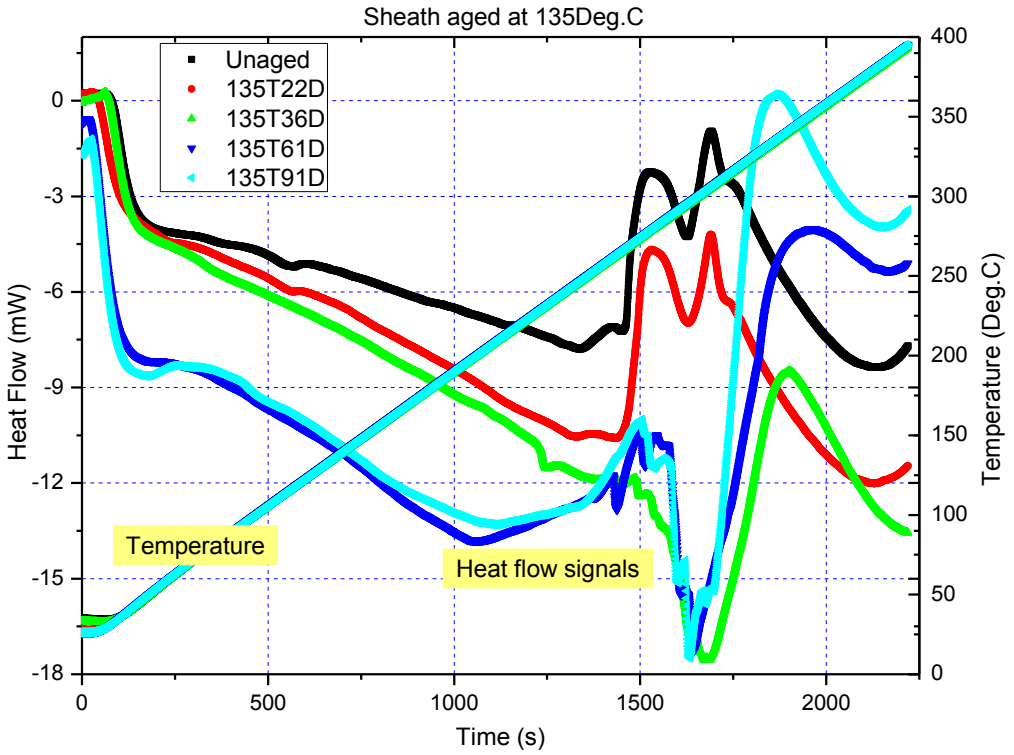

Figure 7.38: DSC thermogram of sheath aged at 135^0C

7.6.1.2 Determination of oxidation induction time from the measured oxidation induction temperature

The procedure employed in calculating the OIT from the measured OITp under radiation ageing was used for thermal ageing as well. The calculated isothermal OITs corresponding to experimental OITp of thermally aged signal cable insulation and sheath at 110^0C and 135^0C are shown in Figure 7.39 and 7.40 respectively.

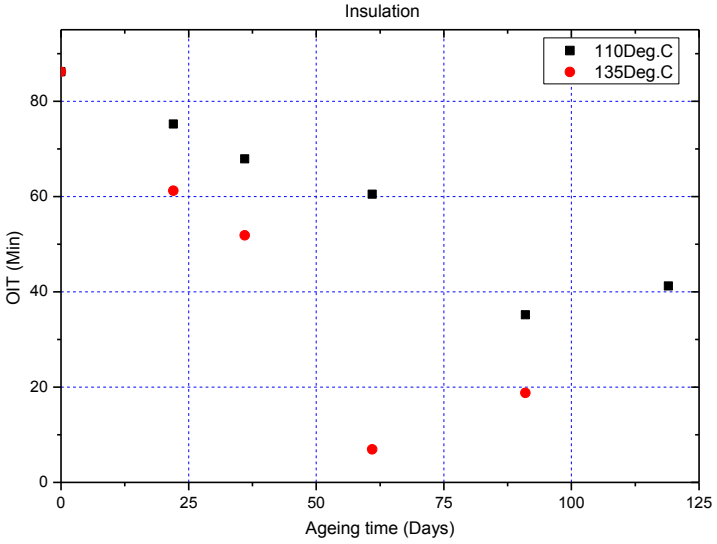

Figure 7.39: OIT vs. ageing time for insulation

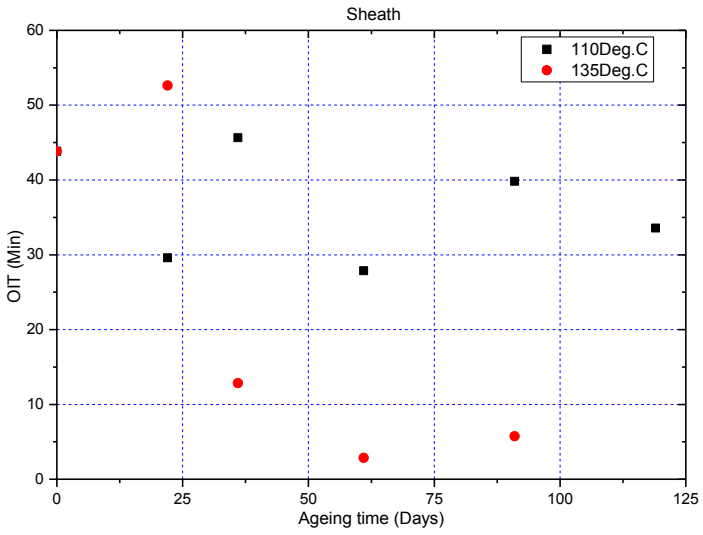

Figure 7.40: OIT vs. ageing time for sheath

7.6.2 Measurement of elongation at break

7.6.2.1 Tensile elongation of cable insulation

Tensile elongation was performed on the thermally aged samples and elongation curves for insulation aged at 110^0C and 135^0C are shown in Figure 7.41 and 7.42 respectively.

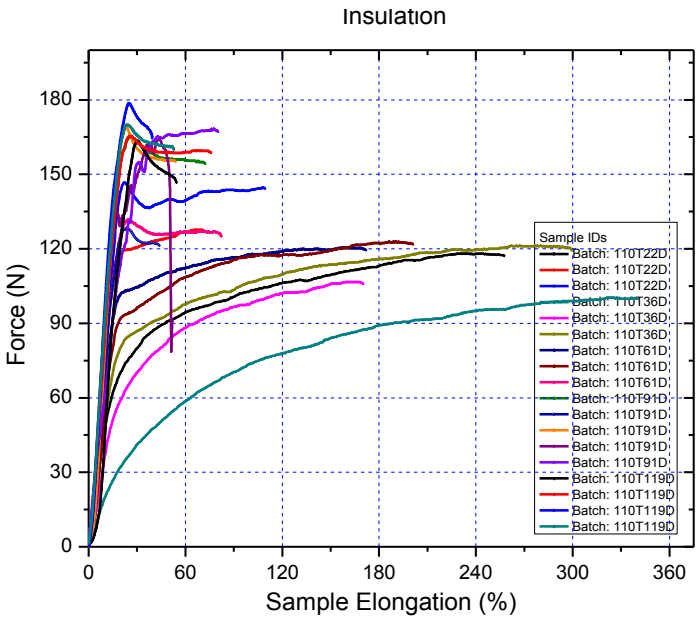

Figure 7.41: Elongation of thermally aged cable insulation at 110^0C

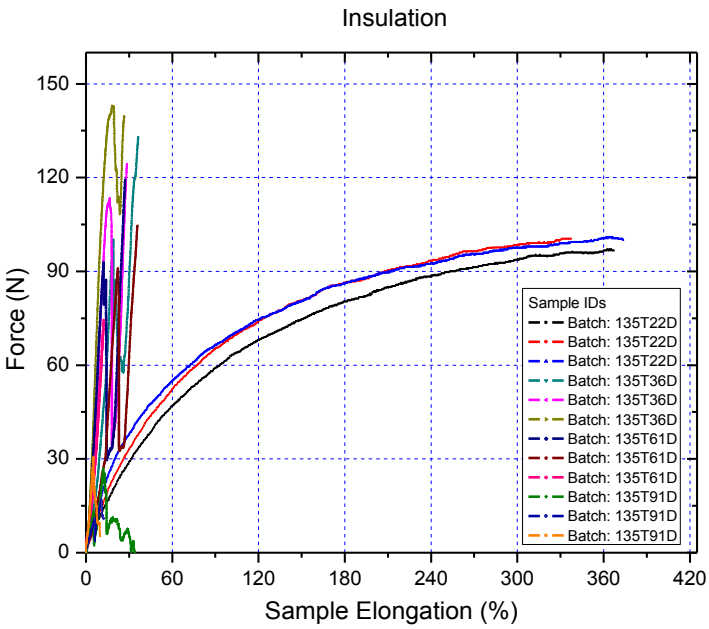

Figure 7.42: Elongation of thermally aged cable insulation at 135^0C

It is observed from the elongation curves that EAB has significantly decreased over the long term accelerated thermal ageing of insulation material. From Figure 7.42, almost all samples failed before 50% of the elongation as samples aged at higher temperature except for the case of 22 days of ageing. The tensile testing results indicate that the insulation materials completely got oxidized at the earlier stages of accelerated ageing at 135^0C and slightly at longer periods at 110^0C. From the tensile testing results, it can be concluded that the OIT or OITp values for the almost oxidized sheath material may not provide any information about remaining life and therefore not useful in life estimation.

In order for better understanding of the degradation due to thermal ageing, the tensile testing results have been compared among the same duration at different temperatures. The resultant plots of EAB are shown in Figures 7.43 and 7.44 for 36 and 91 days of ageing respectively.

From Figure 7.44, it is observed that all the samples show an elongation less than 25% at 135^0C for 36 days of ageing and the elongation for that of 110^0C varies from approximately 175 to 340%. Similar degradation trend can also be seen in Figure 7.44 for 91days of ageing.

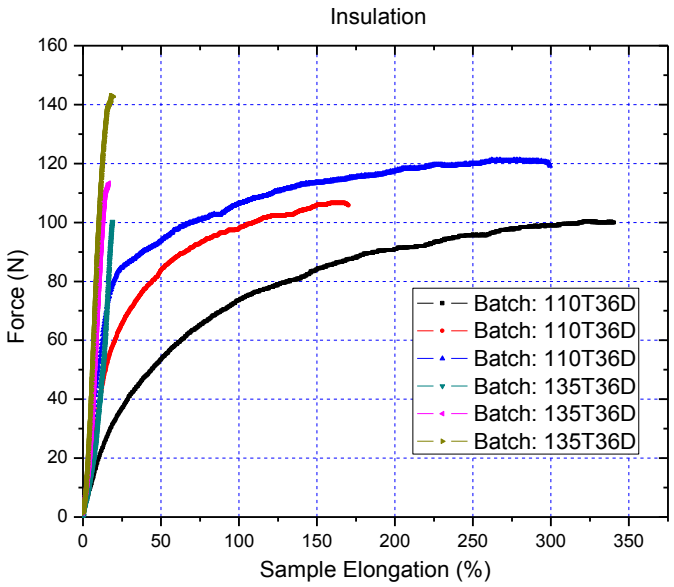

Figure 7.43: Sample elongation for 36 days of ageing at 110^0C and 135^0C

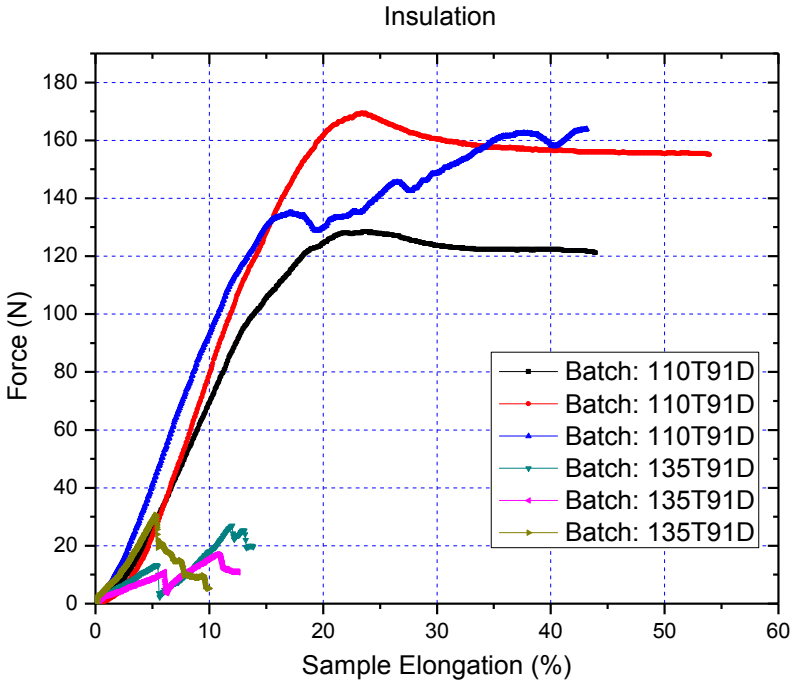

Figure 7.44: Sample elongation for 91 days of ageing at 110^0C and 135^0C

The EAB measurements on thermally aged cable insulation materials were performed. The mean EAB for insulation under 110^0C and 135^0C is shown in Figure 7.45.

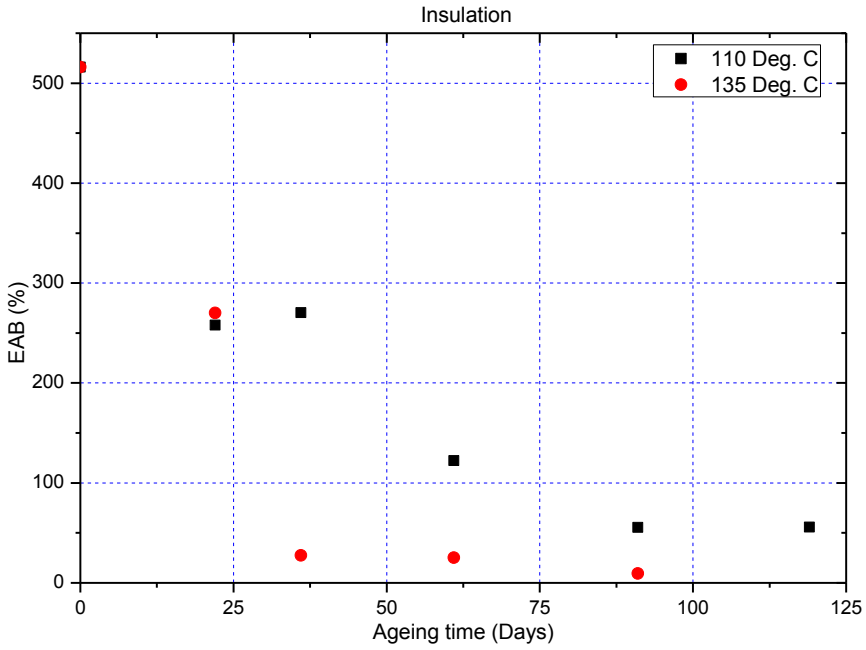

Figure 7.45: EAB vs. ageing time for insulation

7.6.2.2 Tensile elongation of cable sheath

Tensile elongation measurements were performed for cable sheath material under 110^{0}C and 135^{0}C ageing conditions. The EAB results on these thermally aged cable sheath material for two temperature conditions are shown in Figure 7.46 and 7.47.

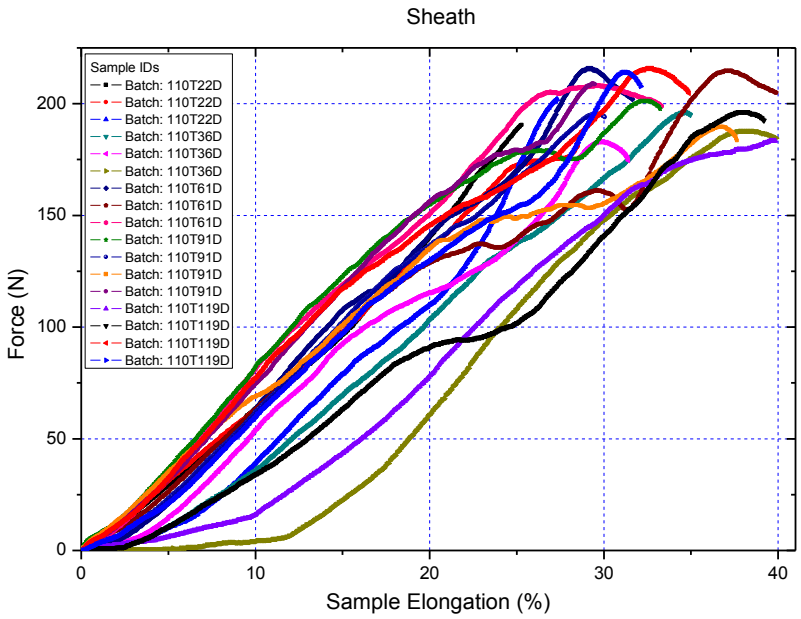

Figure 7.46: Tensile elongation of sheath material at 110^{0}C

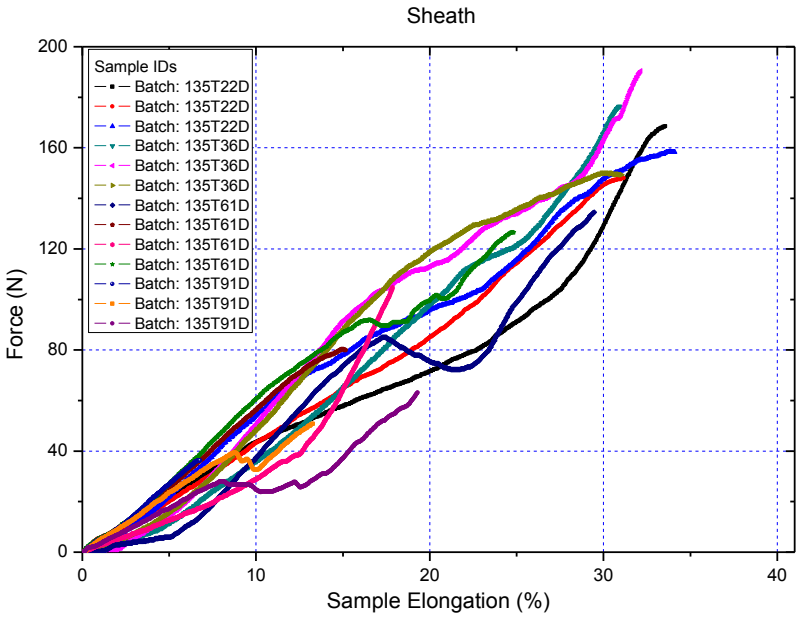

Figure 7.47: Tensile elongation of sheath material at 135^{0}C

It is observed from the elongation curves, all the samples have the EAB less than a benchmark value of 50% for both 110^0C and 135^0C cases. The mean elongation against ageing time for both the ageing conditions is shown in Figure 7.48.

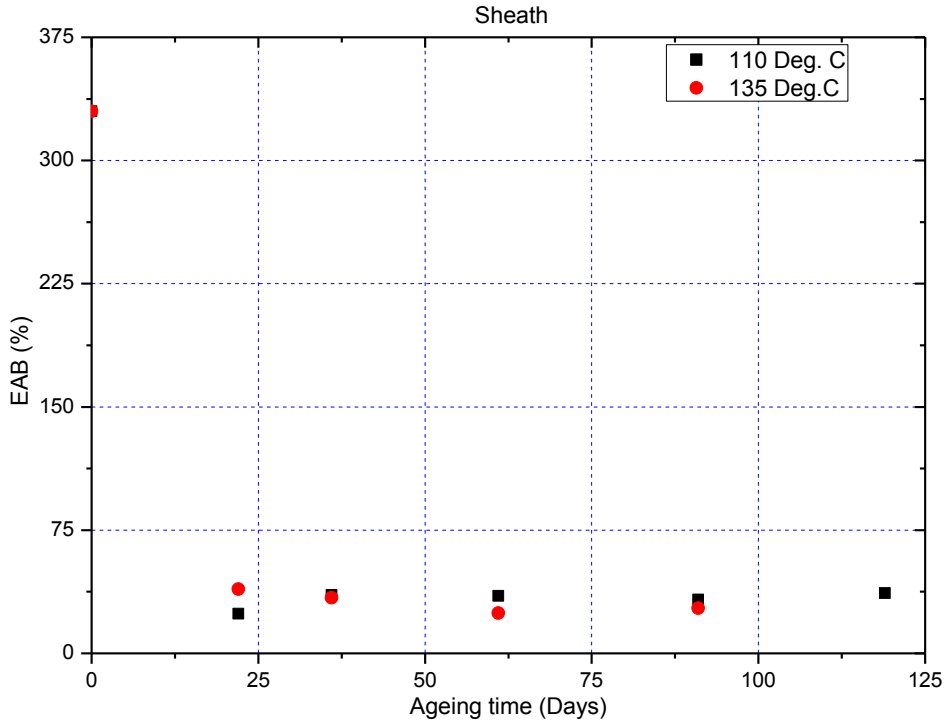

Figure 7.48: Mean elongation vs. ageing time of sheath material

As DSC findings for sheath material are not clear indicative of a particular trend of the ageing effect due to complete decomposition of thermally aged samples, establishing correlation between OIT and EAB will not be logical. Hence, the life prediction of sheath material under thermal ageing was not possible in this study from DSC findings.

7.6.2.3 Correlation between oxidation induction time and EAB

The experimental data was analyzed to derive an empirical model for EAB. An exponential fit of EAB as a function of OIT with coefficient of determination being 0.767 at 110^0C for insulation and 0.989 at 110^0C for sheath are shown in Figure 7.49 and 7.50 respectively.

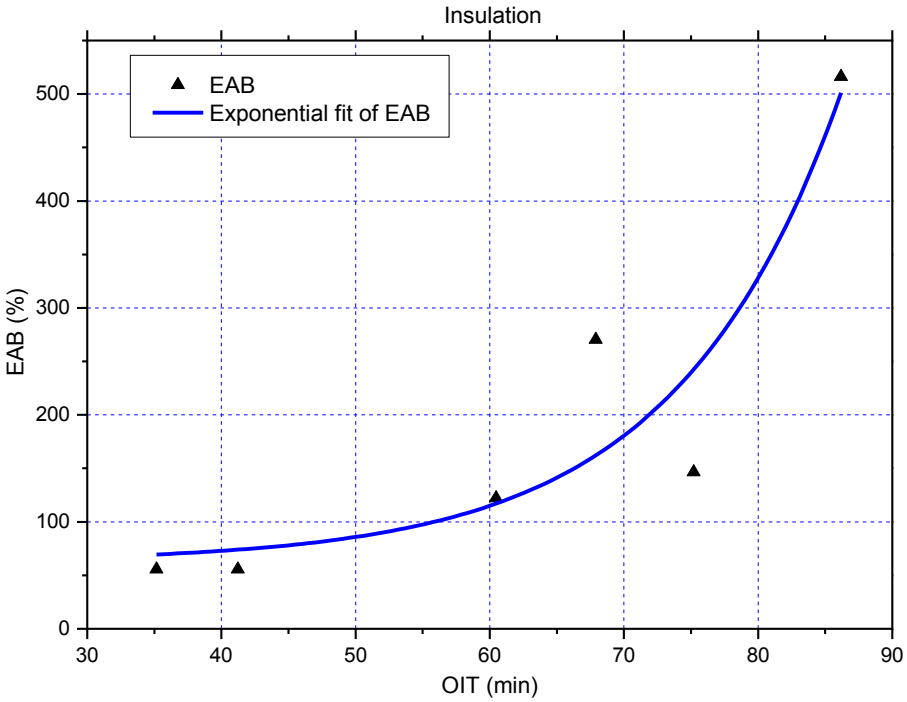

Figure 7.49: Exponential fit of EAB for insulation

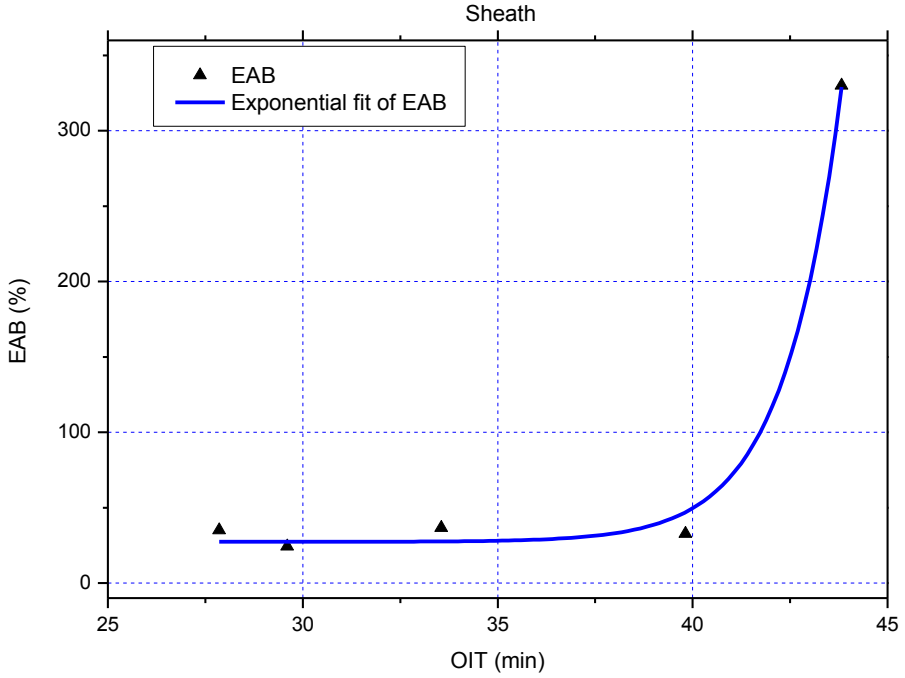

Figure 7.50: Exponential fit of EAB for sheath

The exponential model obtained from the data analysis is shown in Eq. (7.10).

$$EAB = A + Be^{C*OIT_{acc}} \tag{7.10}$$

where, A, B and C are model parameters and OIT_{acc} is the OIT at 200^0C. The parameter values and the standard error obtained from the data analysis for insulation and sheath are shown in Tables 7.17 and 7.18 respectively.

Table 7.17: Model parameters for insulation

Parameter	Value	Standard error
A	62.5	73.1
B	0.405	1.69
C	0.081	0.047

Table 7.18: Model parameters for sheath

Parameter	Value	Standard error
A	29.89	6.54
B	4.18e-11	4.23e-10
C	0.596	0.20

Comparing graphs 7.21, 7.22, 7.49 and 7.50, it is observed that a near exponential degradation phenomenon takes place under thermal and radiation ageing. However, the rates of degradation are significantly different in both thermal and radiation ageing conditions. It is also evident from the experimental evaluations that due to the changes in the chemical structure from both radiation and thermal ageing, a significant reduction in thermo-oxidative stability and mechanical properties of insulation material was observed.

7.6.3 Scanning electron microscopy

7.6.3.1 Fracture surface examination

In order to monitor the state of the fresh and thermally aged cable insulation, the samples of the insulation materials mentioned in Table 7.15 were observed under SEM. The SEM images of fresh and thermally aged samples are shown in Figure 7.51 to 7.68.

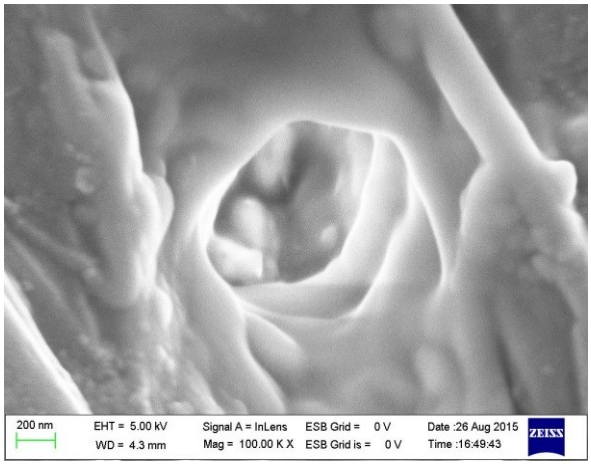

Figure 7.51: SEM micrograph of unaged insulation

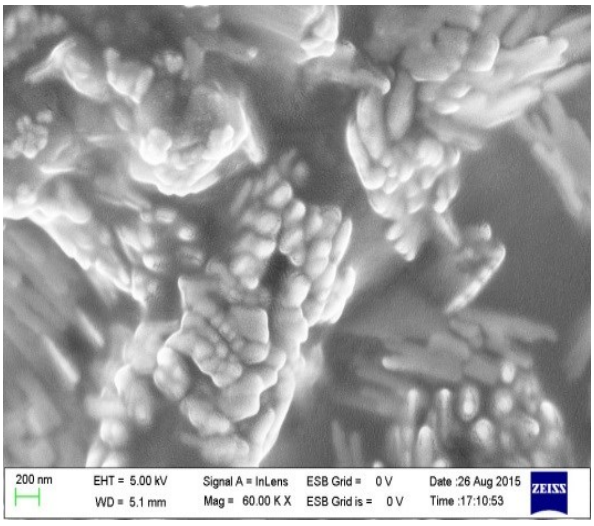

Figure 7.52: SEM micrograph of insulation after 22 days of ageing at 110^0C

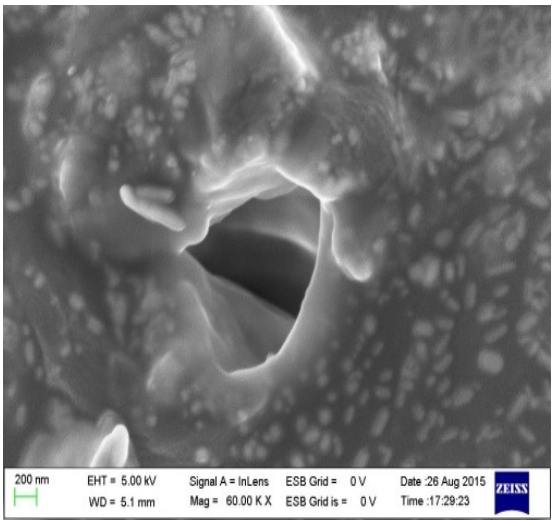

Figure 7.53: SEM micrograph of insulation after 22 days of ageing at 135^0C

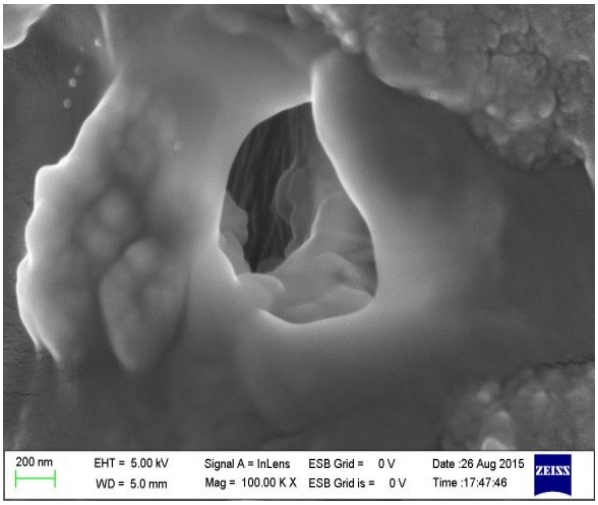

Figure 7.54: SEM micrograph of insulation after 36 days of ageing at 110^0C

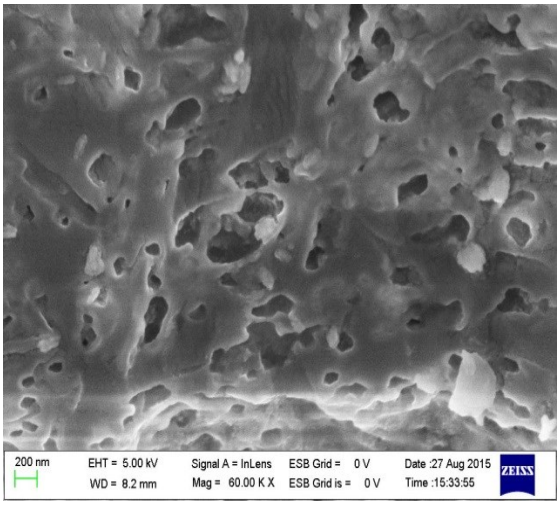

Figure 7.55: SEM micrograph of insulation after 36 days of ageing at 135^0C

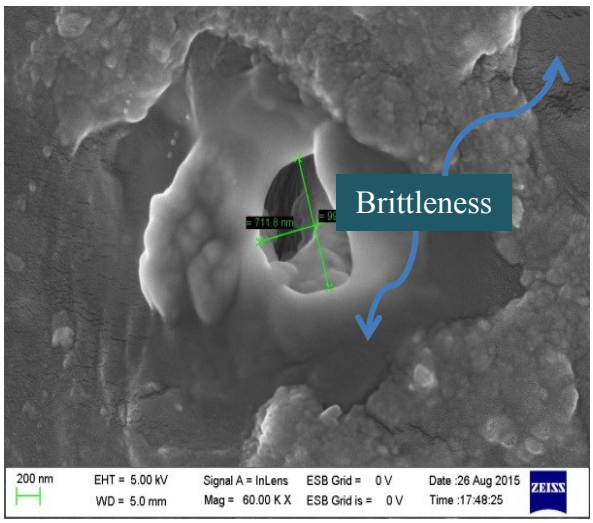

Figure 7.56: SEM micrograph of insulation after 61 days of ageing at 110^0C

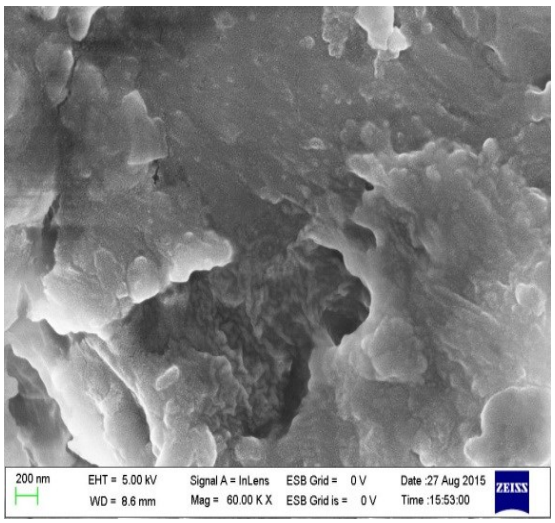

Figure 7.57: SEM micrograph of insulation after 61 days of ageing at 135^0C

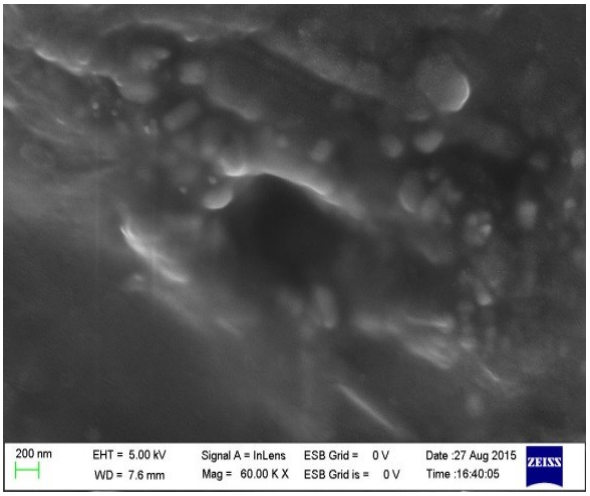

Figure 7.58: SEM micrograph of insulation after 91 days of ageing at 110^0C

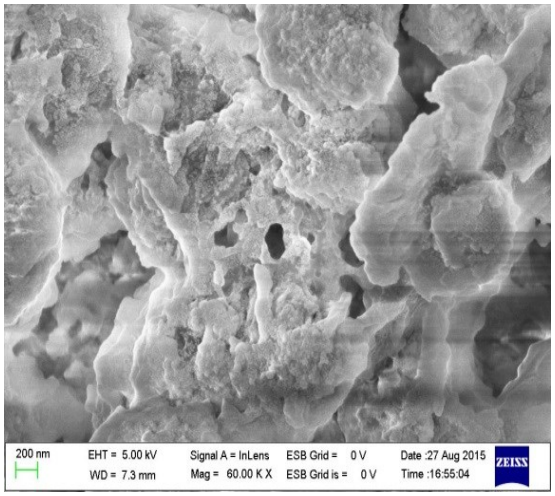

Figure 7.59: SEM micrograph of insulation after 91 days of ageing at 135^0C

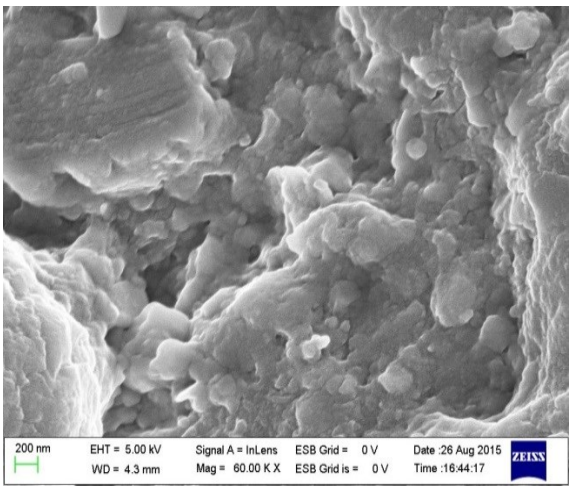

Figure 7.60: SEM micrograph of unaged sheath

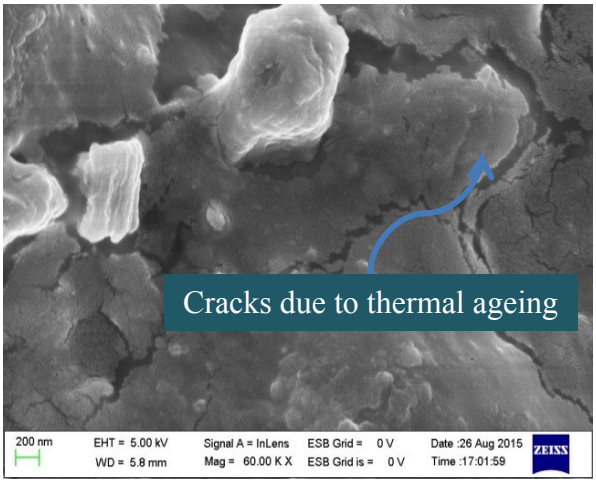

Figure 7.61: SEM micro graph of sheath after 22 days of ageing at 110^0C

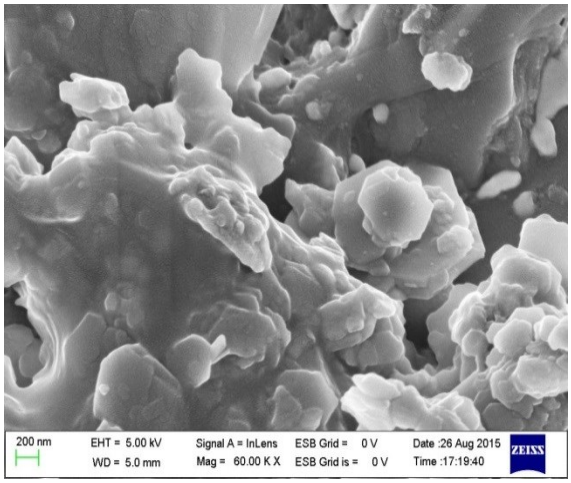

Figure 7.62: SEM micrograph of sheath after 22 days of ageing at 135^0C

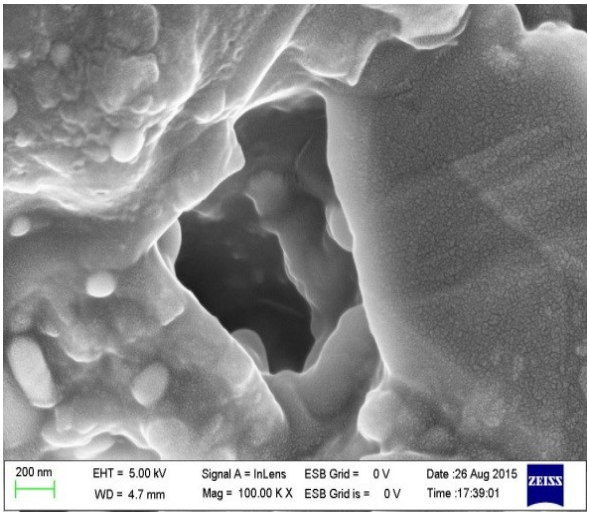

Figure 7.63: SEM micrograph of sheath after 36 days of ageing at 110^0C

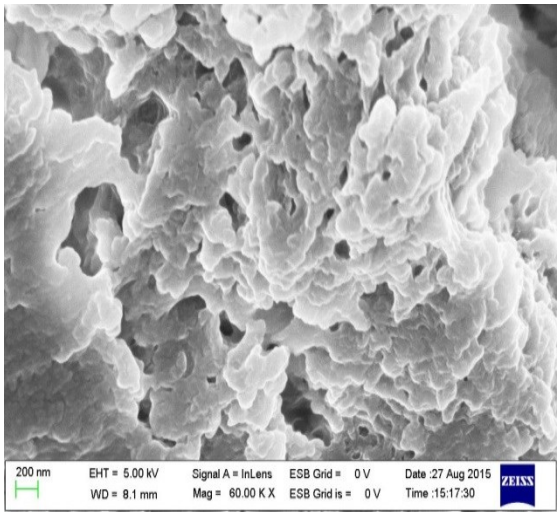

Figure 7.64: SEM micrograph of sheath after 36 days of ageing at 135^0C

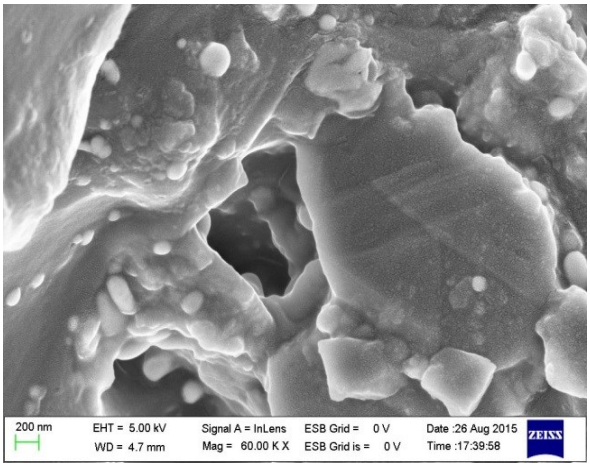

Figure 7.65: SEM micrograph of sheath after 61 days of ageing at 110^0C

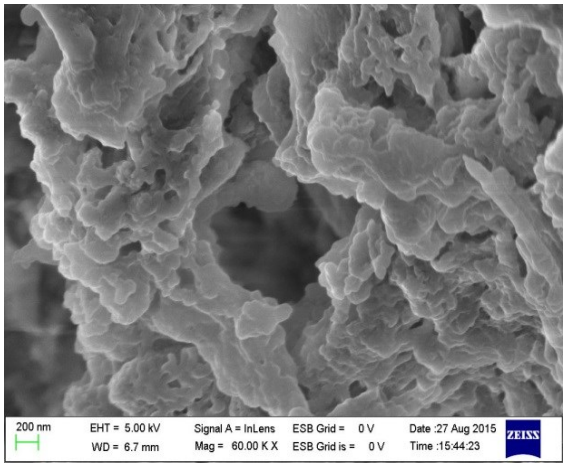

Figure 7.66: SEM micrograph of sheath after 61 days of ageing at 135^0C

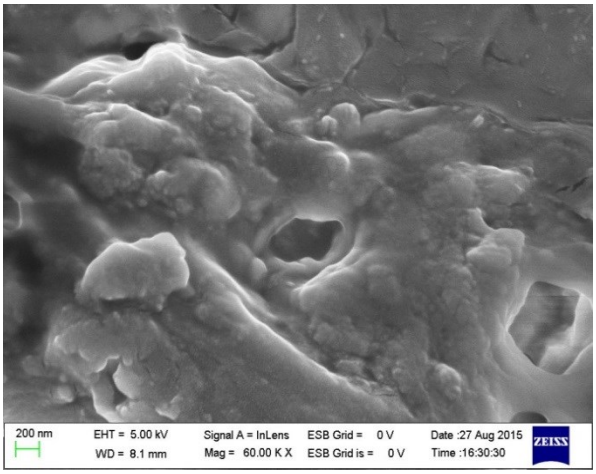

Figure 7.67: SEM micrograph of sheath after 91 days of ageing at 110^0C

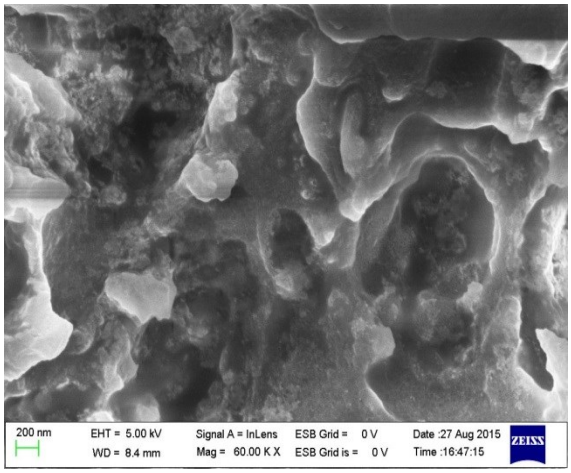

Figure 7.68: SEM micrograph of sheath after 91 days of ageing at 135^0C

The SEM micrographs of thermally aged samples reveal a significant degradation thereby causing a change in the material geometry and structure. It is also evident that the material has become brittle in about 22 days of ageing at relatively high temperature condition and noticeable cracks can be found. It can be concluded that the findings of SEM analysis support the degradation observed from various other techniques and their correlation. As the OITs

determined from the OITp measurement are in good agreement with the benchmark CM techniques, these predicted OITs are used for reliability prediction of I&C cable insulation materials for incorporating the cable ageing into PSA of NPPs.

7.6.3.2 Surface examination

In order to be observed with a SEM the samples were first made conductive for current by coating them with an extremely thin layer (1.5 - 3.0 nm) of gold. The SEM images of fresh and thermally aged samples of the cable insulating materials are shown in Figure 7.69-7.72.

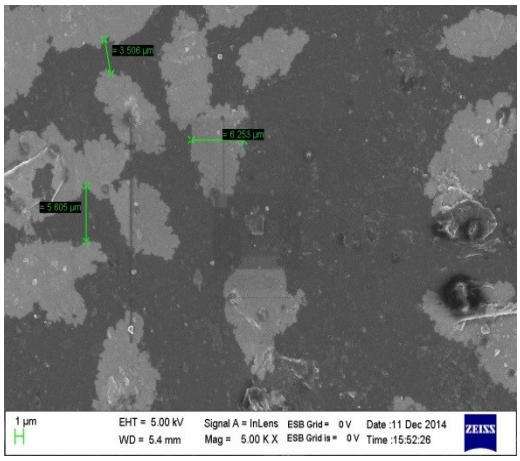

Figure 7.69: Image of unaged insulation

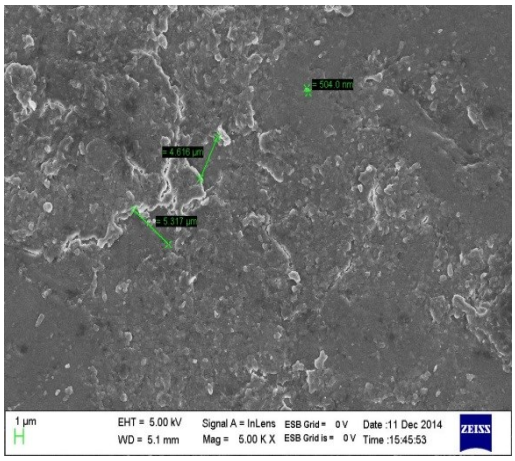

Figure 7.70: Image of unaged sheath

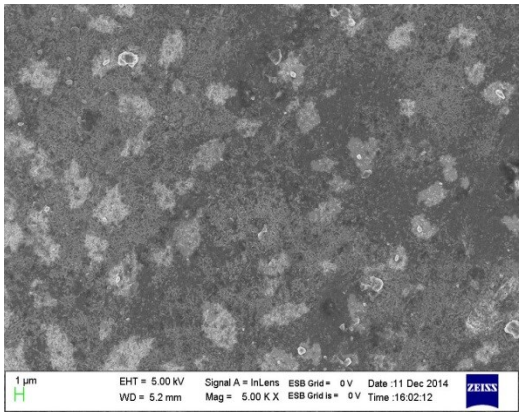

Figure 7.71: Image of insulation aged at 110^0C after 36 days

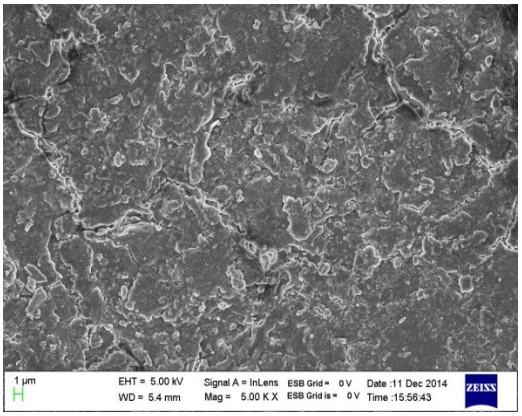

Figure 7.72: Image of sheath aged at 110^0C after 36 days

The SEM images show a significant change in the material geometry under thermal aged samples. Both cross-sectional and surface topography indicates material becoming brittle at high temperature.

7.7 Summary

Insulation resistance measurement was carried out on five I&C cables received from three different manufacturers. IR and polarization index were measured and compared against the recommended values from the standards. It was seen from the study that, there is a significant variation in the IR values among different manufacturers. Also, it was found that though there is a significant variation in IR values, there is not much change in their PI values and the relationship between IR and leakage current. All five cables fit an exponential model with a coefficient of determination being greater than 99%. This indicates that the basic phenomenon is unaffected among the various manufacturers though there is significantly large variation in the IR values. Hence, polarization index along with IR should also be considered in assessing the performance of I&C cables.

A low voltage control cable with PVC insulation and PVC sheath was subjected to gamma radiation and the degradation due to radiation ageing was assessed using FTIR spectroscopy and tensile testing. It was observed that there is an improvement in the tensile properties at lower dose conditions. However, these properties degrade with increased dose levels in both insulation and sheath materials. A near perfect correlation exists between infrared transmittance and elongation in case of insulation material. However, a significant difference in correlation is seen in case of sheath material beyond 25MRad. Therefore, in cases where certain additives are present in polymers a more appropriate condition assessment technique needs to be employed in addition to chemical characterization techniques when mechanical properties are major concern. It was also apparent from Anova

study that there is a significant change in degradation due to radiation in insulation at various dose conditions at 5% significance level compared to that of sheath material. From the data analysis, it can be concluded that EAB alone cannot be a performance indicator for life prediction under radiation ageing as the dose required to reach the acceptable value of EAB is significantly large and practically not feasible. Therefore, a further evaluation of performance indicators is needed for life estimation of polymeric insulating materials.

From the experimental evaluations, it was observed that the EAB fits an exponential function of OIT for both insulation and sheath material under radiation ageing. From the empirical models obtained from the correlation study, the OITs corresponding to 50% elongation were predicted for both insulation and sheath. Differential scanning calorimetry and tensile testing experiments were performed on aged samples to assess the degradation due to thermal ageing and life estimation. The oxidation induction times obtained under non-isothermal condition of thermally aged cable insulation are in good agreement with elongation-at-break values. However, these findings do not indicate clearly a particular trend of the thermal ageing effect for sheath material for 135^0C. This behavior of DSC findings is due to the fact that under 135^0C condition the sheath material has completely oxidized in the earlier stages of thermal ageing which is seen by tensile testing results. Therefore, the life estimation for sheath material under thermal ageing condition was not possible through DSC. The reliability prediction has been carried out for a thermally aged insulation material from EAB and OIT measurements.

Chapter 8 Reliability Prediction from Experimentally Determined Performance Indicators

8.1 Introduction

The performance parameters predicted from various condition assessment techniques in Chapter 7 are used for reliability prediction. Based on the property such as EAB, OIT, etc. an appropriate reliability technique can be applied to estimate the reliability. Since EAB is related to material resistance to the applied load, the stress-strength interference theory is employed to determine the cable reliability. Similarly, the OIT is related to characteristic life or mean time to reach end-of-life, the Weibull reliability model is employed to determine the cable reliability.

8.2 Reliability prediction from EAB

The exponential model obtained from the experimental data for insulation aged at 110^0C is given in Eq. (8.1) and the model parameters are shown in Table 8.1.

$$EAB_{model} = A + Bexp^{-ct} \tag{8.1}$$

Table 8.1: Model parameters for insulation aged at 110^0C

Parameter	Value	Standard error
A	22.72	51.97
B	485.79	57.58
C	0.025	0.007

From the structural reliability methods, the probability of failure is computed from the following relation:

$$P_f = P\ (g(EAB_{Model}, EAB_{th}) = EAB_{model} - EAB_{th} \leq 0) \quad (8.2)$$

Where, g(.) is the limit state function, EAB_{model} is the model derived from the thermal ageing data and EAB_{th} is the 50% absolute elongation which is the threshold value considered as an accepted criteria.

Substituting Eq. (8.1) in Eq. (8.2) we get,

$$P_f = P\ (g(EAB_{Model}, EAB_{th}) = (A + Bexp^{-ct}) - EAB_{th} \leq 0) \quad (8.3)$$

The distribution and coefficient of variation (COV) for basic parameters for structural reliability are shown in Table 8.2. Since parameter A is contributing to the EAB (measured in %) and is related to strength of the material, the lognormal distribution is considered to account for uncertainty in the random variable. Unit of B is in %, C is in days^{-1} and t is in days.

Table 8.2: Input data for structural reliability problem

Parameter	Distribution	Mean	COV
A	Lognormal	22.72	0.1
B	Constant	485.79	----
C	Constant	0.025	----
t	Constant	0	----

Eq. (8.3) has been solved by using the first order reliability method from the COMREL [125], which is one of the modules of STRUREL [126].

8.2.1 Results with lognormal distribution of parameter A

Analysis was carried out by varying the time from 0 to 100 days considering lognormal distribution. The reliability is shown in Figure 8.1 and probability of failure is shown in Figure 8.2.

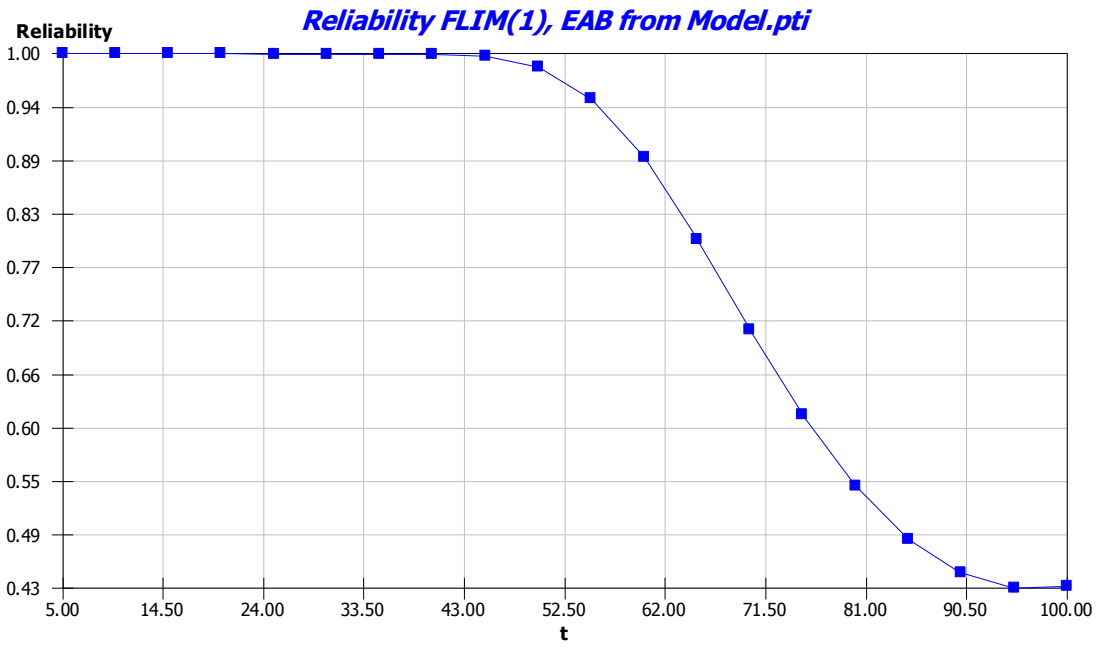

Figure 8.1: Reliability as a function of time in days at 110^0C of ageing

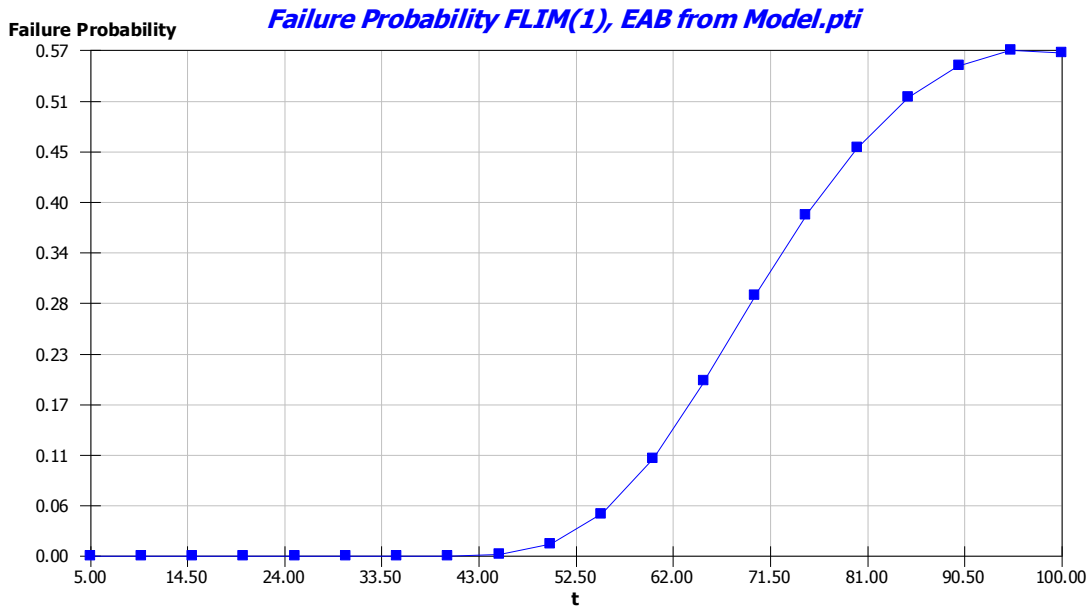

Figure 8.2: Probability of failure as a function of time at 110^0C of ageing

8.2.2 Results with Gumbel (min) distribution of parameter A

Analysis was carried out by varying the time from 0 to 100 days with Gumbel distribution. Gumbel distribution is a Type I extreme value distribution which has two forms. One is based on the smallest extreme and the other is based on the largest extreme. Gumbel

distribution has two parameters namely, location parameter α and scale parameter β [121]. The reliability is shown in Figure 8.3 and probability of failure is shown in Figure 8.4.

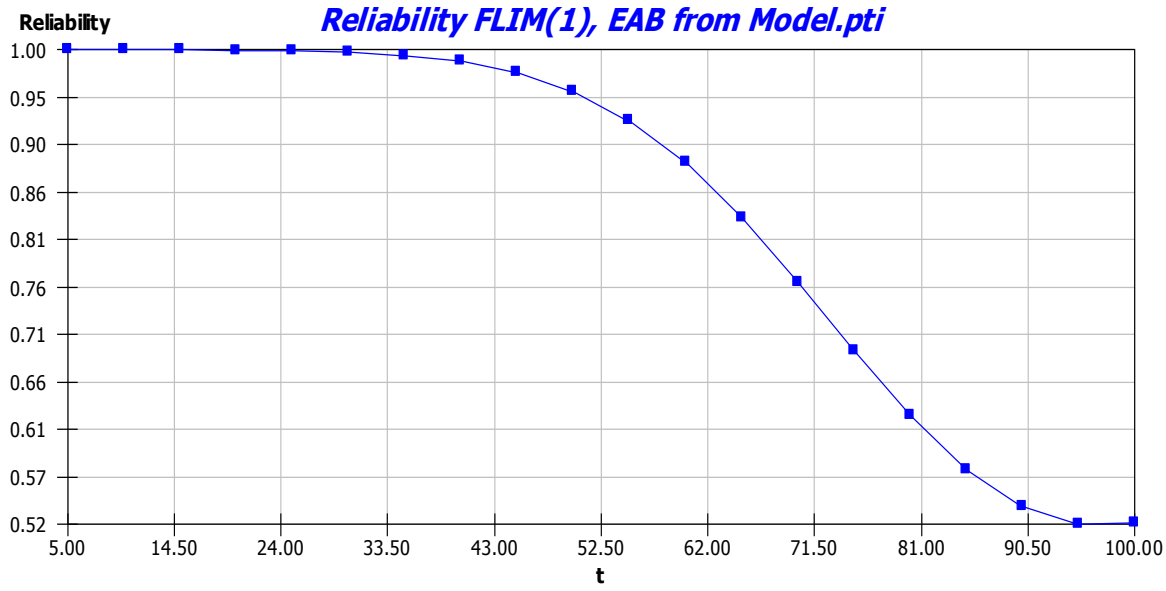

Figure 8.3: Reliability as a function of time in days at 110^0C of ageing

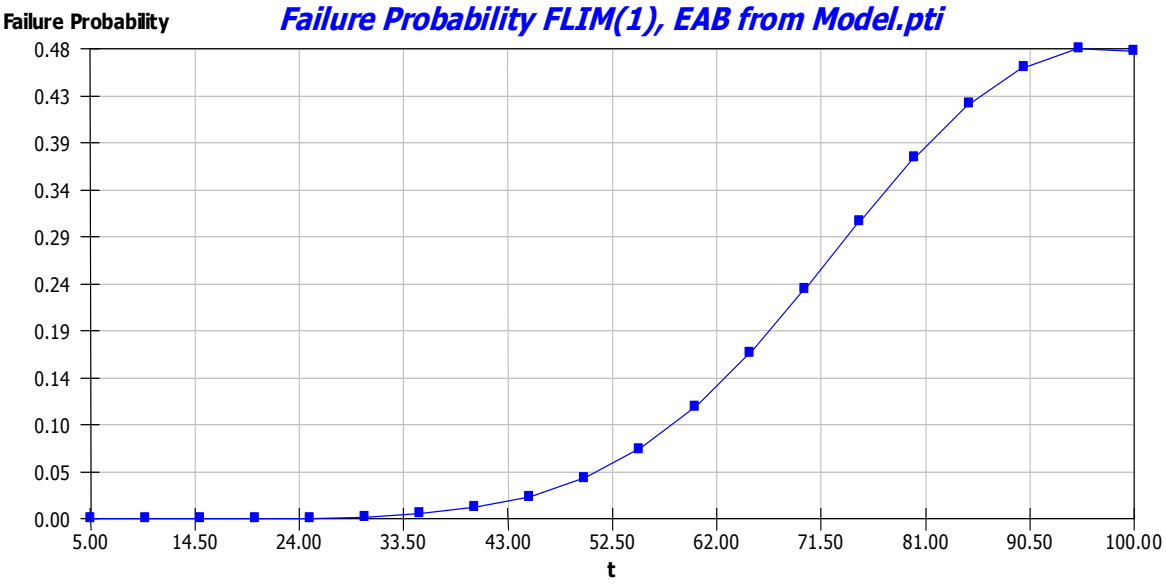

Figure 8.4: Probability of failure as a function of time at 110^0C of ageing

8.3 Reliability prediction from OIT

Generally, OIT decreases exponentially with increase in the isothermal temperature used for the test and this relationship follows Arrhenius behaviour. Therefore, the OIT under isothermal condition can be related to Arrhenius equation as shown in Eq. (8.4).

$$OIT = Ae^{\frac{\Phi}{kT_{OIT}}} \tag{8.4}$$

where, T_{OIT} is the isothermal temperature, A is constant, Φ is the activation energy and k is the Boltzmann constant. OIT in Eq. (8.4) can be considered as characteristic life of insulation to reach end-of-life criterion. Now considering the Arrhenius acceleration factor given by:

$$AF = \frac{t_{use}}{t_{acc}} = \frac{OIT_{use}}{OIT_{acc}} \tag{8.5}$$

Using Eq. (8.4) and (8.5), the OIT at use condition can be estimated from:

$$OIT_{use} = OIT_{acc}e^{\frac{\Phi}{k}\left[\frac{1}{T_{use}}-\frac{1}{T_{acc}}\right]} \tag{8.6}$$

From Eq. (8.6), OIT corresponding to 50% of original EAB is found to be 8.4mins under isothermal temperature of 200^0C for the insulation material subjected to thermal ageing of 110^0C. In general, 40^0C is considered as the normal operating temperature in NPPs. Hence, OIT under 40^0C considering Φ=1.15eV is found to be 29 years from Eq. (8.6). In order for the reliability prediction, an appropriate life distribution is chosen to describe the failure characteristics. The Weibull distribution is commonly employed in reliability studies and it is well suited to fitting the 'weakest-link' properties of typical lifetime data. Different mechanisms of failure can sometimes be distinguished by the Weibull parameters needed to fit the results [140, 163-165]. The reliability function from Weibull distribution is given by:

$$R(t) = e^{-\left(\frac{t}{\eta}\right)^{\beta}} \tag{8.7}$$

where, η is the scale parameter or characteristic life, β is the shape parameter and t is the time. Since OIT is equivalent to characteristic life, the time dependent reliability can be determined from Eq. (8.7). Now with η=OIT=29years and varying t from 0 to 40years, the time dependent reliabilities have been calculated from Eq. (8.7). The time dependent reliabilities of the thermally aged cable insulation for different values of β are shown in Figure 8.5.

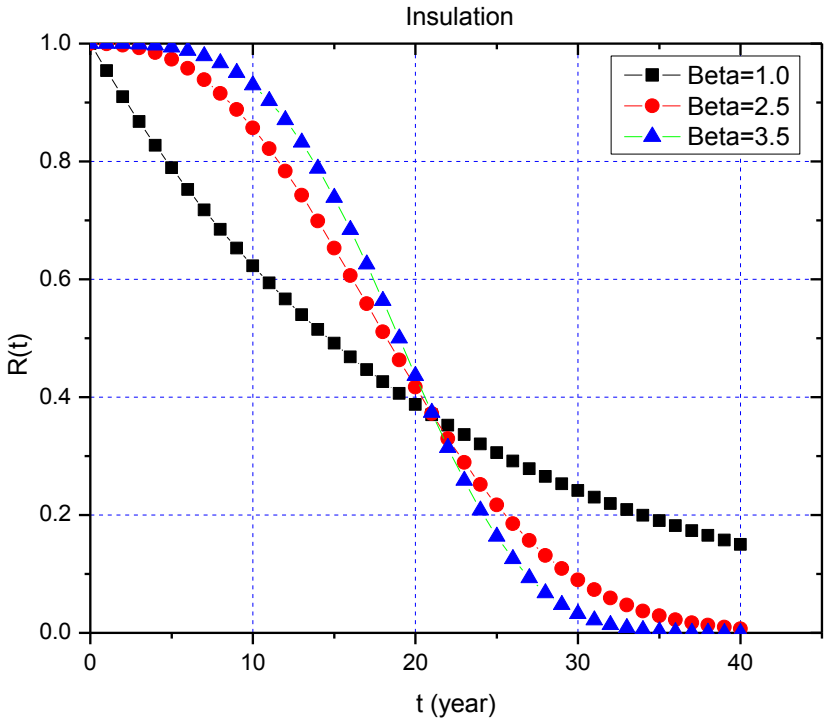

Figure 8.5: Reliability vs. time

It is evident from Figure 8.5 that when times-to-failure of the insulation material follows an exponential distribution, the reliability is substantially high as failures are treated as random failures. Study also demonstrates that under thermal and radiation ageing both insulation and sheath materials exhibited an exponential degradation process; hence the exponential failure rate for modelling cables is found to be appropriate. As samples were

subjected to accelerated ageing other failure distributions were also considered in this study to demonstrate the reliabilities from non-exponential failures. The predicted reliability is used in PSA of NPP to account for the cable failures.

8.4 Application to PSA of NPP

In order to account for cable failures in the PSA of NPP, the reliabilities estimated in this study are used in the system reliability analysis to estimate the overall system failure rate or unavailability. The cable failure rate for an exponential case has been calculated from the Weibull failure rate function as shown in equation (8.8).

$$\lambda(t) = \frac{\beta}{\eta}\left(\frac{t}{\eta}\right)^{\beta-1} \tag{8.8}$$

As a case study to demonstrate the contribution of cable failures in the overall system reliability, the cable failures have been modelled in the secondary shutdown system-2 (SDS-2) of Advanced Heavy Water Reactor. Since SDS-2 is a standby tested system, the basic component failure model for cable is considered to be standby tested model. The fault tree for SDS-2 without cable failures in the corresponding channels of instrumentation is shown in Figure 8.6. The random failures of basic components contributing to SDS-2 failure have been modelled. The SDS-2 has been modelled for its unavailability estimation from all the components leading to failure in addition to cable failures and the minimal cutsets have been generated. The fault tree quantification has been carried out using ISOGRAPH reliability software [166].

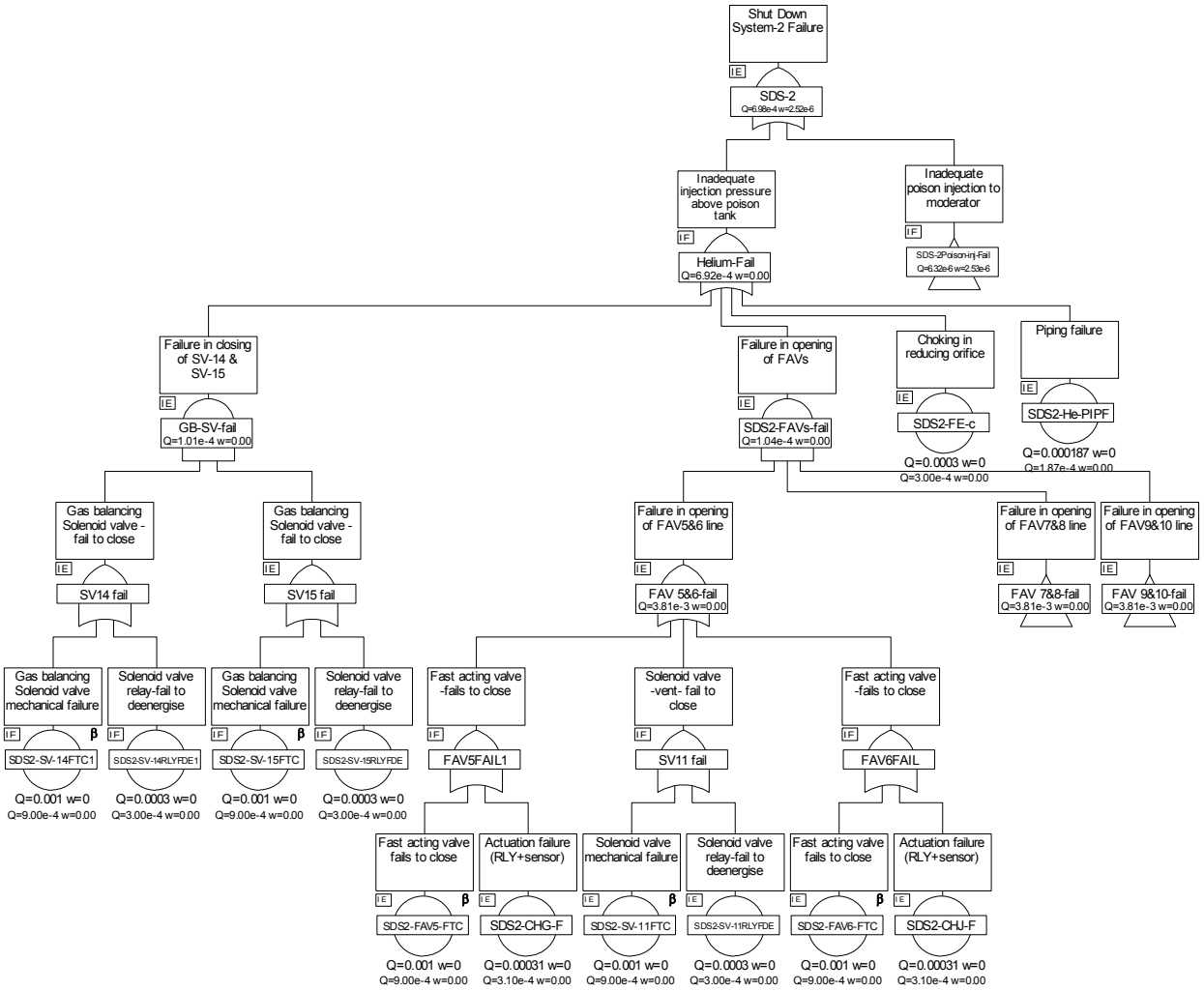

Figure 8.6: Fault tree of SDS-2 without cable failures (Part 1)

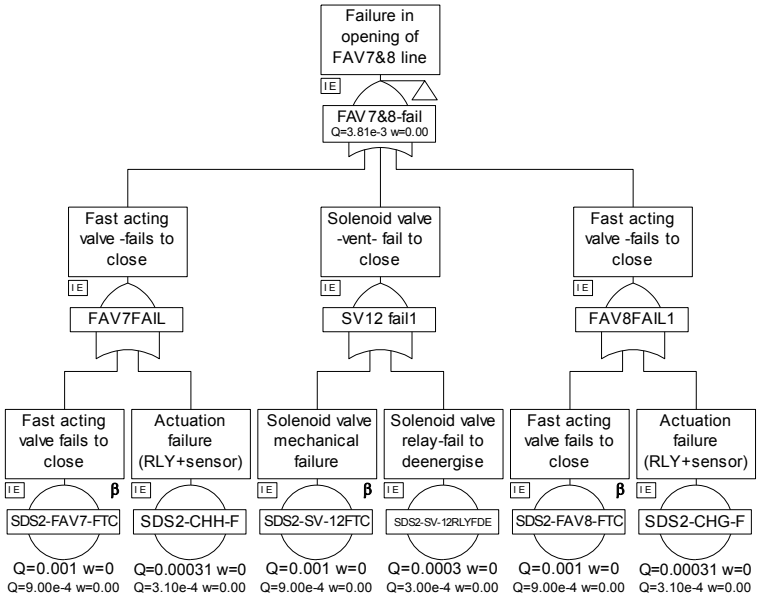

Figure 8.7: Fault tree of SDS-2 without cable failures (Part 2)

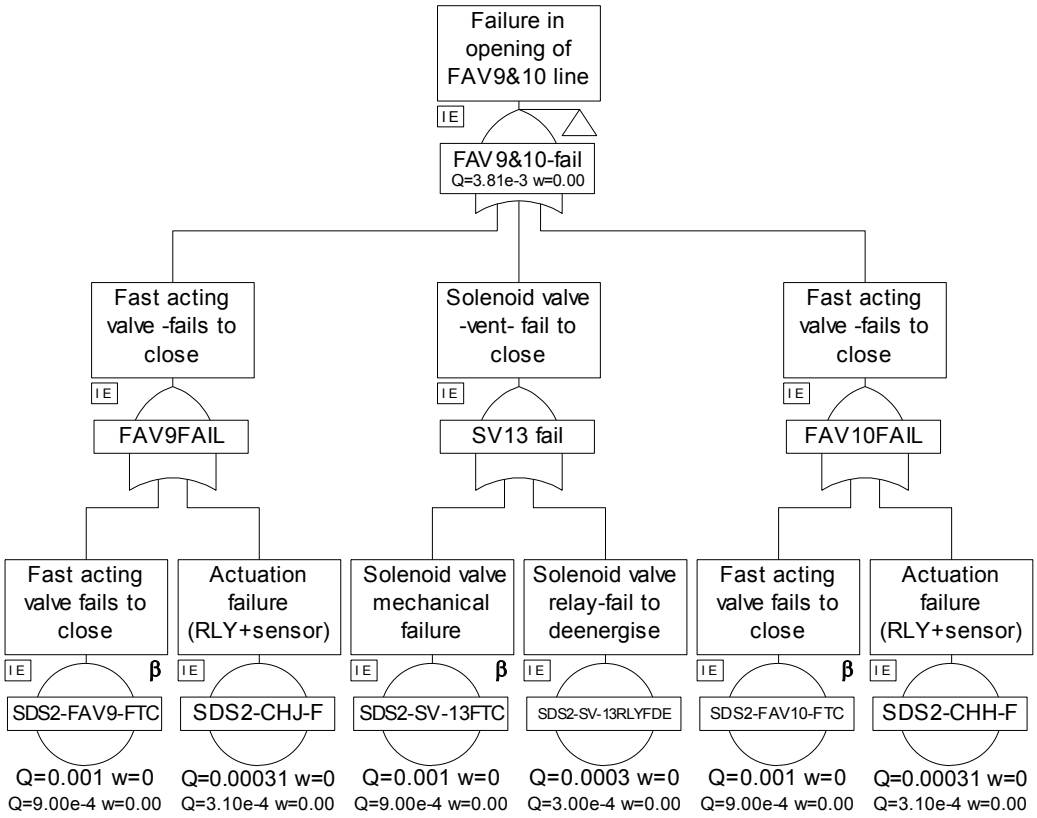

Figure 8.8: Fault tree of SDS-2 without cable failures (Part 3)

The fault tree for SDS-2 with cable failures in the corresponding channels of instrumentation is shown in Figure 8.7.

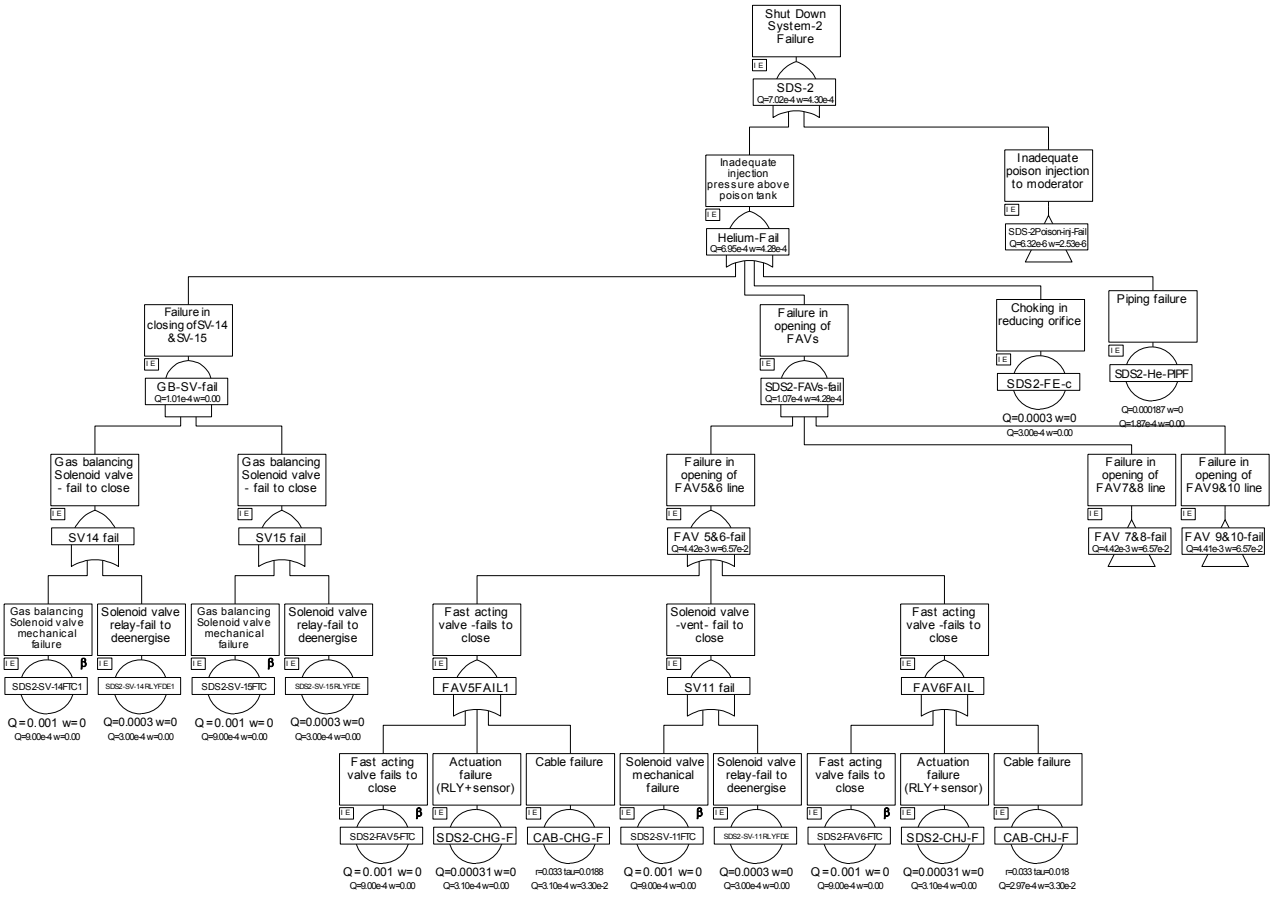

Figure 8.9: Fault tree of SDS-2 with cable failures (Part 1)

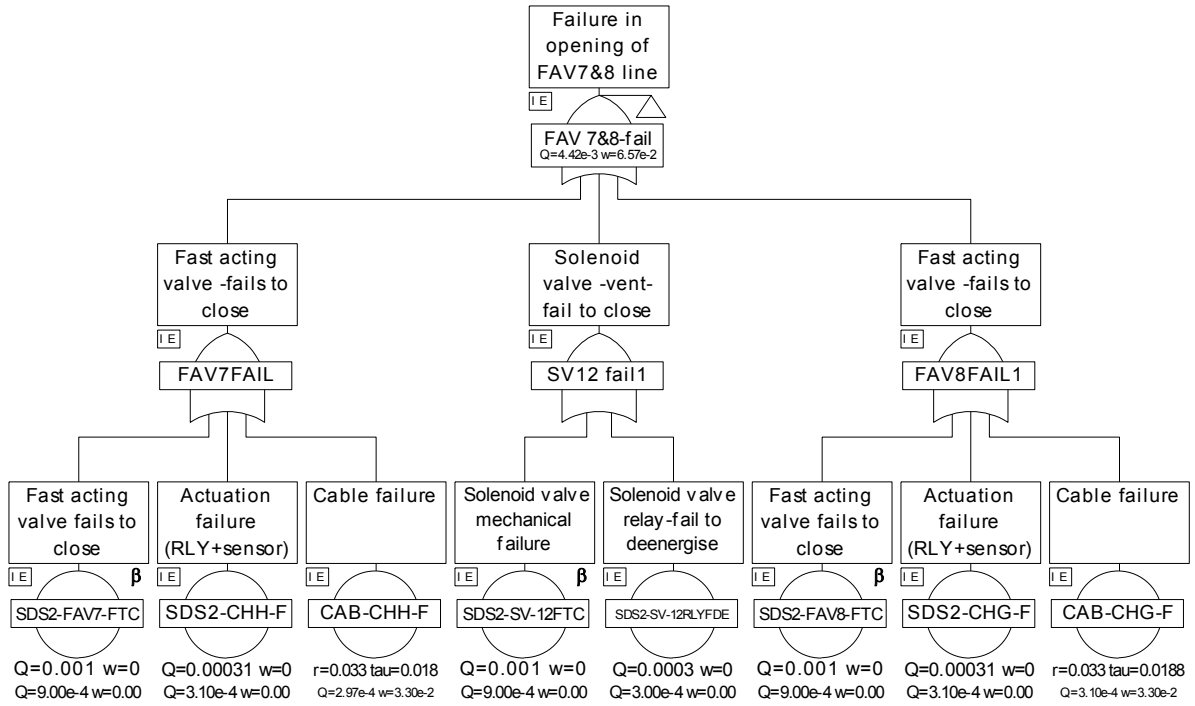

Figure 8.10: Fault tree of SDS-2 with cable failures (Part 2)

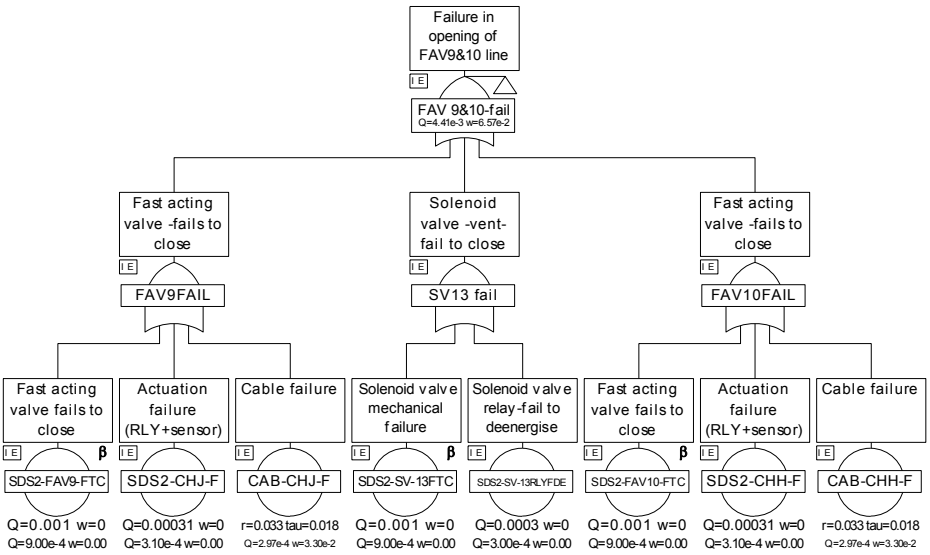

Figure 8.11: Fault tree of SDS-2 with cable failures (Part 3)

It is evident from the system analysis that there is an increase in the system unavailability when cable failures are accounted in the system modelling as shown in Table 8.3.

Table 8.3: Unavailability of SDS-2

Unavailability of SDS-2	
Without cable failures	With cable failures
6.92e-4	7.02e-4

8.5 Summary

From the experimentally determined performance parameters, the reliability of I&C cables of NPPs has been estimated from different approaches. The predicted reliability was then applied to SDS-2 unavailability estimation to account for cable failures in addition to basic component random failures. It is seen from Table 8.3 that the cable failures contribute about 1.5% to overall system unavailability. Hence, it is concluded that the cable failure has an impact on the overall system unavailability and cannot be neglected for realistic evaluation of system reliability.

Chapter 9 Conclusions and Future Scope

9.1 Conclusions

Reliability prediction of I&C cable insulation materials has been carried out by analytical and experimental approaches. A framework for time dependent reliability prediction of I&C cables for use in PSA of NPP has been developed by considering the thermal aging as a part of ageing management. The proposed methodology has been illustrated with the data obtained from the literature on a typical XLPE cable for I&C applications. The behaviour of insulation resistance when the degradation process is linear or exponential has also been modeled. The probability of failure obtained from this framework can be directly used in system reliability analysis to account for cable ageing. The proposed methodology can be extended to other degradation mechanisms such as humidity, voltage etc.

Another approach based on ANNs has been developed for reliability prediction of I&C cables for use in PSA applications. It was evident from the results that with a few sets of accelerated life testing data, the time-to-failure can be predicted from the proposed methodology. The use of ANNs in life assessment of cables not only reduces the laboratory ageing time but also minimizes the cost by accurately predicting the future times-to-failure of an electrical cable. Also, when conducting experiments it is important to note that appropriate test conditions play a significant role in predicting the future property. Therefore, test conditions must be decided judiciously to predict future property with a very limited experimentation.

The polymeric insulation is subjected to both internal (resistive losses in the conductor and shield) and external (environmental temperature) heating. In order to study the effect of such thermal ageing in electrical cables, finite element simulation studies have been carried

out using COMSOL Multiphysics solver. The effect of aluminium screen present in PVC insulated I&C cable was simulated and the heat transfer was studied. The cable was modeled considering maximum outer surface temperature of the conductor being 90^0C due to resistive losses in the conductor and the time dependent analysis were performed to study the maximum temperature rise in the outer surface of the cable insulation and sheath. Study revealed that presence of aluminum screen in the cable significantly contributes to the thermal degradation of insulation materials. Hence, in the remaining life assessment studies the presence of non-polymeric materials which contribute to thermal degradation of the insulation should also be accounted for realistic lifetime evaluations. COMSOL Multiphysics simulations have also been carried to study the impact voids, generated due to radiation ageing, on electrical parameters such as electric field, space charge etc. It was observed from the finite element analysis study that the voids above 0.01mm radius have significantly caused the change in the electric field and other parameters.

Insulation resistance and polarization index readings were measured and compared against the recommended values from the industry standards for cables received from various manufacturers. It was observed that, there is a significant variation in the IR values among different manufacturers. This variation is due to the sensitivity of IR measurements to temperature, moisture and other factors such as the presence of antioxidants, fillers etc., and some manufacturers design cables with significantly high IR. However, a cable with high IR does not always guarantee the reliable performance. As PI being independent of temperature and length of the specimen and will give more reliable and repeatable results, it would be logical to compare the PI values against recommended standards for performance assessment. Also, it was found that though there is a significant variation in IR values of different manufacturers, the trend of leakage current in all the cables found to follow an exponential

process. Hence, polarization index may also be considered in assessing the cable performance.

A low voltage control cable with PVC insulation and PVC sheath was subjected to gamma radiation upto 50MRad at a dose rate of 0.17MRad/hr and the degradation due to radiation ageing was assessed using FTIR spectroscopy and tensile testing. It was observed that there is an improvement in the tensile properties at lower dose condition upto 5MRad. However, these properties degrade with increased dose levels in both insulation and sheath materials. A near perfect correlation between infrared transmittance and elongation in case of insulation material was observed. However, a significant difference in correlation was in case of sheath material beyond 25MRad after 150hrs of ageing. This deviation is expected as the sheath material has other additives which may not affect the basic chemical structure of the polymer but may induce changes in mechanical properties. It was apparent from Anova study that there is a significant change in degradation due to radiation in insulation at various dose conditions at 5% significance level compared to that of sheath material. It is observed from this study that the infrared transmittance is directly related to EAB for polymeric insulation materials where there are no additives. However, precautions must be taken when correlating infrared transmittance with EAB in case of non-standard polymeric materials.

Differential scanning calorimetry and tensile testing experiments were performed on aged samples to assess the degradation due to thermal and radiation ageing. DSC experiments were carried out on several aged samples to determine OIT under isothermal condition. However, due to slow kinetics the exact exothermic peak could not be determined from the DSC thermograms under an isothermal condition. Hence, oxidation induction temperature measurements were carried out which also gives the onset OIT under ramp heating. The OITs obtained under this non-isothermal condition of thermally aged cable insulation are in good agreement with EAB values. However, these findings do not indicate clearly a particular

trend of the thermal ageing effect for sheath material for 135^0C. This is due to the fact that under 135^0C condition the material has completely oxidized during the earlier stages of thermal ageing.

From the experimental evaluations, it was found that the EAB fits an exponential function of OIT for both thermal and radiation ageing of insulation material. From the empirical models obtained from the correlation study, the OITs corresponding to 50% elongation was predicted for cable insulation for both thermal and radiation ageing conditions. From the performance indicators determined using experimental techniques, the time dependent reliabilities have been estimated by employing the developed reliability approaches. The study demonstrates the significance of accounting cables failures in PSA of NPP by modelling cable failure in shutdown system of advanced heavy water reactor. Although the life-stress models and failure distributions have been derived on the basis of strong regression coefficients and statistical confidence tests in this study, certain degree of uncertainty may be expected in the accuracy and confidence in the overall results.

In summary, the time dependent reliability models developed based on SSI theory and ANNs are highly useful in accounting the cable failures in PSA of NPPs. Study demonstrates that with limited accelerated life testing data, it is possible to predict the reliability of cables using ANNs. However, finding a best suitable learning algorithm and network architecture becomes a challenging task. It is also demonstrated that by measuring the OIT and correlating with EAB, it is possible to predict the reliability of a cable for use in PSA applications. Simulation studies carried out in this thesis work highlight the use of FEA tools to study various degradation and ageing related issues in electrical cables. Considering the significant increase in the unavailability of SDS-2 with cable failure accounted, the overall study demonstrates that the cables connected to various NPP systems may be included in the PSA study.

9.2 Future scope

The work reported in this thesis mainly consists of development of reliability models for I&C cables for incorporating the cable failures in PSA of NPPs. The main stressors considered while developing reliability models are temperature and radiation. The reliability frameworks developed based on IR, OIT and EAB using stress-strength interference technique, artificial neural networks and Weibull theory are general approaches and not limited to I&C cables. The possible extensions of this thesis work are the following:

An integrated approach for reliability estimation of cables by combining the thermal, radiation and humidity ageing effect for can be developed in future for accounting the synergistic ageing effect in NPPs. Neural networks approach can be extended to predict the remaining life accounting the multi-stress (temperature, radiation and humidity) ageing effect. The work reported in this thesis on simulation of cable ageing due to thermal and radiation ageing effects can be extended to develop the reliability frameworks. An attempt to develop reliability framework based on the infrared spectroscopy with respect to important chemical bonds can be made to study the cable failures due to radiation ageing.

Bibliography

[1]. M. Villaran and R. Lofaro, Essential elements of an electric cable condition monitoring program, Brookhaven National Laboratory, Upton, New York, NUREG/CR-7000, BNL-NUREG-90318-2009, 2010.

[2]. Robert J. Lofaro, Edward Grove and Peter Soo, An evaluation of condition monitoring techniques for low-voltage electric cables, Brookhaven National Laboratory, BNL-NUREG-67389, 2000.

[3]. Brent D. Shumaker, Jonathan B. Ledlow, Ryan D. O'Hagan, Dan E. McCarter, Hashem M. Hashemian, Remaining useful life estimation of electrical cables in nuclear power plants, Chemical Engineering Transactions, vol. 33, pp. 877-882, 2013,

[4]. IAEA-TECDOC-932, Pilot study on the management of ageing of instrumentation and control cables, International Atomic Energy Agency, 1997.

[5]. K. Anandakumaran, W. Seidl, P.V. Castaldo, Condition assessment of cable insulation systems in operating nuclear power plants, IEEE transactions on dielectrics and electrical insulation, vol. 6, no. 3, pp. 376-384, 1999.

[6]. IAEA-TECDOC-1188, Assessment and management of ageing of major nuclear power plant components important to safety: In-containment instrumentation and control cables, vol. I, International Atomic Energy Agency, 2000.

[7]. IAEA-TECDOC-1188, Assessment and management of ageing of major nuclear power plant components important to safety: In-containment instrumentation and control cables, vol. II, International Atomic Energy Agency, December 2000.

[8]. M. J. Jacobus, Aging, condition monitoring, and loss-of coolant accident tests of class 1E electrical cables: Ethylene propylene rubber cables, NUREG/CR-5772, SAND91-1766/2, vol. 2, 1992.

[9]. NUREG/CR-6794, Evaluation of ageing and environmental qualification practices for power cables used in nuclear power plants, Brookhaven national laboratory, 2003.

[10]. M. Luitel, Statistical approach for predicting remaining life of cross-linked polyethylene insulated cables, thesis, Master of Science, Wichita state university, December 2005.

[11]. NEA/CSNI/R (98)7, Survey on organic components in NPPs, 1999.

[12]. Kröhnke, Polymer Science: A Comprehensive Reference, vol. 8.14-Polymer Additives, Elsevier, 2012.

[13]. International Atomic Energy Agency, Assessing and managing cable aging in nuclear power plants, 2012.

[14]. K. T. Gillen and R. L. Clough, Predictive aging results for cable materials in nuclear power plants, Sandia Laboratories, Tech. Rep., 1990.

[15]. International Atomic Energy Agency, Stability and stabilization of polymers under irradiation, 1997.

[16]. K.L. Simmons, L.S. Fifield, M.P. Westman, P. Ramuhalli, A.F. Pardini, J.R. Tedeschi and A.M. Jones, Determining remaining useful life of ageing cables in nuclear power plants-Interim study FY13, PNNL 22812, US Department of Energy, 2013.

[17]. IEEE Std. 323-1974: IEEE Standard for Qualifying Class 1E Equipment for Nuclear Power Generating Stations, Institute of electrical and electronics engineers, New York, 1974.

[18]. IEEE Std. 383-1974, “IEEE standard for type test of class 1E electrical cables, field splices, and connections for nuclear power generating stations”, Institute of electrical and electronics engineers, New York, 1974.

[19]. KTA 3706 (Draft) 06/94, Wiederkehrender Nachweis der Kühlmittelverlust-Störfallfestigkeitvon elektro- und leittechnischen Komponenten des Sicherheitssystems, 1994.

[20]. M. Subidhi and S. K. Aggarwal, Literature review of environmental qualification of safety related electric cables, NUREG/CR-6384, 1996.

[21]. R J Smith, Electrical equipment qualified life extension through area temperature monitoring, Duke Power Company, EQDB Technical meeting, Tampa, 1995.

[22]. Gröndalen, O., Cable problems in the Barseback Unit 2, Sydkraft Report TV-8807-41, Barseback, 1978-1983.

[23]. Benhabiles, K. and Pinel B., Plasticiser diffusion kinetics for PVC cables: Correlation between electrical properties and plasticiser migration, Journée Internationale CABLE 95, Versailles, pp. 644-648, 1995.

[24]. S.G. Burnay, An overview of polymer ageing studies in the nuclear power industry, Nuclear Instruments and Methods in Physics Research B, Vol. 185, pp. 4-7, 2001.

[25]. R. Clavreul, Ageing of polymers in electrical equipment used in nuclear power plants, Nuclear Instruments and Methods in Physics Research B, vol. 151, pp. 449-452, 1999.

[26]. G.E. Sliter, Overview of research on nuclear plant cable ageing and life extension, in Proc. SMiRT-12, Elsevier Science Publishers, pp. 199-203, 1993.

[27]. D.A. Horvath, D.C Wood and M.J. Wylie, Microscopic void characterization for assessing ageing of electrical cable insulation used in nuclear power stations, in Proc. IEEE conference on electrical insulation and dielectric phenomena (CEIDP 2000), Victoria, BC, pp. 1-5, October, 2000.

[28]. Michael Villaran and Robert Lofaro, Condition monitoring of cables, BNL-90735-2009-IR, 2009.

[29]. Vít Plaček, Jan Kábrt, Vladimír Hnát and Pavel Žák, Acceptance criteria in nuclear power plant cable qualification, 9th International Conference on Insulated Power Cables, Jicable'15, Versailles, 2015.

[30]. Gillen, K.T., Clough, R.L. and Jones, L.H., Cable deterioration in the containment building of the Savannah River Nuclear Reactor, NUREG/CR-2877, SAND81-2613, Sandia National Laboratories, Albuquerque, N.M., 1982.

[31]. IEC 544-2, Guide for determining the effects of radiation on insulating materials, Part 2: Procedures for irradiation and test, International Electrotechnical Commission, 1991.

[32]. NUREG/CR-6869, BNL-NUREG-73676-2005, Reliability Physics Model for Aging of Cable Insulation Materials, Brookhaven National Laboratory, 2005.

[33]. Robert J. Lofaro, Edward Grove and Peter Soo, An evaluation of condition monitoring techniques for low-voltage electric cables, 8th International Conference on Nuclear Engineering, Baltimore, MD USA, 2000.

[34]. Kenneth T. Gillen, Roger A. Assink and Robert Bernstein, Condition monitoring approaches applied to a polychloroprene cable jacketing material, Polymer Degradation and Stability, vol. 84, pp. 419-431, 2004.

[35]. B. Bartonicek, V. Hnat and V. Placek, Assessment of the Insulation Degradation of Cables used in Nuclear Power Plants, Nuclear Instruments and Methods in Physics Research B, vol. 151, pp. 423-426, 1999.

[36]. M. Jevtic and A.M. Andreev, The method of testing of XLPE cable insulation resistance to partial discharges and electrical treeing, Bulletin of material science, vol. 19, No. 5, pp. 823-829, October 1996.

[37]. M.H. Shwehdi, M.A. Morsy and A. Abugurain, Thermal aging tests on XLPE and PVC cable insulation materials of Saudi Arabia, Annual Report Conference on Electrical Insulation and Dielectric Phenomena, 2003.

[38]. IEEE Std. 400-2001, IEEE Guide for Field Testing and Evaluation of the Insulation of Shielded Power Cable Systems (Revision of IEEE Std. 400-1991), IEEE, New York, January 29, 2002.

[39]. IEEE Std. 400.2-2004, IEEE Guide for Field Testing of Shielded Power Cable Systems Using Very Low Frequency (VLF), IEEE, New York, March 8, 2005.

[40]. IEEE Std 141-1993, IEEE Recommended Practice for Electric Power Distribution for Industrial Plants, 1993.

[41]. ASTM Standard D257/IEC 60093, Test Methods for DC Resistance or Conductance of Insulating Materials, ASTM International, 1980.

[42]. IEC 60364-6:2006, Low-voltage electrical installations - Part 6: Verification, 2006.

[43]. IEEE Std. 43-2000 (R2006), IEEE Recommended Practice for Testing Insulation Resistance of Rotating Machinery, 2006.

[44]. Bair H. E., Thermal Analysis of Additives in Polymers: Thermal characterization of polymeric materials (Ed. Turi E. A.), 2nd ed., Academic Press, San Diego, pp. 2263—2410, 1997.

[45]. Clough R. L. and Gillen K. T., Degradation mechanisms and accelerated aging test design, Polymer Materials Science Engineering, no. 52, pp. 592-597, 1985.

[46]. ASTM D638, Standard Test Method for Tensile Properties of Plastics, ASTM International, 2002.

[47]. ASTM D412, Test Methods for Vulcanized Rubber and Thermoplastic Rubbers and Thermoplastic Elastomers-Tension, ASTM International, 2006.

[48]. G. Mazzanti, G.C. Montanari and A. Motori, An insight into thermal life testing and characterization of EPR insulated cables, Journal of physics D: Applied physics, No. 27, pp. 2601-2611, 1994.

[49]. ISO 11357-6, Plastics - Differential scanning calorimetry (DSC) - Part 6: Determination of oxidation induction time (isothermal OIT) and oxidation induction temperature (dynamic OIT), 2011.

[50]. M. Schmid, A. Ritterand S. Affolter, "Determination of oxidation induction time and temperature by DSC:Results of round robin tests", Journal of Thermal Analysis and Calorimetry, vol. 83, no. 2, pp. 367–371, 2006.

[51]. K.T. Gillen, M. Celina, and R.L. Clough, Density measurements as a condition monitoring approach for following the aging of nuclear power plant cable materials," Radiation Physics and Chemistry, vol. 56, pp. 429-447, 1999.

[52]. ASTM Standard D792, Test method for specific gravity (relative density) and density of plastics by displacement, ASTM International, 2013.

[53]. ASTM Standard D1505, Test method for density of plastics by the density gradient method, ASTM International, 2010.

[54]. NUREG/CR-6704, Assessment of environmental qualification practices and condition monitoring techniques for low voltage electrical cables, Brookhaven national laboratory, 2001.

[55]. Kuo-Sung Liao, Hongmin Chen, Somia Awad, Jen-Pwu Yuan, Wei-Song Hung, Kuier-Rarn Lee, Juin-Yih Lai, Chien-Chieh Hu, and Y. C. Jean, Determination of free-volume properties in polymers without orthopositronium components in positron annihilation lifetime spectroscopy, Macromolecules, 44, 6818–6826, 2011.

[56]. David Coats, Jingjiang Wang and Yong-June Shin, Joint Time-Frequency Domain Reflectometry for Diagnostics/Prognostics of Aging Electric Cables in Nuclear Power Plants, The University of South Carolina Research Foundation, 2011.

[57]. Lim, Woo Sang; Ha, Che Wung; Joo, Kwang Ho, VLF Tan Delta Measurement for Used XLPE Power Cables, Korea Hydro and Nuclear Power Co., Korean Nuclear Society, Daejeon, 2011.

[58]. P. Fonseca, A.C.F. Santos and E.C. Montenegro, A very simple way to measure coaxial cable impedance, Revista Brasileira de Ensino de Fisica, v. 29, n. 3, p. 373-375, 2007.

[59]. NRC Regulatory Guide 1.211, Qualification of Safety Related Cables and Field Splices for Nuclear Power Plants, NRC, Washington, DC, 2009.

[60]. IEC 60096-1, Radio-Frequency Cables Part 1: General Requirements and Measuring Methods, IEC, Geneva, 2004.

[61]. L. Reimer, P.W. Hawkes, Scanning electron microscopy: Physics of image formation and microanalysis, Berlin (DE), Springer-Verlag, 2010.

[62]. Kyu-Jin Ktm, Melvyn R. Dicksont, Vicki C1ien and Anthony G. Fane, Applications of field emission scanning electron microscopy to polymer membrane research, Micron and Microscopica Acta, vol. 23, no. 3, pp. 259-271. 1992..

[63]. Luis A. Escobar and William Q. Meeker, A Review of Accelerated Test Models, Statistical Science, vol. 21, no. 4, pp. 552–577, 2006.

[64]. Nicola Bowler and Shuaishuai Liu, Aging Mechanisms and Monitoring of Cable Polymers, International Journal of Prognostics and Health Management, ISSN 2153-2648, no. 029, 2015.

[65]. A. S. Maxwell, W. R. Broughton, G. Dean and G. D. Sims, Review of accelerated ageing methods and lifetime prediction techniques for polymeric materials, National Physical Laboratory, 2005.

[66]. K. T. Gillen, M. Celina, R. L. Clough and J. Wise, Extrapolation of accelerated aging data- Arrhenius or Erroneous?, Review paper in Trends in Polymer Science, no. 5, pp. 250, 1997.

[67]. G. Mazzanti, G.C. Montanari and A. Motori, An insight into thermal life testing and characterization of EPR insulated cables, Journal of physics D: Applied physics, No. 27, pp. 2601-2611, 1994.

[68]. IEC 216, Guide for the determination of thermal endurance properties of electrical insulating materials, 4th issue (1990-1994).

[69]. IEC 610, Principal aspects of functional evaluation of electrical insulation systems: Ageing mechanisms and diagnostic procedures, Geneva (1978).

[70]. S. Z. D. Cheng, Ed.: Handbook of thermal analysis and calorimetry, Vol. 3: Applications to Polymers and Plastics, Elsevier, 2002

[71]. Nelson, Wayne, Accelerated Testing: Statistical Models, Test Plans, and Data Analyses, John Wiley & Sons, Inc., New York, 1990.

[72]. G. Mazzanti, G.C. Montanari and A. Motori, An insight into thermal life testing and characterization of EPR insulated cables, Journal of physics D: Applied physics, No. 27, pp. 2601-2611, 1994.

[73]. Y. R. Shashoua, Effect of indoor climate on the rate and degradation mechanism of plasticized poly (vinyl chloride), Polymer Degradation Stability, vol. 81, no. 1, pp. 29-36, 2003.

[74]. International Electrotechnical Commission, Determination of long term radiation ageing in polymers. Part 2: Procedures for predicting ageing at low dose rates, IEC Technical Report 1244-2, Geneva, 1993.

[75]. International Electrotechnical Commission, Guide for determining the effects of radiation on insulating materials. Part 1: Radiation interaction and dosimetry, IEC 544-1

(1995); Part 2: Procedures for irradiation and test, IEC 544-2 (1991); Part 4: Classification system for service hi radiation environments, IEC 544-4, Geneva, 1985.

[76]. Y. T. Hsu, K.S. Chang-Liao, T.K. Wang, C.T. Kuo, Correlation between mechanical and electrical properties for assessing the degradation of ethylene propylene rubber cables used in nuclear power plants, Polymer degradation and stability, vol. 92, pp. 1297-1303, 2007.

[77]. G. V Gordon, C. Shen, M.T. Shaw, A method for correlating natural ageing data and its application to insulation ageing in nuclear power plants, pp. 694-699, 1992.

[78]. G. C. Montanari and A. Motori, Thermal endurance evaluation of XPLE insulated cables, Journal of physics D: applied physics, No. 24, pp. 1172-1181, 1991.

[79]. Toman, G. and Gardner, J. B., Development of a Non-Destructive Cable Insulation Test, published in NUREG/CP-0135, Workshop on Environmental Qualification of Electric Equipment, U.S. Nuclear Regulatory Commission, November 1993.

[80]. M. Ekelund, H. Edin, U.W. Gedde, Long-term performance of poly (vinyl chloride) cables. Part 1: Mechanical and electrical performances, Polymer degradation and stability, vol. 92, pp. 617-629, 2007.

[81]. Kaisa Simola, Reliability methods in nuclear power plant ageing management, Doctor of Technology, thesis, Helsinki University of Technology, Espoo, Finland, VTT Publications, No. 379, 1999.

[82]. T. Koshy, Environmental qualification of low-voltage instrumentation and control cables, Unites States Nuclear Reactor Regulation, Washington DC, RIS 2003-09.

[83]. D.A. Horvath, D.C Wood and M.J. Wylie, Microscopic void characterization for assessing ageing of electrical cable insulation used in nuclear power stations, in Proc. IEEE conference on electrical insulation and dielectric phenomena (CEIDP 2000), Victoria, BC, pp. 1-5, October, 2000.

[84]. Mohammed Hanif, Principles an applications of insulation testing with DC, IEP-SAC journal, pp. 57-63, 2004-2005.

[85]. D. Allan, T.R. Blackburn and R. Sheehy, Methodologies and models to improve the reliability of service aged electrical insulation, CIGRE, No. 15-303, 2002.

[86]. G.V Gordon, C. Shen and M.T. Shaw, A method for correlating natural ageing data and its application to insulation ageing in nuclear power plants, pp. 694-699, 1992.

[87]. H.M. Banford, R.A. Fouracre, S.J. MacGregor and M. Judd, An investigation of radiation-induced ageing in cable insulation via loss measurements at high and low frequencies, Proc. IEEE International Symposium on Electrical Insulation, Arlington, Virginia, USA, June 7-10, 1998.

[88]. G.C. Montanari and L. Simoni, Ageing phenomenology and modelling, IEEE transactions on electrical insulation, vol. 28, No. 5, pp. 755-776, October 1993.

[89]. M. Jevtic and A.M. Andreev, The method of testing of XLPE cable insulation resistance to partial discharges and electrical treeing, Bulletin of material science, vol. 19, No. 5, pp. 823-829, 1996.

[90]. M.H. Shwehdi, M.A. Morsy and A. Abugurain, Thermal aging tests on XLPE and PVC cable insulation materials of Saudi Arabia, Annual Report Conference on Electrical Insulation and Dielectric Phenomena, 2003.

[91]. G.E. Sliter, Overview of research on nuclear plant cable ageing and life extension, in Proc. SMiRT-12, Elsevier Science Publishers, pp. 199-203, 1993.

[92]. M.J. Sandelin and U.W. Gedde, Long-term performance of cables based on chlorosulphonated polyethylene, Polymer Degradation and Stability, vol. 86, pp. 331-338, 2004.

[93]. Juan Carlos Cano Gonzalez and Paolo F. Fantoni, Experiments on cable ageing assessment and fault detection using modern techniques, OECD Halden Reactor Project, Halden, Norway, 2008.

[94]. T. Tanaka, Ageing of polymeric and composite insulating materials aspects of interfacial performance in ageing, IEEE Transactions on Dielectrics and Electrical Insulation, vol. 9, no. 5, pp. 704-716, 2002.

[95]. G.J. Toman and L.P. Gradin, Power plant practices to ensure cable operability, Electric power research institute, EPRI NP-7485, July 1992.

[96]. Rost, H., Bleier, A., Becker, W., Lifetime of cables in nuclear power plants, Int. Conf. on Operability of Nuclear Systems in Normal and Adverse Environments, OPERA'89, Société Française d'Energie Nucléaire, Lyon, 597-604, 1989.

[97]. Hengkun Xie Xinyan Wu Zongren Peng, The Energy Criterion for Breaking Chemical Bonds in Electrical Breakdown Process of Polymer, Roceedings of the 4th International Conference on Properties and Applications of Dielectric Materials July 378,1994.

[98]. Kao K C. New theory of electrical discharge and breakdown in low-mobility condensed insulators. J Appl Phys, 1984, 55(3):752-755.

[99]. Lebey T, Laurent C. Correlation between charge injection and electroluminecence in polyethylene under prebreakdown a.c. fields. Proc. 2nd ICPADM, Beijing, 1988, 582-585.

[100]. D.C. Wright, 'Failure of Plastics and Rubber Products – Causes, Effects and Case Studies involving Degradation', Rapra Technology Report, 2001, ISBN: 1-85857-261-8.

[101]. Mohammed Hanif, "Principles an applications of insulation testing with DC", IEP-SAC journal, pp. 57-63, 2004-2005.

[102]. D. Allan, T.R. Blackburn and R. Sheehy, Methodologies and models to improve the reliability of service aged electrical insulation, CIGRE, No. 15-303, 2002.

[103]. Jong-Seog Kim, Evaluation of Nuclear Plant Cable Aging through Condition Monitoring, Journal of the Korean Nuclear Society vol. 36, no. 5, pp. 475-484, 2004.

[104]. Jong-seog Kim, Development of cable aging indenter, 99th spring meeting of Korean nuclear society, 1999.

[105]. M.M. Hirschler, "Thermal Decomposition (STA and DSC) of Poly(vinyl chloride) Compounds under a Variety of Atmospheres and Heating Rates," Europ. Polymer J., 22, pp. 153–60, 1986.

[106]. IEC 60068-2-2, Basic environmental testing procedures–Part 2: Tests, Tests B: Dry heat, 1974.

[107]. Carfago and Gibson, A review of equipment ageing theory and technology, EPRI NP-1558, Electric Power Research Institute, Palo Alto, CA, USA, September 1980.

[108]. V. Gueguen, L. Audouin, B. Pinel and J. Verdu, Polymer Degradation and Stability, vol. 46(1), pp. 217-223, 1994.

[109]. H. Kudo, A. Shimada, A. Idesaki, T. Ohshima, K. Tamura, and T. Seguchi, Degradation mechanisms of cable insulation materials during radiation thermal ageing in radiation environment, Proceedings of the International Symposium on the Ageing Management and Maintenance of Nuclear Power Plants, pp. 84-91, 2010.

[110]. T. Kashiwagi, T. Hirata, and J.E. Brown, Thermal and Oxidative Degradation of Poly(methyl methacrylate), Molecular Weight, Macromolecules, 18, pp. 131–138, 1985.

[111]. T. Hirata, T. Kashiwagi, and J.E. Brown, Thermal and Oxidative Degradation of Poly(methyl methacrylate), Weight Loss, Macromolecules, 18, pp. 1410–1418, 1985.

[112]. T. Kashiwagi, A. Inabi, J.E. Brown, K. Hatada, T. Kitayama, and E. Masuda, Effects of Weak Linkages on the Thermal and Oxidative Degradation of Poly(methyl methacrylates), Macromolecules, 19, pp. 2160–2168,1986.

[113]. T. Kashiwagi and A. Inabi, Behavior of Primary Radicals during Thermal Degradation of Poly(methyl methacrylate), Polymer Degradation and Stability, 26, pp. 161–184, 1989.

[114]. M.M. Hirschler, Thermal Analysis and Flammability of Polymers: Effect of Halogen-Metal Additive Systems, Europ. Polymer J., vol.19, pp. 121–129, 1983.

[115]. N. Grassie and G. Scott, Polymer Degradation and Stabilisation, Cambridge University Press, Cambridge, UK, 1985.

[116]. S.M. Lomakin, J.E. Brown, R.S. Breese, and M.R. Nyden, An Investigation of the Thermal Stability and Char-Forming Tendency of Cross-Linked Poly(methyl methacrylate), Polymer Degradation Stability, 41, pp. 229–43, 1993.

[117]. Clough, R. L., and Gillen, K. T., Oxygen diffusion effects in thermally aged elastomers. Polym. Degrad. Stab. 38, 47-56, 1992.

[118]. Clough, R. L., Gillen, K. T., Campan, J. L., Gaussens, G., Schonbacher, H., T., Wilski, H., and Machi, S., Accelerated aging tests for predicting radiation degradation of organic materials. Nucl. Safety, 25, 238, 1984.

[119]. A. J. Alsammarae, A. K. Behera and S. Akhtar, An approach to calculate insulation resistance (IR) at different temperatures and voltages, IEEE Transaction on Nuclear Science, vol. 37, no. 2, April 1990.

[120]. T. V. Santosh, R. K. Saraf, A. K. Ghosh and H. S. Kushwaha, Optimum step length selection rule in modified HL-RF method for structural reliability, International Journal of Pressure Vessels and Piping, vol. 83, pp. 742-748, 2006.

[121]. Achintya Haldar and Sankaran Mahadevan, Reliability assessment using stochastic finite element analysis, John Wiley & Sons Inc., 2000.

[122]. Liping Wang and R. V. Grandhi, Safety index calculations using intervening variables for structural reliability, Computers & Structures, vol. 59, no. 6, pp 1139- 1148, 1996.

[123]. Pei-Ling Liu and Armen Der Kiureghian, Optimization algorithms for structural reliability, Structural Safety, no.9, pp. 161-177, 1991.

[124]. Nowlen Steven, An investigation of the effects of thermal aging on the fire damageability of electric cables, Sandia National Laboratories, Albuquerque, NM, SAND-1990-0696, United States Nuclear Regulatory Commission, Washington, DC, NUREG/CR-5546, 1990.

[125]. COMREL TI+TV, version 7.10. RCP Consulting Software, 1987–2000.

[126]. STRUREL TI+TV, version 7.10. RCP Consulting Software, 1987–2000.

[127]. S. B. Dalal, R. S. Gorur and M. L. Dyer, Aging of distribution cables in service and its simulation in the laboratory, IEEE Transactions on Dielectrics and Electrical Insulation, vol. 12, no. 1, pp. 139-146, 2005.

[128]. Gian Carlo Montanari and Antonio Motori, Thermal endurance evaluation of XLPE insulated cables, J. Phys. D: Appl. Phys., vol. 24, pp. 1172-1181, 1991.

[129]. Johannes G. (Han) Slootweg, Andre Postma and E. Fred Steennis, A practical approach towards estimating remaining MV cable life, 19th International Conference on Electricity Distribution, Vienna, 21-24 May, 2007.

[130]. Michael G. Danikas, Ning Gao and Martti Aro, Neural networks and their role in partial discharge recognition in gas insulated switchgear and transformers: A short review, Journal of Electrical Engineering, vol. 54, no. 3-4, pp. 107-112, 2003.

[131]. Po-Hung Chen and Hung-Cheng Chen, Application of back-propagation neural network to power transformer insulation diagnosis, Springer-Verlag, Berlin Heidelberg, ISNN 2007, LNCS 4493, Part III, pp. 26–34, 2007.

[132]. Mo-yuen Chow, Peter M. Mangum and Sui Oi Yee, A neural network approach to real-time condition monitoring of induction motors, IEEE Transactions on Industrial Electronics, vol. 38, no. 6, pp. 448-453, 1991.

[133]. Zhiqiang Wang, Changliang Zhou, Guofeng LI and Ninghui Wang, Thermal lifetime estimation of ethylene propylene rubber insulated shipboard power cable using artificial neural network, Journal of Computational Information Systems, vol.8, no. 7, pp. 2999–3006, 2012.

[134]. L. Mokhnache and A. Boubakeur, The use of some paradigms of neural networks in prediction of dielectric properties for high voltage liquid solid and gas insulations, IEEE International Symposium on Electrical Insulation, Boston, MA USA, April 7-10, 2002.

[135]. M. Hammer, T. Kozlovsky, R. Szabo and J. Svoboda, The use of neural networks for the life prediction of insulating material of electric rotating machines, International Conference on Solid Dielectrics, Toulouse, France, July 5-9, 2004.

[136]. Khaled Shaban, Ayman El-Hag and Andrei Matveev, A cascade of artificial neural networks to predict transformers oil parameters, IEEE Transactions on Dielectrics and Electrical Insulation, vol. 16, no. 2, pp. 516-523, 2009.

[137]. B. Vahidi, A. H. Ranjbar, H. Omranpour and M. Akbari, Application of artificial neural network in cable life time estimation and its failure rate per 100km, 2nd International Conference on Modern Power Systems MPS 2008, Romania, 12-14 November, 2008.

[138]. T. V. Santosh, A. Shrivastava, V.V.S. Sanyasi Rao, A. K. Ghosh and H. S. Kushwaha, Diagnostic system for identification of accident scenarios in nuclear power plants using artificial neural networks, Reliability Engineering and System Safety, vol. 54, pp. 759-762, 2009.

[139]. S. Deshpande, A. S. Patil and A. N. Cheeran, The applications of Weibull function to partial discharge analysis and insulation ageing: A review, International Journal of Advanced Engineering Sciences and Technologies, vol. 3, no. 2, pp. 111-114, 2011.

[140]. P. J. Tavner, L. Ran, J. Penman and H. Sedding, Condition monitoring of rotating electrical machines, Power and Energy Series, no. 56, IET, 2008.

[141]. Naveen Kumar Sharma and Prashant Kumar Tiwari, Review of artificial intelligence techniques application to dissolved gas analysis on power transformer, International Journal of Computer and Electrical Engineering, vol. 3, no. 4, 2011.

[142]. Bing Liu, Xiao-hua Bao, Jian Liu and Qing-long Zhu, Insulation life prediction of high voltage submersible motor based on BP neural network, no. 978-1-61284-459-6/11, pp. 418-421, IEEE Proceedings, 2011.

[143]. L. Ekonomou, P. D. Skafidas and D. S. Oikonomou, Transformer oil's service life identification using neural networks, 8th WSEAS International Conference on Electric Power Systems, High Voltages, Electric Machines (POWER '08), ISBN: 978-960-474-026-0, pp. 222-226, 2008.

[144]. Simon Haykin, Neural networks: A comprehensive foundation, ISBN 81-7808-300-0, Second Edition, Pearson Foundation, Prentice Hall, 2005.

[145]. Jacek M. Zurada, Introduction to artificial neural systems, ISBN 0-314-93391-3, West Publishing Company, 1992.

[146]. T. V. Santosh, Gopika Vinod, R. K. Saraf, A. K. Ghosh and H. S. Kushwaha, Application of artificial neural networks to nuclear power plant transient diagnosis, Reliability Engineering and System Safety, vol. 92, pp. 1468-1472, 2007.

[147]. Sinem Kulluk, Lale Ozbakir and Adil Baykasoglu, Training neural networks with harmony search algorithms for classification problems, Engineering Applications of Artificial Intelligence, no. 25, pp. 11–19, 2012.

[148]. S. Borucki, T. Boczar and A. Cichoń, The application of the resilient back propagation algorithm and power spectrum density for recognizing the acoustic emission

signals generated by basic partial discharge forms using artificial neuron networks, Research Project no. 3, T10A 018 30, Technical University of Opole, 2006.

[149]. Jovan Nahmana, Miladin Tanaskovicb, Calculation of the ampacity of medium voltage self-supporting cable bunch, vol. 93, pp. 106-112, Electric Power Systems Research, 2012.

[150]. Hanyu Ye, El Mehdi Boudoudou, EikeScholz and Markus Clemens, Coupled Electro-thermal Field Simulation in HVDC-Cables, proceedings of the COMSOL conference, Germany, 2011.

[151]. Jack. P. Holman, Heat Transfer, McGraw Hill, 10th Edition, 2010.

[152]. Bartnikas, R. Dielectrics and Insulators The Electrical Engineering Handbook, CRC Press LLC, 2000.

[153]. IS 10810 (Part 43)-1984, Methods of test for cables: Insulation resistance, 1984.

[154]. Anandakumaran K., Barreca S., Seidl N., Castaldo P. V., Nuclear qualification of PVC insulated cables, IEEE transactions on dielectrics and electrical insulation, vol. 8, no. 5, 2001.

[155]. Rajini V., Experimental evaluation and comparison of performance of polymeric insulating materials in radiation environment, Electrical engineering, Elixir elec. engg., no. 40, pp. 5554-5562, 2011.

[156]. ASTM D 3895-07, Test method for oxidative induction time of polyolefins by thermal analysis, ASTM International, 2007.

[157]. L. R. Mason, A. B. Reynolds, Comparison of oxidation induction time measurements with values derived from oxidation induction temperature measurements for EPDM and XLPE polymers, Polymer Engineering and Science, vol. 38, no.7, pp. 1149-1153, 1998.

[158]. Deepalaxmi R., Rajini V., Performance evaluation of gamma irradiated SiR-EPDM blends, Nuclear Engineering and Design, vol. 273, pp. 602–614, 2014.

[159]. R. López-Castañares, O. Olea-Cardoso, F. Vázquez-Moreno, B. Lizama-Soberanis, E. Camps-Carvajal, Positron annihilation for characterizing polymeric materials, Bulg. J. Phys. 29, 55–178, 2002.

[160]. Y. Kobayashi, W. Zheng, E. F. Meyer, J. D. McGervey, A. M. Jamieson, and R. Simhall, Free volume and physical aging of poly(viny1 acetate) studied by positron annihilation, Macromolecules, 22, 2302-2306, 1989.

[161]. G. Dai, Q. Deng, J. Liu, H. Shi, C. Huang, et al., Free-volume hole distributions of polymers by positron annihilation lifetime spectroscopy, Journal de Physique IV, 03 (C4), pp.C4-233-C4-239, 1993.

[162]. IEC 60216, Guide for the determination of thermal endurance properties of electrical insulating materials, 4th issue, 1994.

[163]. R. M. Bell, T. E. Doyle, and A. B. Reynolds, Correlation of oxidative induction time with thermal and radiation aging of EPR and XPLE cable insulation, IEEE International Symposium on Electrical Insulation, Toronto, Canada, June 3-6, 1990.

[164]. L. A. Dissado, Predicting electrical breakdown in polymeric insulators from deterministic mechanisms to failure statistics, IEEE transactions on dielectrics and electrical insulation, vol.5, pp. 860-875, 2002.

[165]. J. C. Fothergill, L. A. Dissado, Electrical degradation and breakdown in polymers, P. Peregrinus for IEE, London, 1992.

[166]. FaultTree+, ISOGRAPH Reliability Software, Version 10.1, 2002.

Appendix A. Experimental Studies and Results

A.1 Insulation resistance measurement

The experimental results obtained from insulation resistance measurement for insulation and sheath materials of various manufacturer cables are shown in Tables A.1-A.5.

Table A.1: Manufacturer-1 control cable: IR and PI values

Cable type	Specifications	Polymer type		Year of manufacturing
		Insulation	Sheath	
Manufacturer-1 control cable	10 core, 1.5sq.mm, 650/1100V	FRLS PVC	HR PVC	2009

Set test voltage: 1000V	Actual voltage: 1024V	Capacitance: 25.2nF

Sl. No.	Test sequence	Leakage current (nA)		Insulation resistance ($10^9\Omega$)		Polarization index (PI)
		1 min	10 min	1 min	10 min	
1	C1-C2	15.7	10.3	65.2	99.6	1.53
2	C1-C3	11.8	8.21	86.7	125	1.44
3	C1-C4	9.97	7.51	103	136	1.33
4	C1-C5	9.83	7.49	104	137	1.31
5	C2-C3	9.08	6.32	113	162	1.44
6	C2-C4	9.89	7.21	103	142	1.37
7	C2-C5	15.1	12.1	68	84.3	1.24
8	C3-C4	15.7	12.6	65.3	81.3	1.24
9	C3-C5	12.3	9.91	83.4	103	1.24
10	C4-C5	18.7	16	54.6	63.9	1.17

Table A.2: Manufacturer-2 signal cable 1: IR and PI values

Cable type	Specifications	Polymer type		Year of manufacturing
		Insulation	Sheath	
Manufacturer 2 signal cable 1	37 core, 1.5sq.mm, 1100V	FRLS	HRPVC	2011

Set test voltage: 1000V Actual voltage: 1024V Capacitance: 25.2nF

Sl. No.	Test sequence	Leakage current (nA)		Insulation resistance ($10^9\Omega$)		Polarization index (PI)
		1min	10min	1min	10min	
1	C1-C2	4.19	2.84	244	361	1.48
2	C1-C3	1.91	1.65	536	622	1.16
3	C1-C4	2.74	2.34	373	437	1.17
4	C1-C5	0.97	0.74	1050	1380	1.31
5	C2-C3	4.04	2.41	253	425	1.68
6	C2-C4	10.1	8.67	101	118	1.17
7	C2-C5	3.17	2.34	323	438	1.36
8	C3-C4	2.62	2.17	391	472	1.21
9	C3-C5	1.17	0.93	870	1100	1.26
10	C4-C5	3.21	2.45	319	418	1.31

Table A.3: Manufacturer-2 signal cable 2: IR and PI values

Cable type	Specifications	Polymer type		Year of manufacturing
		Insulation	Sheath	
Manufacturer 2 signal cable 2	19 core, 1.5sq.mm, 1100V	FRLS	HRPVC	2011

Set test voltage: 1000V	Actual voltage: 1024V	Capacitance: 25.2nF

Sl. No.	Test sequence	Leakage current (nA)		Insulation resistance ($10^9\Omega$)		Polarization index (PI)
		1min	10min	1min	10min	
1	C1-C2	11.8	8.64	86.4	119	1.37
2	C1-C3	12.1	9.51	84.6	108	1.27
3	C1-C4	11.8	9.27	86.4	110	1.28
4	C1-C5	11	8.07	92.9	127	1.37
5	C2-C3	16.3	13.1	62.8	77.9	1.24
6	C2-C4	15.2	12.8	67.4	80	1.19
7	C2-C5	11.6	9.1	88.1	113	1.28
8	C3-C4	15	12.2	68	84	1.24
9	C3-C5	13.1	10.3	78.3	99.1	1.27
10	C4-C5	15.6	11.3	65.7	91	1.38

Table A.4: Manufacturer-2 instrumentation cable: IR and PI values

Cable type		Specifications	Polymer type		Year of manufacturing	
			Insulation	Sheath		
Manufacturer 2 instrumentation cable		30 core, 1.0sq.mm	FRLS	HRPVC	2012	
Set test voltage: 1000V		Actual voltage: 1024V		Capacitance: 25.2nF		
Sl. No.	Test sequence	Leakage current (nA)		Insulation resistance ($10^9\Omega$)		Polarization index (PI)
		1min	10min	1min	10min	
1	C1-C2	1.39	0.76	740	1340	1.82
2	C1-C3	0.45	0.28	2290	3000	1.31
3	C1-C4	0.46	0.28	2250	3000	1.33
4	C1-C5	0.36	0.07	2860	3000	1.05
5	C2-C3	0.14	0.05	3000	3000	1
6	C2-C4	0.04	0.03	3000	3000	1
7	C2-C5	0.05	0.02	3000	3000	1
8	C3-C4	0.28	0.19	3000	3000	1
9	C3-C5	0.62	0.34	1660	3000	1.81
10	C4-C5	1.02	0.55	1000	1870	1.87

Table A.5: Manufacturer-3 control cable: IR and PI values

Cable type		Specifications	Polymer type		Year of manufacturing	
			Insulation	Sheath		
Manufacturer 3 control cable		37 core, 1.5sq.mm, 1100V	FRLS	HRPVC	2009	
Set test voltage: 1000V		Actual voltage: 1024V		Capacitance: 25.2 nF		
Sl. No.	Test sequence	Leakage current (nA)		Insulation resistance ($10^9\Omega$)		Polarization index (PI)
		1min	10min	1min	10min	
1	C1-C2	1.31	0.9	780	1140	1.46
2	C1-C3	2.44	1.77	420	576	1.38
3	C1-C4	5.67	4.12	180	248	1.38
4	C1-C5	2.22	1.67	461	612	1.33
5	C2-C3	3.55	1.88	288	543	1.89
6	C2-C4	1.65	1.32	620	777	1.25
7	C2-C5	2.02	1.45	506	704	1.39
8	C3-C4	4.36	2.44	235	420	1.79
9	C3-C5	3.29	1.79	311	571	1.83
10	C4-C5	2.54	1.43	403	717	1.78

A.2 Elongation at break measurement

A.2.1 Stress-strain curves of thermally aged insulation materials

A.2.1.1 Stress-strain curves of insulation aged at 110^0C

The stress-strain curves, tensile strength and elongation of insulation aged at 110^0C are shown in Figures A.1-A.3.

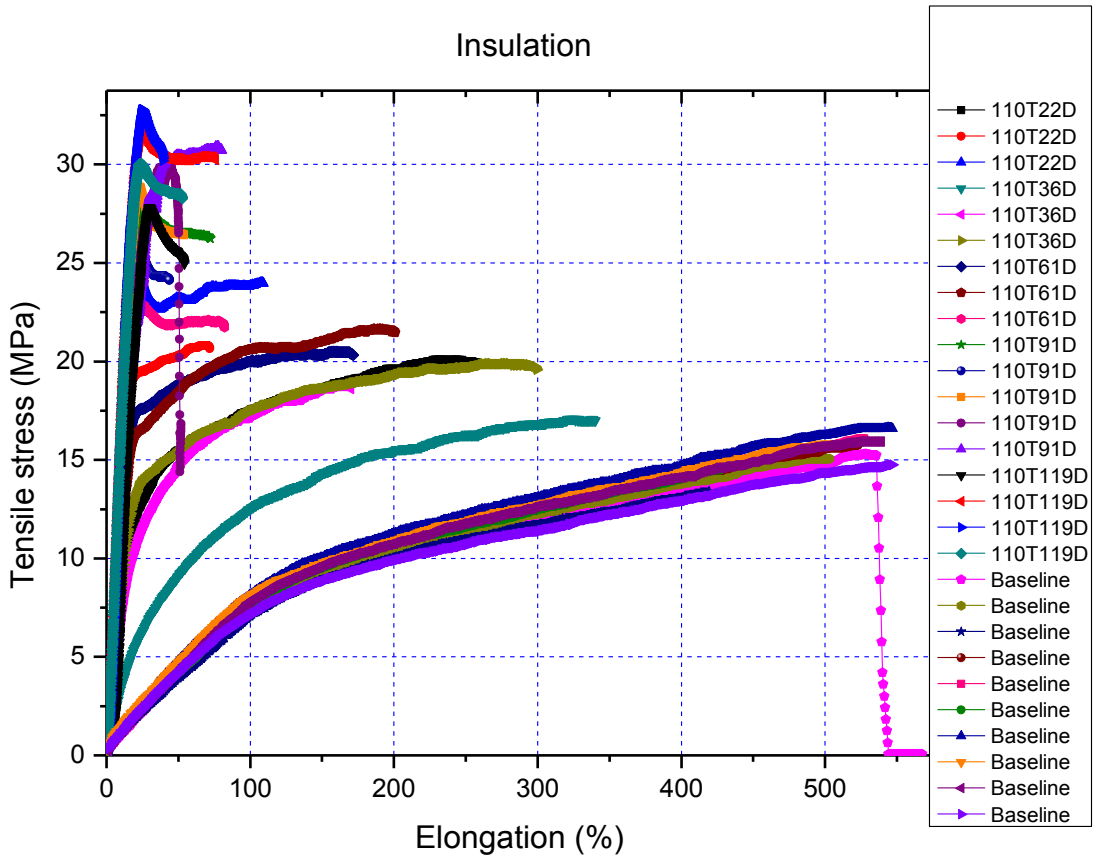

Figure A.1: Stress-strain curves of fresh and aged samples of insulation

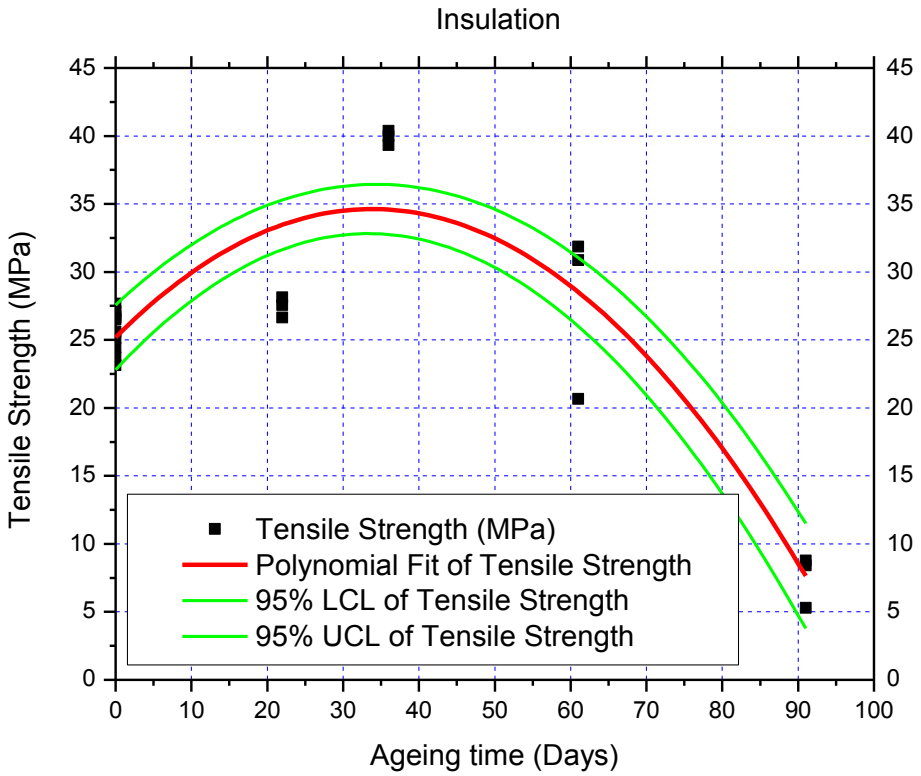

Figure A.2: Tensile strength vs ageing time of insulation aged at 110^0C

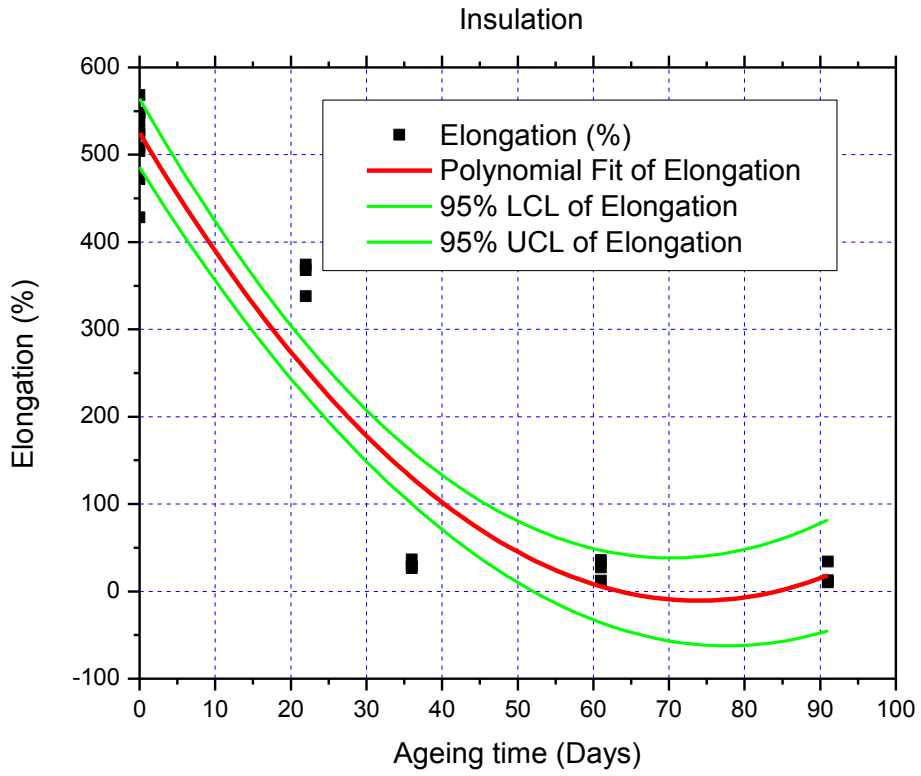

Figure A.3: Elongation vs ageing time of insulation aged at 110^0C

A.2.1.2 Stress-strain curves of sheath aged at 110^0C

The stress-strain curves, tensile strength and elongation of sheath aged at 110^0C are shown in Figures A.4-A.6.

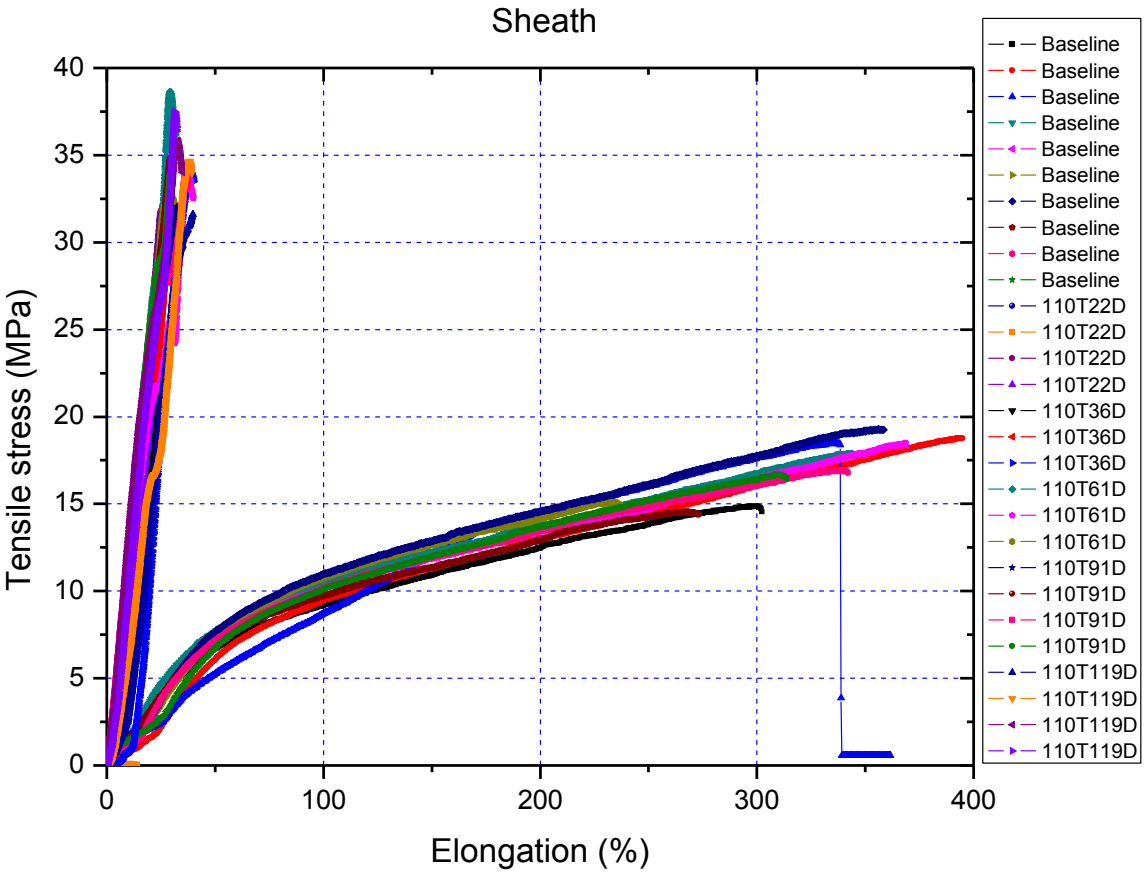

Figure A.4: Stress-strain curves of fresh and aged samples of sheath

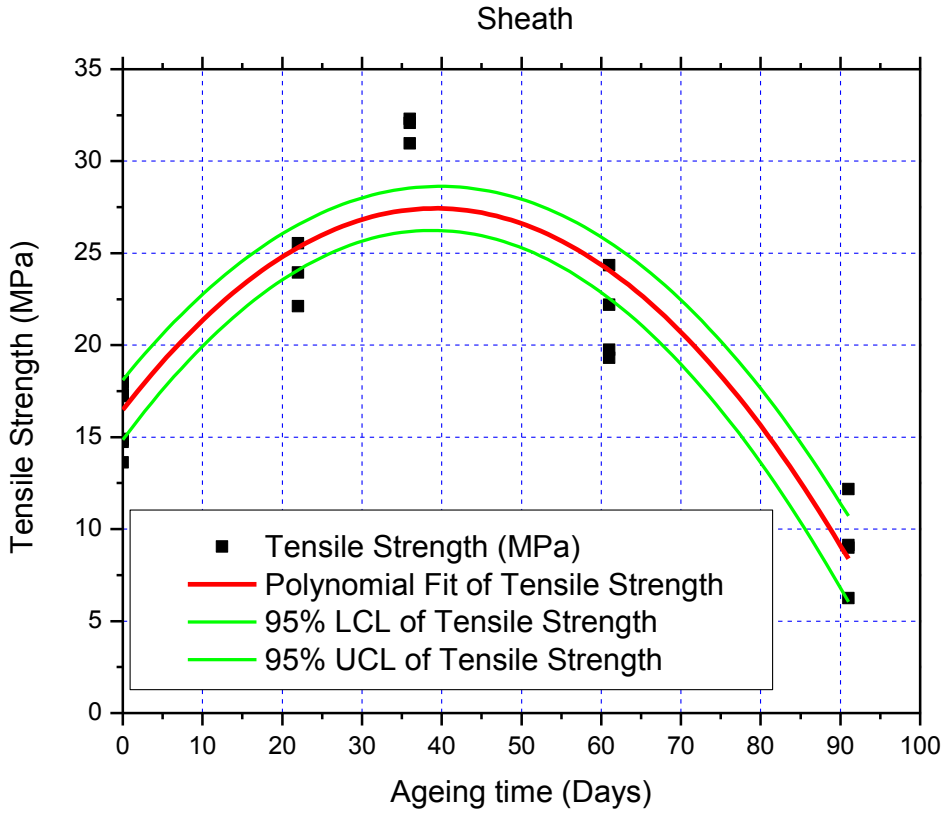

Figure A.5: Tensile strength vs ageing time of sheath aged at 110^0C

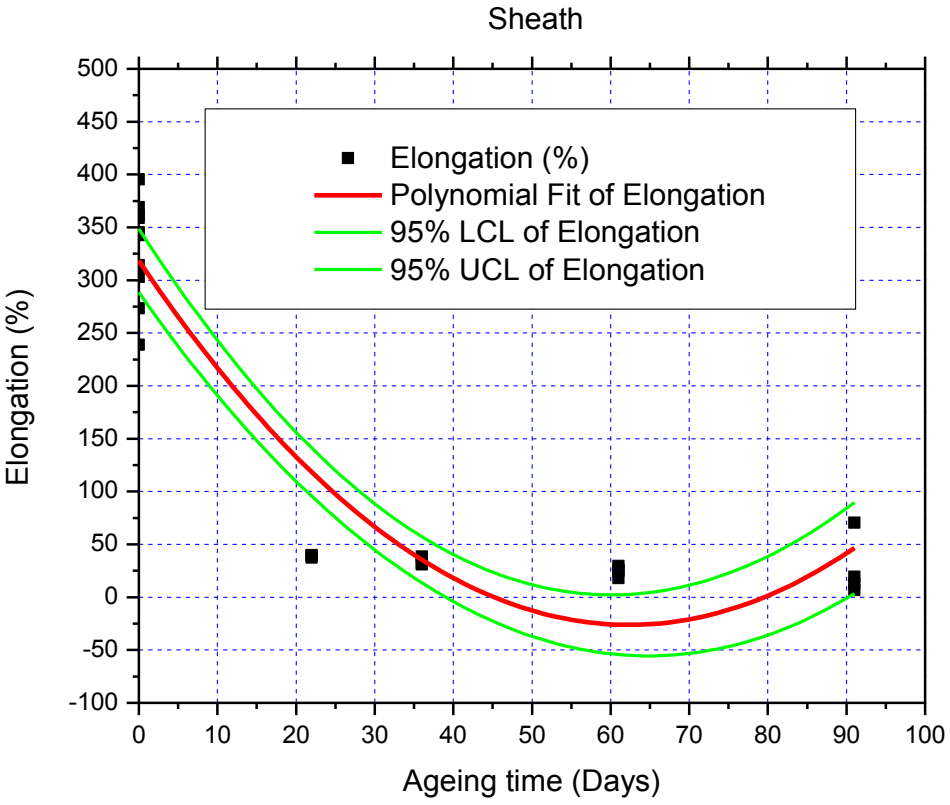

Figure A.6: Elongation vs ageing time of sheath aged at 110^0C

A.2.1.3 Stress-strain curves of insulation aged at 135^{0}C

The stress-strain curves, tensile strength and elongation of insulation aged at 110^{0}C are shown in Figures A.7-A.9.

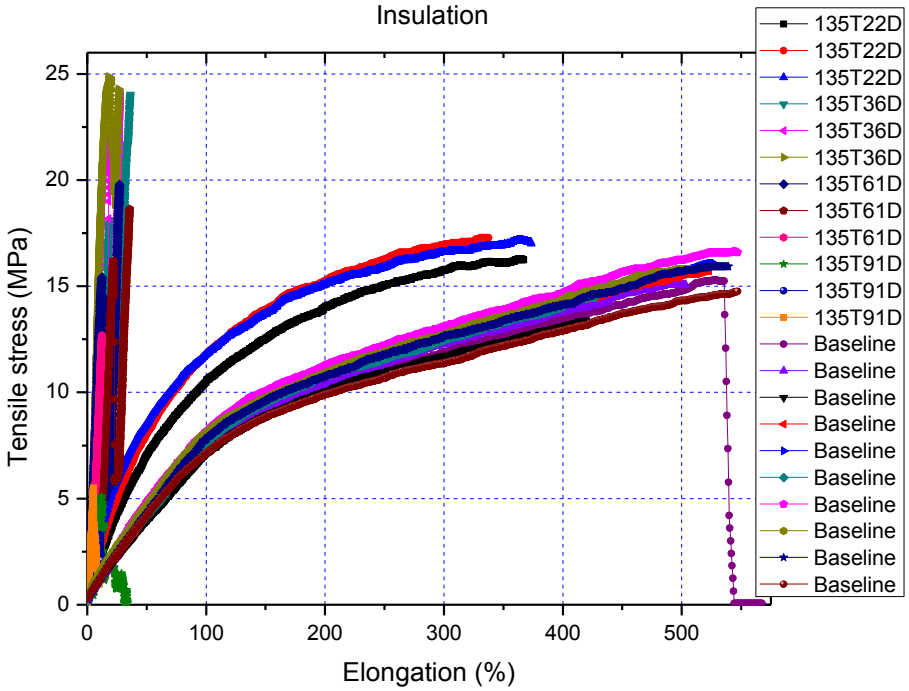

Figure A.7: Stress-strain curves of fresh and aged samples of insulation

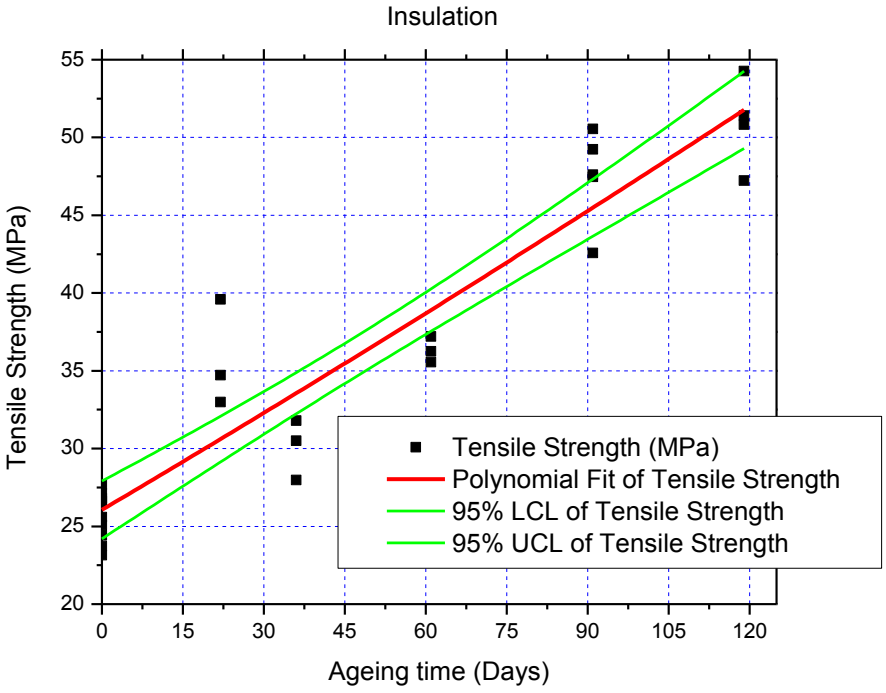

Figure A.8: Tensile strength vs ageing time of insulation aged at 135^{0}C

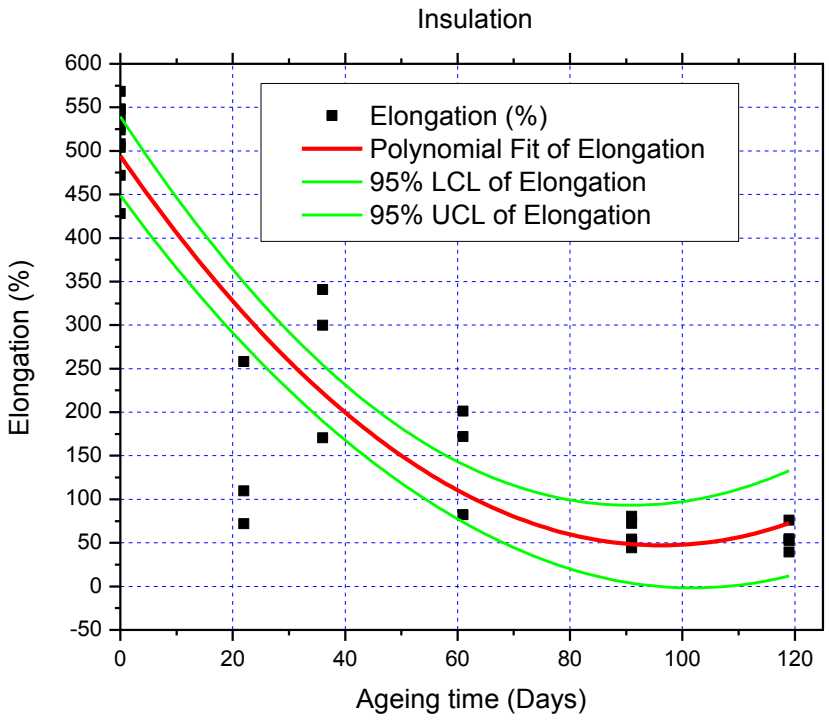

Figure A.9: Elongation vs ageing time of insulation aged at 135^{0}C

A.2.1.4 Stress-strain curves of sheath aged at 135^{0}C

The stress-strain curves, tensile strength and elongation of sheath aged at 110^{0}C are shown in Figures A.10-A.12.

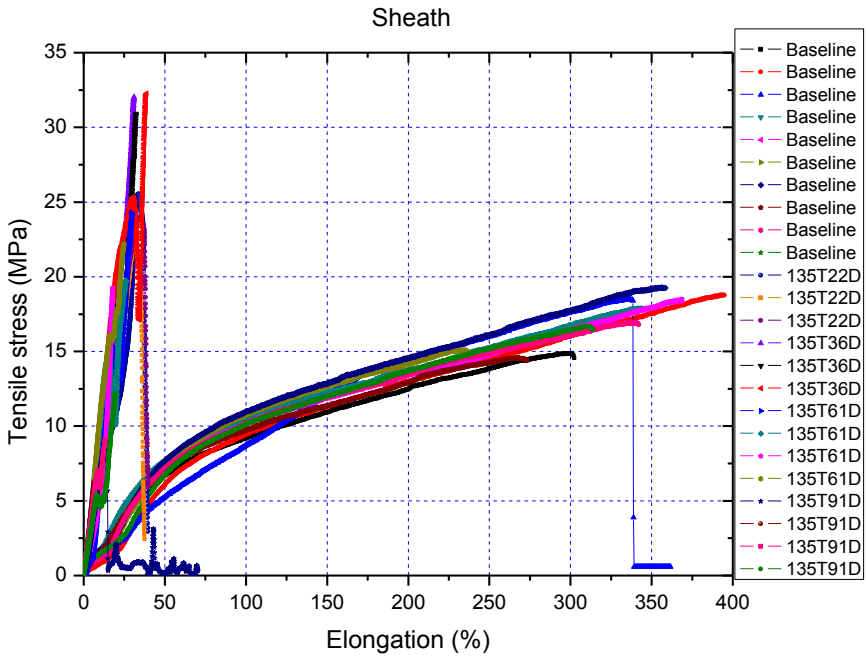

Figure A.10: Stress-strain curves of fresh and aged samples of sheath

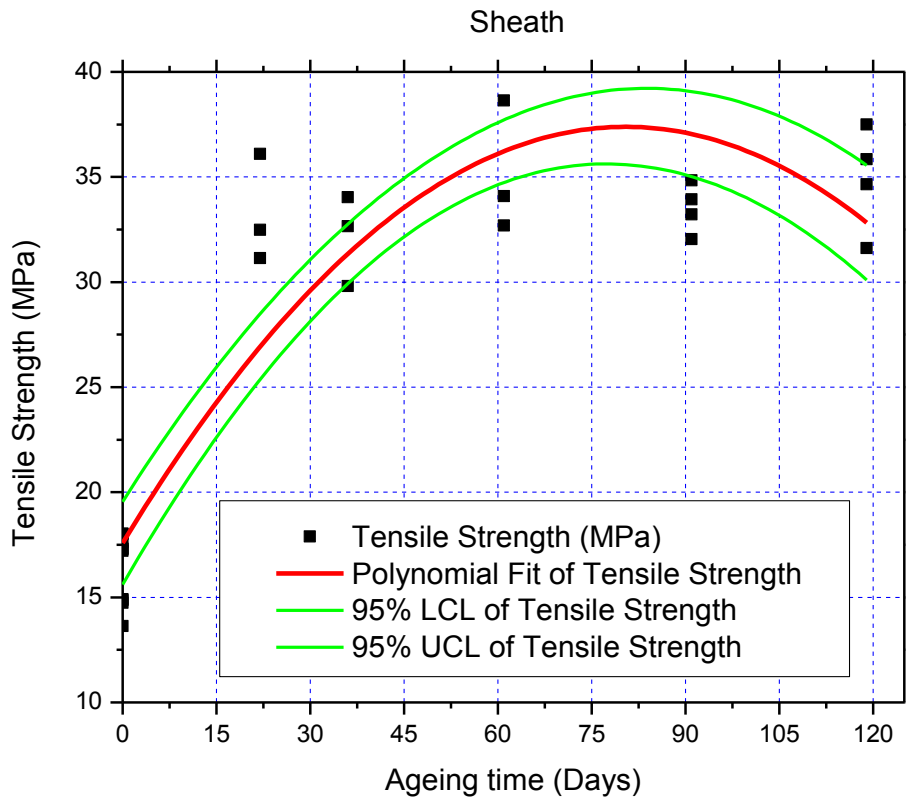

Figure A.11: Tensile strength vs ageing time of sheath aged at 135^0C

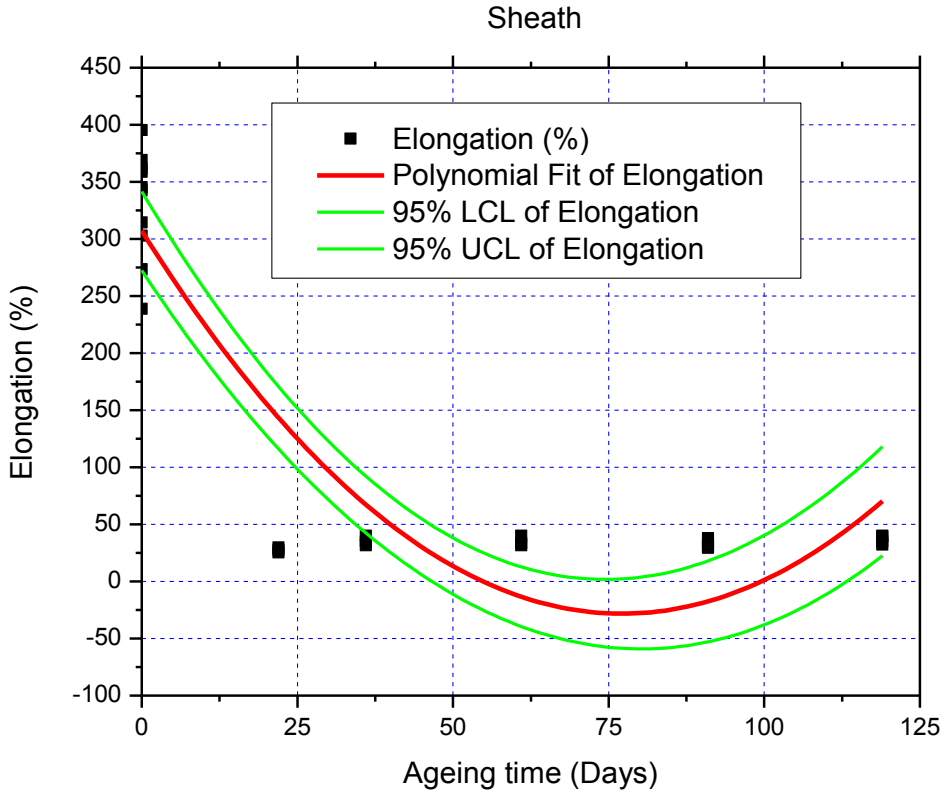

Figure A.12: Elongation vs ageing time of sheath aged at 135^0C

A.2.1.5 Images of thermally aged samples after tensile test

Ageing time (days)	Sheath aged at 110^0C	Insulation aged at 110^0C
Unaged		
22		
36		

61		
91		
119		

Ageing time (days)	Sheath aged at 135^0C	Insulation aged at 135^0C
Unaged		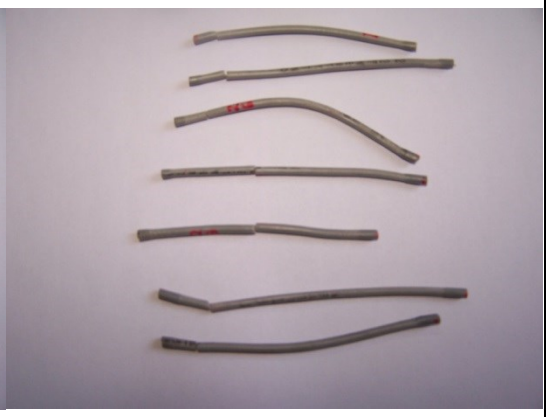
22		
36		

61		
91		

A.2.2 Stress-strain curves of radiation aged insulation materials

A.2.2.1 Stress-strain curves of radiation aged insulation

The important tensile properties and elongation plots of insulation materials for various dose conditions are shown in Figures A.13-A.17.

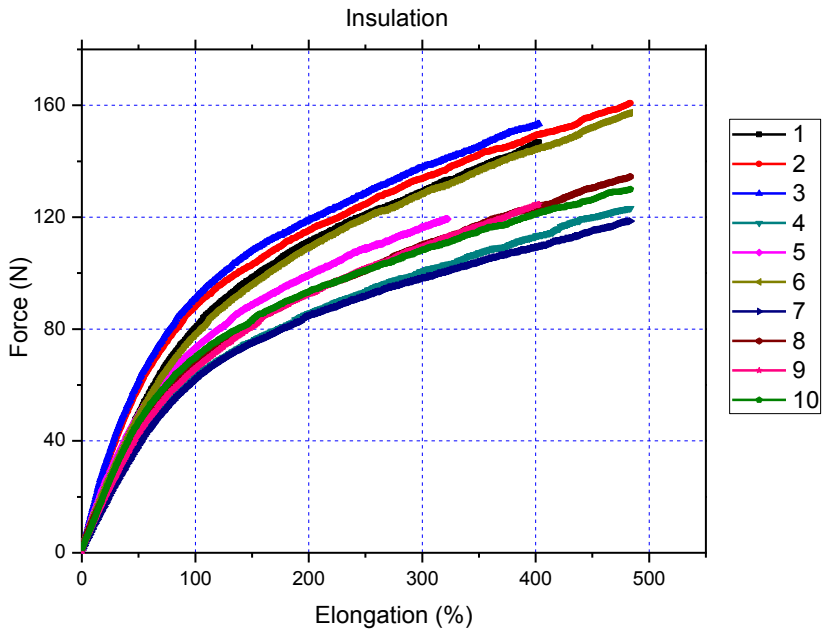

Figure A.13: Elongation of unaged insulation

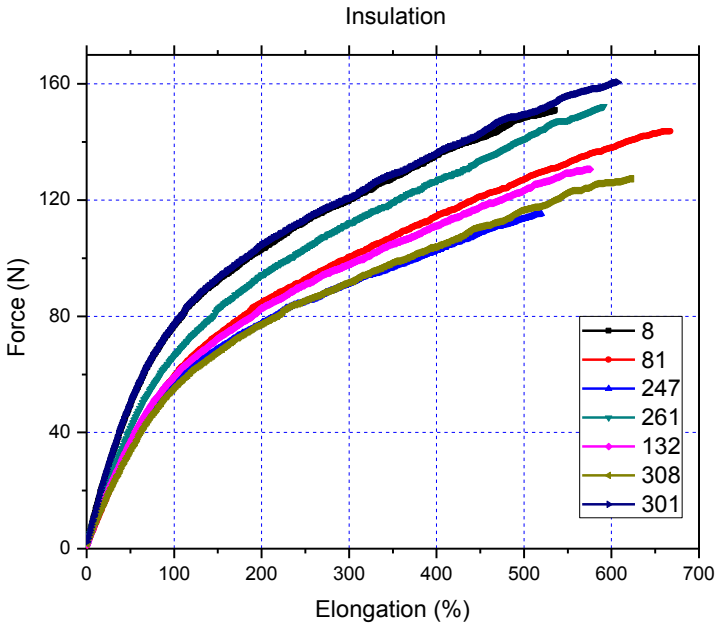

Figure A.14: Elongation of insulation aged at 5MRad

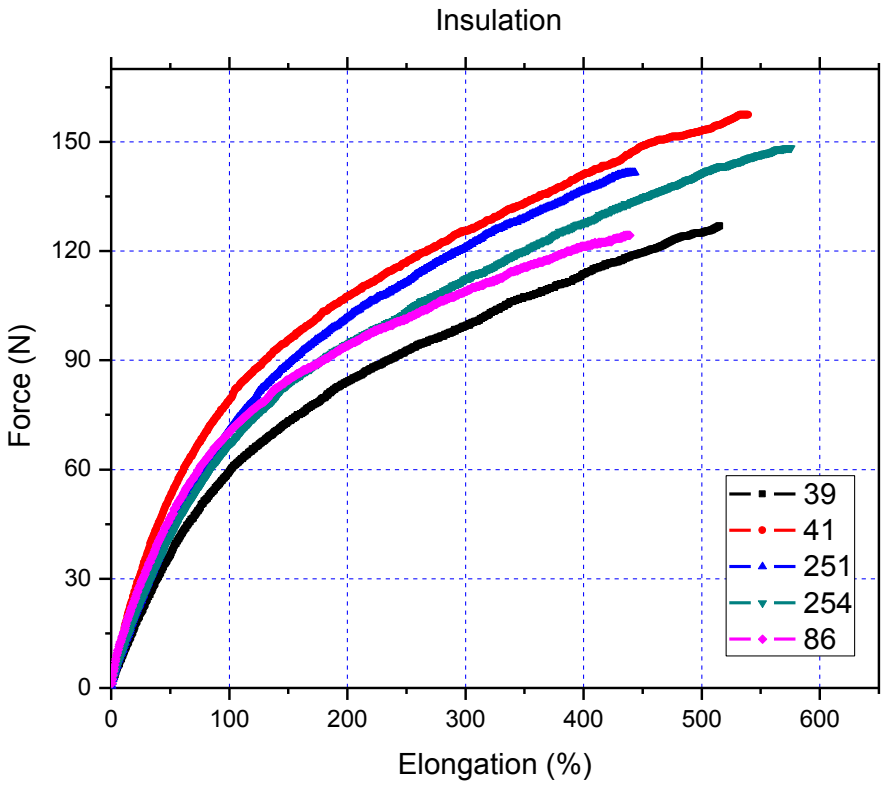

Figure A.15: Elongation of insulation aged at 10MRad

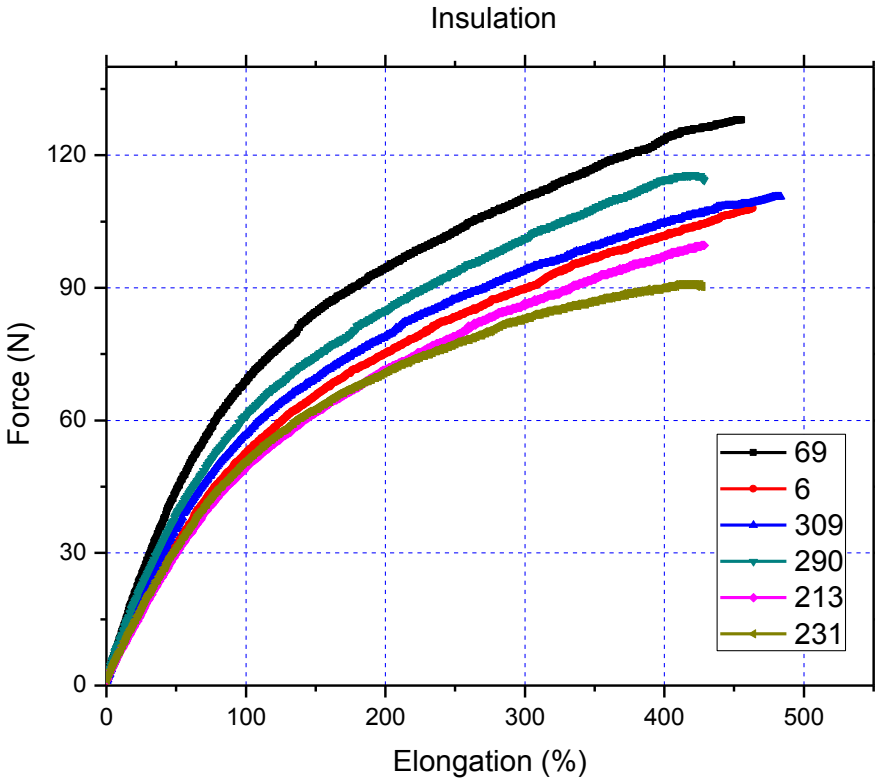

Figure A.16: Elongation of insulation aged at 25MRad

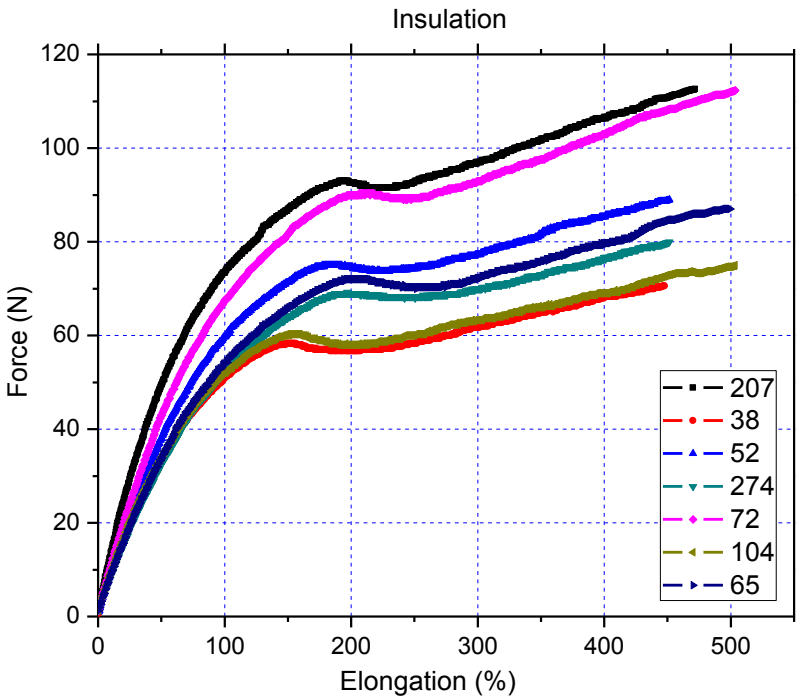

Figure A.17: Elongation of insulation aged at 50MRad

A.2.2.2 Stress-strain curves of radiation aged sheath

The important tensile properties and elongation plots of sheath materials for various dose conditions are shown in Figures A.18-A.22.

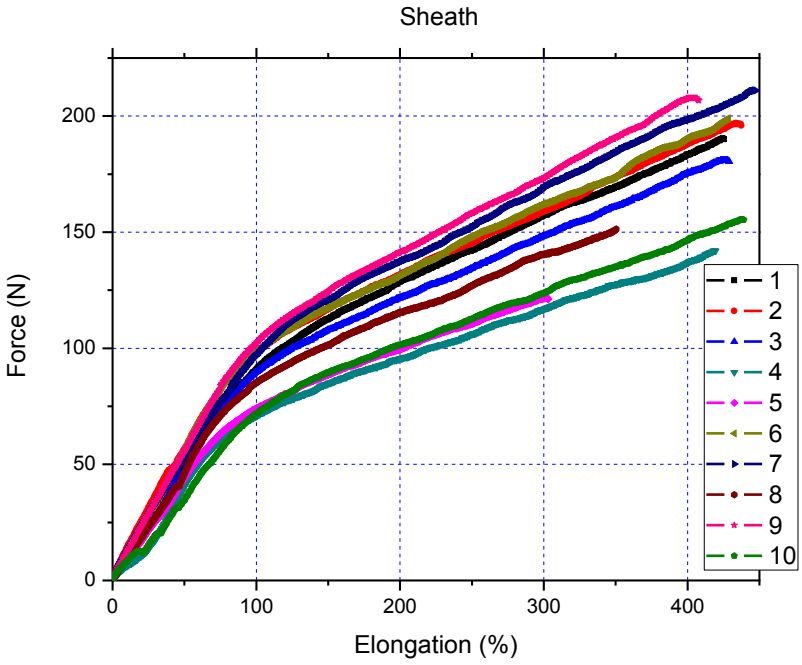

Figure A.18: Elongation of unaged sheath

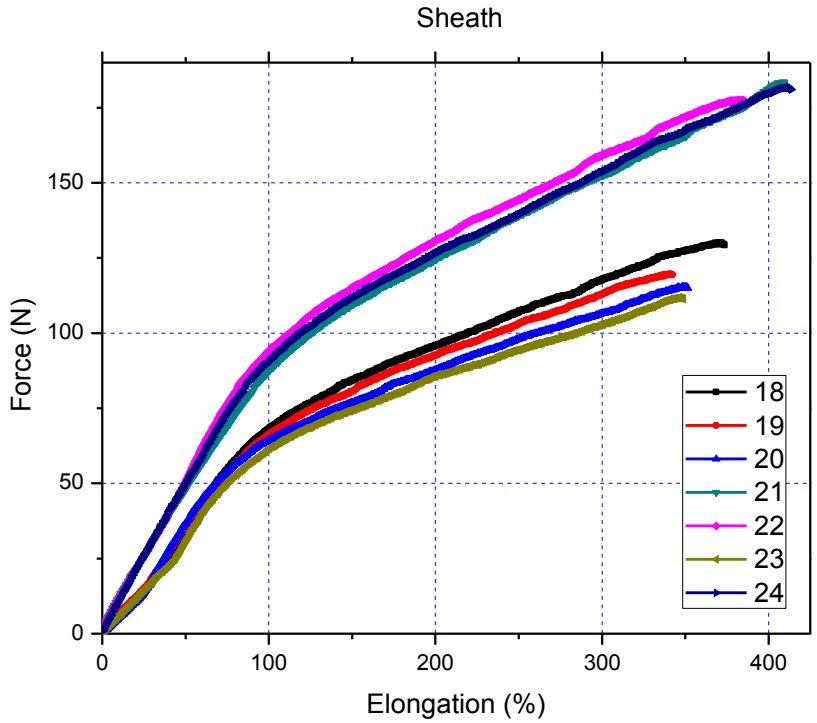

Figure A.19: Elongation of sheath aged at 5MRad

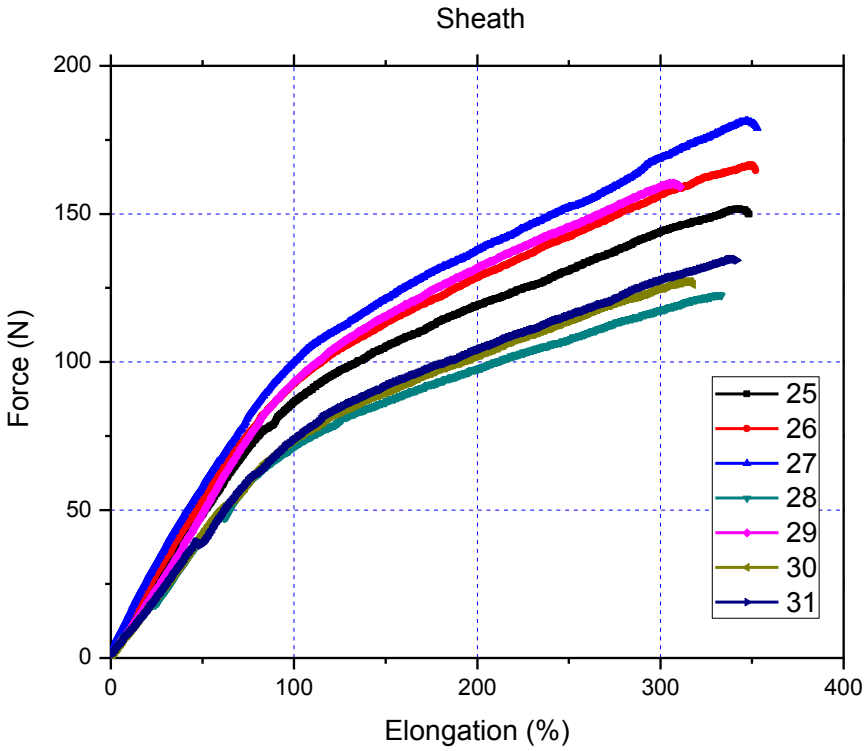

Figure A.20: Elongation of sheath aged at 10MRad

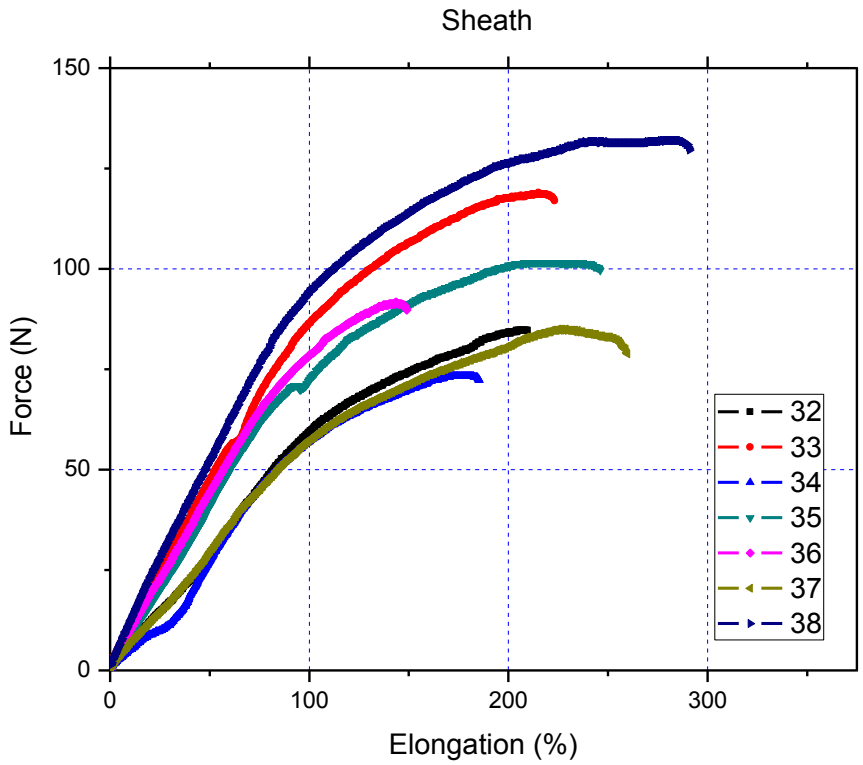

Figure A.21: Elongation of sheath aged at 25MRad

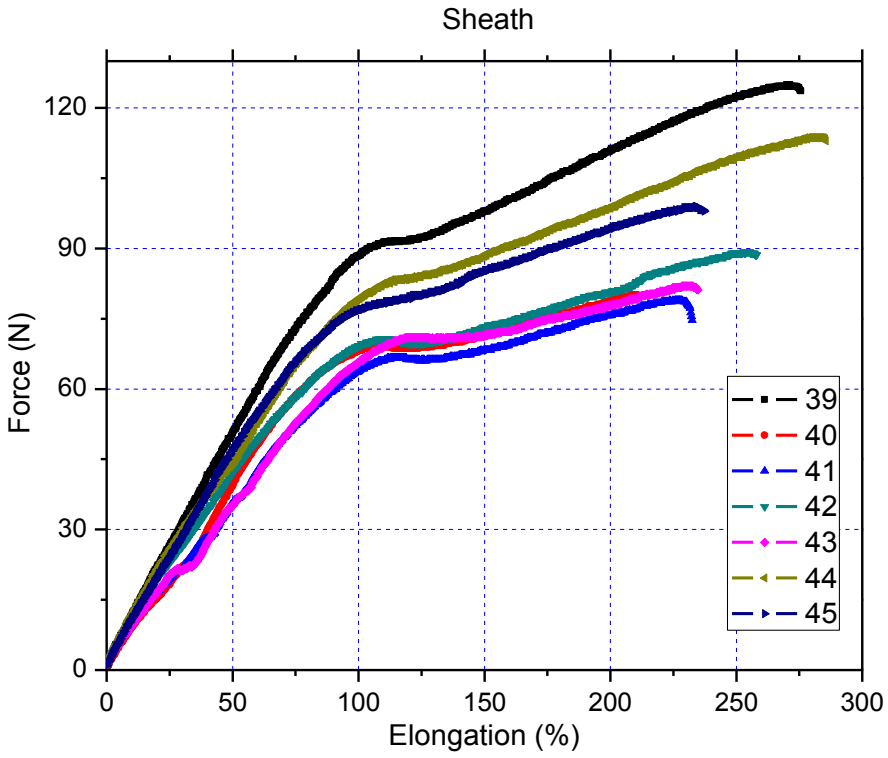

Figure A.22: Elongation of sheath aged at 50MRad

A.3 Infrared spectroscopy

A.3.1 Infrared spectra of insulation

The infrared spectra obtained from FTIR spectroscopy for insulation material are shown in Figures A.23-A.27.

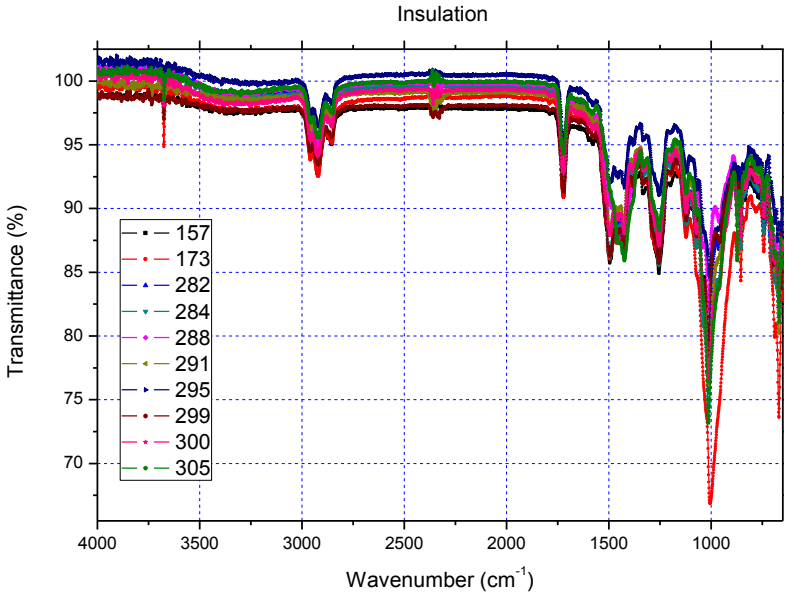

Figure A.23: Baseline spectra of insulation

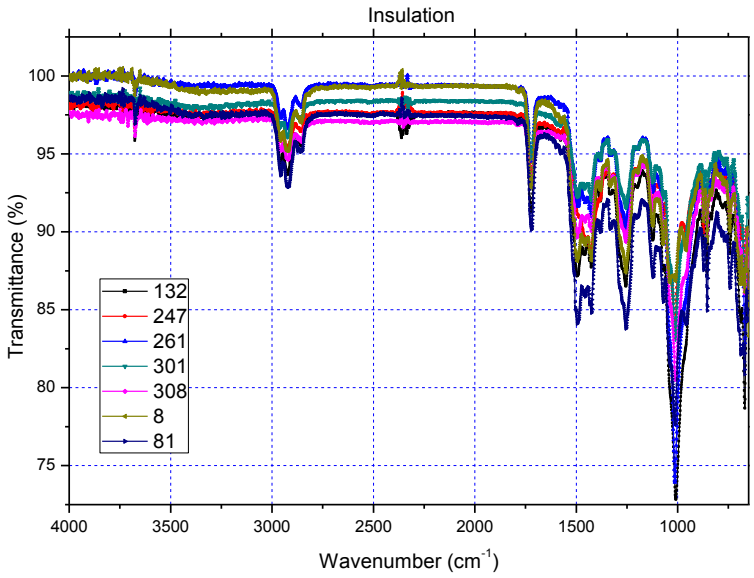

Figure A.24: Spectra of insulation aged at 5MRad

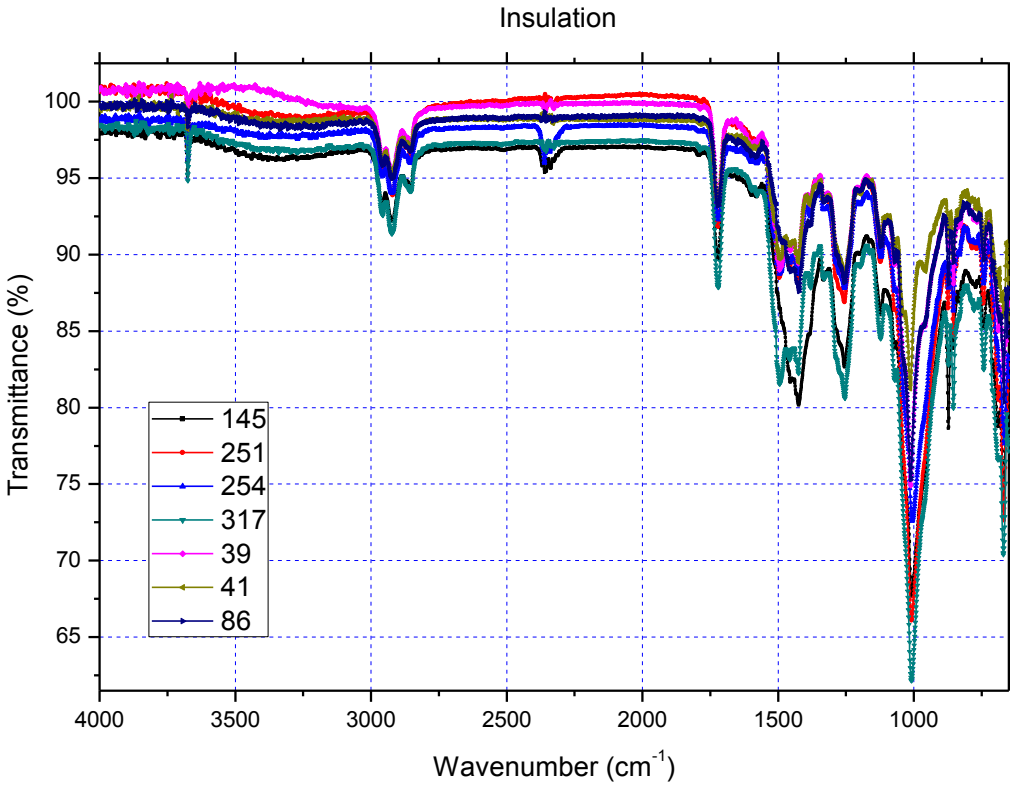

Figure A.25: Spectra of insulation aged at 10MRad

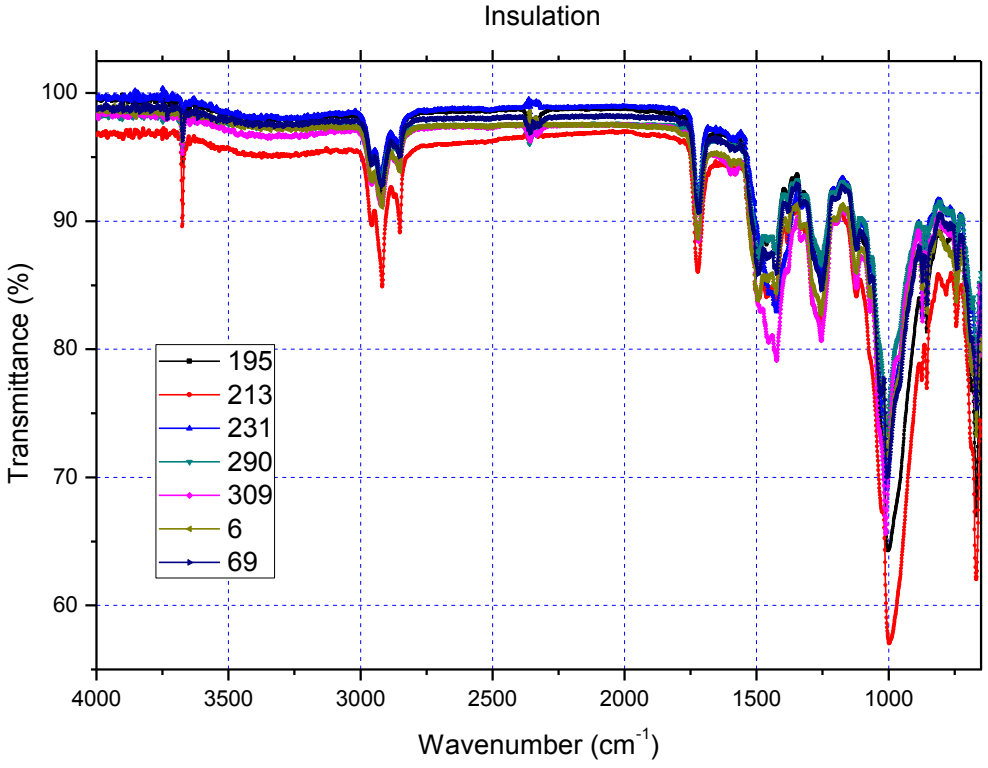

Figure A.26: Spectra of insulation aged at 25MRad

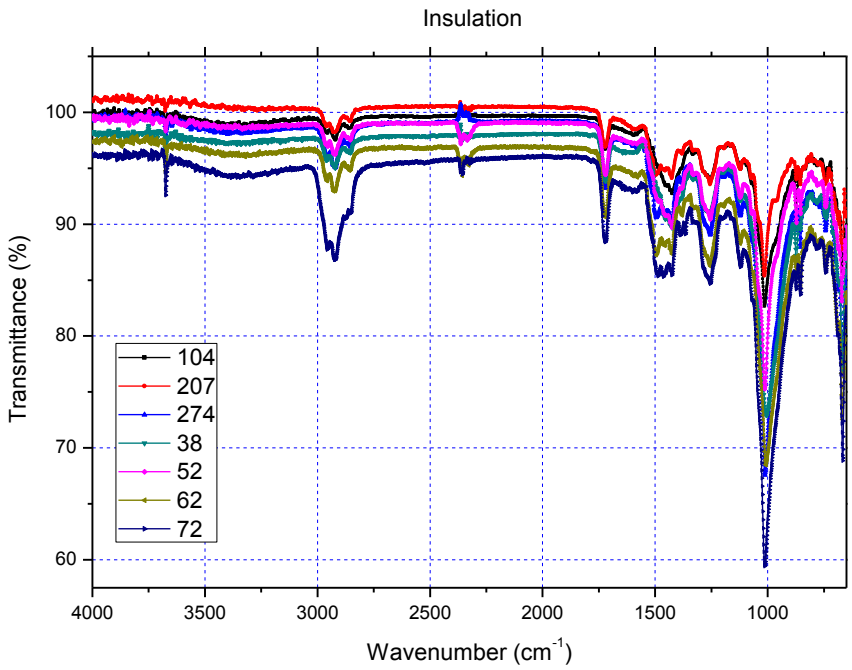

Figure A.27: Spectra of insulation aged at 50MRad

A.3.2 Infrared spectra of sheath

The Infrared spectra obtained from FTIR spectroscopy for sheath material are shown in following Figures A.28-A.32.

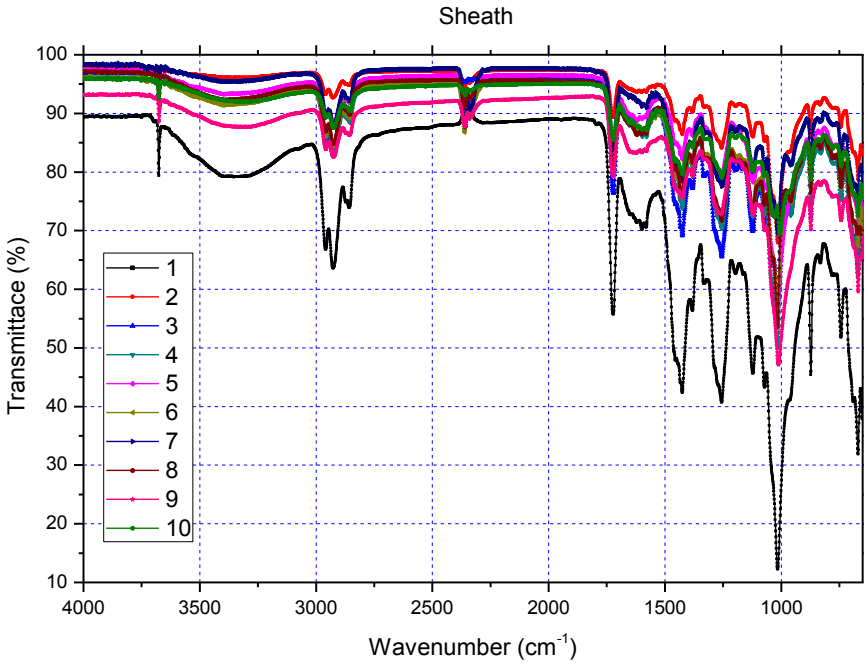

Figure A.28: Baseline spectra of sheath

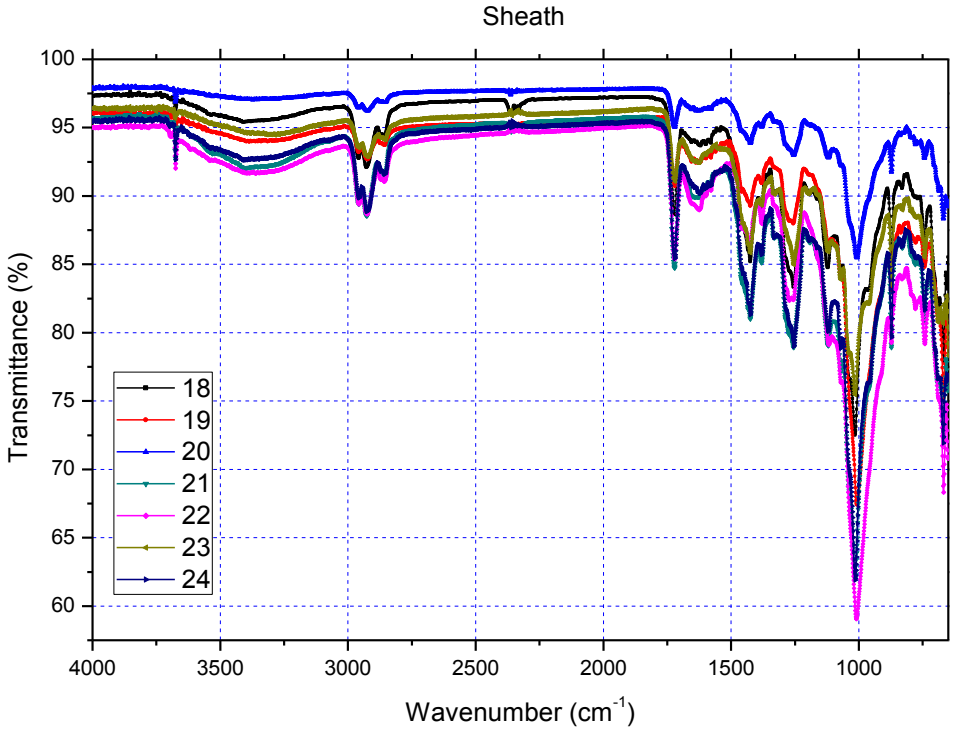

Figure A.29: Spectra of sheath aged at 5MRad

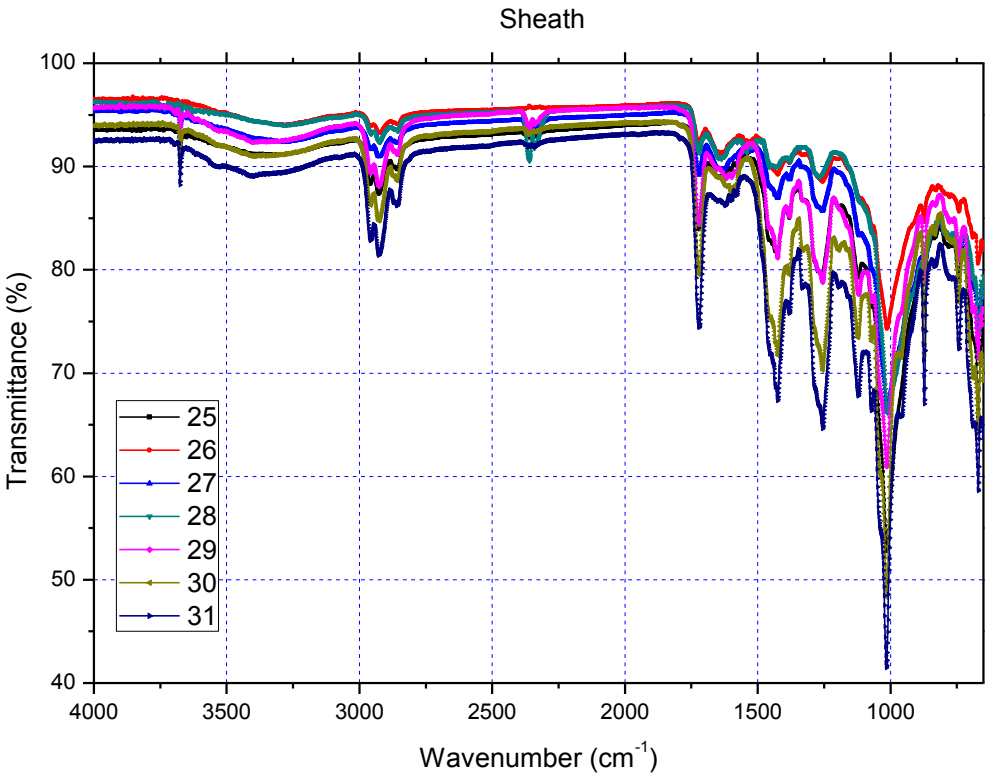

Figure A.30: Spectra of sheath aged at 10MRad

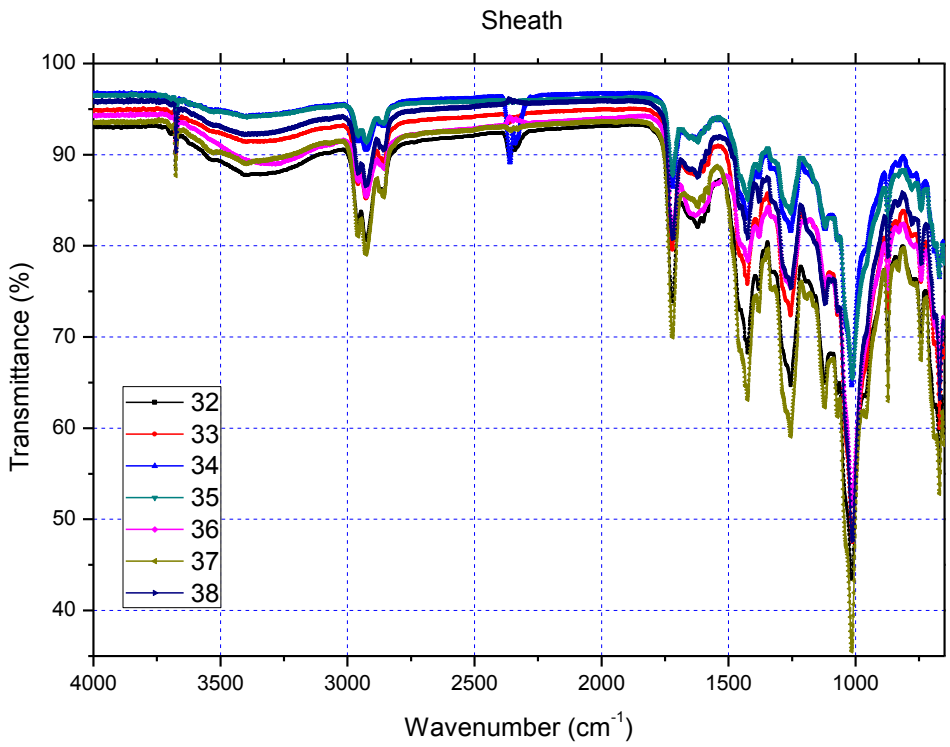

Figure A.31: Spectra of sheath aged at 25MRad

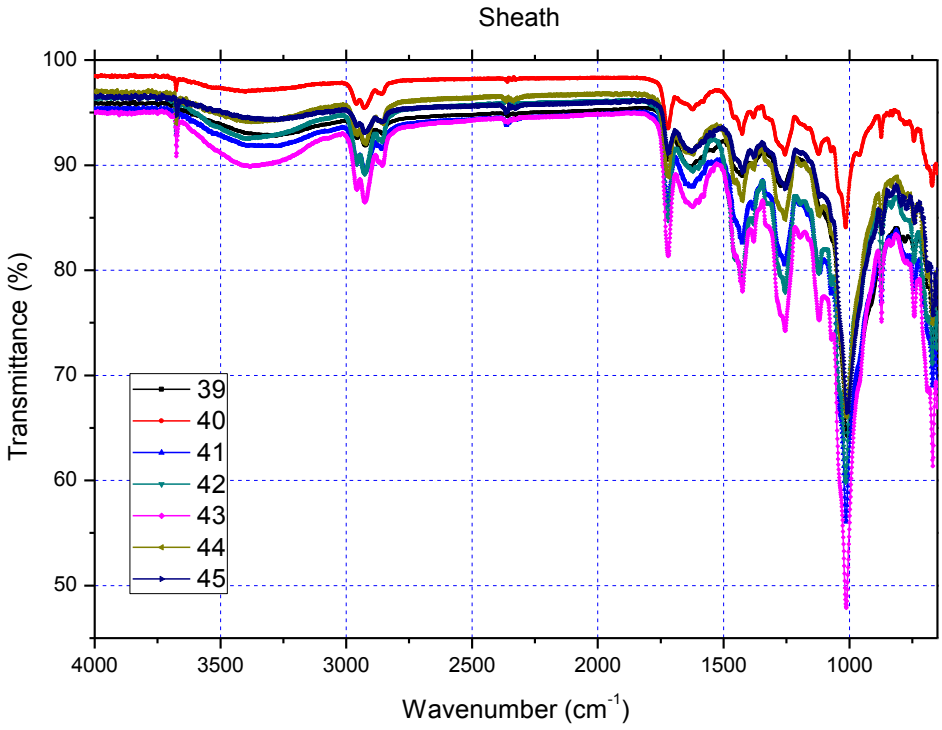

Figure A.32: Spectra of sheath aged at 50MRad

A.4 Oxidation induction time and temperature measurement

A.4.1 Calibration of DSC

The calibration of DSC on standard materials needs to be performed prior to any measurements on actual samples. The first sample to be tested is the Indium or Tin reference material as recommended by ASTM D3895-07 standard. In this study, Indium has been used as a reference material for calibration of DSC131. The recommended heating cycle for Indium is as follows: Nitrogen atmosphere, with a gas flow rate of 50ml/min, heating rate of 10^0C/min from 120^0C to 180^0C, sample mass: ~5-10mg in sealed aluminium pan. The standard melting point of Indium is about 156.63^0C. The calibration of DSC 131 was carried out with the recommended procedure and the heat flow profile obtained for sample of mass 40mg of Indium is shown in Figure A.33.

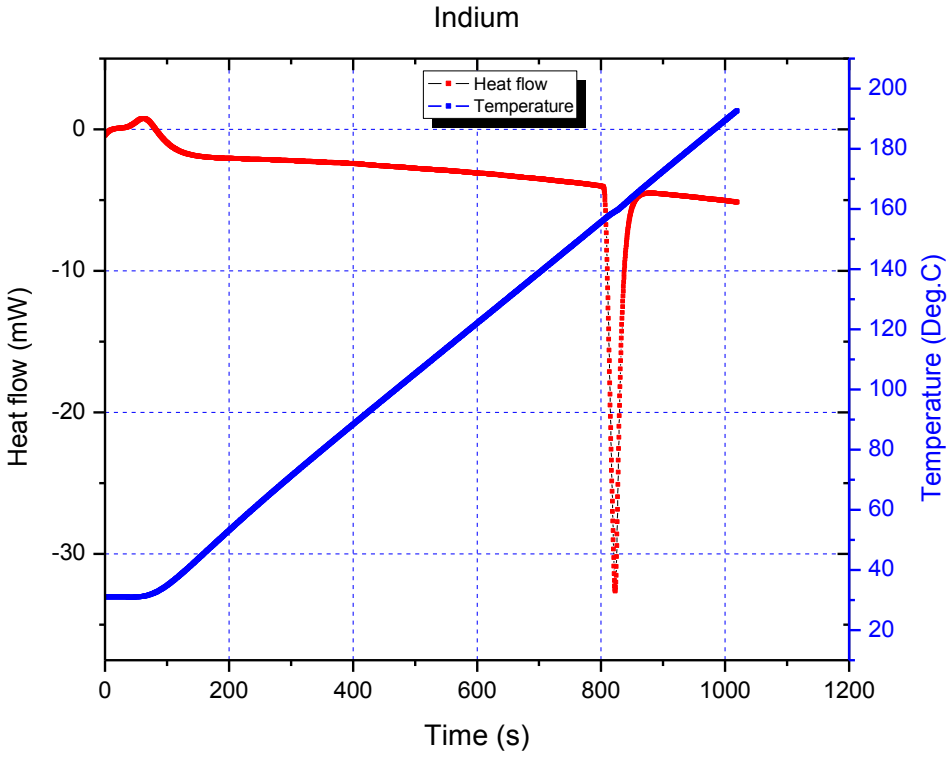

Figure A.33: Calibration signal for sample of Indium of mass 40mg

It can be seen from the calibration curve that the melting temperature of Indium obtained from DSC131 is very close to the standard melting point of Indium.

A.4.2 Determination of oxidation induction time (OIT)

Oxidation induction time (OIT) is a measure of the time at which rapid oxidation of a test material occurs when exposed to a predetermined constant test temperature in a flowing oxygen environment. It is measured with a differential scanning calorimeter (DSC), which is essentially an oven with the capabilities for very precise control and measurement of the heat energy supplied to a test sample. In the OIT test, the DSC supplies heat to a small (approximately 10 mg) sample of material that is placed in a small aluminum pan. An empty pan is placed in the heating chamber of the DSC adjacent to the pan containing the test specimen to act as a control. The difference in heat supplied to the two pans is measured and represents the heat supplied to the sample.

At the beginning of the test, the temperature of the pans is raised to the predetermined test temperature in flowing nitrogen, which takes about 20 minutes. A nitrogen purge is used initially to prevent oxidation from occurring until the test temperature is reached. When the temperature approaches the test temperature, the nitrogen is replaced by oxygen flowing at a specified rate (e.g., 50 ml/min). The OIT is the time from the start of oxygen flow to the time that rapid oxidation of the sample occurs. The onset of oxidation is manifested by the appearance of a large exothermic peak in the oxidation curve (the thermogram), which is monitored as the test progresses. Usually, at least two replicate samples are tested to assure reproducibility. ASTM Standard D3895 provides guidance on performing OIT testing. The test sequences for OIT determination is shown in Figure A.34.

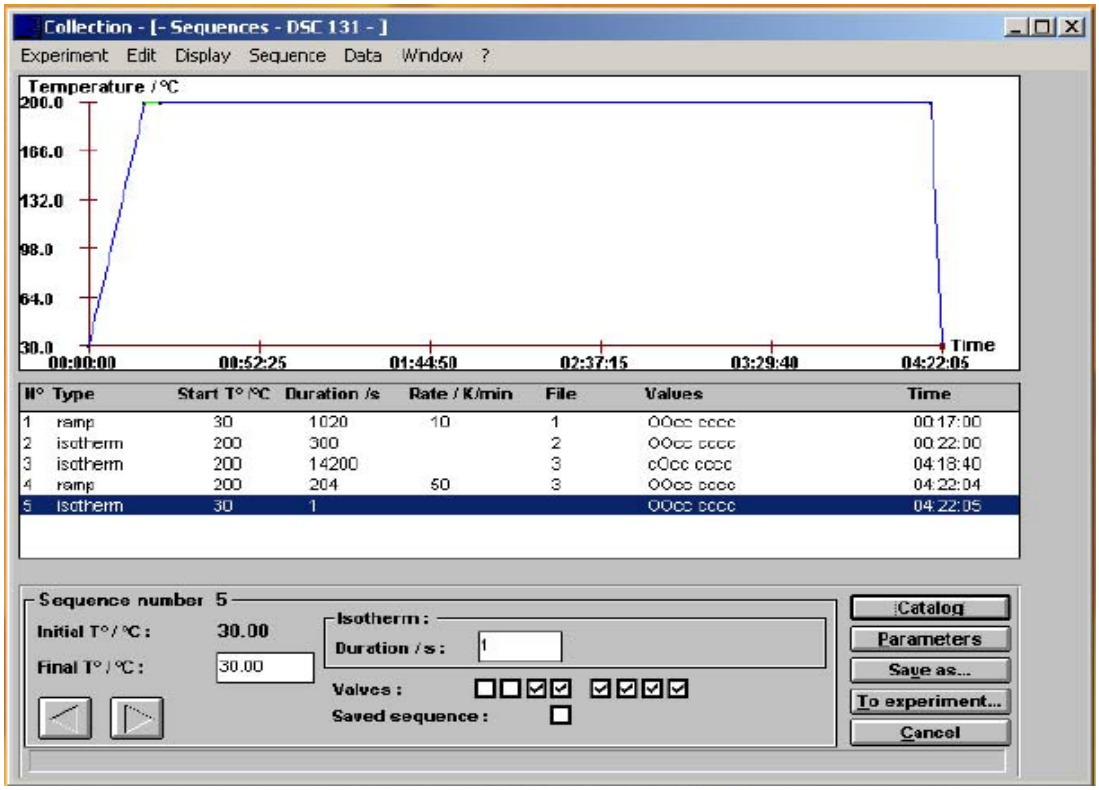

Figure A.34: Test sequence for OIT measurement

Heating and cooling cycles adopted in this study for OIT measurements are summarized below:

- Heating from ambient to 200^{0}C at 10^{0}C/min under nitrogen atmosphere
- Isothermal for about 5min under nitrogen atmosphere
- Isothermal till oxidation under oxygen atmosphere
- Cooling from 200^{0}C to ambient under nitrogen atmosphere

OIT measurements were carried out in the range from 180^{0}C to 220^{0}C, and up to 8 hours on fresh and thermally aged polymeric samples. The DSC output profiles for various samples with and without thermal ageing are shown in Figures A.35-A.37. The yellow curve in Figures A.35 is the heat flow in the sample during heating.

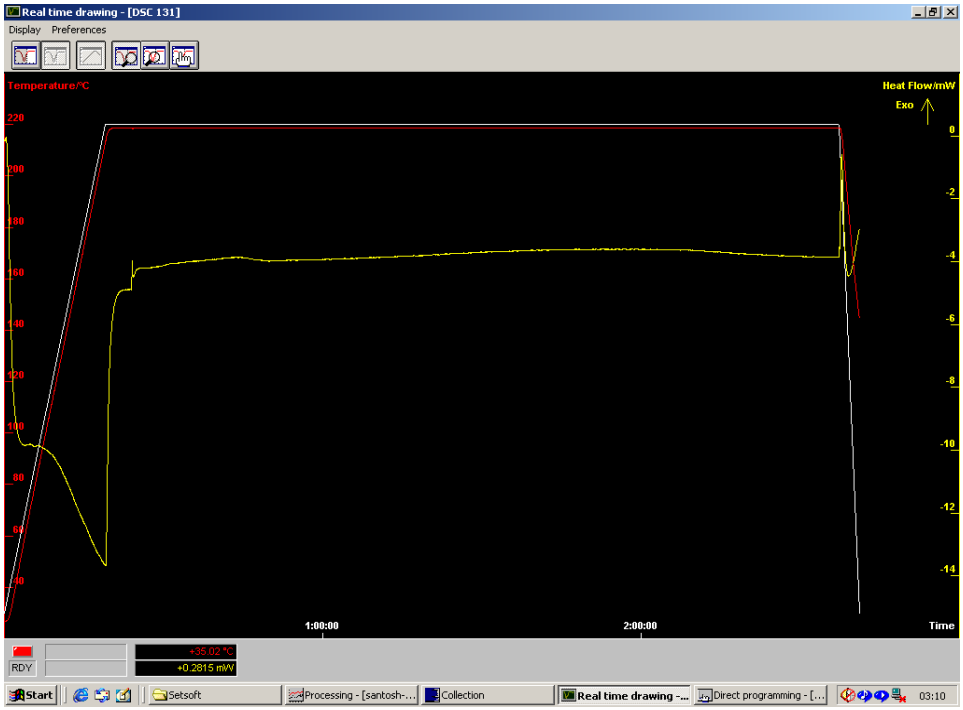

Figure A.35: DSC scan for a baseline sample of mass 13.97mg

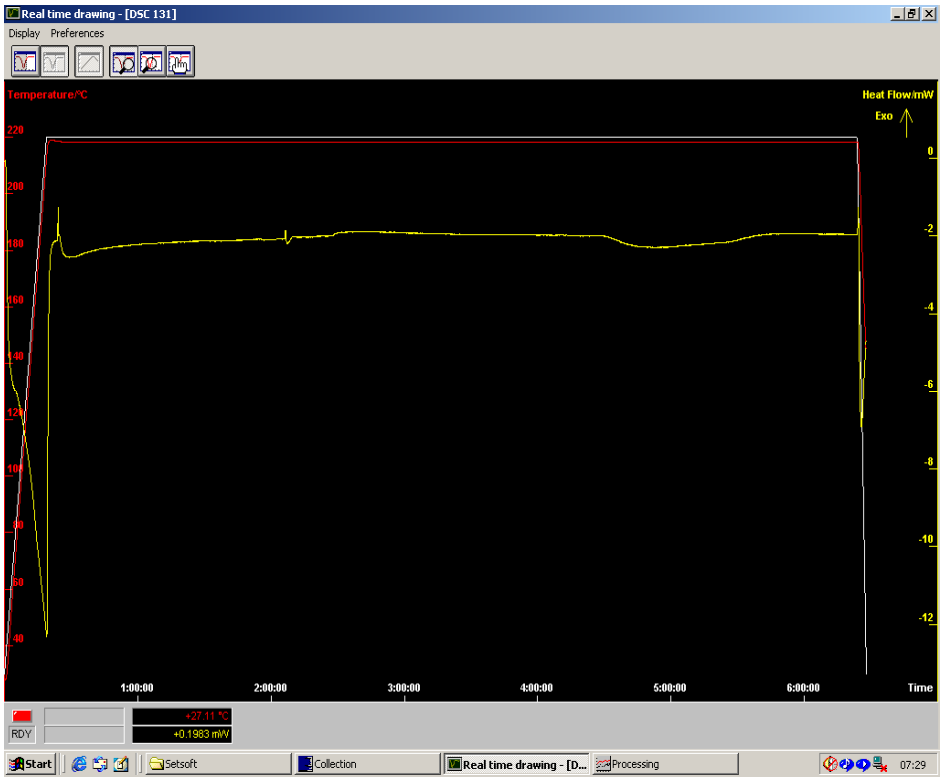

Figure A.36: DSC scan for 22 days of ageing at 110^0C with a sample of mass 8.93mg

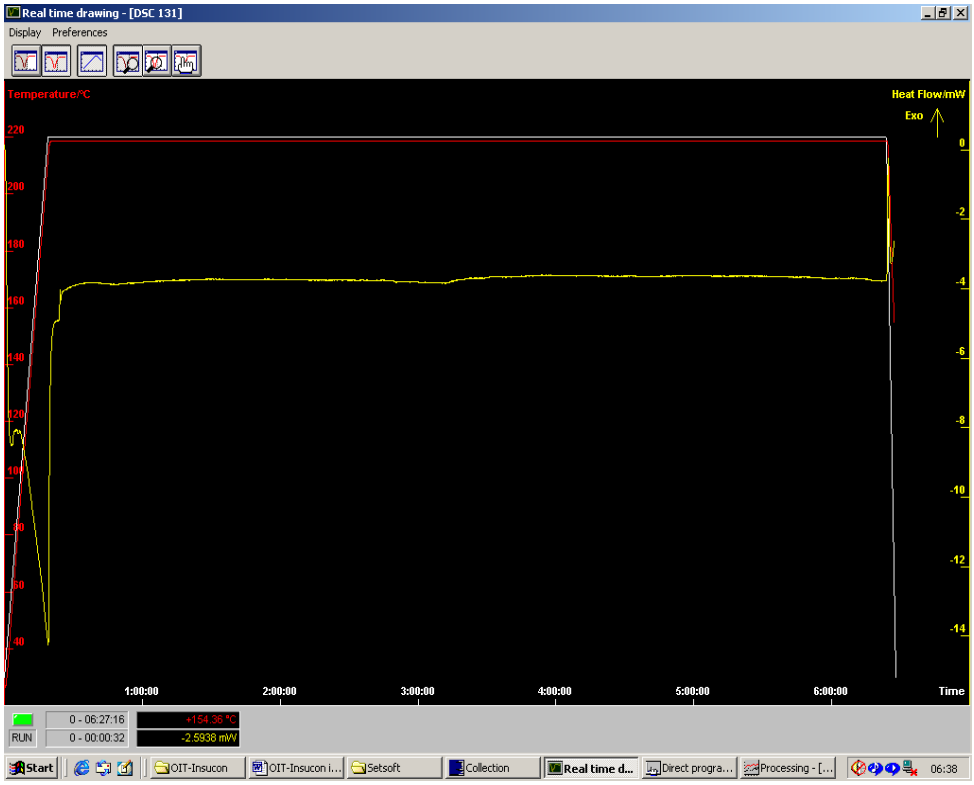

Figure A.37: DSC scan for 36 days of ageing at 110^0C with a sample of mass 10.84mg

It is evident from the OIT curves that it was difficult to determine/identify the exact onset oxidation point (exothermic reaction) from DSC heat flow signals due to slow kinetics. In order to ensure this for the samples under study, low density polyethylene (LDPE) samples (made from base polymers) were taken and OIT measurements were carried out at an isothermal temperature of 200^0C at room temperature with different masses. The resulting DSC scans of the measurements for LDPE samples are shown in Figures A.38-A.41.

Figure A.38: DSC scan for a LDPE sample 1 of mass 22.1mg

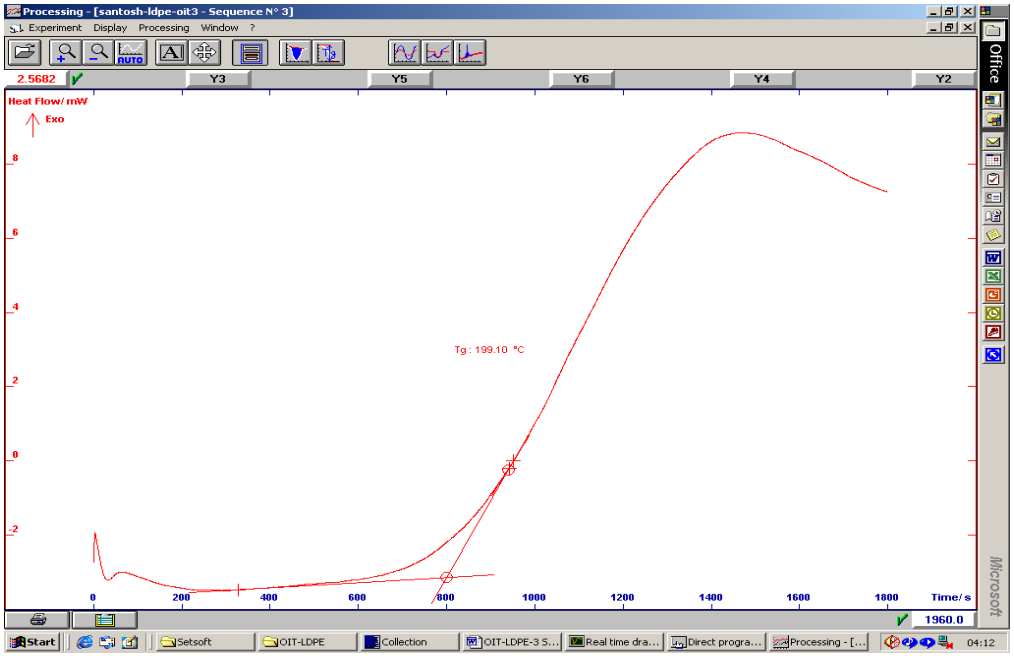

Figure A.39: OIT for LDPE sample 1 is 825 seconds

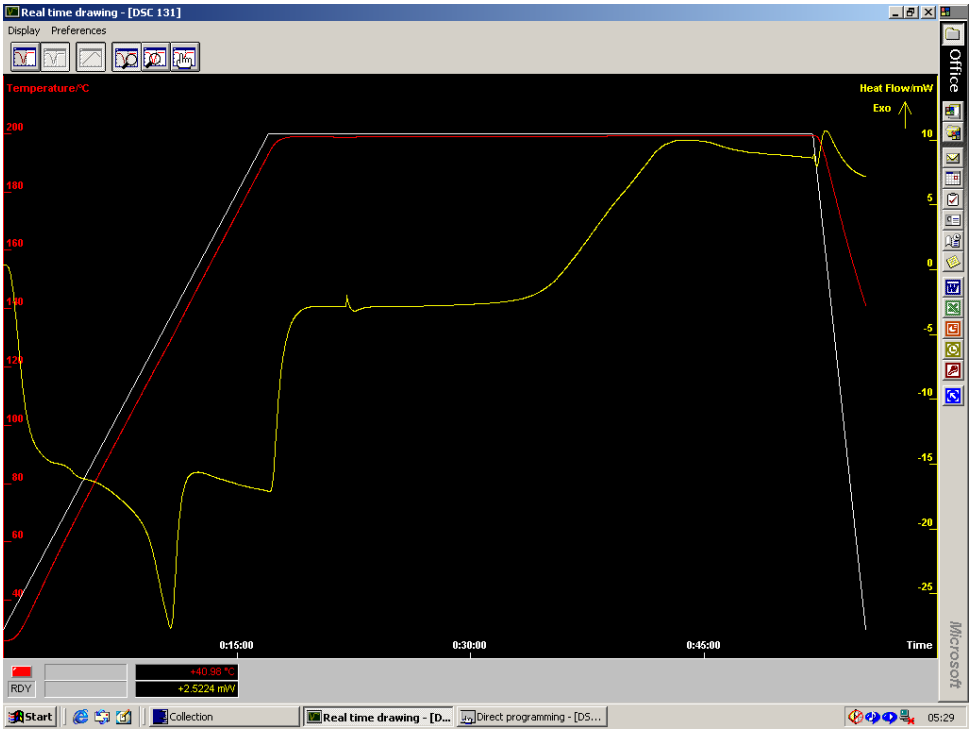

Figure A.40: DSC scan for LDPE sample 2 of mass of 22.51mg

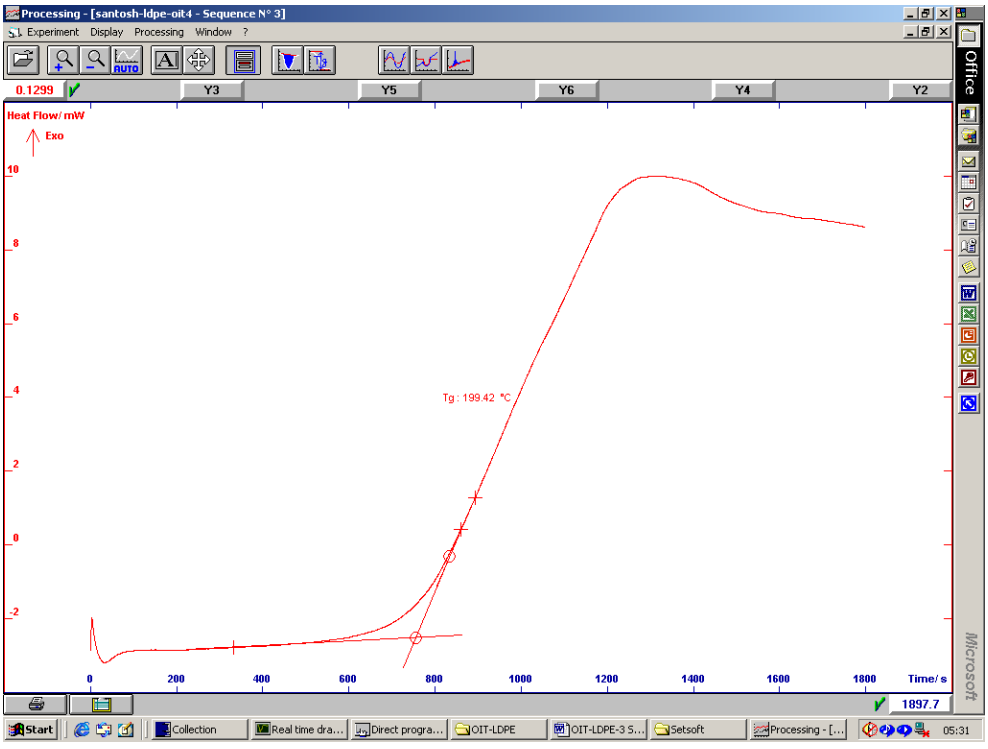

Figure A.41: OIT for LDPE sample 2 is 754 seconds

It is observed from the OIT measurements for LDPE reference samples that the exothermic reaction was unambiguously determined and an accurate OIT was obtained from

the DSC curves. Therefore, it can be concluded that the polymeric cable materials considered in this study were undergoing slow kinetics under OIT measurement. This may be due to the combined effect of many additives/anti-oxidants present in the cable materials resulting in no clear onset oxidation under isothermal condition.

Hence, in order to determine the onset oxidation point, a continuous ramp heating under oxygen atmosphere may be needed. This variation of thermal stability study of polymers is the oxidation induction temperature (OITp) measurement.

A.4.3 Determination of oxidation induction temperature (OITp)

A variation of the OIT test is the oxidation induction temperature (OITp) test, which is also measured using a DSC. In this test, the test specimen is prepared in an identical way to those for OIT. However, instead of maintaining a constant test temperature and measuring the time at which oxidation initiates, the temperature of the sample is increased at a constant specified rate (e.g., 10ºC/min) in flowing oxygen and the temperature at which oxidation initiates is recorded, which is the OITp. The onset of oxidation is usually considered to occur when the sample has become depleted of antioxidants, which allows the main polymer backbone to suffer rapid attack. This measurement will also result in determination of onset oxidation induction time (OIT) corresponding to OITp and can be used to determine the remaining useful life of polymers. The test sequences for performing OITp are shown in Figure A.42.

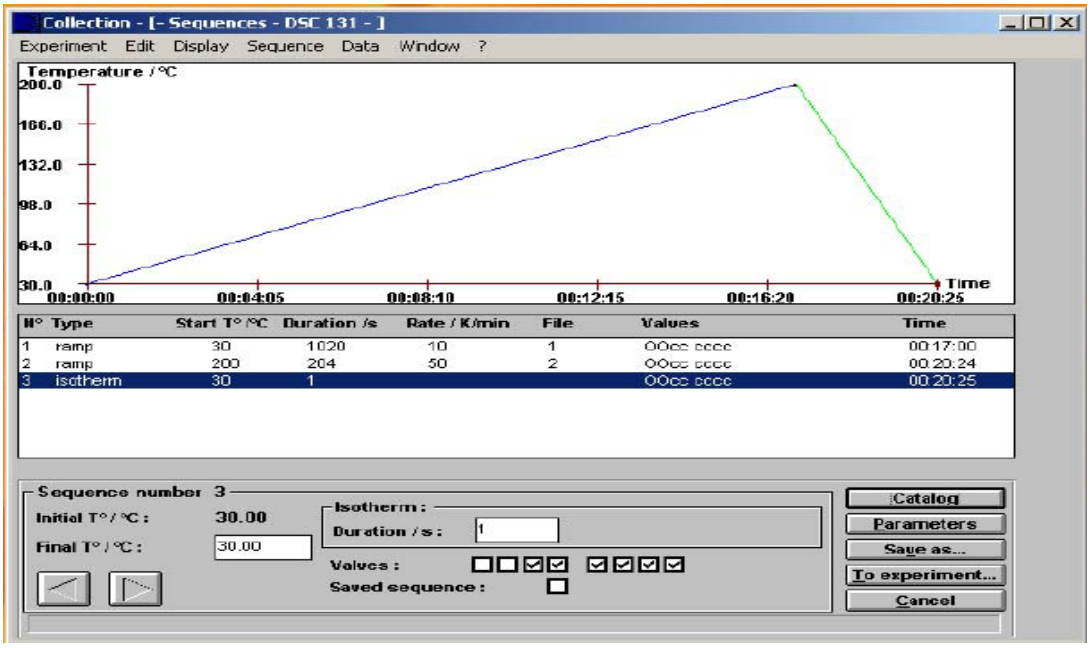

Figure A.42: Test sequences for OITp measurement

Heating and cooling cycles adopted in this study for OITp measurement are summarized below:

- Heating from ambient to above oxidation temperature (around 400^0C at 10^0C/min under oxygen atmosphere.
- Cooling from 400^0C to ambient under nitrogen atmosphere.

OITp measurements were carried out on fresh and thermally aged polymeric samples. Following are the DSC output profiles for various samples with and without thermal ageing are shown in Figures A.43-A.51.

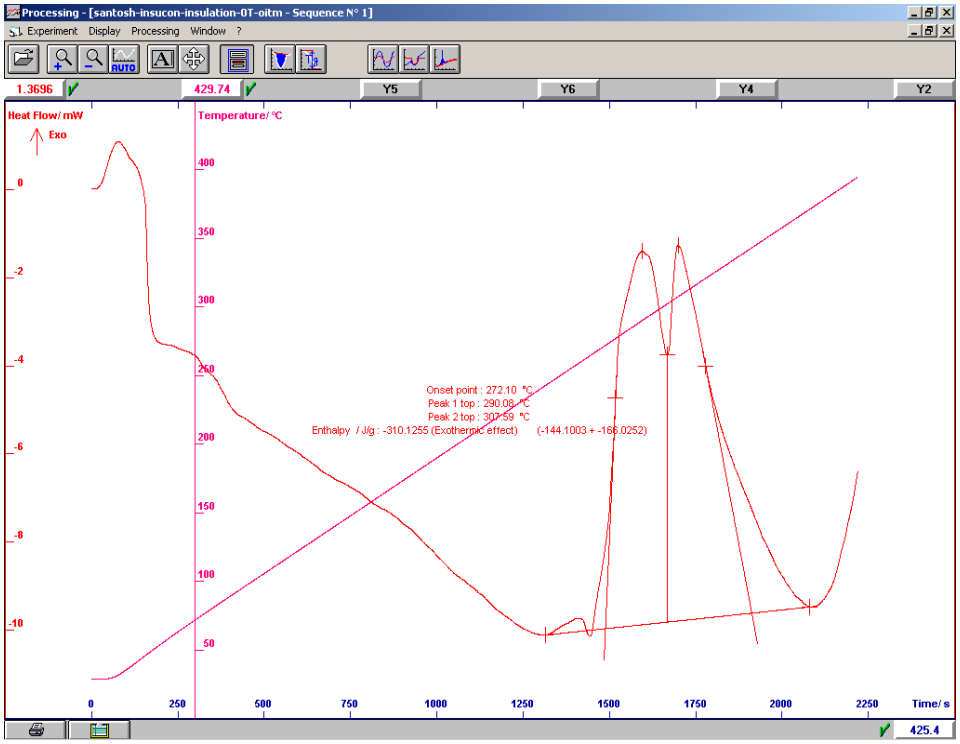

Figure A.43: DSC scan of unaged insulation

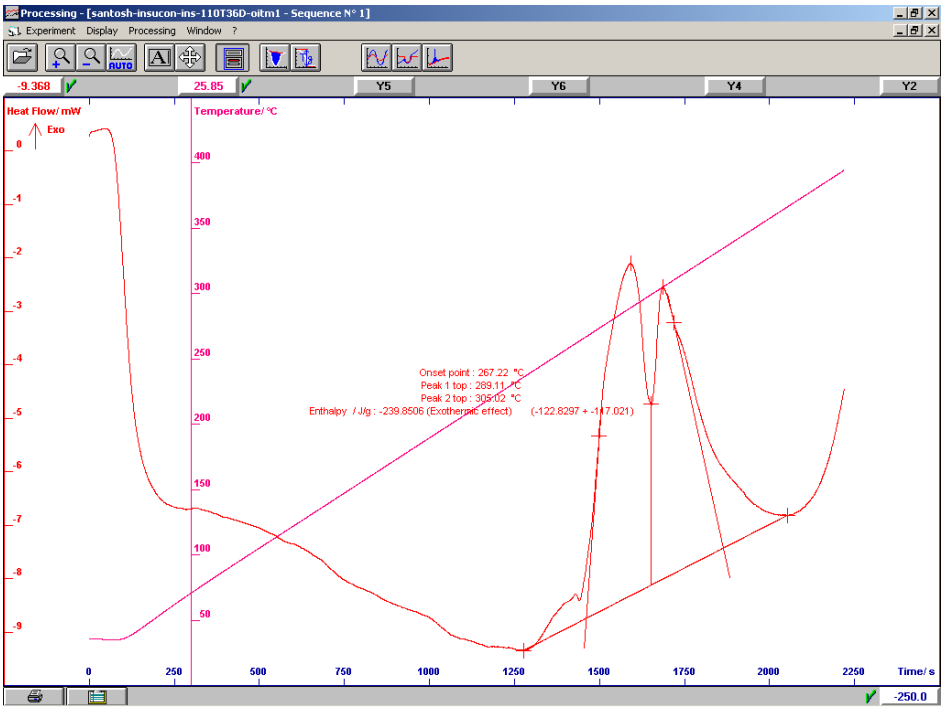

Figure A.44: DSC scan of insulation after 36 days of ageing at 110^0C

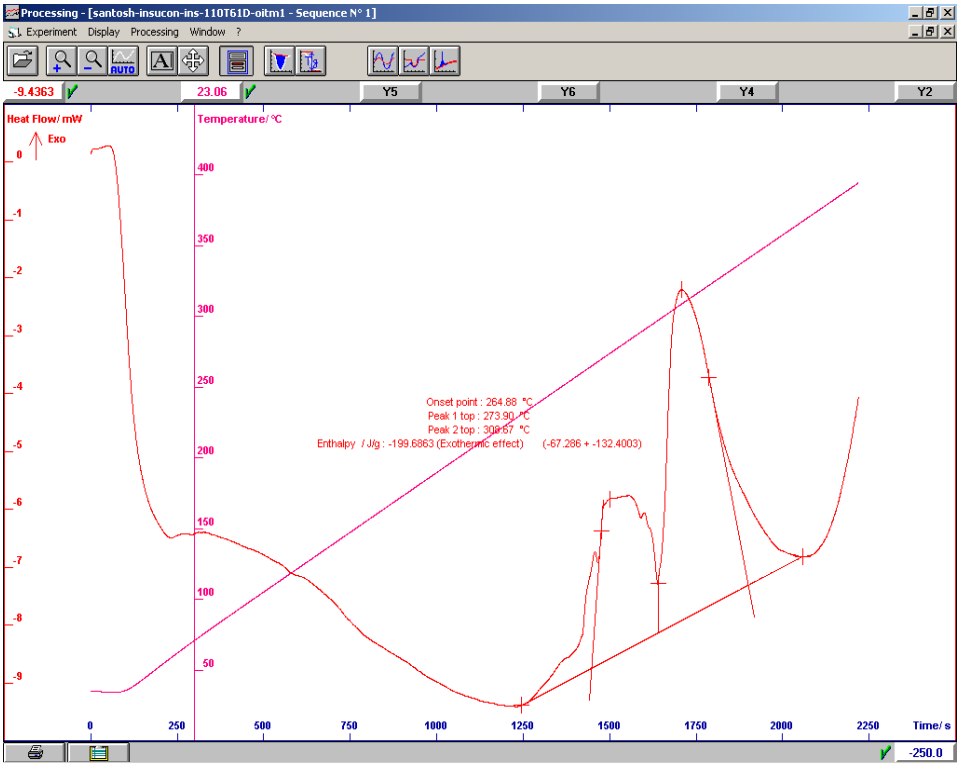

Figure A.45: DSC scan of insulation after 61 days of ageing at 110^0C

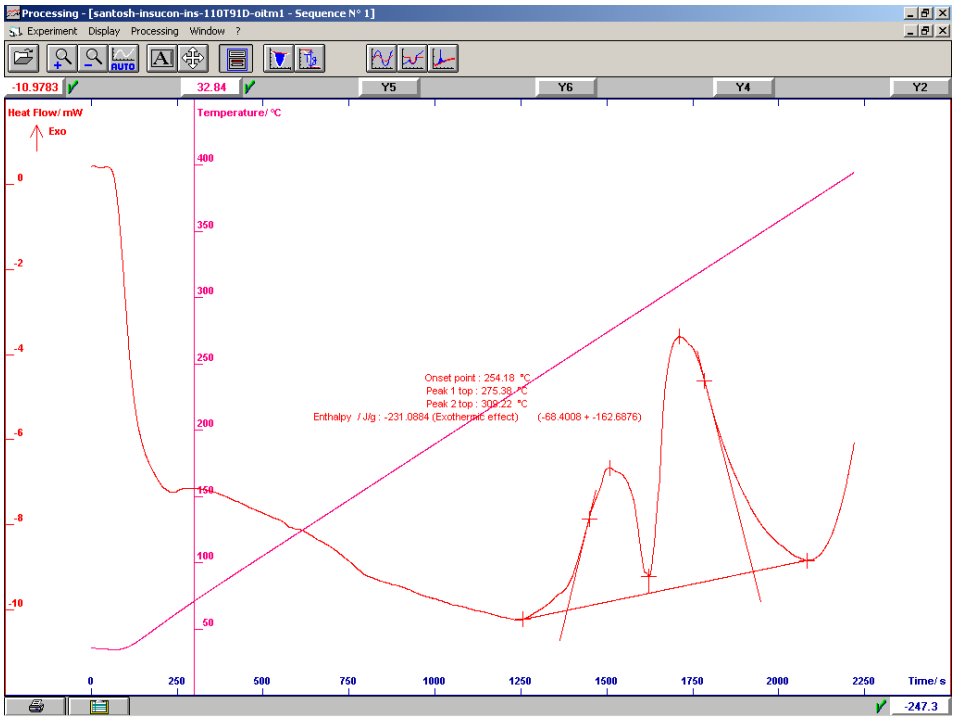

Figure A.46: DSC scan of insulation after 91 days of ageing at 110^0C

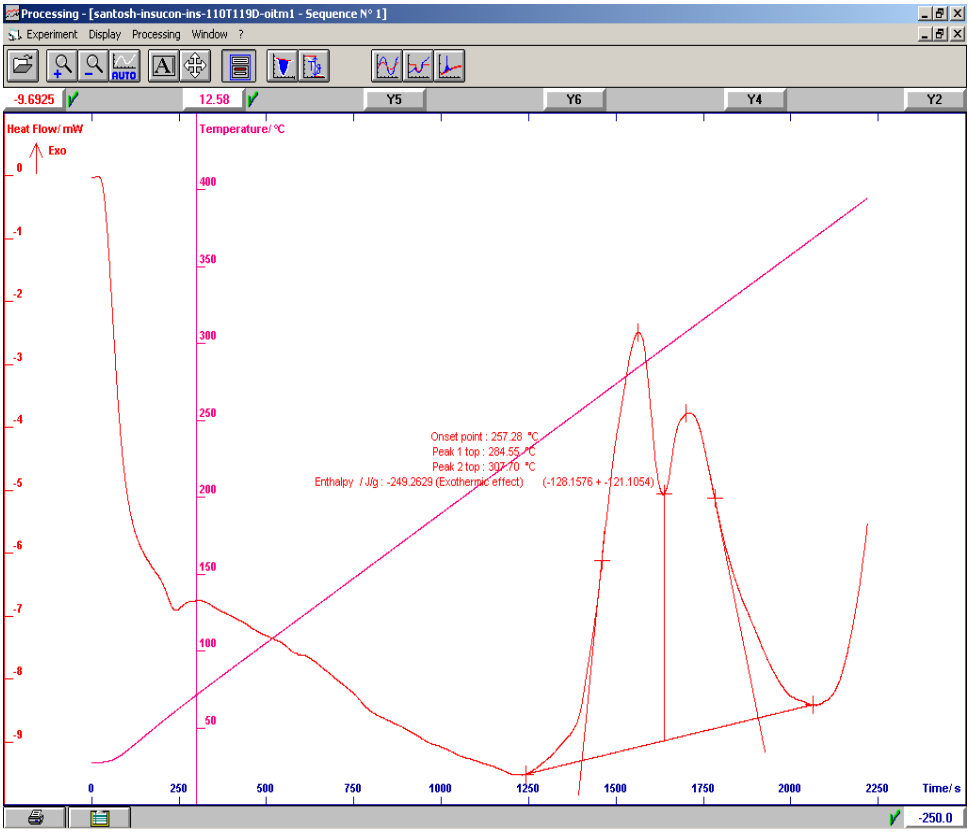

Figure A.47: DSC scan insulation after 119 days of ageing at 110^0C

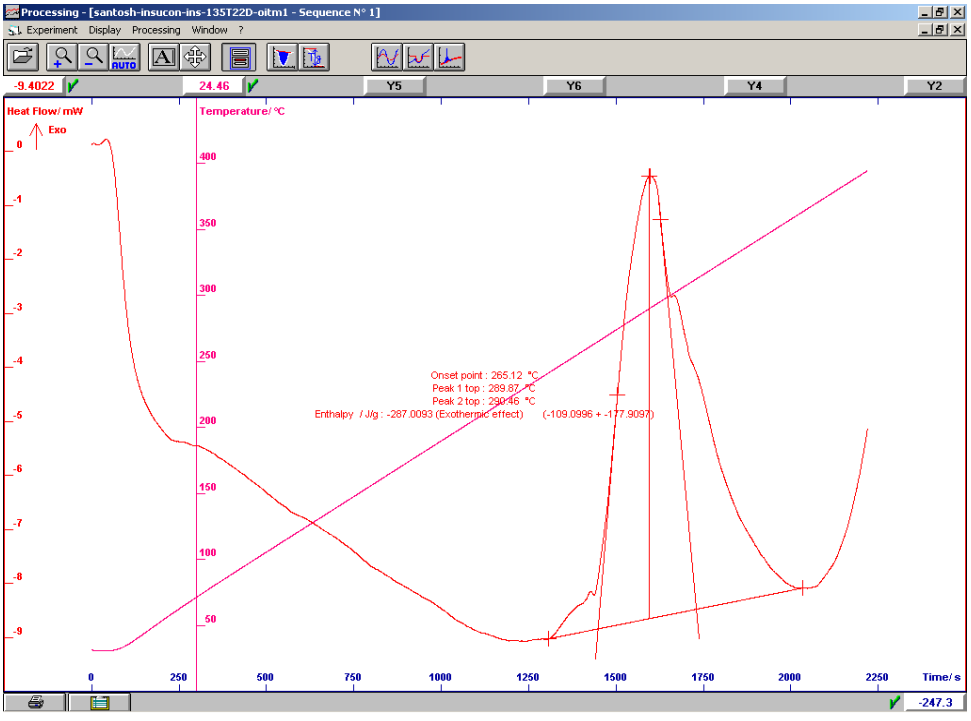

Figure A.48: DSC scan of insulation after 22 days of ageing at 135^0C

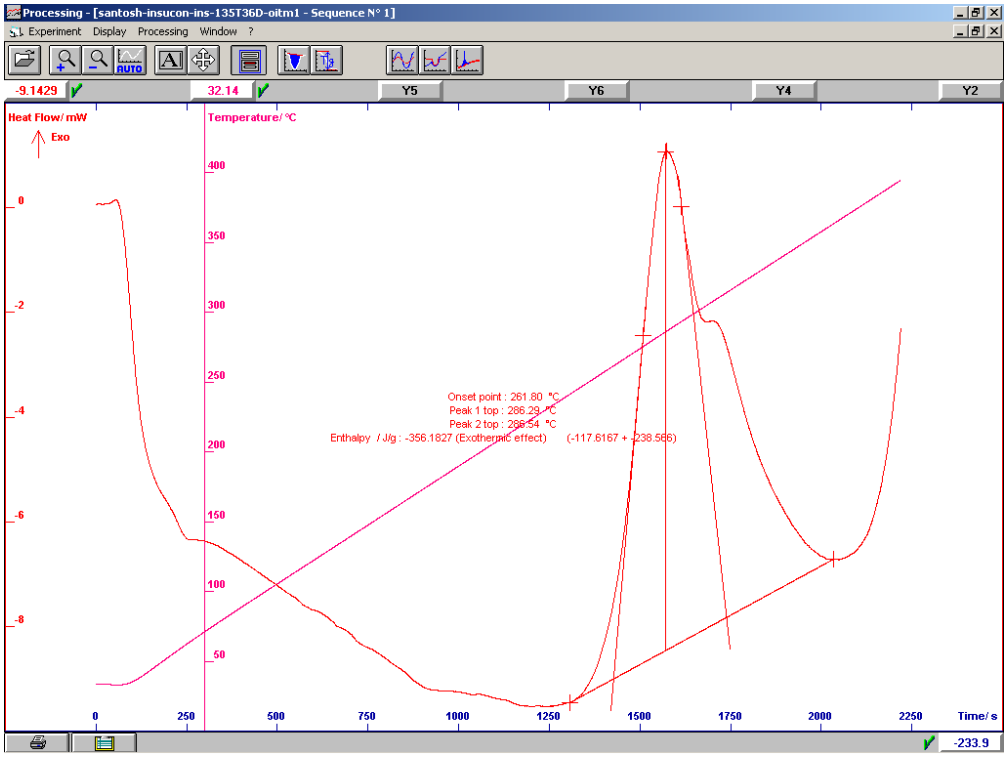

Figure A.49: DSC scan of insulation after 36 days of ageing at 135^0C

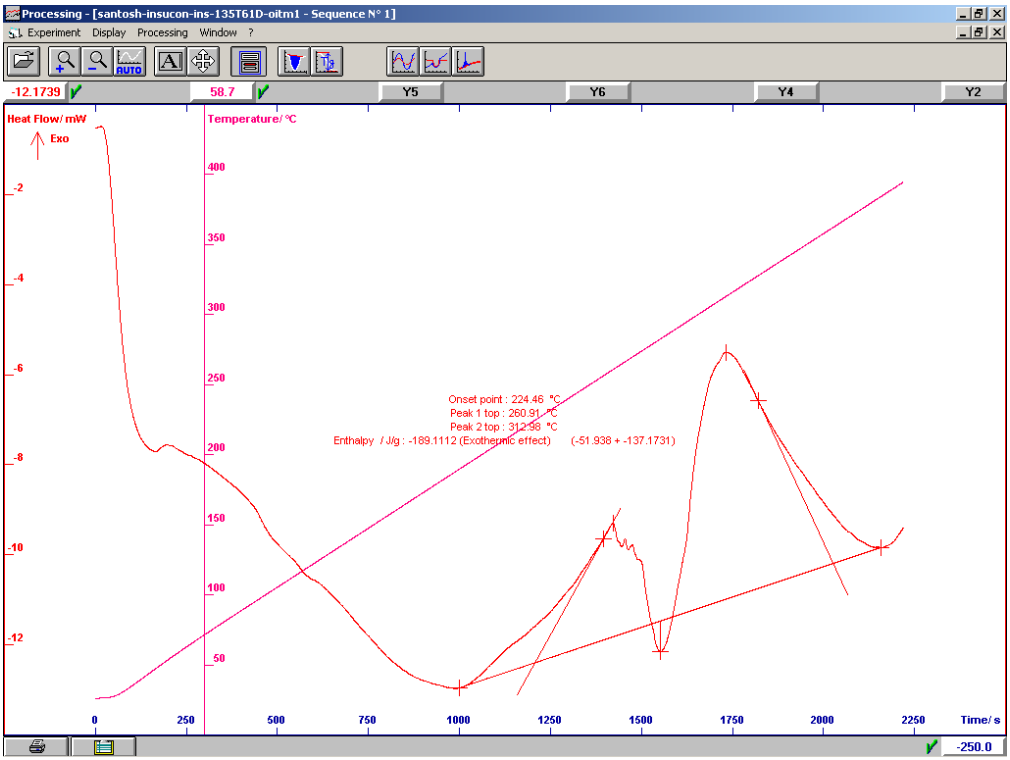

Figure A.50: DSC scan of insulation after 61 days of ageing at 135^0C

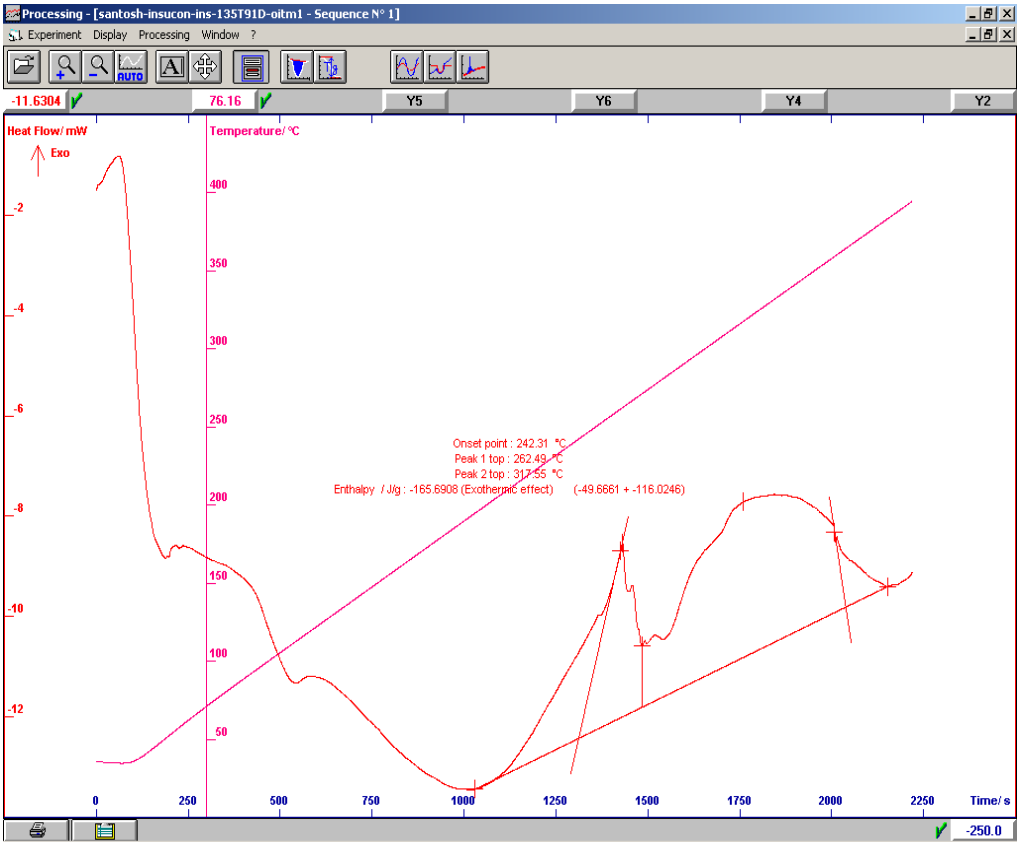

Figure A.51: DSC scan of insulation after 91 days of ageing at 135^0C

Similar DSC profiles were observed for sheath under thermal ageing and for both insulation and sheath under radiation ageing.

Appendix B. Determination of Life Distribution for Reliability Prediction

The EAB data of irradiated insulation and sheath was analysed with several probability distributions through Histograms and Probability plots. The Anderson-Darling goodness-of-fit statistic and associated p-values indicate the best fit distribution. For a better fit, the Anderson-Darling statistic will be small, and the associated p-value will be larger than a chosen confidence level. The analysis is performed with a confidence level of 95%. The results of various distributions fit for insulation and sheath are shown in the following sections.

B.1 EAB data of irradiated insulation

B.1.1 Normal distribution fit of the data

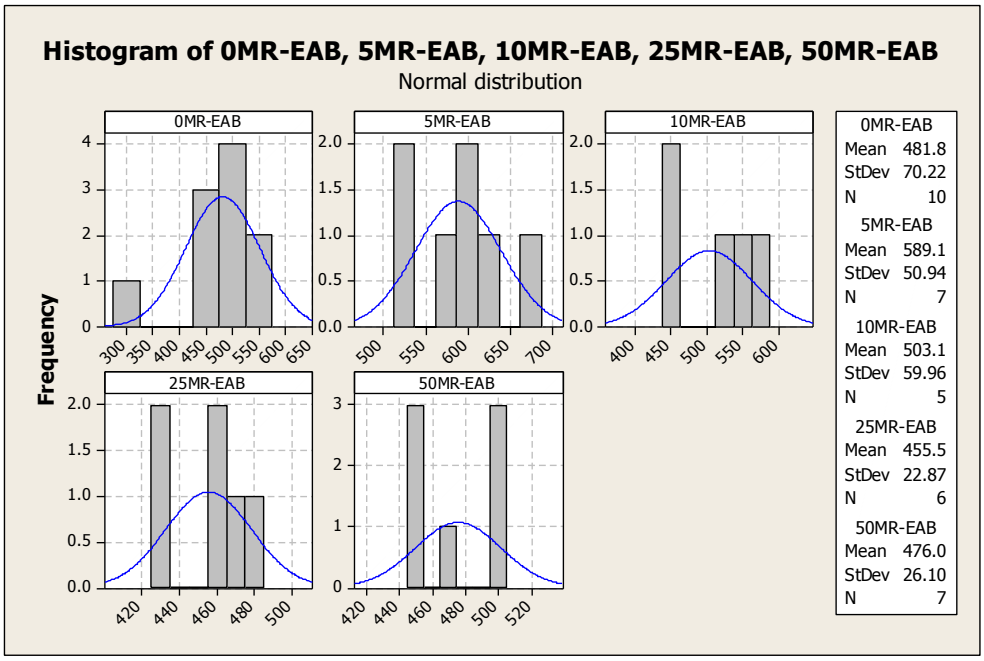

Figure B.1: Histogram of EAB data at various doses for insulation with Normal distribution

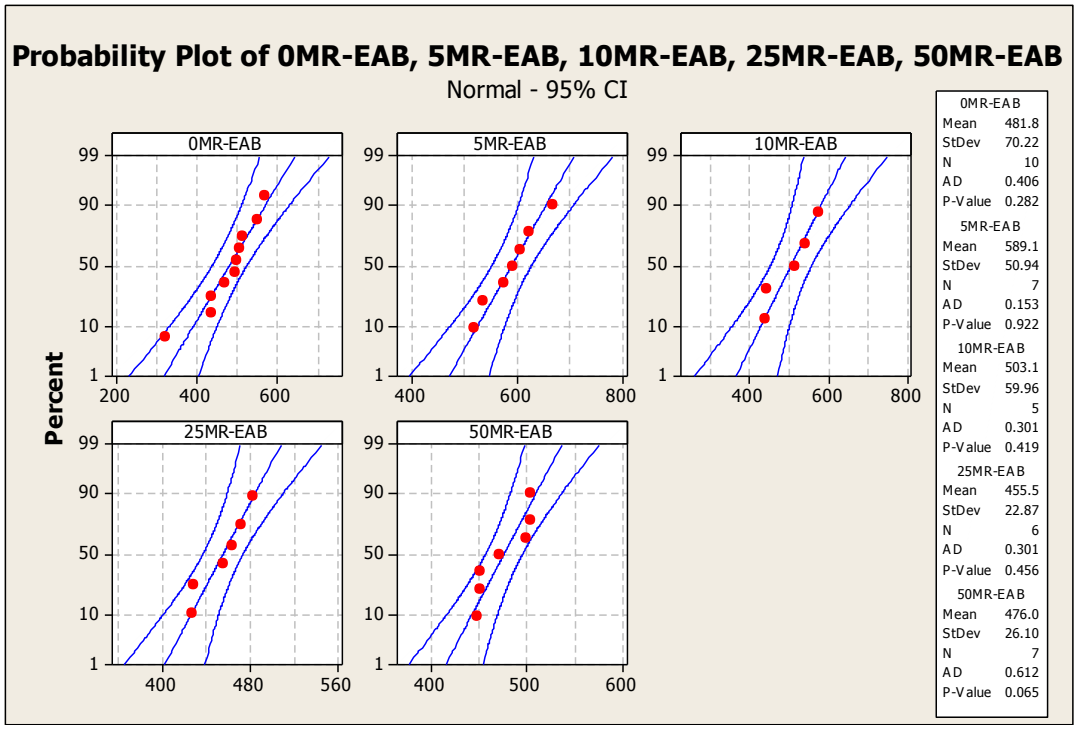

Figure B.2: Probability plot of EAB data at various doses for insulation with Normal distribution

B.1.2 Lognormal distribution fit of the data

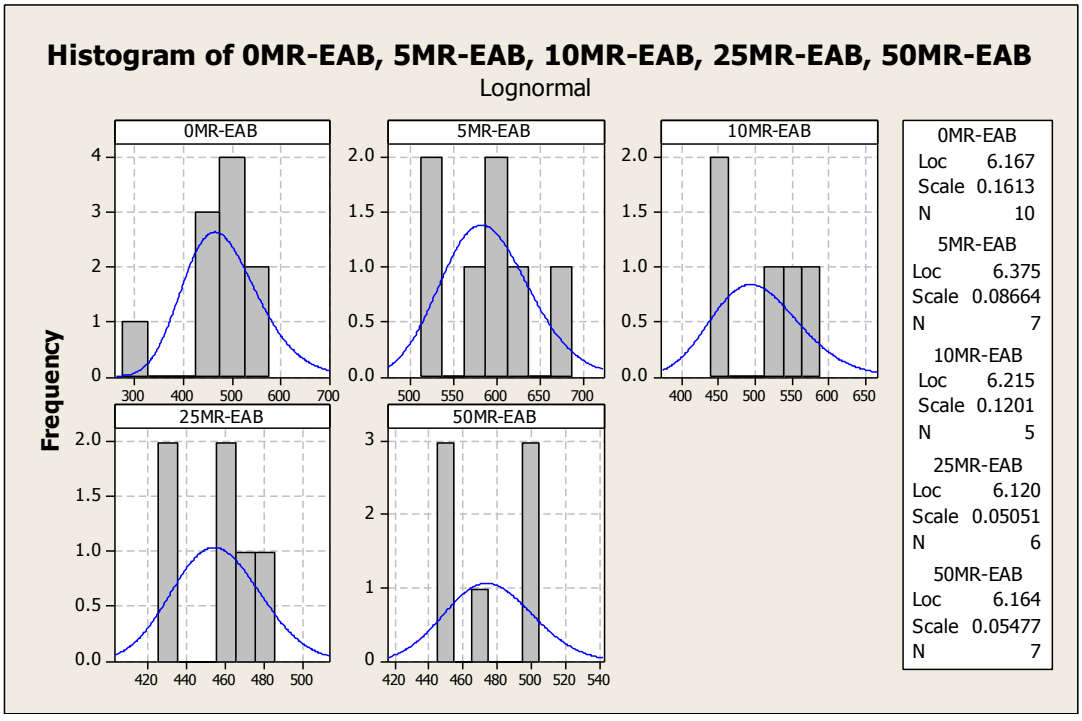

Figure B.3: Histogram of EAB data at various doses for insulation with Lognormal distribution

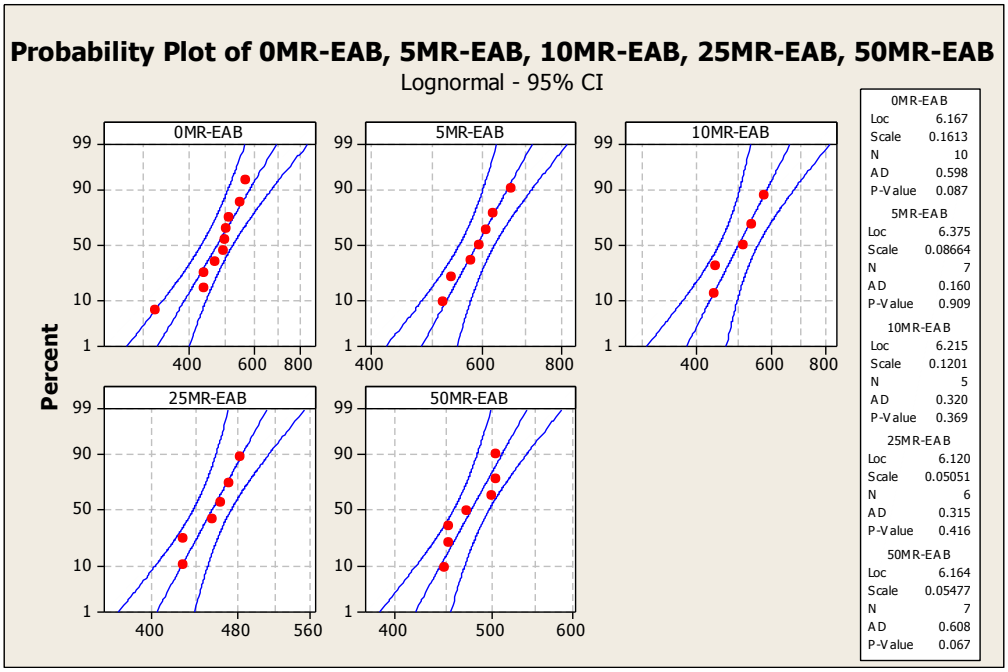

Figure B.4: Probaility plot of EAB data at various doses for insulation with Lognormal distribution

B.1.3 Smallest extreme value distribution fit of the data

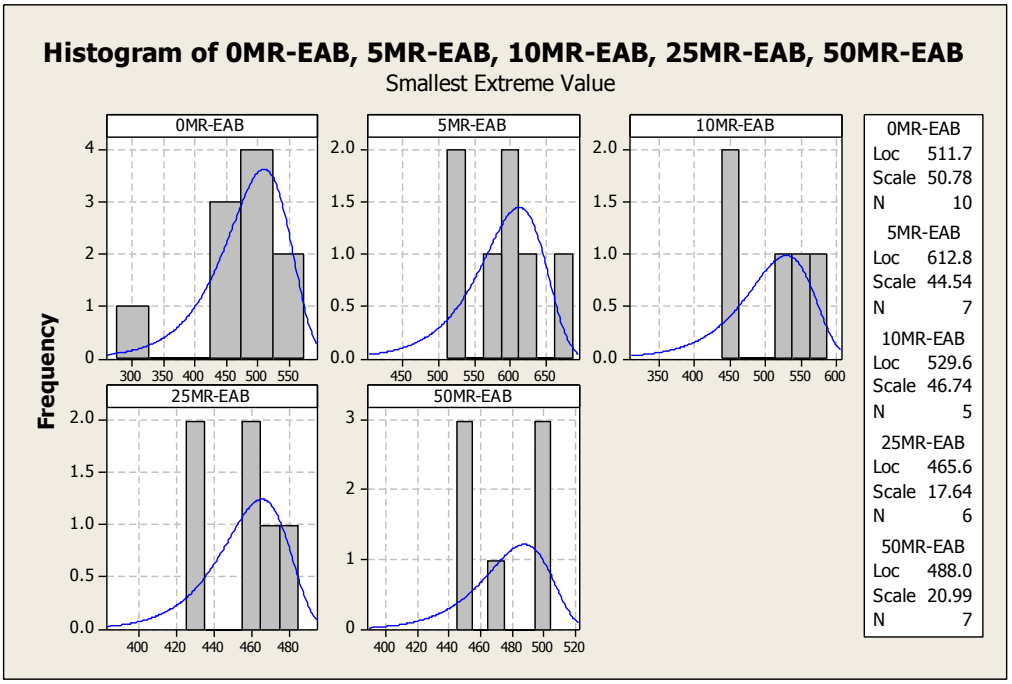

Figure B.5: Histogram of EAB data at various doses for insulation with Smallest Extreme value distribution

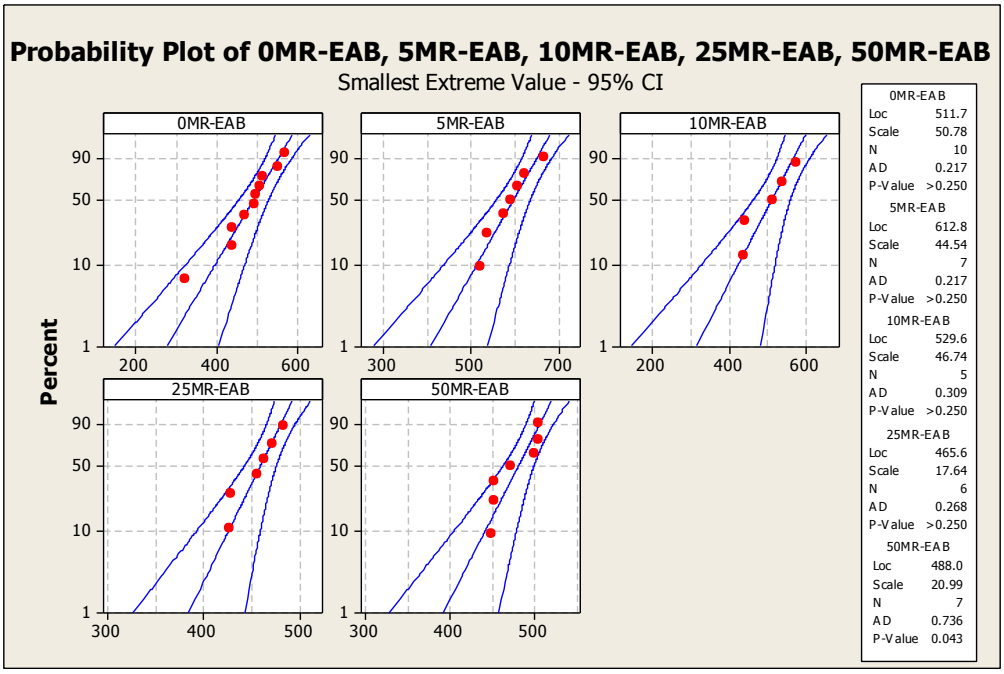

Figure B.6: Probability plot of EAB data at various doses for insulation with Smallest Extreme value distribution

B.1.4 Weibull distribution fit of the data

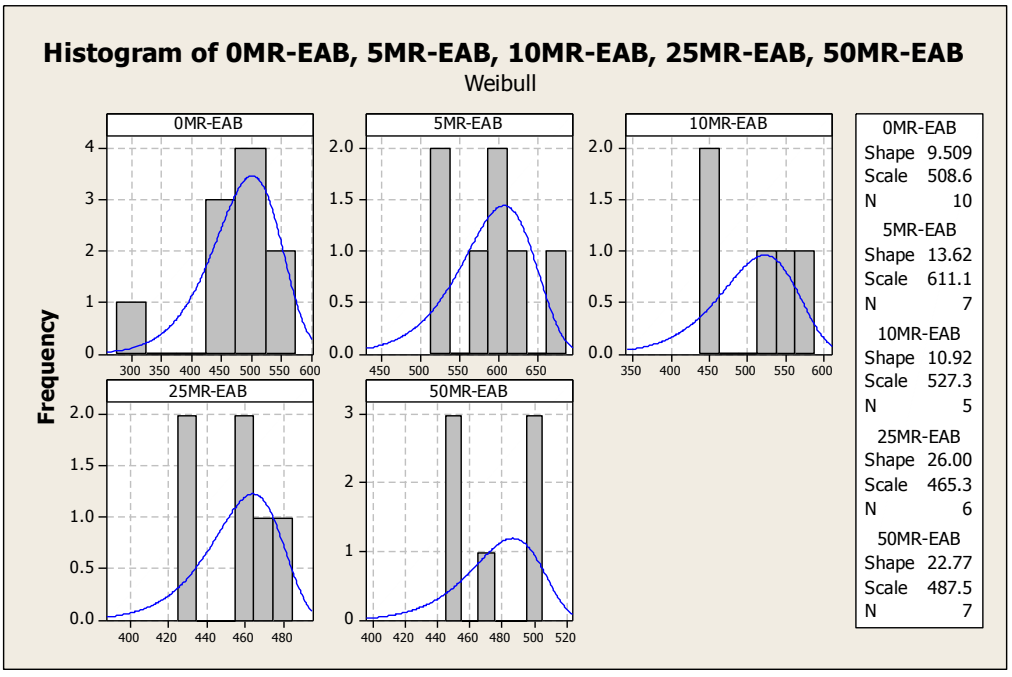

Figure B.7: Histogram of EAB data at various doses for insulation with Weibull distribution

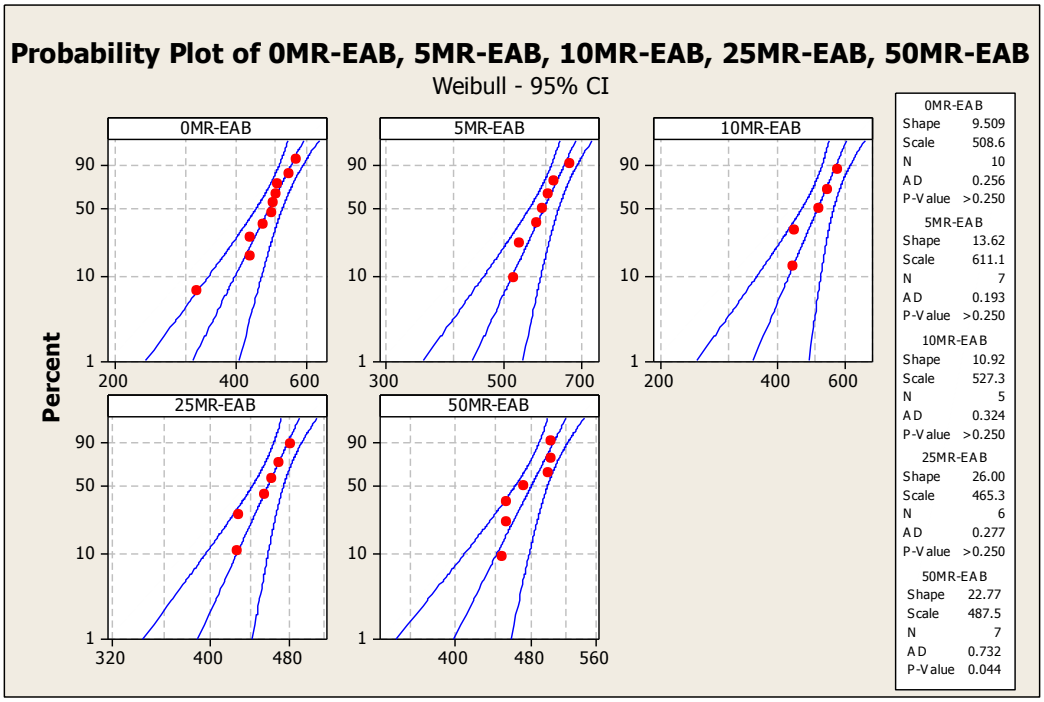

Figure B.8: Proability plot of EAB data at various doses for insulation with Weibull distribution

B.1.5 3-Parameter Weibull distribution fit of the data

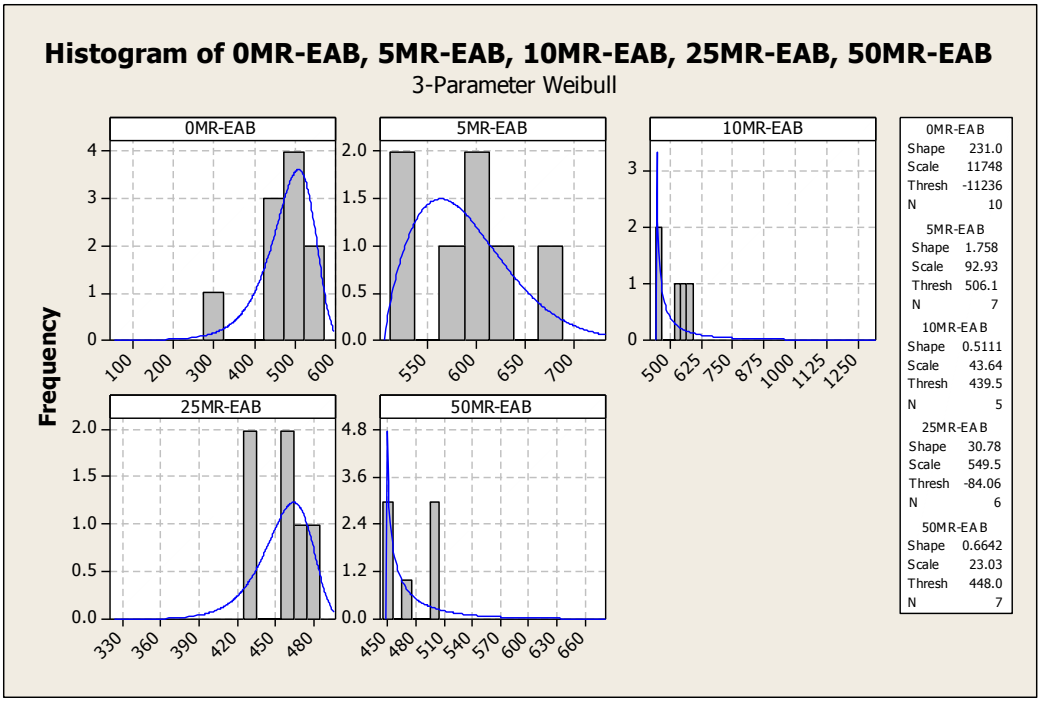

Figure B.9: Histogram of EAB data at various doses for insulation with 3-Parameter weibull distribution

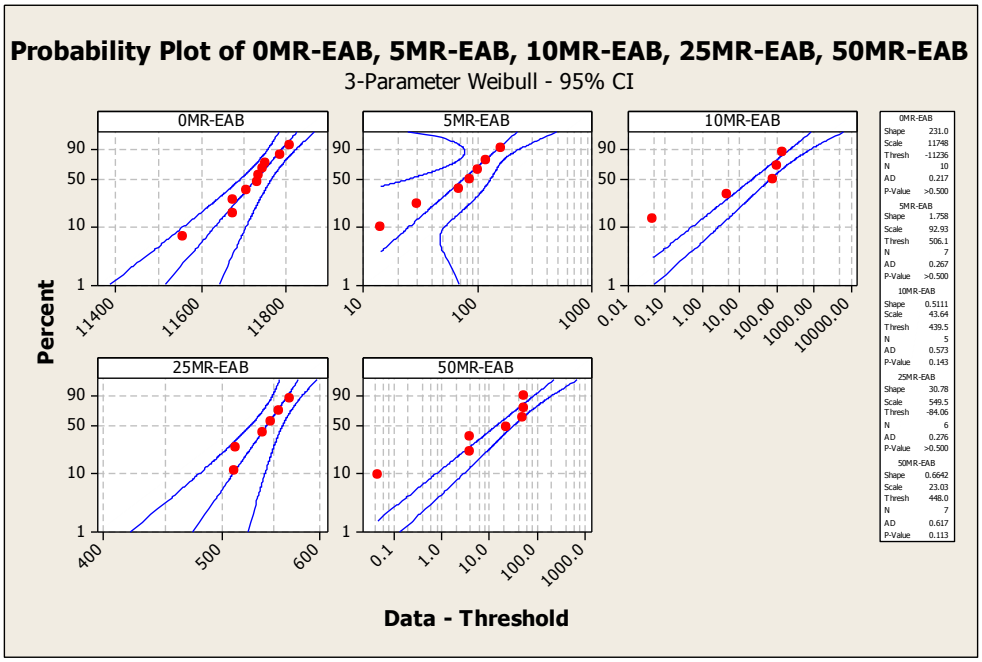

Figure B.10: Probability plot of EAB data at various doses for insulation with 3-Parameter weibull distribution

B.1.6 Largest extreme value distribution fit of the data

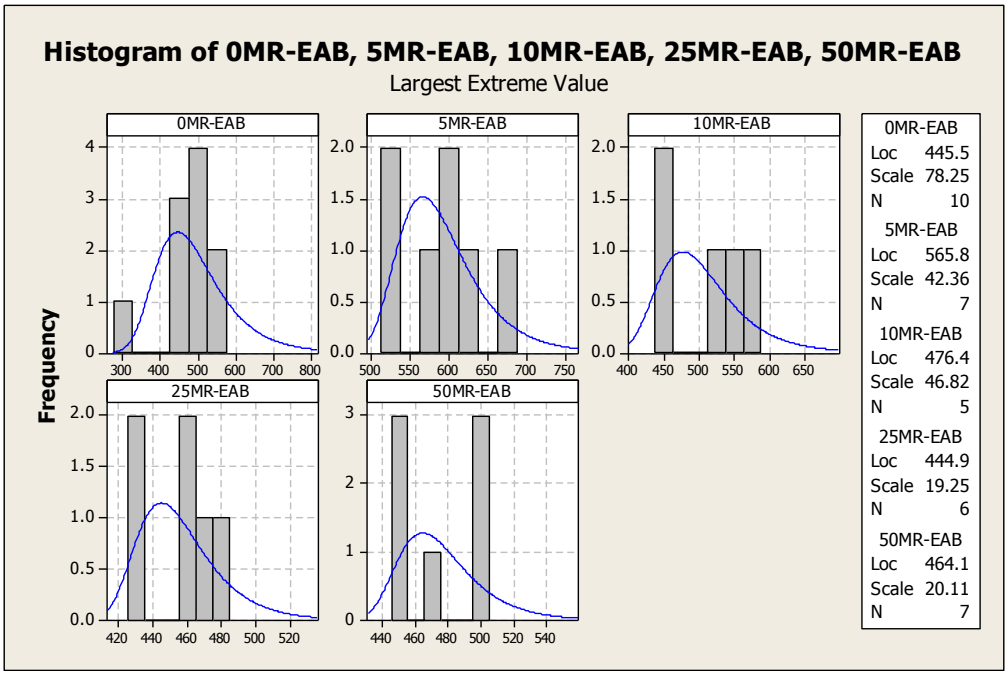

Figure B.11: Histogram of EAB data at various doses for insulation with Largest Extreme value distribution

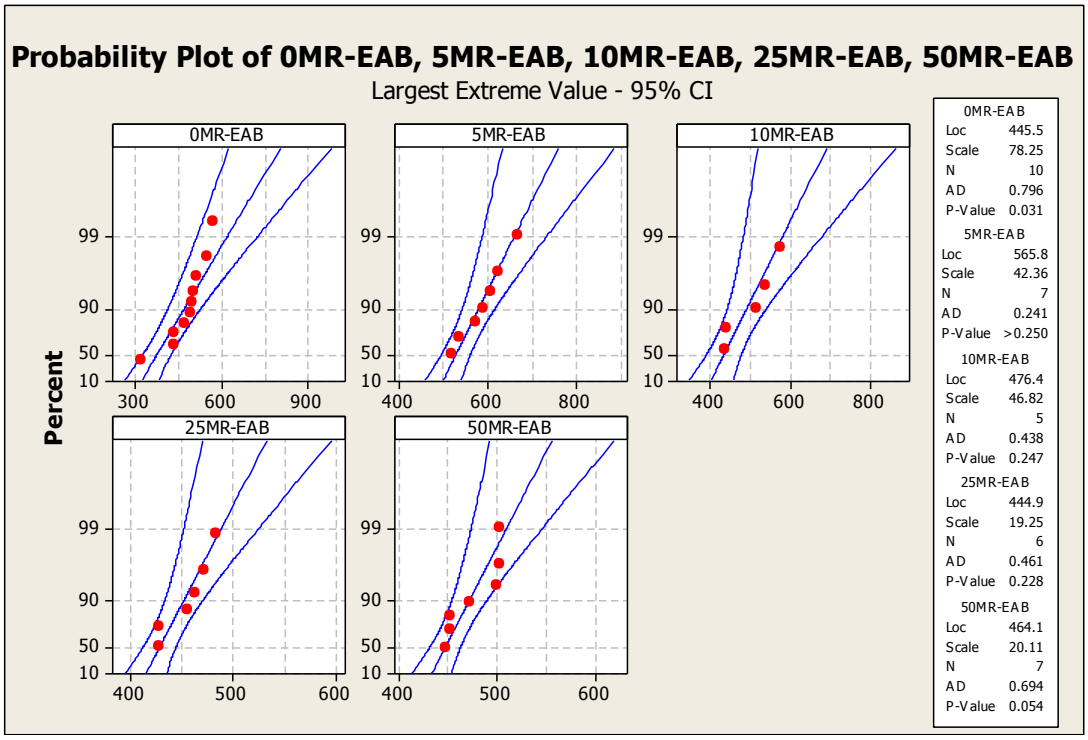

Figure B.12: Proability of EAB data at various doses for insulation with Largest Extreme value distribution

B.1.7 Summary of the distributions

The summary of distribution analysis for insulation is shown in Table B.1.

Table B.1: Summary of distribution analysis for insulation.

Dose (MRad)	Samples	Distribution	Anderson Darling	P-value	Correlation coefficient
0	10	Normal	0.406	0.282	0.944
		Lognormal	0.598	0.087	0.912
		Weibull	0.256	>0.25	0.955
		3-Parameter Weibull	0.217	>0.500	0.973
		Smallest extreme value	0.217	>0.25	0.973
		Largest extreme value	0.796	0.031	
5	7	Normal	0.153	0.922	0.991
		Lognormal	0.160	0.909	0.991
		Weibull	0.193	>0.25	0.981
		3-Parameter Weibull	0.267	>0.500	0.988
		Smallest extreme value	0.217	>0.25	0.976
		Largest extreme value	0.241	>0.25	

10	5	Normal	0.301	0.419	0.963
		Lognormal	0.320	0.369	0.959
		Weibull	0.324	>0.25	0.947
		3-Parameter Weibull	0.573	0.143	0.947
		Smallest extreme value	0.309	>0.25	0.947
		Largest extreme value	0.438	0.247	
25	6	Normal	0.301	0.456	0.966
		Lognormal	0.315	0.416	0.963
		Weibull	0.277	>0.25	0.958
		3-Parameter Weibull	0.276	>0.500	0.958
		Smallest extreme value	0.268	>0.25	0.958
		Largest extreme value	0.461	0.228	
50	7	Normal	0.612	0.065	0.919
		Lognormal	0.608	0.067	0.920
		Weibull	0.732	0.044	0.904
		3-Parameter Weibull	0.617	0.113	0.959
		Smallest extreme value	0.736	0.043	0.902
		Largest extreme value	0.694	0.054	

B.2 EAB data of irradiated sheath

B.2.1 Normal distribution fit of the data

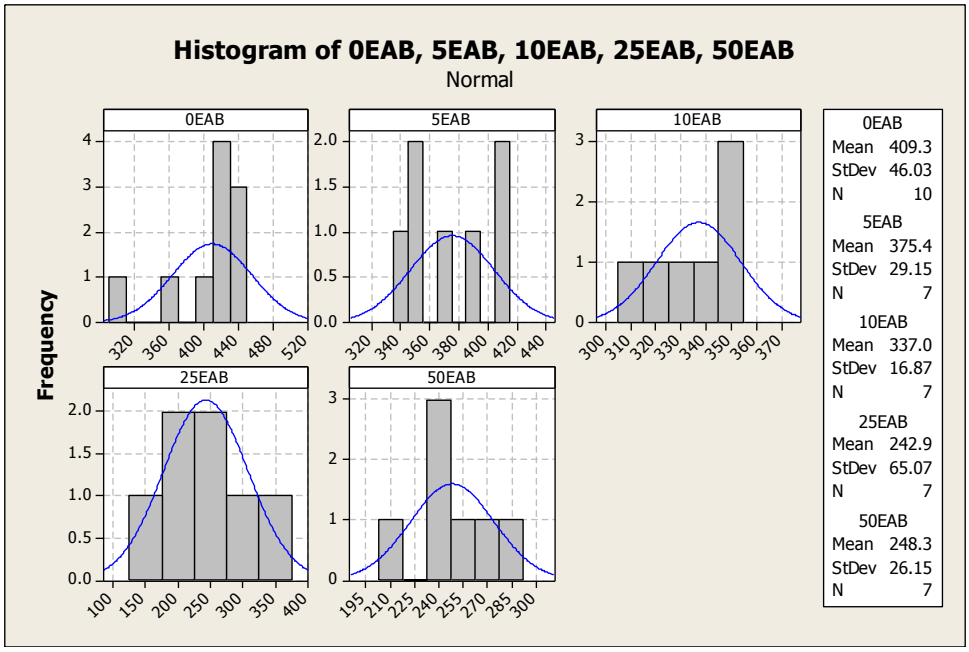

Figure B.13: Histogram of EAB data at various doses for sheath with Normal distribution

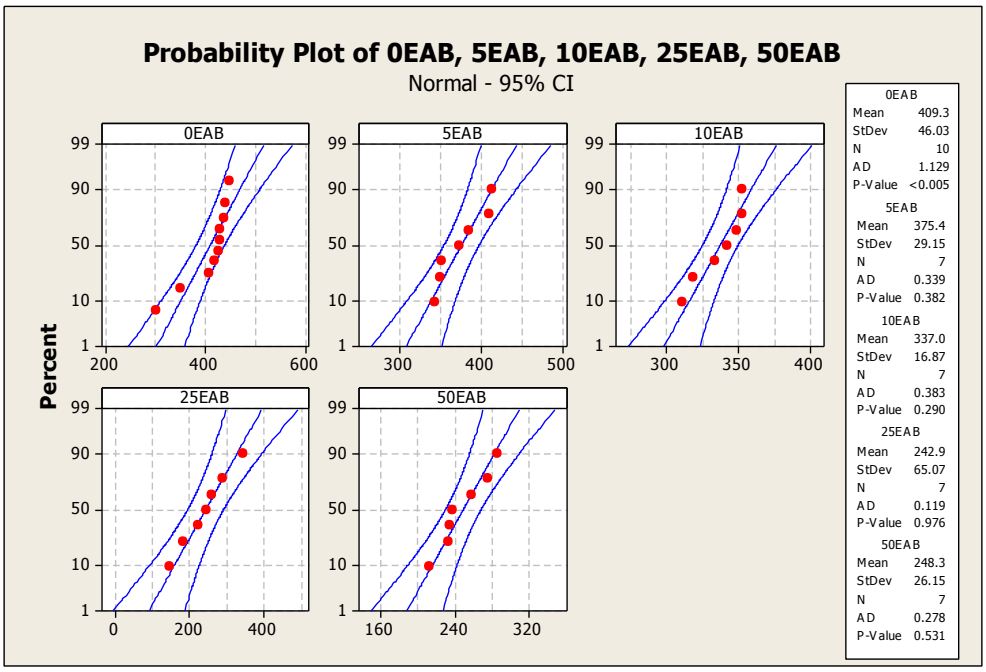

Figure B.14: Probability plot of EAB data at various doses for sheath with Normal distribution

B.2.2 Lognormal distribution fit of the data

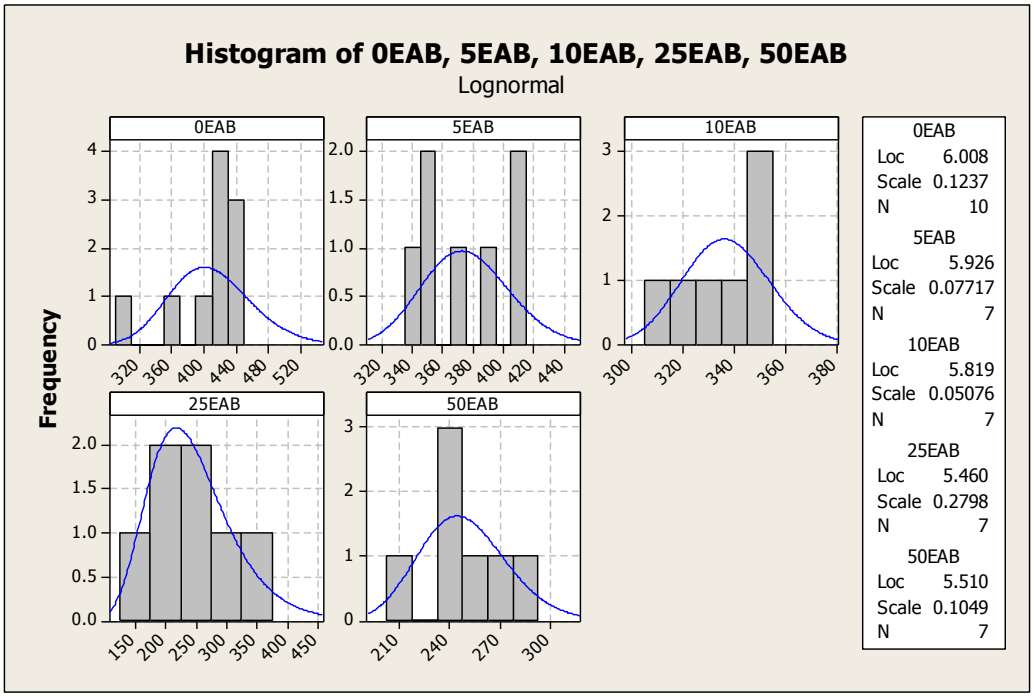

Figure B.15: Histogram of EAB data at various doses for sheath with Lognormal distribution

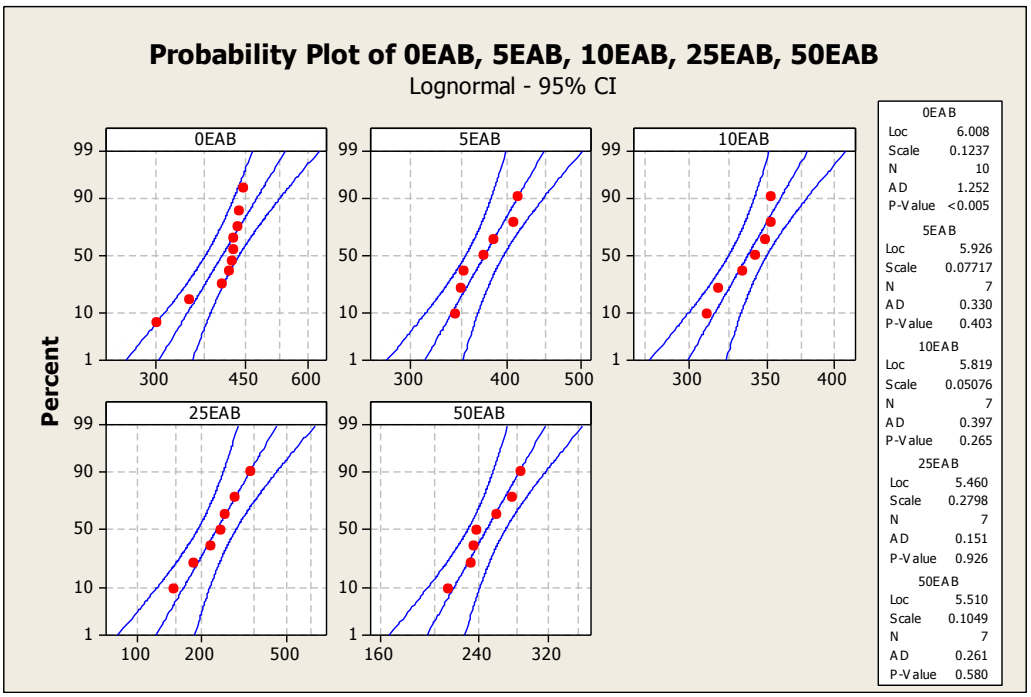

Figure B.16: Probability plot of EAB data at various doses for sheath with Lognormal distribution

B.2.3 Smallest extreme value distribution fit of the data

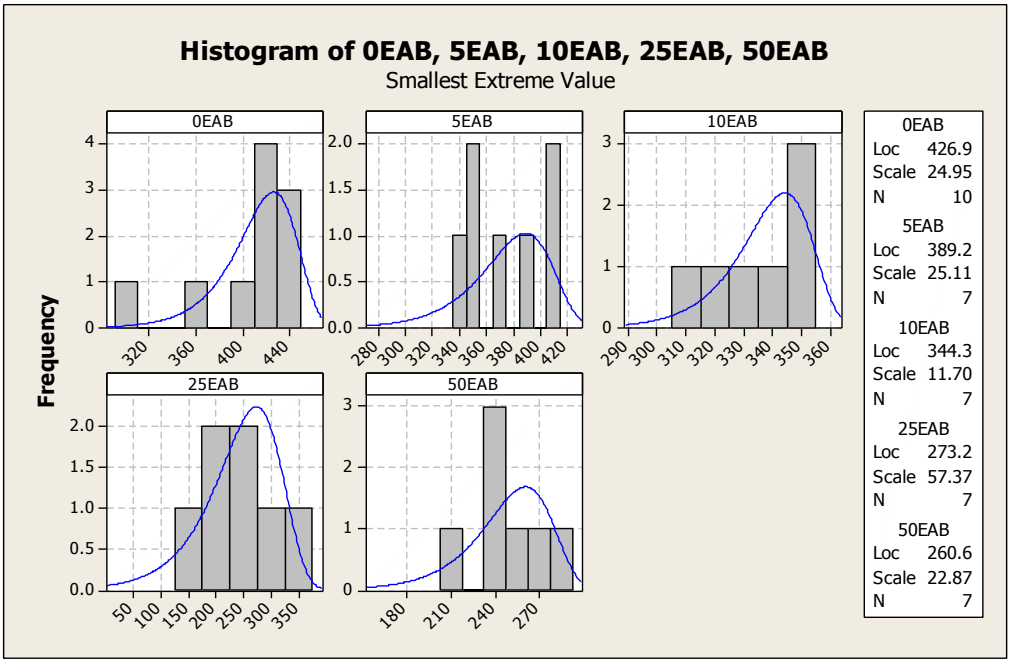

Figure B.17: Histogram of EAB data at various doses for sheath with Smallest Extreme value distribution

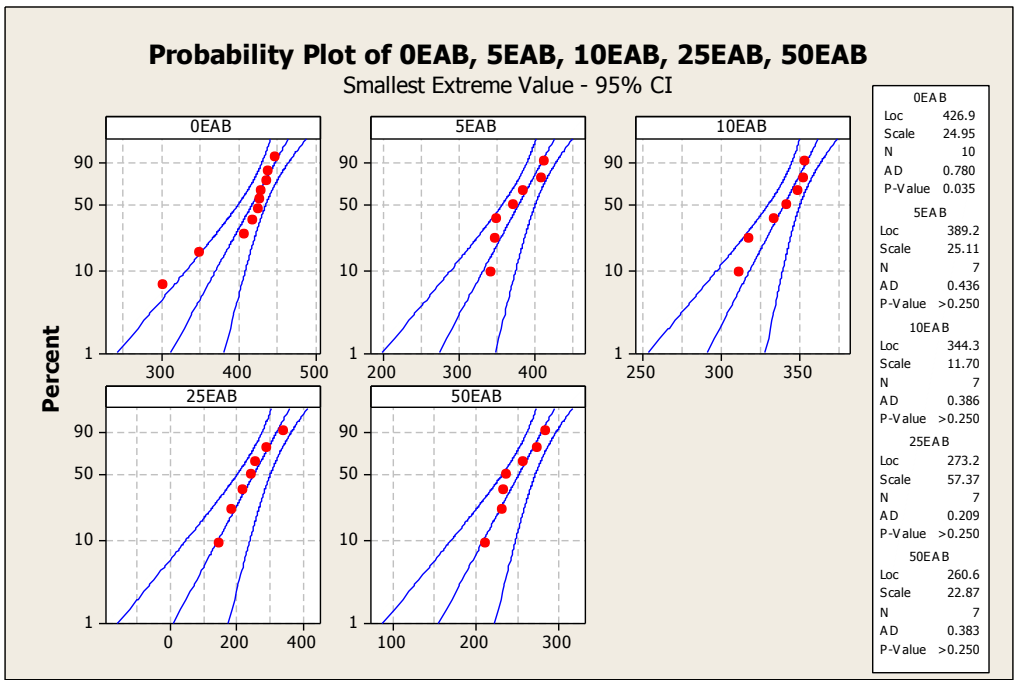

Figure B.18: Proability plot of EAB data at various doses for sheath with Smallest Extreme value distribution

B.2.4 Weibull distribution fit of the data

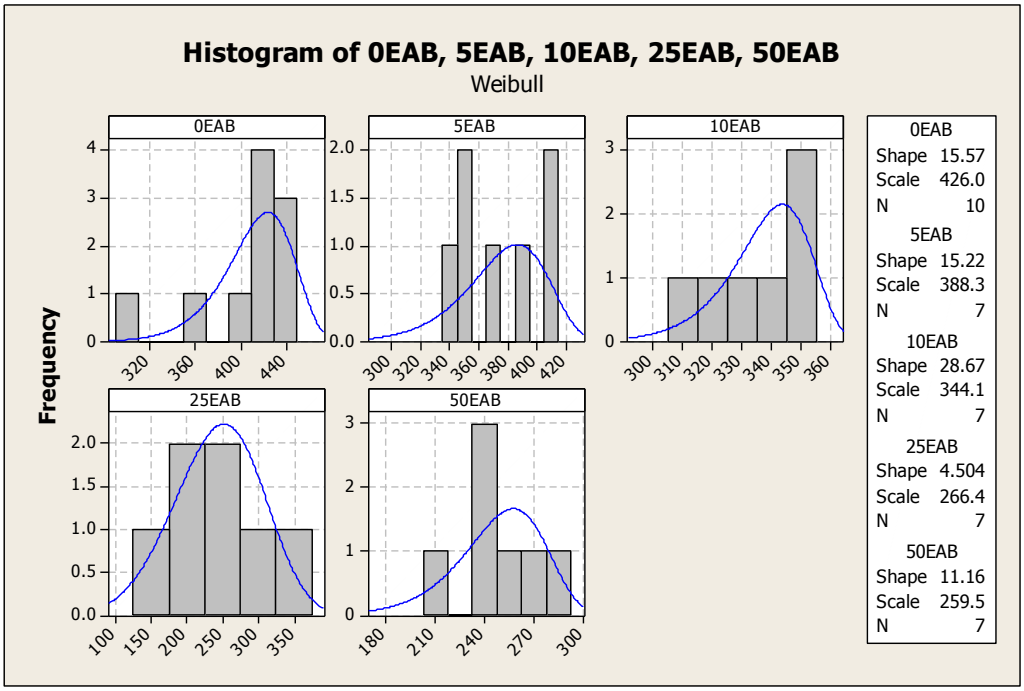

Figure B.19: Histogram of EAB data at various doses for sheath with Weibull distribution

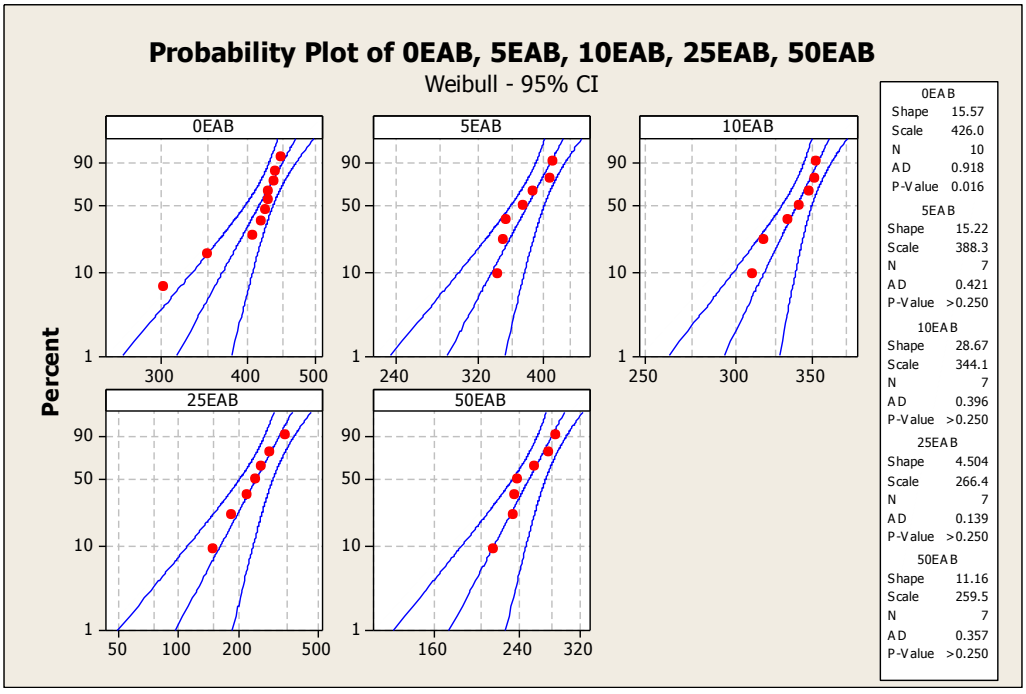

Figure B.20: Probability plot of EAB data at various doses for sheath with Weibull distribution

B.2.5 3-Parameter Weibull distribution fit of the data

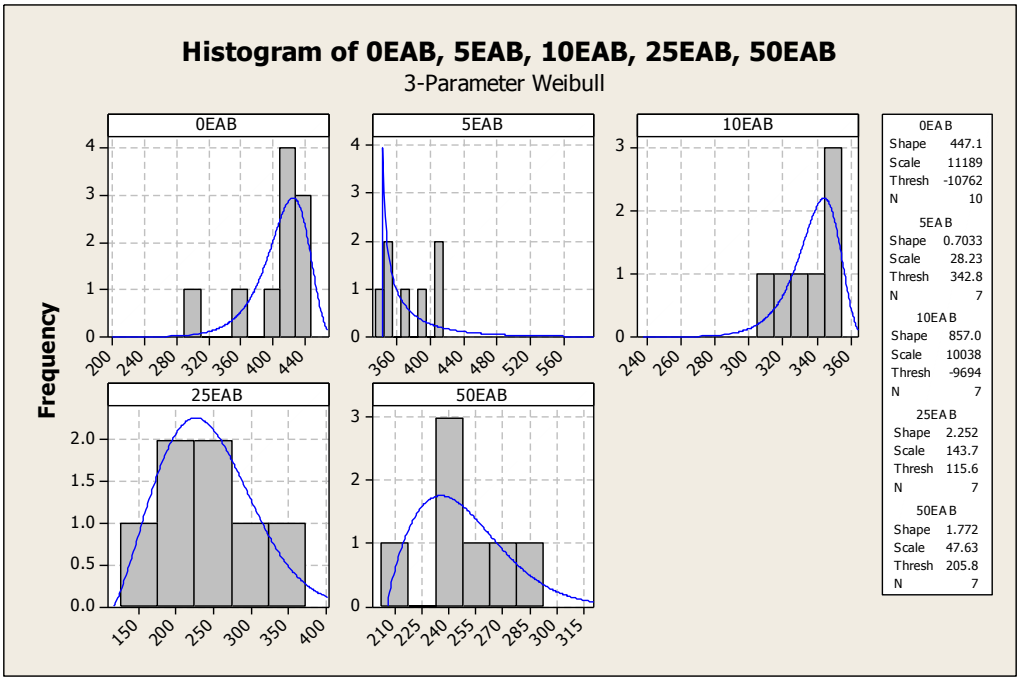

Figure B.21: Histogram of EAB data at various doses for sheath with 3-Parameter Weibull distribution

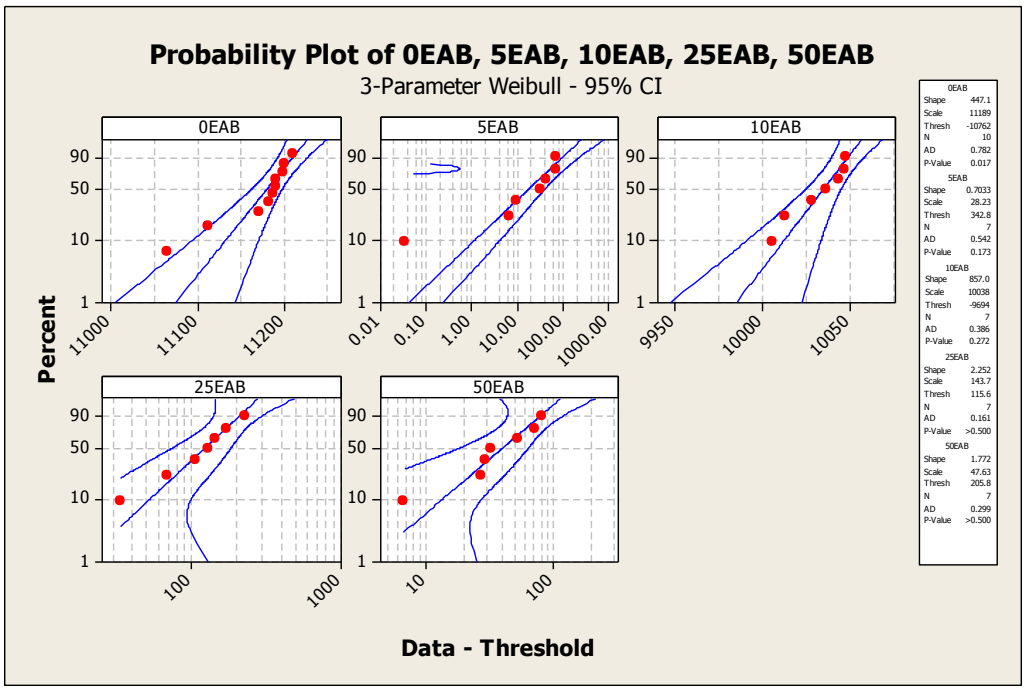

Figure B.22: Probability plot of EAB data at various doses for sheath with 3-Parameter Weibull distribution

B.2.6 Largest extreme value distribution fit of the data

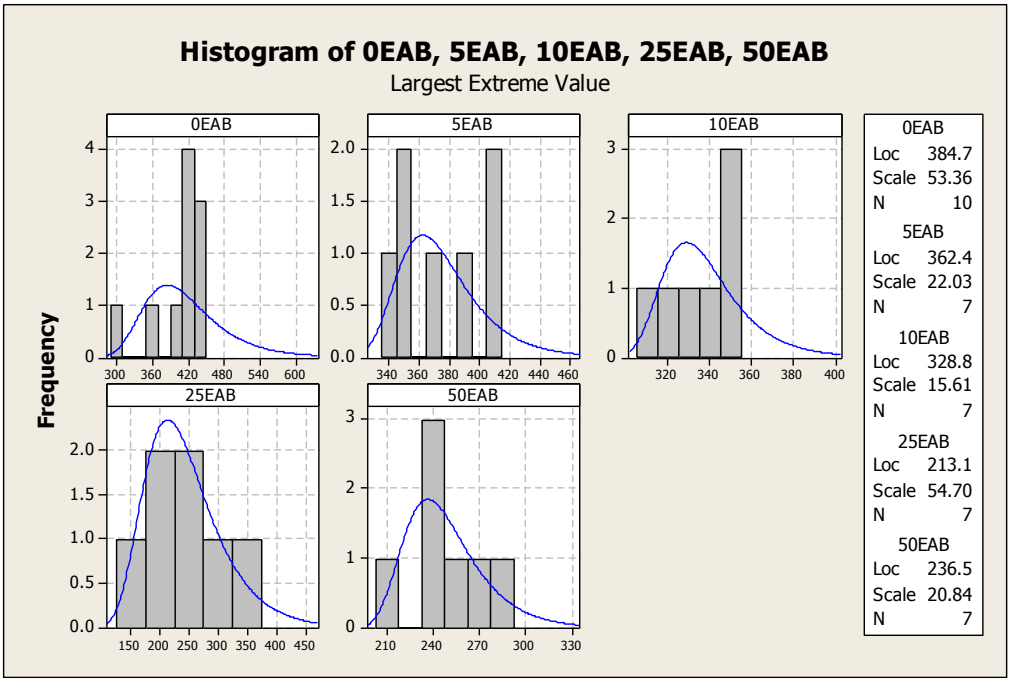

Figure B.23: Histogram of EAB data at various doses for sheath with Largest Extreme value distribution

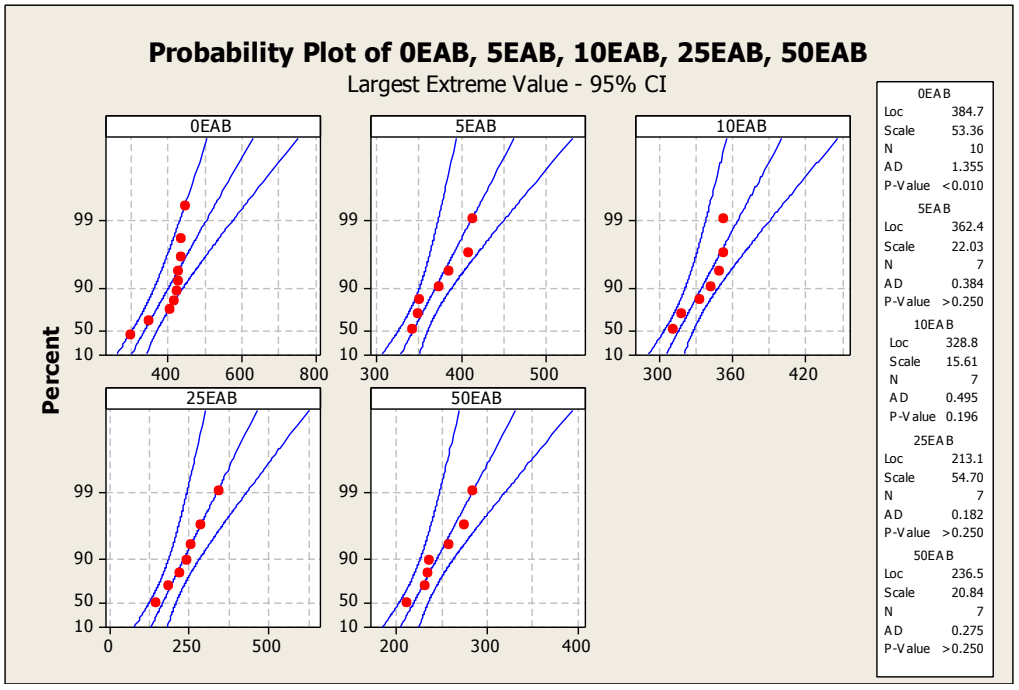

Figure B.24: Probability plot of EAB data at various doses for sheath with Largest Extreme value distribution

B.2.7 Summary of the distributions

The summary of distribution analysis for sheath is shown in Table B.1.

Table B.1: Summary of distribution analysis for sheath.

Dose (MRad)	Samples	Distribution	Anderson Darling	P-value	Correlation coefficient
0	10	Normal	1.129	<0.005	0.861
		Lognormal	1.252	<0.005	0.843
		Weibull	0.918	0.016	0.913
		3-Parameter Weibull	0.782	0.017	0.925
		Smallest extreme value	0.78	0.035	0.926
		Largest extreme value	1.355	<0.01	
5	7	Normal	0.329	0.382	0.962
		Lognormal	0.330	0.403	0.964
		Weibull	0.421	>0.25	0.939
		3-Parameter Weibull	0.542	0.173	0.982
		Smallest extreme value	0.436	>0.25	0.934
		Largest extreme value	0.384	>0.25	

10	7	Normal	0.383	0.290	0.952
		Lognormal	0.397	0.265	0.949
		Weibull	0.396	>0.25	0.973
		3-Parameter Weibull	0.386	0.272	0.973
		Smallest extreme value	0.386	>0.25	0.973
		Largest extreme value	0.495	0.196	
25	7	Normal	0.119	0.976	0.996
		Lognormal	0.151	0.926	0.991
		Weibull	0.139	>0.25	0.997
		3-Parameter Weibull	0.161	>0.5	0.997
		Smallest extreme value	0.209	>0.25	0.982
		Largest extreme value	0.182	>0.25	
50	7	Normal	0.278	0.531	0.975
		Lognormal	0.261	0.580	0.977
		Weibull	0.357	>0.25	0.961
		3-Parameter Weibull	0.299	>0.5	0.977
		Smallest extreme value	0.383	>0.25	0.953
		Largest extreme value	0.275	>0.25	